Analyse der Hämokompatibilität und zeitabhängigen Plasmaproteinadsorption auf Medizinprodukten zur Etablierung neuartiger Beschichtungen

Dissertation

der Mathematisch-Naturwissenschaftlichen Fakultät
der Eberhard Karls Universität Tübingen
zur Erlangung des Grades eines
Doktors der Naturwissenschaften
(Dr. rer. nat.)

vorgelegt von:
Katharina Große-Berkenbusch (geb. Gerling)
aus Tübingen

Tübingen
2025

Gedruckt mit Genehmigung der Mathematisch-Naturwissenschaftlichen Fakultät der Eberhard Karls Universität Tübingen.

Tag der mündlichen Qualifikation:	13.02.2026
Dekan:	Prof. Dr. Thilo Stehle
1. Berichterstatter/-in:	Prof. Dr. Meltem Avci-Adali
2. Berichterstatter/-in:	Prof. Dr. Boris Maček
3. Berichterstatter/-in:	Prof. Dr. Tassula Proikas-Cezanne

Danksagung

Zunächst möchte ich meinen herzlichen Dank an Frau Prof. Dr. Meltem Avci-Adali, Frau Dr. Sandra Stoppelkamp und Herrn Prof. Dr. Hans-Peter Wendel richten, die mir die Möglichkeit gegeben haben, meine Promotion im klinischen Forschungslabor der Thorax-, Herz- und Gefäßchirurgie am Universitätsklinikum Tübingen zu verwirklichen.

Ein besonderer Dank gilt Frau Prof. Dr. Avci-Adali für die stets wertvolle Beratung, engagierte Betreuung und umfassende Unterstützung in allen Belangen während der gesamten Promotionszeit. Liebe Meltem, ich danke dir von Herzen für alles!

Mein Dank gilt außerdem Herrn Prof. Dr. Boris Maček für seine Bereitschaft, die Betreuung und Begutachtung dieser Dissertation zu übernehmen.

Ein weiterer Dank geht an Frau Prof. Dr. Tassula Proikas-Cezanne für die spontane Bereitschaft das 3. Gutachten zu übernehmen.

Ein großer Dank geht an Frau Dr. Sandra Stoppelkamp, die mich seit meinem Praxissemester über meine Masterarbeit hinweg bis zum Ende dieser Dissertation begleitet hat. Liebe Sandra, ich danke dir für die Projektidee, die inspirierenden Anregungen, die gemeinsame Planung und Entwicklung der Projekte sowie für das Vertrauen, das du mir entgegengebracht hast. Dein stets offenes Ohr und deine Unterstützung waren unbezahlbar – von Herzen vielen Dank!

Ebenso danke ich allen Mitarbeitenden und Studierenden des klinischen Forschungslabors der THG-Chirurgie sowie allen Kooperationspartnern, die mit ihrer Freundlichkeit, Hilfsbereitschaft und ihrem Engagement maßgeblich zum Erfolg dieser Arbeit beigetragen haben

Ein herzliches Dankeschön geht an meine Eltern für ihre bedingungslose Unterstützung und Förderung schon mein ganzes Leben lang. Danke, dass ihr stets an mich geglaubt habt – ohne euch wäre ich nicht dort, wo ich heute bin.

Zuletzt möchte ich mich bei meiner kleinen Familie bedanken. Lieber Andy, danke für deine Geduld und Unterstützung bis zum Schluss.

Inhaltsverzeichnis

Abkürzungsverzeichnis

AK	Antikörper
ADP	Adenosindiphosphat
API	aktive pharmazeutische Substanz
ATIII	Antithrombin III
APOB	Apolipoprotein B
APOE	Apolipoprotein E
β-TG	β-Thromboglobulin
C	Komplementkomponente
C1-INH	C1-Esterase-Inhibitors
C1qrs	C1-Komplex (bestehend aus den Untereinheiten C1q, C1r und C1s)
C4BP	C4-Bindungsprotein
CD11b/CD18	Integrin-Molekül Mac-1
CD56	Neural Cell Adhesion Molecule (NCAM)
CFHR	Komplementfaktor-H-verwandte Proteine
COVID-19	Coronavirus-Krankheit
CPB	kardiopulmonalen Bypass
CPB2	Carboxypeptidase B2
CRP	C-reaktives Protein
ECMO	extrakorporale Membranoxygenierung
F	Gerinnungsfaktor
FGA	Fibrinogen alpha chain
FGB	Fibrinogen beta chain
FGG	Fibrinogen gamma chain
FIII	Gewebefaktor
FH	Flüssigphasenfaktor H
FI	Flüssigphasenfaktor I
Fa	Aktivierte Form eines Gerinnungsfaktors
HCII	Heparin-Co-Faktor II
HEMA	2-Hydroxyethylmethacrylat
HIT	heparininduzierten Thrombozytopenie

HK	hochmolekulares Kininogen
HLM	Herz-Lungen-Maschine
HMWK	hochmolekulares Kininogen
IL	Interleukin
KI	Künstliche Intelligenz
MS	Massenspektrometrie
KNG	Kininogen
MASPs	MBL/Ficolin-assoziierten Serinproteasen
MBL	Mannose-bindende Lektin
MDR	Medizinprodukteverordnung
NET	neutrophile extrazelluläre Fallen
PAF	Plättchenaktivierender Faktor
PC	Protein C
PCI	Protein-C-Inhibitor
PF4	Plättchenfaktor 4
PK	Präkallikrein
PET-Membran	Polyethylenterephthalat (Wärmeaustausch) Membran
PMN-Elastase	Polymorphonuklear-Elastase
PMP-Membran	Polymethylpenten (Gasaustausch) Membran
PRMs	Mustererkennungsmoleküle
PS	Protein S
PSGL-1	Leukozyten-P-Selektin-Glykoprotein-Ligand-1
SIRS	Systemisches inflammatorisches Response-Syndrom
SOFA	Sepsis-related organ failure assessment
TAT	Thrombin-Antithrombin-III-Komplexes
TF	Tissue-Faktor
TFPI	Tissue-Faktor-Pathway-Inhibitor
VWF	von-Willebrand-Faktor

Zusammenfassung

Biomaterialien bieten vielfältige Möglichkeiten zur Verbesserung der Lebensqualität von Patienten, insbesondere im Bereich von implantierbaren oder blutkontaktierenden Medizinprodukten. In den letzten Jahren wurden in diesem Bereich signifikante Fortschritte erzielt. Dennoch bleibt die Hämokompatibilität von Biomaterialien eine zentrale Herausforderung. Der Kontakt zwischen Biomaterialien und Blut birgt das Risiko thrombotischer Reaktionen sowie initialer Immunreaktionen, die durch die Adsorption von Plasmaproteinen an der Materialoberfläche ausgelöst werden. Ein besseres Verständnis der Proteinadsorption und der damit verbundenen Abwehrreaktionen kann gezielte Modifikationen der Biomaterialien ermöglichen, um eine verbesserte Hämokompatibilität zu erreichen. Diese Modifikationen können sowohl durch spezifische Oberflächenbeschichtungen als auch durch die Veränderung der Materialeigenschaften erfolgen.

In der vorliegenden Arbeit wurde die Proteinadsorption auf verschiedenen Biomaterialien mittels massenspektrometrischer Analysen untersucht. Dabei konnten erstmals Bindungsprofile von über 500 Proteinen über einen Zeitraum von sechs Stunden identifiziert werden. Auf Basis dieser Ergebnisse wurde eine neuartige hämokompatible Beschichtung entwickelt, die auf der kovalenten Bindung des C1-Esterase-Inhibitors (C1-INH) basiert. C1-INH hemmt nicht nur das Komplementsystem, sondern verhindert auch die Aktivierung von Faktor XII (FXII), wodurch die Blutgerinnung bereits in einem frühen Stadium unterbrochen wird. Die Hämokompatibilität der entwickelten Beschichtungen wurde durch dynamische Inkubation mit humanem Vollblut getestet. Die Analyse der Blut- und Plasmaparameter ergab, dass die C1-INH-Beschichtung die Aktivität von FXIIa signifikant stärker reduzierte als herkömmliche Heparin-Beschichtungen.

Darüber hinaus wurde in einer weiteren Studie gezeigt, dass die Materialeigenschaften ebenfalls einen Einfluss auf die Hämokompatibilität haben. So konnte nachgewiesen werden, dass der Wechsel von Baumwoll- zu synthetischen Bauchtüchern während Operationen zu einer Reduktion der Thrombozyten- und Neutrophilenaktivierung sowie der Freisetzung von inflammatorischen Zytokinen wie Interleukin (IL) 1β und IL-6 führt. Jedoch bewerteten alle an dieser Studie beteiligten Chirurgen und Chirurginnen die synthetischen Materialien hinsichtlich ihrer Absorptionsfähigkeit und Formbarkeit als minderwertig.

Insgesamt liefert diese Arbeit wertvolle Erkenntnisse über die Proteinadsorption auf Biomaterialien und deren Konsequenzen. Zu den zentralen Ergebnissen zählen die schnelle und dynamische Schichtbildung, die zeitabhängige Veränderung der adsorbierten Proteine sowie der Einfluss von Oberflächenmodifikationen, Materialeigenschaften und Flussraten auf die Zusammensetzung der Proteinschicht. Diese Erkenntnisse bilden eine fundierte Grundlage für die Entwicklung innovativer Strategien zur Verbesserung der Hämokompatibilität und zur Optimierung von Biomaterialien.

Abstract

Biomaterials offer diverse opportunities to improve the quality of life for patients, particularly in the field of implantable or blood-contacting medical devices. In recent years, significant progress has been made in this area. Nevertheless, the hemocompatibility of biomaterials remains a major challenge. Contact between biomaterials and blood carries the risk of thrombotic reactions as well as initial immune responses, which are triggered by the adsorption of plasma proteins onto the material surface. A better understanding of protein adsorption and the associated defense mechanisms can enable targeted modifications of biomaterials to achieve improved hemocompatibility. These modifications can be implemented through specific surface coatings or by altering the material properties.

In the present study, protein adsorption on various biomaterials was investigated using mass spectrometric analyses. For the first time, binding profiles of over 500 proteins were identified over a six-hour period. Based on these findings, a novel hemocompatible coating was developed, based on the covalent binding of C1-esterase inhibitor (C1-INH). C1-INH not only inhibits the complement system but also prevents the activation of factor XII (FXII), thereby interrupting the coagulation cascade at an early stage. The hemocompatibility of the developed coatings was tested by dynamic incubation with human whole blood. Analysis of blood and plasma parameters revealed that the C1-INH coating significantly reduced FXIIa activity compared to conventional heparin coatings.

Furthermore, an additional study demonstrated that material properties also influence hemocompatibility. It was shown that switching from cotton to synthetic surgical swabs during operations led to a reduction in platelet and neutrophil activation as well as the release of inflammatory cytokines such as interleukin (IL) 1β and IL-6. However, all surgeons involved in the study rated the synthetic materials as inferior in terms of absorption capacity and moldability.

Overall, this work provides valuable insights into protein adsorption on biomaterials and its consequences. Key findings include the rapid and dynamic formation of protein layers, the time-dependent changes in adsorbed proteins, and the influence of surface modifications, material properties, and flow rates on the composition of the protein layer. These insights form a solid foundation for the development of innovative strategies to improve hemocompatibility and optimize biomaterials for clinical applications.

1 Einleitung

1.1 Biomaterialien

Biomaterialien werden verwendet, um die Funktion von geschädigten oder degenerierten Geweben und Organen zu ersetzen oder zu verbessern. Der Einsatz führt zu einer Verbesserung der Lebensqualität von Patienten [1]. Schon die Römer, Azteken und Chinesen verwendeten Gold für zahnmedizinische Anwendungen. Auch die Mayas verwendeten Zahnimplantate aus Muscheln, deren Ergebnisse auf eine tatsächliche Knochenintegration hinwiesen [2]. Auch Silber wurde schon vor über 1000 Jahren in verschiedenen Formen als antimikrobielles Mittel zur Verhinderung von Infektionen eingesetzt [3]. Heute ist durch den Einsatz von Biomaterialien vieles möglich. Künstliche Gelenke verbessen die Lebensqualität von Millionen von Menschen [4], resorbierbares Nahtmaterial vereinfacht chirurgische Eingriffe [5] und verschiedene kardiovaskuläre Geräte retten Millionen von Menschenleben [6]. Das Aufkommen des *Tissue Engineering* und der Organregeneration verschiebt heute die Grenzen der Wissenschaft, und bietet eine große Forschungsbandbreite im Bereich der Biomaterialien.

Biomaterialien interagieren direkt mit biologischen Systemen. Die Biokompatibilität ist deshalb ein entscheidender Punkt bei der Entwicklung von Biomaterialien. Ein biokompatibles Material sollte die ihm zugedachte Funktion in einer bestimmten Anwendung erfüllen, ohne dass es zu unerwünschten Reaktionen kommt [7]. Bei Biomaterialien, die mit Blut in Kontakt kommen, wie beispielsweise kardiovaskuläre Produkte, spielt die Hämokompatibilität eine bedeutende Rolle im Rahmen der Biokompatibilität. Die Hämokompatibilität bezieht sich auf die Fähigkeit eines Materials, mit dem Blut in einer Weise zu interagieren, die keine schädlichen Auswirkungen auf die Blutzellen, die Gerinnung oder andere wichtige physiologische Prozesse hat. Obwohl eine perfekte Biokompatibilität sehr schwer zu erreichen ist, funktionieren viele kardiovaskuläre Produkte mit einem geringen oder akzeptablen Risiko von Komplikationen [8].

1.2 Blutkontakt mit Biomaterialien

Unter normalen Bedingungen kommt das Blut ausschließlich mit dem Endothel in Kontakt. Das Endothel besitzt gerinnungshemmende und antithrombotische Eigenschaften. Bei der Verwendung von kardiovaskulären Geräten kommt es zum Kontakt des Blutkreislaufes mit einer fremden Oberfläche, ohne die positiven Eigenschaften des

Endothels. Durch die Wechselwirkungen zwischen Blut und Material kommt es zur Proteinadsorption, dies stellt das erste bedeutende Ereignis nach Oberflächenkontakt dar. Die Proteinadsorption bei Blutkontakt ist der Vorläufer für nachfolgende Körperabwehrreaktionen wie die plasmatische Gerinnung, Thrombozytenadhäsion und -aktivierung, Immunreaktionen und Inflammation (**Abbildung 1**). Gerinnung, Thrombozytenadhäsion und -aktivierung sind die wichtigsten Herausforderungen einer oberflächeninduzierten Thrombose, die die größte Einschränkung bei der Verwendung von Produkten mit Blutkontakt darstellt.

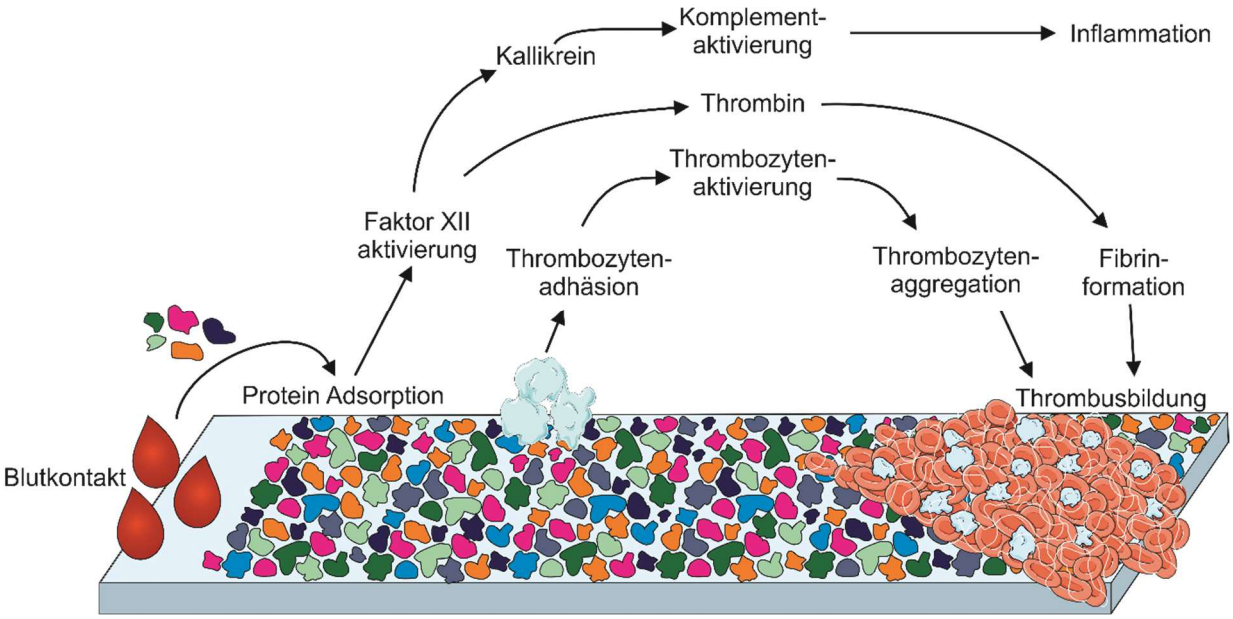

Abbildung 1: Thrombusbildung auf Biomaterialien nach Blutkontakt. Die Adsorption von Proteinen auf der Oberfläche von Medizinprodukten führt zur Adhäsion, Aktivierung und Aggregation von Blutplättchen. Der an der Oberfläche adsorbierte Faktor XII wird autoaktiviert, und der daraus resultierende Faktor XIIa wandelt Präkallikrein in Kallikrein um und leitet die Gerinnung und Thrombinbildung ein. Thrombin führt zur Ablagerung von Fibrin auf der Oberfläche und fördert die Aktivierung der Blutplättchen. An der Oberfläche abgelagerte Thrombozytenaggregate werden durch Fibrinstränge stabilisiert und bilden einen Thrombozyten-Fibrin-Thrombus. Kallikrein, Thrombin und andere Gerinnungsproteine aktivieren das Komplement und lösen eine lokale Entzündungsreaktion aus.

1.2.1 Protein Adsorption

Die Proteinadsorption auf der Oberfläche eines Biomaterials spielt eine entscheidende Rolle bei dem Ablauf von biologischen Reaktionen und zellulären Interaktionen [9]. Kommt ein Material mit einem lebenden System in Kontakt kommt, bildet sich innerhalb von Sekunden eine Proteinschicht [10]. Die genaue Zusammensetzung der Proteinschicht ist jedoch unbekannt, nicht vorhersehbar und stark abhängig von der Oberfläche [11]. Als vorherrschenden Faktoren, die die Proteinadsorption beeinflussen gelten allgemein die Eigenschaften der Proteine [12, 13], die Eigenschaften der Substrate und Medien [14-16] und die Protein-Substrat-Wechselwirkungen [17-20]. **Abbildung 2** zeigt eine schematische Darstellung der Einflussfaktoren auf die Proteinadsorption.

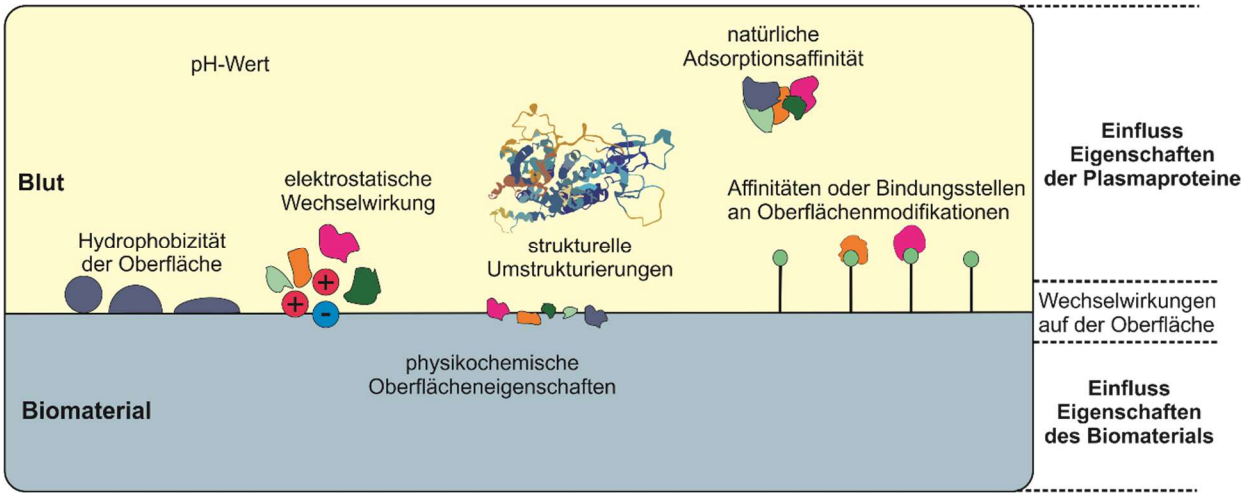

Abbildung 2: Einflussfaktoren der Proteinadsorption. Die Bindung der Proteine hängt sowohl von den Eigenschaften der Proteine selbst als auch von den Eigenschaften des Biomaterials sowie deren Wechselwirkungen ab.

Die adsorbierte Proteinschicht ist komplex und enthält viele der im Plasma vorkommenden Proteine. Die Häufigkeit der einzelnen adsorbierten Proteine spiegelt im Allgemeinen nicht die Proteinzusammensetzung des Plasmas wider [21, 22]. Zu den auf den meisten blutkontaktierenden Oberflächen vorhandenen Proteinen gehören Albumin, Fibrinogen, Immunglobuline, Vitronectin und Apolipoproteine [23]. Es gibt Hinweise darauf, dass die Zusammensetzung der Proteinschicht mit der Zeit variiert [24]. Die kurzfristige Veränderung der adsorbierten Proteinschicht wurde eingehend untersucht. Es wird davon ausgegangen, dass Proteine aufgrund ihrer Größer, Anzahl und ihres adsorptionsverhalten unterschiedlich schnell an der Oberfläche binden. Die um-

fangreichsten Informationen über die zeitabhängige Plasmaproteinadsorption stammen aus Studien über den Vroman-Effekt [25, 26]. Es zeigte sich, dass Fibrinogen kurzfristig adsorbiert, aber relativ schnell durch andere Plasmabestandteile verdrängt wird. Hierfür sind hauptsächlich die Proteine des intrinsischen Gerinnungsweges, insbesondere hochmolekulares Kininogen (HMWK), verantwortlich [26, 27]. Ganz allgemein hatte Vroman die Hypothese, dass die Adsorption im Plasma sequenziell erfolgt und dass im Laufe der Zeit häufiger vorkommende Proteine mit geringerer Oberflächenaffinität durch weniger häufig vorkommende Proteine mit höherer Oberflächenaffinität ersetzt werden [28].

1.2.2 Zelladhäsion

Adsorbierte Proteine vermitteln die Anhaftung von Thrombozyten, Leukozyten und Erythrozyten an künstliche Oberflächen [29]. Fibrinogen spielt hierbei eine entscheidende Rolle, da es an spezifische Rezeptoren auf der Oberfläche von Thrombozyten bindet. Diese Bindung zwischen Fibrinogen und den Fibrinogenrezeptoren auf den Thrombozyten führt zur Aktivierung der Thrombozyten und fördert so die Bildung von Blutgerinnseln. Auch andere Proteine wie von-Willebrand-Faktor und Fibronektin sind dafür bekannt die Thrombozytenadhäsion zu fördern [30]. Aktivierte Thrombozyten sekretieren Agonisten (wie ADP und Thromboxan A_2) und Gerinnungsfaktoren, fördern dadurch die Thrombozytenaggregation und sorgen für eine Beschleunigung der Thrombinbildung. Auch Leukozyten, insbesondere neutrophile Granulozyten, haften über CD11b/CD18 an adsorbiertem Fibrinogen [31]. Adhärente Thrombozyten fördern die Leukozytenadhäsion über eine Interaktion zwischen P-Selektin auf der Oberfläche aktivierter Thrombozyten und Leukozyten-P-Selektin-Glykoprotein-Ligand-1 (PSGL-1) [32]. Auch aktivierte Komplementkomponenten fördern durch spezifische Oberflächenrezeptoren die Leukozytenadhäsion [33]. Adhärente Leukozyten erzeugen freie Radikale und schütten durch Degranulation Substanzen wie den Plättchenaktivierender Faktor (PAF), Interleukine und den Tumornekrosefaktor aus. Diese Faktoren verstärken die lokale Thrombozytenaktivierung und induzieren die Expression des Gewebefaktors (FIII) durch umliegende Monozyten. Im Gegensatz zur rezeptorvermittelten Adhäsion von Thrombozyten und Leukozyten an die Proteinschicht ist die Adhäsion von Erythrozyten passiv [34]. Adhärente Erythrozyten setzten ADP frei, das durch das durch den ADP-rezeptor auf den Thrombozyten zu deren Aktivierung führt [35].

1.2.3 Aktivierung des Gerinnungssystems

Durch die Adsorption von Faktor (F) XII wird die Aktivierung des intrinsischen Gerinnungsweges eingeleitet. F XII wird durch Autoaktivierung in FXIIa umgewandelt, das dann Präkallikrein (PK) und FXI aktiviert. Auch das als Kofaktor fungierende hochmolekulare Kininogen (HK) bindet an künstliche Oberflächen, wodurch es zu einer weiteren Aktivierung von FXII kommt. Die Aktivierung von PK führt zur Bildung von Kallikrein, das dann seinerseits wiederum FXII aktiviert. Die Aktivierung von FXI durch FXII setzt eine Reihe von proteolytischen Reaktionen in Gang, die zur Thrombinbildung führen. Thrombin wandelt Fibrinogen in Fibrinmonomere um und ist ein potenter Thrombozyten Agonist, der die lokale Thrombozytenaggregation fördert. Durch die Polymerisierung der Fibrinmonomere kommt es zur Stabilisierung der Thrombozyten Aggregate, wodurch es zur Thrombusbildung kommt. Der Ablauf der Gerinnungskaskade ist in **Abbildung 3** dargestellt.

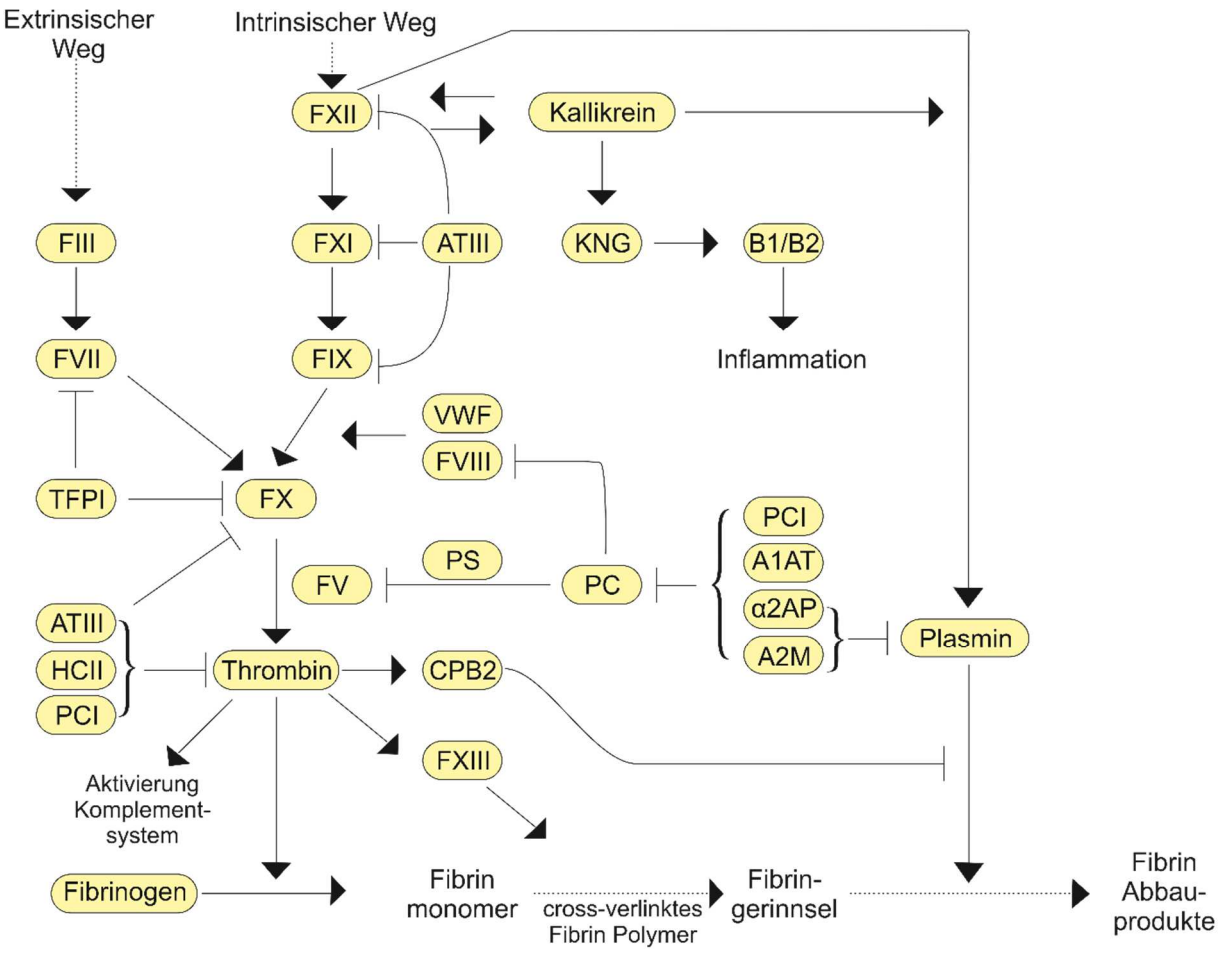

Abbildung 3: Schematischer Ablauf der Gerinnungskaskade. Die Aktivierung des extrinsischen Weges erfolgt durch die Freisetzung des Gewebefaktors (FIII). FIII interagiert mit dem Gerinnungsfaktor (F) VII, was zu einer Aktivierung dieses Faktors führt. Aktivierter FVII führt zur FX Aktivierung.Beim intrinsischen Weg wird FXII aktiviert und aktiviert wiederum FXI, was zur FIX Aktivierung führt. FIX bildet zusammen mit FVIII und Calciumionen einen Komplex (Tenase Komplex). Der Tenase Komplex aktiviert FX. Durch die Aktivierung von FX durch den extrinsischen oder intrinsischen Weg wird die Umwandlung von Prothrombin zu Thrombin gefördert. Thrombin spaltet Fibrinogen zu Fibrin, das das Gerinnsel bildet und die Blutung stoppt. Abbildung mittels KEGG-Datenbank [36] erstellt.

Durch Thrombenbildung kommt es zum Fouling von Biomaterialien, was zu deren Versagen führen kann. Außerdem können sich Teile des Thrombus von der Oberfläche lösen, durch den Blutkreislauf wandern und sich in Gefäßen festsetzen, die wichtige Organe mit Blut versorgen.

1.2.4 Komplementaktivierung

Das Komplementsystem besteht aus einem streng regulierten Netz von Proteinen, die eine wichtige Rolle bei der Erregerabwehr und bei Entzündungen spielen. Die Aktivierung des Komplementsystems führt zur Opsonisierung von Krankheitserregern und ihrer Beseitigung durch Phagozyten sowie zur Lyse [37]. Die Komplementkaskade wird über drei verschiedene Wege ausgelöst: den klassischen, den alternativen und den Lektin-Weg (**Abbildung 4a**). Alle drei Wege führen zur Aktivierung der C5-, C6-, C7-, C8- und C9-Proteine, was zur Bildung des Membranangriffkomplexes auf der Zielzelle führt (**Abbildung 4b**) [38].

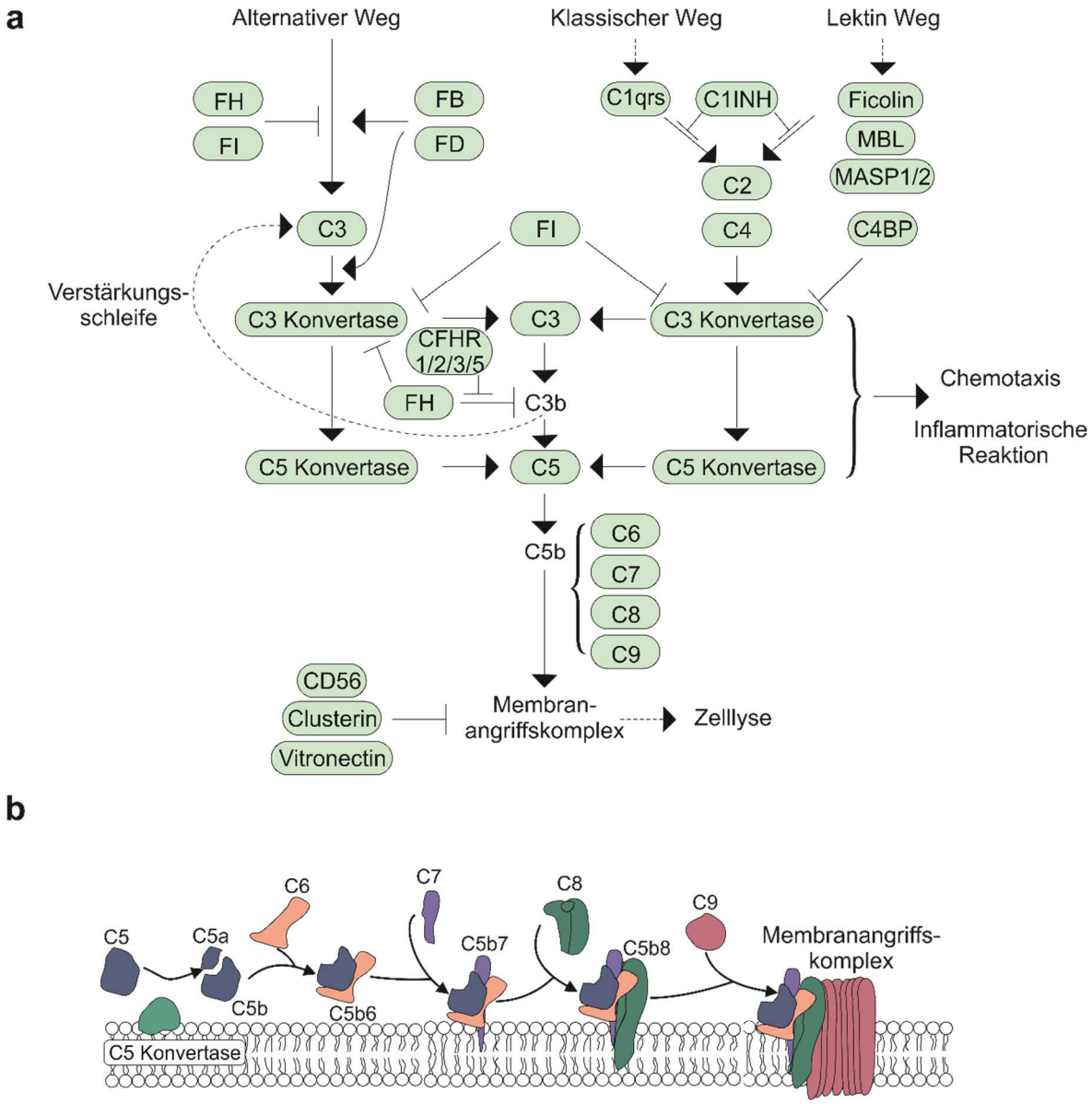

Abbildung 4: (a) Schematischer Ablauf der Komplementaktivierung. Die Bildung und der Zusammenbau der Komplementkomponente (C) 5-Konvertase erfolgen entweder über den klassischen, den alternativen oder den Mannose-bindenden Lektin-Weg. Die C5-Konvertase bindet an C5 und spaltet es, um C5a und C5b zu erzeugen was zum Aufbau des terminalen Komplementkomplexes führt (b). Nach der Bindung an C5b erlangt C6 die Fähigkeit, mit der Lipiddoppelschicht zu interagieren und einen bimolekularen C5b6-Komplex zu bilden. C7 und dann C8 binden nacheinander an C5b und fügen sich weiter in die Lipiddoppelschicht ein und bilden C5b-7- bzw. C5b-8-Komplexe. Ein C9-Molekül bindet an das in die Membran eingefügte C8, woraufhin die Polymerisation mehrerer C9-Moleküle zur Bildung des C5b-9-Komplexes erfolgt. Abbildung mittels KEGG-Datenbank [36] erstellt.

Biomaterialien lösen die Komplementaktivierung wahrscheinlich über den klassischen und den alternativen Weg aus [39]. Das auf den Biomaterialien gebildete Kallikrein spaltet FXIIa und erzeugt β-FXIIa, was neben der Aktivierung durch Antikörper (AK), zur Einleitung des klassischen Weges führt. Des Weiteren kommt es zur Ablagerung von C3 und C5 auf Biomaterialien. Kallikrein aktiviert abgelagertes C3 und C5. Zudem wird C5 durch FIXa, FXa und Thrombin aktiviert [40]. Durch die Aktivierung entstehen C3a und C5a, die als starke Chemoattraktoren für Leukozyten dienen und dadurch ihre Anhaftung an der Oberfläche und ihre anschließende Aktivierung fördern [41].

1.3 Hämokompatibilität von Medizinprodukten am Beispiel der extrakorporalen Membranoxygenierung

Die Hämokompatibilität von Medizinprodukten hängt nicht nur von den Biomaterialien selbst ab, sondern auch von einer Reihe anderen Faktoren, wie z. B. den Einsatzbedingungen und dem Zustand des Patienten. In vielen Fällen besteht jedoch nur die Möglichkeit, die Blutverträglichkeit der Produkte zu regulieren in dem die Eigenschaften des Medizinproduktes verändert werden [42]. Dies ist besonders wichtig bei kardiovaskulären Medizinprodukten da es hier häufig zu vollständigem und langfristigem Blutkontakt kommt. Beispiele für kardiovaskuläre Medizinprodukte sind künstliche Herzklappen, Koronarstents oder endovaskuläre Transplantate. Eine besonders große Herausforderung für die Hämokompatibilität stellen extrakorporale Unterstützungssystem dar.

Die extrakorporale Membranoxygenierung (ECMO) wird in der Intensivmedizin bei Patienten mit schwerem Lungen- und Herzversagen eingesetzt, u. a. zur Unterstützung bei septischem Schock, Herz-Lungen-Stillstand und Spende nach Herztod sowie zur Zieltherapie und Überbrückung von Patienten mit chronischen Erkrankungen bis zur Transplantation oder Langzeitunterstützung [42, 43]. Nach dem Ausbruch der Coronavirus-Krankheit (COVID-19) im Jahr 2019 hat die ECMO noch mehr an Bedeutung gewonnen, da sie eine wichtige Rolle bei der Versorgung von kritischen COVID-19-Patienten spielte [44].

Obwohl vielen Patienten durch den Einsatz der ECMO geholfen werden kann, hat die ECMO immer noch ihre Grenzen, insbesondere die Morbidität und Mortalität sind in-

akzeptabel hoch. Auch die Aufrechterhaltung der extrakorporalen Perfusion ohne Blutungs- und Thrombosekomplikationen ist eine weitere Herausforderung der ECMO [45, 46]. Trotz intensiver Forschungsbemühungen bleibt die unzureichende Hämokompatibilität der verwendeten Materialien ein ungelöstes Problem. Dies spielt bei der ECMO eine besonders wichtige Rolle, da ein ECMO-System bis zu 30 Tage verwendet werden kann.

Die ECMO besteht aus Kanülen, Schläuchen, einer Pumpe, einem Wärmetauscher und einem Hohlfasermembran-Oxygenator. Das Herzstück und zugleich die kritischste Komponente der ECMO ist der Oxygenator. Mit 0,8 bis 2,5 m^2 stellt der Oxygenator die größte blutberührende Fläche während der ECMO dar. Die Schläuche bieten eine zusätzliche Oberfläche von 0,05–0,15 m^2 [47]. Die in Kapitel 1.2 beschrieben Blutreaktionen können zu einer Thrombusbildung führen [7]. Die Thrombenbildung führt zu einer Blockade des Oxygenators, was zu dessen Versagen führen kann. Darüber hinaus können sich Teile des Thrombus von der Oberfläche lösen, durch den Blutkreislauf wandern und sich in Gefäßen festsetzen, die lebenswichtige Organe mit Blut versorgen. Laut dem internationalen Bericht 2020 des ELSO-Registers (Extracorporeal Life Support Organization) liegt die Inzidenz der Thrombenbildung in Kreislaufkomponenten bei 5–30 %. Eine Thrombose im Oxygenator tritt bei etwa 10–16 % der Patienten auf, abhängig von der Art des Kreislaufs und dem Alter des Patienten [46].

Um eine Thrombose im ECMO-Kreislauf zu verhindern ist neben dem Einsatz von hämokompatiblen Materialien eine kontinuierliche systemische Antikoagulation z.B. mit fraktioniertem Heparin erforderlich. Heparin bindet an Antithrombin III (ATIII); der entstehende Komplex wirkt als unmittelbarer Inhibitor der Blutgerinnung. Er ist in der Lage, die Gerinnungsfaktoren FII, FIX, FX, FXI und FXII zu binden und damit deren Wirkung zu unterdrücken. Darüber hinaus hemmt der Heparin-Antithrombin-Komplex auch Kallikrein und die Wirkung des Membranangriffskomplexes des Komplementsystems [48]. Die Antikoagulation mit Heparin birgt jedoch auch die Gefahr einer heparininduzierten Thrombozytopenie (HIT) [48]. Des weiteren führt die systemische Antikoagulation zu einem erhöhten Blutungsrisiko und damit zu einem Ungleichgewicht zwischen Blutung und Thrombose [49]. Treten thrombotische Komplikationen auf, so werden diese häufig durch den Ersatz von Kreislaufkomponenten, zum Beispiel durch einen Oxygenator Wechsel, behandelt. Blutungskomplikationen werden in der Regel

durch die Verabreichung von Thrombozyten und Gerinnungsfaktoren und die Reduzierung oder Beendigung der systemischen Antikoagulation behandelt [50].

1.4 Verbesserung der Hämokompatibilität durch Beschichtungen

Im Allgemeinen gibt es zwei Hauptmechanismen für antithrombotische Oberflächenbeschichtungen, biopassive Beschichtungen und bioaktive Beschichtungen [51]. Biopassive Beschichtungen minimieren die Wechselwirkung zwischen Blut und fremden Oberflächen durch Unterdrückung der Proteinadsorption [50]. Bioaktive Beschichtungen wirken, indem sie Gerinnungsfaktoren, Blutplättchen oder andere an der Blutgerinnung beteiligte Faktoren gezielt hemmen. Oberflächeneigenschaften wie Benetzbarkeit, Ladung, Rauheit und Topografie können gezielt beeinflusst werden [51]. Biopassive Beschichtungen haben die längste Tradition und sind vor allem für Geräte mit langfristigem Blutkontakt notwendig. Hier werden sie auch als ergänzende Strategie eingesetzt, wenn die bioaktiven Modifikationen erschöpft sind [52]. Da bei bioaktiven Beschichtungen ein erhöhtes Risiko besteht, dass die Aktivität aufgrund von Sättigung, Verbrauch und Abbau abnimmt [53]. Ein prominentes Beispiel einer antithrombotischen Oberflächenbeschichtung ist die Heparin Beschichtung. Bereits 1963 berichteten Gott et al. über eine Heparinbeschichtung auf mit kolloidalem Graphit vorbehandelten Kunststoffen [54]. Um die Hämokompatibilität von Fremdoberflächen zu verbessern, versuchten Marcum und Rosenberg 1989 Heparansulfat zu imitieren, um antithrombotische Effekte zu erzielen. Zu diesem Zweck beschichteten sie Kunststoffoberflächen mit Heparin. Die erste kommerziell erhältliche Heparinbeschichtung wurde 1983 von Carmeda entwickelt [55]. Seitdem wurden mehrere neue Beschichtungen mit unterschiedlichen Bindungsmechanismen entwickelt und auf den Markt gebracht. Durch diese Beschichtungen konnte die Hemokompatibilität von ECMO Systemen und anderen Biomaterialien deutlich erhöht werden. Videm et al. zeigte, dass Heparinbeschichtungen die Komplementaktivierung um fast die Hälfte reduzieren können [56]. Auch andere Körperabwehrreaktionen können im Vergleich zu unbeschichteten Biomaterialien durch eine Heparinbeschichtung reduziert werden. Dazu gehören die aktivierung der Gerinnungskaskade, die Aktivierung von Granulozyten, Entzündung und pulmonale Komplikationen, Thrombozytenaktivierung, Störung der Homöostase, Blutverlust und zerebrale Schäden [57]. Die Vorteile von heparinbeschichteten Materialien

haben jedoch auch ihre Grenzen. Kovalent und ionisch gebundene Heparinbeschichtungen auf Biomaterialien verringerten zwar einige Auswirkungen der Entzündungsreaktion und Thrombusbildung, andere Komplikationen bleiben jedoch im Vergleich zu unbeschichteten Biomaterialien gleich [39]. Des Weiteren besteht eine Kontraindikation bei Patienten mit einer heparininduzierten Thrombozytopenie (HIT) [48].

Neben Heparinbeschichtungen gibt es weitere Ansätze der Oberflächenmodifkation. Eine Möglichkeit ist die Modifizierung der Oberfläche mit Polyethylenoxide, Sulfat- und Sulfonatgruppen, die zu einer hydrophilen und negativ geladen Oberfläche führt [58]. Eine weitere Möglichkeit ist die Reduzierung der Oberflächenspannung durch eine Beschichtung mit Derivaten aus Rizinusöl [59]. Auch Beschichtungen mit Phosphorylcholin sind möglich. Durch den Einsatz von Phosphorylcholin wird die modifizierte Oberfläche der Zellmembran ähnlicher und dadurch als weniger Fremd erkannt [60]. Weitere Möglichkeiten von Beschichtungen bestehen durch eine Passivierung der Oberfläche zum Beispiel durch Albumin [61] oder Silicone [62].

2 Zielsetzung

Durch den Einsatz von Biomaterialien wird die Funktion von geschädigten oder degenerierten Geweben und Organen ersetzt oder verbessert. Des Weiteren können Biomaterialien als Hilfsmittel zum Beispiel während einer Operation eingesetzt werden. Dadurch wird die Lebensqualität von vielen Patienten erheblich verbessert. Trotz vielen Fortschritten und Entwicklungen in diesem Bereich stellt die Hämokompatibilität dieser Produkte immer noch ein großes Problem dar. Es muss immer mit dem Risiko einer thrombotischen Reaktion oder einer initialen Immunreaktion gerechnet werden. Ausgelöst werden diese Reaktionen durch die Proteinadsorption auf den Biomaterialien. Umso genauer die Adsorptionsmuster auf den Biomaterialien verstanden werden, umso effizienter ist es möglich die Hämokompatibilität von Biomaterialien zu verbessern. Aus diesem Grund ist das Ziel dieser Arbeit die Adsorptionsmuster der Plasmaproteine genau zu untersuchen. Dazu sollen die derzeit verwendeten synthetischen Materialien von Membranoxygenatoren mit und ohne spezifische Beschichtungen verwendet werden. In einem der klinischen Anwendung angepassten Simulationsmodel sollen die Biomaterialien über einen Zeitraum von sechs Stunden mit Humanen Plasma bzw. Humanen Vollblut inkubiert werden. Mit Hilfe von genauen und empfindlicheren Proteomics-Technologien (z. B. Progenesis LC-MS) soll die Identifizierung von mehreren 1000 auf der Oberfläche adsorbierten Proteinen möglich sein. Eine andere Möglichkeit die Auswirkung von Biomaterialien auf die Abwehrreaktionen der Patienten besser zu verstehen ist das mit Biomaterialien inkubierte Blut genauer zu untersuchen. Hierfür soll, dass im Rahmen einer klinischen Studie bei Operationen mit einer Herz-Lungen-Maschine gewonnen Patientenblut auf verschiedene Biomarker wie zum Beispiel Gerinnungsfaktoren, Komplementfaktoren und Inflammatorische Marker wie Cytokine und Interleukine untersucht werden.

Die Untersuchung der Plasmaproteinadsorption auf den Biomaterialien sowie die Untersuchung des Verwendeten Humanen Vollblutes bzw. Plasmas bietet die Chance, komplexe Interaktionen auf Oberflächen aufzuklären und besser zu verstehen. Die so gewonnen Erkenntnisse sollen dazu in einem weiteren Schritt dieser Arbeit dafür verwendet eine neuartige hämokompatible Beschichtung für Biomaterialien zu entwickeln.

3 Ergebnisse:

3.1 Publikation I: Profiling of time-dependent human plasma protein adsorption on non-coated and heparin-coated oxygenator membranes

Katharina Große-Berkenbusch, Meltem Avci-Adali, Madeleine Arnold, Linda Cahalan, Patrick Cahalan, Ana Velic, Boris Maček, Christian Schlensak, Hans Peter Wendel, Sandra Stoppelkamp

Biomaterials Advances

Volume 139, August 2022, 213014

Zusammenfassung:

Patienten mit schweren Lungenerkrankungen sind in hohem Maße auf Lungenersatzsysteme angewiesen. Die Anwendung ist jedoch zeitlich begrenzt. Die limitierenden Faktoren sind hier die starken Abwehrreaktionen des Körpers (z.B. Gerinnung, Komplementsystem, Entzündung und Zellaktivierung). Durch umfassende massenspektrometrische Analysen der desorbierten Proteine konnte in dieser Studie erstmals Bindungsprofile von über 500 Proteinen über einen Zeitraum von sechs Stunden auf unbeschichteten und Heparin beschichteten PMP-Hohlfasermembranen identifiziert werden. Hierbei zeigte sich, dass die Plasmaproteinschicht über die Zeit auf der beschichteten Membran stabiler als auf unbeschichteten Membran war. Zusätzlich war die Gesamtmenge der einzelnen gemessenen Proteine auf der unbeschichteten Membran höher, mit Ausnahme von Proteinen mit einer spezifischen Heparin-Bindungsstelle. Die Fokussierung auf die wichtigsten Pathways zeigte, dass fast alle Gerinnungsfaktoren in höheren Mengen an die nicht beschichteten Membranen gebunden wurden. Darüber hinaus konnten gezeigt werden, dass die Initiatorproteine des Komplementsystems stärker an die heparinisierten Membranen gebunden haben, wohingegen die späteren Proteine des Komplementsystem stärker an die nicht-beschichteten Membranen gebunden haben. Durch das Durchführen dieser Studie konnte ein umfassender Einblick auf die Adsorption von Plasmaproteinen auf Oxygenatormembranen im Laufe der Zeit sowie auf den darauffolgenden Ablauf verschiedener Abwehrreaktionen gewonnen werden. Dadurch ist es möglich die Prozesse auf den Membranen besser zu verstehen und neue spezifische Oberflächenmodifikationen zu entwickeln.

3.2 Publikation II: Comparative study of flow rate- and material-dependent human plasma protein adsorption on oxygenator membranes and heat exchanger materials

Katharina Große-Berkenbusch, Meltem Avci-Adali, Patrick Cahalan, Linda Cahalan, Ana Velic, Boris Maček, Christian Schlensak, Hans Peter Wendel, Sandra Stoppelkamp

Frontiers in Cardiovascular Medicine

2025, 12. Jg., S. 1578538.

Zusammenfassung:

Diese Studie baut auf den Ergebnissen der ersten Veröffentlichung auf und erweitert diese, indem sie zusätzlich den Einfluss verschiedener Heparin beschichteten Membranarten sowie den Zusammenhang zwischen unterschiedlichen Blutflussraten und der Proteinadsorption untersucht. Zu diesem Zweck wurden miniaturisierte extrakorporale Kreisläufe mit Heparin beschichteten Gas- (PMP) und Wärmeaustausch- (PET) Hohlfasermembranen bei hohen und niedrigen Flussraten untersucht. Die Hämokompatibilität sowie die Adsorption von Plasmaproteinen wurden über einen Zeitraum von einer Minute bis sechs Stunden mittels Massenspektrometrie (MS) analysiert. Auf den Membranen wurden etwa 150 bis 200 verschiedene Proteine nachgewiesen, wobei die zehn häufigsten Proteine nur geringe Variationen aufwiesen. Die Proteinadsorption an beiden Membrantypen unterschied sich nur geringfügig, jedoch verringerte sich bei niedriger Flussrate der Unterschied in der Proteinadsorption zwischen den beiden Membranarten signifikant, was zu einer deutlich höheren Anhaftung der inhibitorischen Proteine C1-INH und α1-AT führte. Bei höherer Flussrate adsorbierten gerinnungsassoziierte Proteine signifikant stärker an der PET-Membran, während auf der PMP-Membran Proteine, die mit der Komplementaktivierung in Verbindung stehen, stärker adsorbiert wurden. Unsere Ergebnisse unterstreichen die Bedeutung der Analyse aller Kreislaufkomponenten, um die Aktivierung von Blutkomponenten während der ECMO zu verstehen. Der Hauptfaktor für die erhöhte Proteinadsorption und Aktivierung von Blutbestandteilen war die erhöhte Flussrate. Daher sollte die Anpassung der Flussrate idealerweise darauf abzielen, eine optimale Oxygenierung von etwa 80 % zu erreichen und gleichzeitig die Proteinadsorption sowie die Aktivierung von Blutbestandteilen während der ECMO zu minimieren.

3.3 Publikation III: A Novel C1-Esterase Inhibitor Oxygenator Coating Prevents FXII Activation in Human Blood

Katharina Gerling, Sabrina Ölschläger, Meltem Avci-Adali, Bernd Neumann, Ernst Schweizer, Christian Schlensak, Hans Peter Wendel,
Sandra Stoppelkamp

biomolecules - *MDPI*

Biomolecules 2020, 10(7), 1042

Zusammenfassung:

Die begrenzte Hämokompatibilität der derzeit verwendeten Oxygenatormembranen verhindert den dauerhaften Einsatz von Lungenersatzsystemen am Patienten. Durch die Untersuchungen von Adsorptionsmuster in der vorherigen beschriebenen Studie zeigte sich, dass der Einsatz von Inhibitoren des Komplementsystems ein vielversprechender Ansatz für neuartige Beschichtungen sein kann. Auf Grund dieser Erkenntnisse wurde in dieser Veröffentlichung eine Beschichtung mit dem Komplementinhibitor C1-INH entwickelt. Der C1-INH wurde ausgewählt, da er zusätzlich zur Komplementinhibierung auch noch positive Auswirkungen auf die Gerinnungskaskade, den Fibrinabbau und Entzündungsreaktionen hat. Kovalent beschichtetes Heparin, die zurzeit meistangewendete Beschichtung, diente als Kontrolle. Zusätzlich wurde eine Kombination aus beiden Beschichtungen (C1-INH und Heparin) entwickelt. Die Beschichtungen wurden durch dynamische Inkubation mit frisch abgenommenem menschlichem Vollblut auf ihre Hämokompatibilität getestet. Die Analyse verschiedener Blut- und Plasmaparameter ergab, dass C1-INH-haltige Beschichtungen die FXIIa-Aktivität im Vergleich zur Heparin Beschichtung deutlich reduzieren konnte. Dadurch kann die Gerinnungskaskade durch die C1-INH Beschichtung schon zu einem sehr frühen Zeitpunkt gestoppt werden, was zu einen erheblichen Vorteil gegenüber der Heparin Beschichtung führt. Die kombinierte C1-INH-/Heparin-zeigte auf den Rasterelektronenmikroskopischen Aufnahmen eine eindeutig verringerte Adhäsion von Monozyten und Thrombozyten sowie eine verringerte Bildung von Fibrinnetzwerken. So konnte in dieser Studie erstmals gezeigt werden, dass durch die kovalente Beschichtung des Komplementinhibitor C1-INH auf Biomaterialien die Hämokompatibilität signifikant verbessert werden kann, auch im Vergleich zu den Standardmäßig eingesetzten Heparin Beschichtungen.

3.4 Publikation IV: Synthetic Material Abdominal Swabs Reduce Activation of Platelets and Leukocytes Compared to Cotton Materials

Katharina Gerling*, Lisa Maria Herrmann*, Christoph Salewski, Melanie Wolf, Pia-Müllerbader, Dorothea Siegel-Axel, Hans-Peter Wendel, Christian Schlensak, Meltem Avci-Adali und Sandra Stoppelkamp

* *gleichermaßen beigetragen*

biomolecules - *MDPI*

Biomolecules 2021, 11(7), 1023

Zusammenfassung:

Der Schwerpunkt der vorangegangenen Publikationen lag bei der Langzeitanwendung der extrakorporalen Membran Oxygenierung. Eine weitere Anwendung der extrakorporale Membran Oxygenierung ist der Einsatz während Operationen mit kardiopulmonalem Bypass (CPB). Trotz der kürzeren Anwendungszeiten ist auch hier eine Ausreichende Hämokompatibilität von großer Bedeutung. Erschwerend kommt noch der Einsatz von weiteren Biomaterialien zum Beispiel Bauchtüchern hinzu. Bauchtücher werden verwendet, um Organe zurückzuhalten und Blut oder andere Körperflüssigkeiten aufzunehmen. Bei CPB-Operationen kann sich ein hohes Blutvolumen in der Brusthöhle ansammeln, dass schnell über die Herz-Lungen-Maschine (HLM) retransfundiert wird. Dies kann zur aktivierung von Blutzellen und Plasmaproteine führen. Um diese Effekte genau zu untersuchen, wurde in dieser Studie Blut von Patienten während einer CPB-Operation auf entzündliche und gerinnungsassoziierte Aktivierung nach Kontakt mit der HLM und nach Kontakt mit Bauchtüchern aus Baumwolle oder synthetischen Fasern untersucht. Der Kontakt mit Baumwolle führte zu einer signifikanten Erhöhung der Thrombozyten- und Neutrophilen-Aktivierung im Vergleich zu synthetischen Bauchtüchern. Die entzündlichen Zytokine, IL 1β und IL6, waren in der Baumwollgruppe ebenfalls signifikant höher als in der synthetischen Patientengruppe. Diese Daten zeigten zum ersten Mal, dass Baumwollmaterialien trotz einer hohen Antikoagulation, Thrombozyten und Leukozyten aktivieren können und dass diese Aktivierung durch synthetischen Materialien signifikant reduziert werden kann. Dies zeigt, dass der Standardmäßige Einsatz von Bauchtüchern aus Baumwolle überdacht werden sollte, und besser auf synthetische Materialien umgestellt werden sollte.

4 Diskussion:

4.1 Plasmaproteinadsorption über die Zeit

Um die Proteinadsorption über die Zeit zu charakterisieren wurden Heparin beschichtete und unbeschichtete PMP-Oxygenatormembranen mit Blut inkubiert. Für die Heparin Beschichtung wurde ein standardisiertes Herstellungsverfahren mit endpunktgebundenem, biologisch aktivem Heparin verwendet. Die Funktionalität der Beschichtung konnte durch eine verbesserte Hämokompatibilität gezeigt werden.

Nach der Blutinkubation erfolgte eine MS Analyse der gebundenen Plasmaproteine. Die Adsorption von Plasmaproteinen erfolgte direkt unmittelbar nach Blutkontakt, so dass innerhalb der ersten Minute viele verschiedene Proteine auf die Membranen gelangten. Außerdem wurde eine Veränderung in der Schichtzusammensetzung im Laufe der Zeit beobachtet. Die Veränderung der Proteinschicht in den ersten Sekunden ist für die wichtigsten Plasmaproteine bekannt. Zunächst adsorbieren kleine, hochkonzentrierte und schnell diffundierende Proteine wie Albumin. Diese werden jedoch in sehr kurzer Zeit durch größere, stärker affine Proteine wie Fibrinogen oder Immunglobuline verdrängt, was zu einer dynamischen Umstrukturierung der Proteinschicht führt. [25].

Bis zum jetzigen Zeitpunkt gab es keine Studien über die weitere Entwicklung der Plasmaproteinschicht im Laufe der Zeit. Diese Arbeit zeigt zum ersten Mal über 500 zeitabhängige Proteinbindungsprofile auf Biomaterialien innerhalb von sechs Stunden.

Werden die Proteinbindungsprofile nach der Plasmainkubation im Zeitverlauf betrachtet, so fällt auf, dass die Proteine auf der Heparin-beschichteten und auf der unbeschichteten Membranen unterschiedlich schnell gebunden haben. Dies deutet auf unterschiedliche Adsorptionsmechanismen auf den verschiedenen Oberflächen hin. Besonders auffällig ist, dass ein erheblicher Anteil der Proteine auf der nicht beschichteten Membran im Laufe der Zeit abnahm (reversible Bindung). Ein Phänomen, das auf der Heparin-beschichteten Membran fast nicht auftrat. Auch Weber et al. entdeckten unterschiedliche Bindungsmechanismen zwischen beschichteten und unbeschichteten PVC-Schläuchen, doch konnten in ihren Experimenten keine mit der Zeit abnehmenden Proteinkonzentrationen festgestellt werden [63]. Im Gegensatz zu den aktuellen anspruchsvollen MS-Analysen verwendeten die Autoren damals SDS-PAGE und

spezifische Antikörper, um ausgewählte desorbierte Proteine nachzuweisen. Insgesamt waren die Zeitspanne (120 min) und die Anzahl mit nur zwölf untersuchten Proteine viel geringer [63]. Die vorübergehende Adsorption von Plasmaproteinen in den ersten Sekunden, insbesondere für Fibrinogen, ist als Vroman-Effekt bekannt [25]. Dieser tritt jedoch unmittelbar nach dem Blutkontakt auf und konnte daher in unserer Studie, bei der der erste Zeitpunkt bei einer Minute lag, nicht direkt gezeigt werden.

Hervorzuheben ist, dass Fibrinogen zu allen Zeitpunkten das am häufigsten vorkommende Protein auf der nicht beschichteten Membran war. Auch auf der beschichteten Membran war Fibrinogen nach 60 und 360 Minuten das am häufigsten vorkommende Protein. Studien zeigten, dass Thrombin in der Lage ist an das in hoher Anzahl adsorbierte Fibrinogen auf der Oberfläche zu binden. Dies führt dazu das Thrombin aktiv bleibt und nicht durch das systemisch zugeführte Heparin neutralisiert werden kann. Infolgedessen bleibt eine hohe Thrombinaktivität auf der Oberfläche bestehen [64]. Dies könnte ein Grund der verbesserten Hämokompatibilität der Heparin beschichteten Oxygenatormembranen sein.

Sowohl bei der unbeschichteten als auch bei der Heparin-beschichteten Membran wurden bei allen Zeitpunkten Fibrinogen, Albumin oder Apolipoproteine am häufigsten nachgewiesen. Auch die Literatur beschreibt das diese Proteine unabhängig von der Oberflächenbeschaffenheit am häufigsten binden [23]. Das Vorhandensein von Albumin wird im Allgemeinen als wünschenswert beschrieben, da angenommen wird, dass Thrombozytenrezeptoren aufgrund fehlender Aminosäuresequenzen nicht binden können, was zu einer Resistenz gegenüber der Thrombozytenadhäsion führt [65]. Sivaraman und Latour zeigten jedoch, dass Thrombozyten durch eine Konformationänderung, die zur Freilegung der Aminosäuresequenz von Albumin führt, in der Lage sind an Albumin zu binden [66]. In dieser Arbeit konnten keine Unterschiede in der Albumin Bindung zwischen der beschichteten und der unbeschichteten Membran festgestellt werden. Das Albumin scheint also nicht zur verbesserten Hämokompatibilität der Heparin Beschichtung beizutragen. Es ist auch unklar, ob der Schutz durch Albumin über einen längeren Zeitraum anhält, da die Literatur davon ausgeht, dass Albumin im Laufe der Zeit durch andere Blutbestandteilen ausgetauscht wird [11]. In dieser Arbeit wurde auf der nicht beschichteten Membran eine Albumin Abnahme im Laufe der Zeit beobachtet, was die Hypothese des Albumin Austausches durch andere Blutbestandteile unterstützt.

Unsere Ergebnisse zeigen, dass eine Veränderung der Proteinschicht nicht nur in der Startphase auftritt, sondern über den gesamten Zeitraum von sechs Stunden dynamisch ist. Brash et al. wiesen bereits darauf hin, dass die Wechselwirkungen zwischen Proteinen und Oberflächen im Blutkontakt dynamisch sind und es unwahrscheinlich erscheint, dass die Schicht ihre Zusammensetzung über lange Zeiträume beibehält [11]. Diese Hypothese kann durch unsere Ergebnisse eindeutig unterstützt werden.

4.2 Einfluss der Plasmaproteinadsorption auf die Aktivierung der Gerinnungskaskade

Mit den umfassenden Daten aus der MS-Analyse konnte das Verhalten des Gerinnungssystems auf unbeschichteten und Heparin-beschichteten PMP-Membranen eingehend untersucht werden. Die plasmatische Gerinnung wird durch eine komplexe Kaskade von Zymogen-Enzym-Umwandlungen in Gang gesetzt, die miteinander verknüpft sind und sich selbst verstärken, wobei sie letztlich zur Bildung von Thrombin führen. Am Ende dieser Kaskade katalysiert Thrombin die Umwandlung von Fibrinogen in Fibrinmonomere, die sich zu einem oligomeren Netzwerk verbinden und so die Plasmakoagulation auslösen.[67].

Zu den frühen Proteinen der Blutgerinnung gehören FXII, Präkallikrein, HMWK und FXI. Diese Proteine reagieren auf das Vorhandensein von Oberflächen mit negativer Ladung, wie sie beispielsweise an Biomaterialien oder beschädigten Blutgefäßen zu finden sind. [68, 69] [70]. Die Aktivierung FXII, Präkallikrein, HMWK und FXI erfolgt in den ersten Sekunden nach Oberflächenkontakt, wobei die Oberflächenbeschaffenheit eine entscheidende Rolle spielt.

In dieser Arbeit konnte bereits nach einer Minute (erster Messzeitpunkt) eine signifikant höhere Menge an FXII, Präkallikrein, HMWK und FXI auf der unbeschichteten Membranen gezeigt werden. FXI konnte jedoch nach 10 Minuten nicht mehr nachgewiesen werden. Eine deutlich niedrigere Proteinbindung zeigte sich auf der Heparin-beschichteten Membran. Eine Ausnahme bildete FXI, das aufgrund seiner Heparin-Bindungsstelle [71] stark an die beschichtete Membran adsorbierte. Das Abfangen von FXI durch Heparin senkt den FXI-Spiegel im Blut, was zu einer geringeren Aktivierung von FXI führt. Dies könnte eine Erklärung für die kaum vorhandenen FIX-Bindung auf der beschichteten Membran sein.

Gorbet et al. formulierten jedoch die Ansicht, dass die Aktivierung von FXII, Präkallikrein, HMWK und FXI für die Auslösung der Gerinnung durch Biomaterialien nur eine untergeordnete Rolle spielt [7]. Einige Studien stützen diese Hypothese, indem sie zeigen, dass FXII an Biomaterialien wie Gefäßimplantate [72] und Hämodialysatoren [73] adsorbiert wird, jedoch keine Aktivierung von FXII nachgewiesen werden konnte [74].

In den hier angewandten Analysen ist eine Unterscheidung zwischen der aktivierten und inaktiven Form von FXII nicht möglich. Allerdings können Rückschlüsse auf die Aktivierung der Kaskade durch die Bindungsprofile nachfolgender Faktoren gezogen werden. So könnte die fehlende Bindung von FXI auf der unbeschichteten Membran auch auf inaktives FXII hinweisen. Dennoch gibt es Berichte, die von einer In-vitro-Aktivierung von FXII und Kallikrein durch Biomaterialien berichten [75-77] ohne jedoch eine signifikante Aktivierung der Gerinnung nachzuweisen. Die Bindungsprofile von FXII, Präkallikrein, HMWK und FXI stimmten darüberhinaus nicht mit denen späterer Komponenten wie Thrombin überein. Es gibt Hinweise darauf, dass Leukozyten für die Aktivierung der Gerinnungskaskade erforderlich sind [78]. [79]. Auch in vivo hat sich gezeigt, dass die Aktivierung durch FXII, Präkallikrein, HMWK und FXI eher eine untergeordnete Rolle spielt [80].

Nach der Aktivierung von FXII, Präkallikrein, HMWK und FXI erfolgt die Gerinnung nicht mehr direkt an der Oberfläche [81], dies erschwert die Interpretation der nachfolgenden Gerinnungsfaktoren. Dennoch konnten Unterschiede in der Bindung zwischen der Heparin-beschichteten und der unbeschichteten Membran beobachtet werden. Die späteren Komponenten Plasmin, FX und Thrombin zeigten untereinander ähnliche Bindungsprofile. Alle drei Proteine banden im Laufe der Zeit konstant an die unbeschichtete Membran und nahmen im Laufe der Zeit auf der beschichteten Membran in unserer Studie zu. Allerdings unterschieden sich die Bindungsmengen von FX und Plasmin nur in der frühen Startphase, nach einer Minute und für Thrombin überhaupt nicht. Aktiviertes FX wandelt zusammen mit aktiviertem FV Prothrombin in aktives Thrombin um [82]. FX und Thrombin sind also direkt miteinander verbunden. Das gleiche Bindungsverhalten deutet darauf hin, dass die Bindung nicht zufällig ist und in direktem Zusammenhang mit einer laufenden Gerinnungskaskade steht. Das betroffene FV passt jedoch nicht in dieses Muster. Das Bindungsverhalten von FV weicht jedoch von diesem Muster ab. Obwohl FV konstant in höheren Mengen an die unbe-

schichtete Membran bindet, konnte dort keine erhöhte Menge an Thrombin nachgewiesen werden. Anti-Thrombin III bindet aufgrund seiner hohen Affinität für Heparin stärker an die beschichtete Membran. Die Bindung von Proteinen, die die Gerinnung hemmen, wie Antithrombin, wird im Allgemeinen als positiv angesehen [83].

4.3 Einfluss der Plasmaproteinadsorption auf die Aktivierung der Komplementkaskade

Es wird angenommen, dass der anfänglich gebildete Proteinfilm aus einer Monoschicht besteht, auf der die Komplementaktivierung stattfindet [84, 85]. Der Lektinweg des Komplementsystems wird durch lösliche Mustererkennungsmoleküle (Pattern Recognition Molecules, PRMs) aktiviert, die an spezifische Kohlenhydratstrukturen binden, welche auf fremden Mikroorganismen oder veränderten Wirtszellen vorkommen. Zu den wichtigsten PRMs gehören die Ficoline (Ficolin-1, -2 und -3) sowie das Mannose-bindende Lektin (MBL). In dieser Arbeit konnten weder Ficolin-1 noch MBL auf den beschichteten oder unbeschichteten Membranen nachgewiesen werden. Da Ficoline häufiger im Plasma vorkommen als MBL [86] sind sie wahrscheinlich von größerer Bedeutung. Sowohl die Ficoline 2 als auch 3 banden zu mehreren Zeitpunkten signifikant mehr an die beschichtete Membran als an die unbeschichtete Membran. Hein et al. beobachteten einen ähnlichen Effekt für Ficolin-2, indem sie die PRM-Spiegel nach einer kardiopulmonalen Bypass-Behandlung mit zwei verschiedenen beschichteten Systemen verglichen [87]. In ihrer Studie wies das Blut in dem mit Heparin beschichteten System signifikant niedrigere Ficolin-2-Spiegel auf als das Blut in dem System ohne Heparin. Hein et al. erklärten dies mit der spezifischen Bindung von Ficolin-2 an Heparin [87]. Die erhöhte Bindung von Ficolinen und der daraus resultierende niedrigere Plasmaspiegel könnten zu einer erhöhten postoperativen Infektionsanfälligkeit nach extrakorporaler Zirkulation führen. Sobald PRMs an einen Liganden gebunden sind, wird die Kaskade durch Aktivierung von MBL/Ficolin-assoziierten Serinproteasen (MASPs) eingeleitet. Sowohl MASP1 als auch MASP2 wurden in dieser Arbeithäufiger auf der Heparin-beschichteten Membran nachgewiesen. Dies deutet darauf hin, dass die Eigenschaften von Ficolin auch nach der Bindung an Heparin erhalten bleiben.

Der klassische Komplementweg weist strukturelle Ähnlichkeiten zum Lektinweg auf und wird durch den C1-Komplex aktiviert, der als Pathogen-Sensormolekül fungiert.

Der C1-Komplex kann direkt mit Pathogenoberflächen, Antikörpern oder mit auf der Oberfläche abgelagertem C-reaktivem Protein (CRP) interagieren. Der C1-Komplex besteht aus einer großen Untereinheit, C1q, und zwei Serinproteasen, C1r und C1s. C1r und C1s bilden zusammen Tetramere, die sich in die Arme von C1q falten, wobei ein Teil des C1r:C1s-Komplexes außerhalb von C1q liegt. C1q zeigte eine signifikant häufigere Bindung an die Heparin-beschichtete Membran, was auf die hohe Bindungsaffinität von C1q zu Heparin hinweist. Auf unbeschichteten Membranen scheint C1q dagegen vorwiegend an zuvor gebundenes IgG zu binden. Eine ähnliche Beobachtung wurde von Nilsson et al. im Jahr 1993 gemacht, als sie die Wirkung von Heparin-beschichtetem Polystyrol auf das Komplementsystem untersuchten [85]. Auch in dieser Studie konnte eine erhöhte Bindung von C1r und C1s sowie eine erhöhte Bindung des C1-Esterase-Inhibitors auf der Heparin-beschichteten Membran beobachtet werden. Ähnlich wie beim Lektinweg ist dies ein starkes Indiz dafür, dass die Eigenschaften von C1q nach der Bindung erhalten bleiben und eine Aktivierung des klassischen Weges über eine direkte Bindung von C1q und Heparin möglich wäre. Betrachtet man jedoch die weiteren Komponenten des Weges, so erscheint dies nicht sehr wahrscheinlich. Die Erkennungsfunktion von C1 befindet sich in den sechs globulären Köpfen von C1q. Sobald zwei oder mehr dieser Köpfe mit einem Liganden interagieren, wird die autokatalytische Enzymaktivität von C1r stimuliert. Dies führt zur Abspaltung und Aktivierung des assoziierten C1s-Moleküls. Das aktivierte C1s-Molekül wirkt auf C4 und C2. Das dabei entstehende C4b bindet sich wie beim Lektinweg kovalent an die Oberfläche des Erregers. Außerdem bindet C4b an C2, das von C1s gespalten wird, um die Serinprotease C2a zu bilden. Auf diese Weise entsteht die aktive C3-Konvertase C4b2a des klassischen und des Lektin-Wegs. C2 wurde in dieser Arbeit nur sporadisch und in sehr geringen Mengen auf den Membranen nachgewiesen (auf der Heparin beschichteten Membran nur nach 5 und nach 30 Minuten). Auf der nicht beschichteten Membran war die C2-Bindung nach 10 Minuten deutlich höher. Darüber hinaus verhält sich die C4-Bindung komplementär zu den Mustererkennungsmolekülen und bindet auf der nicht beschichteten Membran stärker als auf der Heparin-beschichteten Membran. Die Aktivierungsereignisse des Lektin- und des klassischen Weges finden an der Erregeroberfläche statt. Dies wird hauptsächlich durch die kovalente Bindung von C4b an die Erregeroberfläche erreicht. Im Gegensatz dazu deutet die verstärkte Bindung von C4 an die nicht beschichtete Membran auf eine stärkere

Aktivierung des klassischen und des Lektinwegs durch die nicht beschichtete Membran hin, trotz der anfänglichen Befunde einer verstärkten Ficolin- und C1-Adsorption an die Heparin-beschichtete Membran. Dieses Ergebnis weicht von der Erklärung von Nilsson et al. ab, die eine verstärkte Aktivierung des klassischen Weges durch die erhöhte Bindung von C1q annahmen. Sie erklärten die dennoch reduzierte Komplementaktivität, d.h. die geringere C3-Bindung an die heparinmodifizierte Oberfläche, mit der Verhinderung der Aktivierung des alternativen Weges. Auch wenn die erhöhte Bindung von Ficolin und C1q nicht zu einer verstärkten Aktivierung des Lektin- und des klassischen Weges führt, kann sich dieser Effekt dennoch negativ auf die Patienten auswirken. Da durch die erhöhte Bindung die entsprechenden Mustererkennungsmoleküle im Plasma fehlen, könnten mögliche Infektionen schlechter erkannt werden.

Da auf den Heparin-beschichteten Membranenim Vergleich zur unbeschichteten Membran kein Anstieg von C2 zu beobachten war, ist es unwahrscheinlich, dass mehr funktionelles C4b2a gebildet wurde und die Aktivierung über den klassischen oder Lektin-Weg erfolgte. Unsere Ergebnisse legen daher nahe, dass der Hauptauslöser für die Aktivierung des Komplementsystems der alternative Weg ist. Bei diesem Weg wird C3 spontan zu C3(H2O) hydrolysiert (der "Tick-over"-Mechanismus), was durch FB, FD und Properdin verstärkt wird. Die durch den alternativen Weg produzierte C3-Konvertase kann sich selbst reproduzieren, indem sie C3b produziert. Das bedeutet, dass der alternative Weg als Verstärkerschleife fungieren und die C3b-Produktion schnell steigern kann, sobald einige C3b-Moleküle gebildet worden sind [88]. Ausgelöst wird dies durch Fremdoberflächen, die keine ausreichende Down-Regulation der Konvertase bewirken [89]. Kürzlich fanden Riedel et al. auch Hinweise darauf, dass der alternative Weg des Komplementsystems durch den "Tick-Over"-Mechanismus der spontanen C3-Aktivierung eine wichtige Rolle beim Fouling auf Oberflächen spielt, die mit Poly(2-hydroxyethylmethacrylat)-Polymerbürsten beschichtet sind [90]. Antifouling-Polymerbürsten unterdrücken das Fouling meist erfolgreich, aber einige Beschichtungen zeigen eine extrem hohe Variabilität des Foulings durch verschiedene Spender, was wahrscheinlich auf die Aktivierung des Komplementsystems zurückzuführen ist [90]. Die wichtige Rolle der Verstärkung durch den alternativen Weg spiegelt sich in unseren Ergebnissen auch in der Tatsache wider, dass die C3-Bindung auf der beschichteten Membran nur zu den späten Zeitpunkten (90 und 360 Minuten) signifikant geringer war als auf der unbeschichteten Membran.

Alle drei Wege des Komplementsystems kulminieren in der Bildung des Membranangriffskomplexes. In Übereinstimmung mit der erhöhten Bindung der Komponenten des Membranangriffskomplexes an die PMP-Membran wurde in dieser Arbeit ein zeitabhängiger Anstieg von sC5b-9 im Blut beobachtet. Dies deutet auf eine Initiierung der Komplement Aktivierung mit anschließender Bindung der späten Komplementproteine an die Gasaustauschmembran hin. Trotz umfangreicher Forschungsarbeiten gibt es in der Literatur immer noch keinen klaren Konsens darüber, welche(s) Protein(e) die Komplementaktivierung auf Biomaterialien auslösen. Gebundenes IgG, C1q und C4 wurden als Auslöser diskutiert [89, 91, 92]. Die Ergebnisse dieser Arbeit legen nahe, dass C1q nicht der Hauptauslöser der Komplementkaskade auf Biomaterialien ist. C1q bindet signifikant häufiger an die Heparin beschichtete Membran, obwohl die Heparin Beschichtung die Aktivierung des Komplementsystems reduziert [56].

Die Komplementaktivierung unterliegt einer strengen Kontrolle durch mehrere Regulatoren, darunter der Flüssigphasenfaktor H (FH) und das C4-Bindungsprotein (C4BP), die die C3-Konvertase des alternativen, des klassischen und des Lektin- Wegs hemmen. Die Kontrolle der C3-Konvertasen erfolgt dadurch, dass die Proteine den Zerfall der Konvertasen erhöhen und/oder als Kofaktoren für die Flüssigphasenprotease Faktor I wirken. FI spaltet das abgelagerte C3b und C4b zu iC3b und iC4b und unterbricht damit die weitere Komplementaktivierung. Alle diese Regulatoren (FH, C4BP und FI) nahmen in dieser Arbeit überraschenderweise im Laufe der Zeit auf den nicht beschichteten Membranen deutlich ab, während C4BP auf der beschichteten Membran konstant blieb. Engberg et al. wiesen nach, dass gebundenes C4BP auf der Biomaterialoberfläche in der Lage ist, die Komplementaktivierung über den klassischen Weg zu hemmen [93]. C4BP besteht aus sieben identischen α-Ketten, die jeweils in der Lage sind, C4b zu binden. Durch diese Bindung wird die Spaltung von C4b durch Faktor I zu iC4b erleichtert, was zur Regulation der Komplementaktivierung beiträgt. Dies ist der Grund, warum C4BP nach der Bindung an ein Biomaterial einen wesentlichen Teil seiner Co-Faktor-Funktion beibehält [94]. Daher kann die gezeigte Abnahme der C4BP-Menge auf den nicht beschichteten Membranen im Laufe der Zeit durchaus eine verstärkende Wirkung auf die Komplementaktivierung haben. Die C4BP-Bindung ist eine mögliche Erklärung für das Fehlen der C2-Bindung, da C2 durch C4BP verdrängt wird [95]. Im Gegensatz dazu hat FH eine einkettige Struktur, die mehrere Bindungsstellen für C3b aufweist. Alle Bindungsstellen müssen C3b binden, um einen effizienten Abbau zu iC3b zu ermöglichen. In der Literatur konnte gezeigt werden, dass die

Kofaktoraktivität verloren geht, wenn Faktor H in einer denaturierten Konformation gebunden ist [84, 93]. Darüber hinaus verfügt FH über mehrere Heparin-Bindungsstellen mit einer hohen Affinität für Heparin [96, 97]. Die in dieser Arbeit gemessenen FH-Bindungen auf der beschichteten Membran sind daher wahrscheinlich eher auf die Bindung an Heparin als an C3b zurückzuführen. Diese Annahme wird durch das kaum vorhandene FI auf der beschichteten Membran unterstützt. Aufgrund der fehlenden C3b-Bindung ist kein FI an FH gebunden. C1-INH ist ein weiterer Regulator des Komplementsystems. In dieser Arbeit konnte bei einer erhöhten C1-Bindung auf der beschichteten Membran auch teilweise eine erhöhte C1-INH-Bindung festgestellt werden. Die Bindung von C1-INH an C1, führt zur Hemmung der Serinproteasen C1r und C1s, was zu einer Verringerung der Komplementaktivierung führt. Des Weiteren führt die kovalente Bindung von C1-INH an C1 zu einer dauerhaften Inaktivierung des C1-Moleküls.

4.4 Einfluss weiterer Komponenten und Parameter der ECMO auf die Hämokompatibilität

Zusätzlich zu den bisher diskutierten Vergleichen zwischen beschichteten und unbeschichteten PMP-Membranen wurden in dieser Arbeit auch der Einfluss verschiedener Heparin-beschichteter Membrantypen (PMP-Gasaustauschmembran; PET-Wärmetauschmembran) sowie der Zusammenhang zwischen unterschiedlichen Blutflussraten und der Proteinadsorption untersucht, um ein tiefergehendes Verständnis der Plasmaproteinadsorption und ihrer Auswirkungen auf die Körperabwehrreaktionen zu gewinnen.

Die Ergebnisse zeigten, dass die Gesamtmenge der Proteine unter beiden Flussraten (0.2 l/min und 1.0 l/min) und auf beiden Membrantypen vergleichbar war. Allerdings war die Anzahl der unterschiedlichen Proteine insbesondere auf PMP-Membranen bei hoher Flussrate über die Zeit am höchsten. Der Vergleich zwischen heparinbeschichteten PMP- und PET-Membranen verdeutlichte zudem, dass höhere Flussraten die Adsorption verschiedener Proteine auf beiden Membrantypen erhöhten. Zu den zehn häufigsten Proteinen unter allen Bedingungen zählten Apolipoprotein B (APOB), Albumin, ATIII, Fibrinogen gamma chain (FGG), Fibrinogen alpha chain (FGA), Fibrinogen beta chain (FGB), Apolipoprotein E (APOE) und Fibronektin, was teilweise mit früheren Studien übereinstimmt. [11]. Der Unterschied in der Häufigkeit wurde jedoch

durch die Heparinisierung der Membran beeinflusst, da viele dieser Proteine Heparin-Bindungsstellen besitzen (z. B. APOB, APOE, Fibronektion, Ficolin-2 und ATIII). Interessanterweise wurde in unserer Studie Albumin, obwohl es keine Heparin-Bindungsstelle besitzt, auf allen Membranen nachgewiesen, während Transferrin nur sporadisch unter den ersten 10 Proteinen auftauchte. Andere Proteine mit Heparin-Bindungsstellen und hoher Blutkonzentration wie SERPING1 wurden erst unter den ersten 50-100 detektierten Proteinen gefunden.

Obwohl in anderen Studien ein Displacement-Effekt von Fibrinogen durch HMWK und HDL beschrieben wurde [11], konnte in unserer Untersuchung über 6 Stunden hinweg kein Displacement-Effekt nachgewiesen werden. Bei höheren Flussraten war die Adsorption von Proteinen der Koagulationskaskade (PMP: VWF, FX, Heparin-Cofaktor II, FV; PET: VWF, FII) besonders bei späteren Zeitpunkten (360 min) erhöht, während Komplementinhibitoren (Vitronectin, Clusterin) zu Beginn (10 min, 1 l/min) stärker gebunden wurden. Obwohl der allgemeine Trend einer erhöhten Proteinbindung bei höheren Flussraten beobachtet wurde, wurde Fibrinogen, FXIIIb und α-1-Antitrypsin signifikant häufiger auf PMP-Membranen bei niedriger Flussrate gefunden. Eine höhere Fibrinogenablagerung bei niedriger Flussrate wurde bereits in früheren Studien beobachtet [98].

Unsere Ergebnisse zeigen, dass niedrigere Flussraten weniger signifikante Proteinänderungen auf den Membranen verursachen als höhere Flussraten, was in Übereinstimmung mit der Literatur [99] steht, die eine erhöhte Aktivierung von Thrombozyten, Neutrophilen und dem Komplementsystem bei höheren Flussraten beschreibt, was zu einer Verschlechterung der Hämokompatibilität führt. Für die Langzeit-ECMO sind mittlere Flussraten daher wünschenswert, um die Proteinadsorption an der Membran zu verringern und gleichzeitig den Scherstress auf Zellbestandteile zu minimieren [99].

Bezüglich der Membrantypen zeigte sich, dass die Flussrate einen größeren Einfluss auf die Proteinadsorption hatte als der Membrantyp selbst. Dennoch sollte der Materialeinfluss nicht unterschätzt werden. PMP und PET sind beide thermoplastische Materialien, die in medizinischen Geräten verwendet werden, jedoch weisen sie Unterschiede in ihren Eigenschaften auf. Die Proteinbindung war auf PET-Membranen bei höherer Flussrate stärker ausgeprägt, insbesondere bei Proteinen der Koagulation wie Fibrinogen und einigen Inhibitoren der Koagulation (Heparin-Cofaktor II). Auf PMP-Membranen wurden Proteine des Komplementsystems und der Entzündungsreaktion

häufiger gebunden. Diese Unterschiede zeigten, dass bei hoher Flussrate die Aktivierung der Koagulation durch PET-Membranen stärker und die Aktivierung des Komplementsystems durch PMP-Membranen ausgeprägter war. Bei niedrigen Flussraten wurden auf den PMP-Membranen mehr Inhibitoren der Entzündung und des Komplementsystems gebunden, was auf den potenziellen Vorteil hinweist, die Flussrate zu senken, um die Proteinadsorption und die Aktivierung von Komplementsystem und Entzündungen zu reduzieren.

Insgesamt zeigt diese Studie, dass sowohl die Flussrate als auch der Membrantyp einen Einfluss auf die Proteinbindung haben, wobei die Flussrate der entscheidende Faktor für die Adsorption von Plasmaproteinen ist

4.5 Ansatz für neue Oberflächenbeschichtungen

Die im Kapitel 4.3 beschriebene Ergebnisse deuten darauf hin, dass die Bindung von Proteinen, die an der Komplementinhibierung beteiligt sind, eine entscheidende Rolle für die Hämokompatibilität von Biomaterialien spielen. Mit Hilfe der in dieser Arbeit gewonnen Erkenntnissen wurde festgestellt, dass der alternative Weg eine wichtige Rolle bei der Aktivierung des Komplementsystems durch die Oxygenatormembran spielt. Daher könnte der Einsatz von Inhibitoren des alternativen Weges von Vorteil sein, um die Aktivierung des Komplementsystems zu verringern und so die Hämokompatibilität des Biomaterials zu erhöhen. Die Ergebnisse dieser Arbeit zeigten außerdem, dass das auf der Heparin-beschichteten Membran gebundenes Fibrinogen durch Albumin verdrängt werden kann (Fibrinogen Bindung nimmt ab und Albumin Bindung nimmt zu). Dieser Effekt war jedoch zeitlich begrenzt und hielt nur bis zu 180 Minuten an. Eine kombinierte Beschichtung mit Albumin und Heparin-ATIII-Komplexen könnte diesen Verdrängungseffekt möglicherweise verlängern. Albumin-Beschichtungen wurde bereits früher zur Verbesserung der Hämokompatibilität von Gefäßprothesen eingesetzt, was zu einer geringeren Zellablagerung führte [65]. Die kommerziell verwendete Bioline®-Beschichtung besteht aus Albuminschichten mit kovalent gebundenem Heparin [100]. Die höchste Hämokompatibilität wurde laut Andersson et al. bei der Verwendung heparinisierter Oberflächen mit einer Antithrombin-III-Bindungskapazität von 6–12 pmol/cm² nachgewiesen, was der Bioaktivität von etwa 1,5 µg Heparin/cm^2 entspricht [101]. Die in unserer Studie verwendete Heparin Beschichtung ent-

sprach etwa 3,5 µg bioaktivem Heparin/cm^2 und lag damit im Bereich der beschriebenen ATIII-Bindungskapazität von Andersson et al. Bisher wurden keine vergleichbaren Proteinadsorptionsstudien zu anderen Beschichtungsansätzen veröffentlicht. Die in der aktuellen Studie vorgestellten Daten deuten darauf hin, dass eine Kombination aus einer biopassiven Schicht aus Albumin mit einem bioaktiven Heparin-ATIII-Komplex geeignete Kandidaten für eine neuartige Beschichtung zur Verbesserung der langfristigen Hämokompatibilität sein könnten. Des Weiteren könnten aktive Beschichtungen mit Komplementinhibitoren ein vielversprechender Ansatz sein.

4.6 Entwicklung einer neuartigen Beschichtung auf Basis des C1-INH

Aufgrund der in dieser Arbeit gewonnen Ergebnissen mit endpunktgebundenem Heparin ist davon auszugehen, dass Proteine mit Affinitäten zu den für die Oberflächenbeschichtung verwendeten Molekülen von der Membran angezogen werden. So könnte zum Beispiel das C1-Protein von einer mit dem C1-INH beschichten Oberfläche abgefangen werden. So wird die Proteinadsorption und die Hämokompatibilität beeinflusst. Diesen Ansatz wurde für eine neuartige Beschichtung gewählt. Hierfür wurde eine PMP-Membran mit dem C1-INH beschichtet. Des Weiteren wurde eine Kombinierte Beschichtung aus C1-INH und Heparin entwickelt.

Der Serin-Protease-Inhibitor C1-INH ist ein Plasmaprotein, das als Komplementinhibitor sowie als Inhibitor anderer Signalwege wie des Kontaktsystems, der Fibrinolyse und der Gerinnung wirkt [102]. In dieser Arbeit konnte gezeigt werden, dass die Beschichtung mit C1-INH die Hämokompatibilität verbessert. Dies zeigte sich insbesondere in der ausgeprägten Hemmung des frühen Gerinnungsfaktors XIIa durch die C1-INH-Beschichtung. Durch das Fortlaufen der Gerinnungskaskade kommt es zum Anstieg des Thrombin-Antithrombin-III-Komplexes (TAT). Dieser Anstieg ist proportional zur Aktivierung von FX, da FXa (als katalytischer Teil des Prothrombinase-Komplexes) Prothrombin zu Thrombin spaltet, das von ATIII zur Bildung des TAT-Komplexes abgefangen wird [103, 104]. Erwartungsgemäß verringerte in dieser Arbeit gebundenes Heparin, das bekanntermaßen die Wirkung von ATIII verstärkt, den TAT-Plasmaspiegel erheblich. Im Gegensatz zur Heparin-Beschichtung zeigte die C1-INH-Beschichtung keinen Einfluss auf die TAT-Plasmaspiegel. Dies deutet darauf hin, dass die be-

obachtete FX-Aktivierung – und damit der Anstieg des TAT-Komplexes – nicht ausschließlich durch FXII und dessen nachgeschaltete Aktivierungskaskade verursacht wurde. Obwohl in der Literatur häufig berichtet wird, dass die Einleitung der Gerinnung durch Medizinprodukte mit einer Aktivierung von FXII beginnt, die zu einer nachgeschalteten Aktivierung von FXI, FIX und FX führt [105], scheint diese genaue Abfolge von Ereignissen hier unwahrscheinlich, da FXII durch die C1-INH-Beschichtung signifikant gehemmt wurde, während der TAT-Spiegel nicht reduziert wurde. Es ist möglich, dass die Aktivierung der Gerinnung unabhängig von FXII durch die Autoaktivierung von FXI eingeleitet wurde. In der Literatur wurde berichtet, dass FXI selbst durch negativ geladene Oberflächen autoaktiviert wird und so die Aktivierung durch Thrombin beschleunigt wird [106]. Somit kann eine geringe Menge an gebildetem Thrombin FXI autoaktivieren, was zu weiteren nachgeschalteten Ereignissen führt. C1-INH ist ein Inhibitor von FXI [107], daher reichte entweder die Menge an C1-INH nicht aus, um sowohl FXII als auch FXI zu blockieren, oder es gab andere aktivierende Ereignisse. Zusätzlich zur C1-INH-Beschichtung wurde in dieser Arbeit eine kombinierte Beschichtung entwickelt, die sowohl C1-INH als auch Heparin enthält. Im Gegensatz zur alleinigen C1-INH-Beschichtung, die keinen Einfluss auf den TAT-Plasmaspiegel zeigte, führte die kombinierte C1-INH/Heparin-Beschichtung zu TAT-Werten, die denen der reinen Heparin-Beschichtung entsprachen. Dies ist insofern von Interesse, als die eingesetzte Heparinmenge in der Kombination etwa dreimal geringer war als bei der Heparin-Beschichtung ohne C1-INH.Die Einbindung von C1-INH in die Heparinbeschichtung deutet also auf eine Verbesserung der Heparinwirkung auf der Oberfläche hin. Obwohl es keinen offensichtlichen Unterschied in der Aktivierung von Neutrophilen (Polymorphonuklear-Elastase; PMN-Elastase), Komplementaktivierung (C3a) und Thrombozytenaktivierung (β-Thromboglobulin; β-TG) zwischen den Beschichtungen gab, wurde eine signifikante Reduzierung der Leukozytenanhaftung an den mit C1-INH beschichteten Membranen festgestellt. Die Beschichtungen mit C1-INH und Heparin zeigten sogar einen signifikanten Rückgang der Leukozytenanheftung. Dies deutet darauf hin, dass die Adhäsion von Zellen durch den Einbau von C1-INH in Heparinbeschichtungen weiter verringert werden könnte. Die Untersuchung der Fibrinbildung und der Thrombozytenadhäsion mittels REM untermauert diese Vermutung. Auf Membranen, die mit C1-INH beschichtet waren, konnte fast keine Thrombozytenadhäsion oder Fibrinnetzwerke festgestellt werden und noch weniger bei den kombinierten

Beschichtungen aus Heparin und C1-INH. Die Heparin-beschichtete Membranen wiesen eine geringere Adhäsion von Thrombozyten und eine geringere Bildung von Fibrinnetzwerken auf als unbeschichtete Membranen. Dieses Ergebnis zeigt, dass der C1-INH-Beschichtung eine andere Wirkung zugrunde liegen muss als die alleinige Verhinderung der Aktivierung der Gerinnung. Die Adhäsion von Plasmaproteinen könnte einer der zugrundeliegenden Vorgänge sein. Wie bereits in Kapitel 4.3 beschrieben, konnte eine erhöhte C1-INH Adsorption auf heparinisierten Oberflächen nachgewiesen werden. Durch die direkte Beschichtung der Oberfläche der PMP-Membran mit C1-INH wurde die Adsorption von Plasmaproteinen möglicherweise auf eine hämokompatible, nicht aktivierende Oberfläche gelenkt. Außerdem kann FXII durch fehlgefaltete Proteine aktiviert werden [108]. Die Hemmung der FXII-Aktivierung durch C1-INH könnte daher auch die negative Wirkung von Proteinen verringern, die an der Oberfläche adsorbieren und eine Konformationsänderung eingehen. Diese Aktivierung von FXII würde normalerweise unerwünschte Entzündungen fördern, während die Verhinderung der Adsorption und Fehlfaltung von Proteinen an der Oberfläche die Bindung von Fibrinogen und Blutplättchen an die Oberfläche verringern kann [42]. Ein wesentlicher Vorteil der C1-INH-Beschichtung gegenüber der Heparin-Beschichtung zeigt sich bei Patienten und Patientinnen mit Heparin-induzierter Thrombozytopenie (HIT). Während HIT Typ 1 nicht immunvermittelt ist und sich der Abfall der Thrombozytenzahl bei kontinuierlicher Heparin Behandlung stabilisiert [109], handelt es sich bei HIT Typ 2 um eine Immunreaktion mit lebensbedrohlichen thromboembolischen Komplikationen [110]. IgG-Antikörper werden innerhalb von fünf Tagen gebildet und bilden einen Komplex mit Heparin und Plättchenfaktor 4 (PF4), was zu Thrombozytenaggregation und Thrombose führt [111] [112]. Daherh könnte die Substitution der Heparin Beschichtung durch C1-INH eine HIT verhindern und die ECMO für solche Patienten sicherer machen. Im Falle einer HIT können die gebildeten Antikörper zur Aktivierung des klassischen Komplementwegs führen, was eine Entzündung auslöst [105].

4.7 Einfluss der Materialeigenschaften von Biomaterialien auf die Hämokompatibilität

Ein kardiopulmonarer Bypass ist ähnlich wie eine ECMO aufgebaut. Bei einer Operation mit einem kardiopulmonalen Bypass wird das Blut durch die HLM gepumpt. Durch den Kontakt mit der Oberfläche kommt es zur Aktivierung von Zellen und zur Ausschüttung von entzündungsfördernden und gerinnungsaktivierenden Faktoren [113]. Um die Aktivierung der Blutgerinnung zu verhindern, wird das Blut des Patienten mit ca. 3 IU/ml hochmolekularem Heparin antikoaguliert, was zu einer aktivierten Gerinnungszeit (ACT) von >300–480 s führt. Durch die starke Antikoagulation, ist es in vielen Herzzentren üblich, das Blut aus den während der Operation verwendeten Bauchtüchern auszuwringen und über das Kardiotomiereservoir in den Patienten zurückzuführen. Dabei wird das Blut ohne Aufreinigung durch einen Cellsaver retransfundiert. Eine mögliche Aktivierung des Gerinnungssystems wird dabei als vernachlässigbar angesehen [114]. Im Rahmen einer klinischen Studie in dieser Arbeit wurde analysiert, ob abdominale Bauchtücher die Blutparameter wie die Aktivierung der Gerinnung, Entzündung oder des Komplementsystems zusätzlich zur kardiopulmonalen Bypass-Operation beeinflussen können und ob die Materialeigenschaften der Bauchtücher eine Rolle bei der Aktivierung von Abwehrprozessen spielen. Hierfür wurden zwei verschiedene Bauchtuchmaterialien (Baumwolle und synthetisch hergestellte Bauchtücher) verwendet. Baumwollbauchtücher werden standardmäßig, aufgrund ihrer hohen Saugfähigkeit eingesetzt. Baumwolle als Naturprodukt unterliegt jedoch während des Wachstumsprozesses verschiedenen Einflüssen, die die Qualität des Rohmaterials beeinträchtigen können [115]. Darüber hinaus kann der Herstellungsprozess die Hämokompatibilität beeinflussen [116]. Seit einigen Jahren gibt es vergleichbare Bauchtücher aus synthetischen Fasern, z. B. Viskose oder Polyester [117]. Die meisten Schritte während des Herstellungsprozesses von Kunstfasern können kontrolliert werden, so dass es möglich ist, die Qualität und die Eigenschaften des synthetischen Produkts zu beeinflussen. Dies könnte sich Vorteilhaft auf die Hämokompatibilität auswirken. Deshalb wurden die während dieser Studie erhaltenen Daten unter den folgenden zwei Aspekten diskutiert: (1) Veränderungen, die während der Behandlung mit der HLM auftraten. Diese spiegelten die kombinierten Auswirkungen der Operation, des HLM-Kreislaufs und des Bauchtuches wieder, (2) Hämokompatibilitätsparameter, die aus dem Bauchtuch ausgewrungen Blut gemessen wurden. Diese sind hauptsächlich

auf die Auswirkungen des Materials und der angewandten Scherspannung zurückzuführen.

Das Blut der zwei Patientengruppen (Patientengruppe 1: behandelt mit Baumwollbauchtüchern, Patientengruppe 2: behandelt mit synthetischen Bauchtüchern) zeigte unterschiedliche Aktivierungsparameter während der Behandlung mit der HLM, die auf einen Material-Effekt hinweisen. So können die nur in der Baumwollgruppe beobachteten pathologisch erhöhten Leukozyten am Ende der Behandlung mit der HLM wahrscheinlich auf eine stärkere Aktivierung [118] durch das Material zurückzuführen.

Die PMN-Elastase, die von aktivierten Neutrophilen freigesetzt wird, war am Ende der HLM und im Blut der Baumwollbauchtücher im Vergleich zu den synthetischen Bauchtüchern signifikant höher. Dies deutet darauf hin, dass neben dem HLM-Verfahren auch das Material selbst eine erhöhte neutrophile Degranulation auslöste. Da sich das Blut am Ende der HLM nicht signifikant unterschiedet, verdeckt die aktivierende Wirkung des extrakorporalen Verfahrens wahrscheinlich die Wirkung des Materials.

Die signifikant höhere Aktivierung von Thrombozyten, im aus dem Baumwollbauchtuch ausgewrungenen Blut könnte mit für die erhöhte Neutrophilenaktivierung verantwortlich sein. Aktivierte Thrombozyten sezernieren Thrombozyten aktivierende Faktoren (z. B. plättchenaktivierender Faktor, ADP, von-Willebrand-Faktor, [119]), aber auch neutrophilen aktivierende Faktoren (neutrophilenaktivierendes Peptid 2) und andere entzündungsauslösende Mediatoren [120]. Thrombozyten selbst werden leicht an negativ geladenen Oberflächen [121] oder durch Scherbelastung [122] zum Beispiel durch die HLM oder das Auswringen der Bauchtücher aktiviert.

Gewebefaktor-exprimierende Zellen wie aktivierte Monozyten [123] oder neutrophile extrazelluläre Fallen (NET) aus aktivierten Neutrophilen [124] können die Gerinnungskaskade auslösen [125]. Ebenfalls können Gerinnung und Entzündungen durch die künstlichen Oberflächen der HLM oder der Bauchtücher (Hydrolyse von FXII [126]) ausgelöst werden [127-129]. Eine signifikante Gerinnungsaktivierung (gemessen durch die Bildung des TAT-Komplexes) wurde in dieser Studie im Blut aus der HLM trotz der hohen Antikoagulation beobachtet. Allerdings war die Aktivierung durch Baumwolle signifikant stärker als bei den synthetischen Bauchtüchern, was auf eine stärkere Aktivierung der Gerinnungskaskade oder Thrombozytenaktivierung hindeutet.

Die signifikant höhere IL6-Sekretion im aus den Baumwollbauchtüchern ausgewrungenen Blut spiegelt wahrscheinlich eine materialbedingte entzündliche Aktivierung von Monozyten wider [116]. [130], während der signifikante Anstieg am Ende der HLM in der Baumwollgruppe im Vergleich zur synthetischen Gruppe für beide entzündlichen Zytokine (IL1β und IL6) durch aktivierte Monozyten, Thrombozyten oder Endothelzellen induziert sein kann [131, 132]. Die SDF-1α-Expression kann durch Entzündungsmediatoren wie IL1β oder TNFα hochreguliert werden [133, 134]. In dieser Arbeit war dieses Chemokin während der HLM in beiden Gruppen signifikant erhöht, aber im Blut, das aus den Bauchtüchern ausgewrungen wurde, induzierten die synthetischen Bauchtücher eine signifikant höhere Expression als die Baumwollbauchtücher. Diese Beobachtung scheint im Widerspruch zu anderen Beobachtungen zu stehen, da das Chemokin bei Bindung an die Thrombozytenoberflächenrezeptoren CXRC4 oder CXCR7 eine verstärkende Wirkung auf die Thrombozytenaggregation hat [135]. Im Einklang mit der stärkeren Aktivierung von Thrombozyten und Leukozyten durch Baumwolle wurde daher der gegenteilige Effekt erwartet. Obwohl lange Zeit davon ausgegangen wurde, dass SDF-1α hauptsächlich aus dem Knochenmark und dem Endothel stammt [136], gibt es auch einen Pool von SDF-1α, der von Thrombozyten freigesetzt wird [137]. Insbesondere dieses SDF-1α fördert nachweislich das Überleben von Thrombozyten [135] und reguliert die Differenzierung und das Überleben von Monozyten [138]. Somit kann das aus den Bauchtüchern und während der HLM gemessene SDF-1α aus unterschiedlichen Quellen stammen. Während sich die SDF-1α-Konzentrationen im Blut, das bei HLM entnommen wurde, zwischen den Patientengruppen nicht unterscheiden, sind die aus den Bauchtüchern gemessenen Konzentrationen unterschiedlich, was auf eine mögliche Rolle von aus Thrombozyten stammendem SDF-1α nach direktem Kontakt mit den Materialien hindeutet und somit in diesem Fall eher eine schützende als eine zerstörende Rolle für Thrombozyten und Monozyten darstellen könnte.

Die in dieser Arbeit gewonnenen Daten deuten stark darauf hin, dass eine entzündliche Aktivierung von Monozyten, eine Degranulation von Neutrophilen und eine Aktivierung von Thrombozyten durch die Baumwolle stattgefunden hat, nicht zuletzt aufgrund der starken IL1β-Sekretion in vitro bei Kontakt mit Baumwolle. Obwohl die meisten gemessenen Parameter am Ende der HLM in beiden Patientengruppen ähnlich erhöht waren, kam es in der Baumwollgruppe zu einem deutlichen Anstieg der Ent-

zündungsparameter am Ende der HLM. Diese stärkere Aktivierung von Blutbestandteilen durch Baumwolle stellt ein zusätzliches Risiko für die Patienten dar, ein Systemisches inflammatorisches Response-Syndrom (SIRS) zu entwickeln, wenn die aktivierten Blutbestandteile in den systemischen Kreislauf gelangen. Es wurde berichtet, dass die PMN-Elastase die Freisetzung von Zytokinen fördert [139], und auch die anderen proinflammatorischen Mediatoren und Substanzen, die von aktivierten Thrombozyten freigesetzt werden, tragen dazu bei. Bei Betrachtung des C-reaktives Protein (CRP)-Werte und des SOFA-Scores (Sepsis-related organ failure assessment score) in beiden Gruppen konnten keinen signifikanten Unterschied zwischen den Gruppen festgestellt werden. Allerdings wies in der Baumwollgruppe die Hälfte der Patienten Symptome eines SIRS auf, während in der Gruppe, die mit den synthetischen Bauchtücher behandelt wurden, nur zwei Patienten SIRS-Symptome hatten. Daher scheint das synthetische Material die sicherere Wahl für Patienten bei CPB-Operationen zu sein.

Ähnliche Beobachtungen in Bezug auf synthetische Materialien wurden auch in anderen Studien gemacht. Hernández et al. konnten bei Hämodialysepatienten zeigen, dass die Leukozytenaktivierung höher war, wenn Zellulosemembranen verwendet wurden als bei Verwendung synthetischer Membranen [140]. Bei Affen zeigten orale Nähte aus Nylon fast keine entzündlichen Gewebereaktionen und waren daher den Nähten aus Baumwolle überlegen [141].

Allerdings bezeichneten alle Chirurgen in unserer Studie die synthetischen Bauchtücher als minderwertig in Bezug auf Saugfähigkeit und Formbarkeit. Diese subjektive Einschätzung könnte darauf beruhen, dass die Chirurgen mit den Baumwollbauchtüchern vertraut sind. Zumindest bei der Adsorptionsfähigkeit des synthetischen Materials Polyurethan konnte auch nach wiederholter Verwendung eines Bauchtuches kein Nachteil gegenüber Baumwollmaterialien festgestellt werden [117]. Beim Vergleich der Ausbreitung von Bluttropfen auf diesen Materialien war zu erkennen, dass die Ausbreitung auf dem synthetischen Material geringer war. In der klinischen Anwendung könnte dies ein Vorteil bei der Lokalisierung des genauen Ursprungs von Blutungen sein [117]. Die beschriebene Steifigkeit des synthetischen Materials ist jedoch ein Nachteil, der berücksichtigt werden muss. Zur Verbesserung der Benetzbarkeit und haptischen Eigenschaften synthetischer Materialien können Modifikationen wie die UV-initiierte

kovalente Anbindung von 2-Hydroxyethylmethacrylat (HEMA) an Polypropylen eingesetzt werden. HEMA, ein potenzielles Material für biokompatible Hydrogele, führte dabei zu einer deutlich erhöhten Absorptionsfähigkeit und einer verkürzten Wasserbenetzungszeit des Polymers [142].

5 Ausblick

Die vorliegende Arbeit hat wertvolle Erkenntnisse zur Verbesserung der Hämokompatibilität von medizinischen Biomaterialien geliefert, insbesondere im Zusammenhang mit der Anwendung extrakorporaler Membransysteme und ihrer Auswirkungen auf das Immunsystem, die Gerinnung und Entzündungsprozesse. Die gewonnenen Ergebnisse eröffnen neue Perspektiven für die Weiterentwicklung von innovativen Beschichtungen, die die Langzeitkompatibilität dieser Systeme fördern können. Dennoch gibt es weiterhin zahlreiche Herausforderungen, die sowohl die Forschung als auch die praktische Umsetzung in der klinischen Anwendung betreffen.

Durch umfassende massenspektrometrische Analysen von konnten in dieser Arbeit etwa 3000 verschiedenen desorbierten Plasmaproteinen auf Hohlfasermembranen nachgewiesen werden. Durch die Anwendung unterschiedlicher Materialien, variierender Blutflussraten und der Analyse zu verschiedenen Zeitpunkten ist ein sehr umfangreicher Datensatz entstanden. Die detaillierte Auswertung dieser Daten ermöglichte es, wertvolle Rückschlüsse auf die biologischen Prozesse nach Blutkontakt zu ziehen und eine neue Beschichtung zu entwickeln. Jedoch könnte das Potenzial dieser umfangreichen Daten durch die Zusammenarbeit mit Bioinformatikern und den gezielten Einsatz fortschrittlicher Künstlicher Intelligenz (KI) noch erweitert werden. Insbesondere KI-gestützte Algorithmen könnten dabei helfen, Muster und Zusammenhänge zu erkennen, die für den menschlichen Analysten nur schwer greifbar wären. Moderne KI-Methoden, wie maschinelles Lernen und Deep Learning, könnten auf Basis dieser großen Datenmengen Modelle zur Identifikation potenziell relevanter biologischer Marker entwickeln. Solche Modelle könnten helfen, vorherzusagen, welche Protein-Muster mit spezifischen biologischen Reaktionen, wie der Aktivierung des Komplementsystems oder der Blutgerinnung, korrelieren.

Der in dieser Arbeit entstandene Datensatz basiert ausschließlich auf in-vitro erzeugten Daten, was die Interpretation und Übertragbarkeit der Ergebnisse auf klinische Anwendungen einschränken kann. Um die gewonnenen Erkenntnisse weiter zu vertiefen und ihre Relevanz für die Praxis zu bestätigen, wäre es sinnvoll, in-vivo-Daten hinzuzufügen. Dies könnte durch die Durchführung einer klinischen Studie erreicht werden.

In einer solchen Studie könnten Plasmaproteine, die sich nach der Anwendung von Oxygenatoren im Blutkreislauf von Patienten ablagern, analysiert werden. Dies würde nicht nur die in-vitro-Daten validieren, sondern auch neue Einblicke in die tatsächlichen biologischen Prozesse und Wechselwirkungen unter klinischen Bedingungen ermöglichen. Durch die Analyse der Proteinzusammensetzung könnten spezifische Proteine identifiziert werden, die als Biomarker für unerwünschte Reaktionen wie Gerinnung oder Entzündungen dienen. Darüber hinaus könnte die Integration von in-vivo-Daten den Weg für personalisierte Ansätze ebnen, bei denen die Auswahl oder Anpassung von Biomaterialien auf die individuellen Bedürfnisse eines Patienten abgestimmt wird. Kombiniert mit den zuvor erwähnten KI-Methoden könnten Modelle entwickelt werden, um die Verträglichkeit und Effektivität extrakorporaler Membransysteme unter realen Bedingungen besser vorherzusagen. Solche Studien könnten entscheidend dazu beitragen, die Translation der Forschungsergebnisse in die klinische Praxis zu beschleunigen und die Sicherheit sowie die Langzeitkompatibilität von ECMO-Systemen weiter zu optimieren.

Die Entwicklung der C1-INH-basierten Beschichtung auf Grundlage der gewonnenen massenspektrometrischen Daten stellt einen bedeutenden Fortschritt in der Optimierung der Hämokompatibilität dar. Trotz dieses vielversprechenden Ansatzes bestehen jedoch noch erhebliche Herausforderungen, bevor eine klinische Anwendung und eine kommerzielle Verfügbarkeit möglich sind. Insbesondere die regulatorischen Anforderungen im Rahmen der europäischen Medizinprodukteverordnung (MDR) stellen eine hohe Hürde dar. Kombinationsprodukte, die sowohl ein Medizinprodukt als auch eine aktive pharmazeutische Substanz (API) wie den C1-INH enthalten, unterliegen besonders strengen Auflagen. Neben den Anforderungen an die Sicherheit und Wirksamkeit dieser Produkte ist eine umfassende Bewertung von klinischen Daten und potenziellen Langzeitwirkungen erforderlich. Um die Marktzulassung solcher innovativen Beschichtungen zu beschleunigen, ist eine enge Zusammenarbeit zwischen Forschungseinrichtungen, klinischen Partnern und Zulassungsbehörden essenziell.

Darüber hinaus bietet der generierte massenspektrometrische Datensatz weitere Entwicklungsmöglichkeiten. Insbesondere könnten darauf aufbauend alternative Beschichtungen entwickelt werden, die keine aktive pharmazeutische Substanz enthalten und somit geringeren regulatorischen Anforderungen unterliegen. Solche Lösungen

könnten beispielsweise durch die gezielte Modifikation physikalisch-chemischer Eigenschaften von Biomaterialien erreicht werden, um eine vergleichbare Hämokompatibilität zu gewährleisten.

.

6 Literaturverzeichnis

1. Hudecki, A., G. Kiryczyński, and M.J. Łos, *Biomaterials, definition, overview*, in *Stem Cells and Biomaterials for Regenerative Medicine*. 2019, Elsevier. p. 85-98.
2. Bose, S. and A. Bandyopadhyay, *Introduction to biomaterials*, in *Characterization of Biomaterials*. 2013, Elsevier. p. 1-9.
3. Barillo, D.J. and D.E. Marx, *Silver in medicine: A brief history BC 335 to present.* Burns, 2014. **40**: p. S3-S8.
4. Shen, G., J.-F. Zhang, and F.-Z. Fang, *In vitro evaluation of artificial joints: A comprehensive review.* Advances in Manufacturing, 2019. **7**(1): p. 1-14.
5. Singhal, J.P., H. Singh, and A.R. Ray, *Absorbable suture materials: preparation and properties.* Polymer Reviews, 1988. **28**(3-4): p. 475-502.
6. Jaganathan, S.K., et al., *Biomaterials in cardiovascular research: applications and clinical implications.* BioMed research international, 2014. **2014**.
7. Gorbet, M.B. and M.V. Sefton, *Biomaterial-associated thrombosis: roles of coagulation factors, complement, platelets and leukocytes.* Biomaterials, 2004. **25**(26): p. 5681-5703.
8. Hanson, S.R., *Device thrombosis and thromboembolism.* Cardiovascular Pathology, 1993. **2**(3): p. 157-165.
9. Chen, H., et al., *Biocompatible polymer materials: role of protein–surface interactions.* Progress in Polymer Science, 2008. **33**(11): p. 1059-1087.
10. Baier, R.E. and R.C. Dutton, *Initial events in interactions of blood with a foreign surface.* Journal of biomedical materials research, 1969. **3**(1): p. 191-206.
11. Brash, J.L., et al., *The blood compatibility challenge. Part 2: Protein adsorption phenomena governing blood reactivity.* Acta biomaterialia, 2019. **94**: p. 11-24.
12. Chen, J. and S.M. Cramer, *Protein adsorption isotherm behavior in hydrophobic interaction chromatography.* Journal of Chromatography A, 2007. **1165**(1-2): p. 67-77.
13. Chuang, H.Y., W.F. King, and R.G. Mason, *Interaction of plasma proteins with artificial surfaces: protein adsorption isotherms.* The Journal of laboratory and clinical medicine, 1978. **92**(3): p. 483-496.
14. Noh, H., S.T. Yohe, and E.A. Vogler, *Volumetric interpretation of protein adsorption: ion-exchange adsorbent capacity, protein pI, and interaction energetics.* Biomaterials, 2008. **29**(13): p. 2033-2048.
15. Chen, J., et al., *Classification of protein adsorption and recovery at low salt conditions in hydrophobic interaction chromatographic systems.* Journal of Chromatography A, 2007. **1139**(2): p. 236-246.
16. Allen, L.T., et al., *Surface-induced changes in protein adsorption and implications for cellular phenotypic responses to surface interaction.* Biomaterials, 2006. **27**(16): p. 3096-3108.
17. Daculsi, G., et al., *In vivo cell interactions with calcium phosphate bioceramics.* Journal of submicroscopic cytology and pathology, 1988. **20**(2): p. 379-384.
18. Aissaoui, N., et al., *Silane layers on silicon surfaces: mechanism of interaction, stability, and influence on protein adsorption.* Langmuir, 2012. **28**(1): p. 656-665.
19. Shen, B., *Lipid-protein interaction at solid-water interface. Adsorption of human apo-high density lipoprotein to amphiphilic interfaces.* Journal of Biological Chemistry, 1985. **260**(2): p. 1032-1039.

20. Höland, W., et al., *Interface reactions between machinable bioactive glass-ceramics and bone.* Journal of biomedical materials research, 1985. **19**(3): p. 303-312.
21. Cornelius, R.M., et al., *Adsorption of proteins from infant and adult plasma to biomaterial surfaces.* Journal of Biomedical Materials Research: An Official Journal of The Society for Biomaterials, The Japanese Society for Biomaterials, and The Australian Society for Biomaterials and the Korean Society for Biomaterials, 2002. **60**(4): p. 622-632.
22. Wojciechowski, P., P. Ten Hove, and J. Brash, *Phenomenology and mechanism of the transient adsorption of fibrinogen from plasma (Vroman effect).* Journal of colloid and interface science, 1986. **111**(2): p. 455-465.
23. Brash, J.L., *Protein surface interactions and biocompatibility: A forty year perspective*, in *Proteins at Interfaces III State of the Art*. 2012, ACS Publications. p. 277-300.
24. Hadjidemetriou, M., Z. Al-Ahmady, and K. Kostarelos, *Time-evolution of in vivo protein corona onto blood-circulating PEGylated liposomal doxorubicin (DOXIL) nanoparticles.* Nanoscale, 2016. **8**(13): p. 6948-6957.
25. Vroman, L. and A.L. Adams, *Identification of rapid changes at plasma–solid interfaces.* Journal of biomedical materials research, 1969. **3**(1): p. 43-67.
26. Vroman, L., et al., *Interaction of high molecular weight kininogen, factor XII, and fibrinogen in plasma at interfaces.* 1980.
27. Schmaier, A.H., et al., *The effect of high molecular weight kininogen on surface-adsorbed fibrinogen.* Thrombosis research, 1984. **33**(1): p. 51-67.
28. Vroman, L. *The importance of surfaces in contact phase reactions*. in *Seminars in thrombosis and hemostasis*. 1987. Copyright© 1987 by Thieme Medical Publishers, Inc.
29. Courtney, J.M. and C.D. Forbes, *Thrombosis on foreign surfaces.* Br Med Bull, 1994. **50**(4): p. 966-81.
30. Grunkemeier, J., et al., *The effect of adsorbed fibrinogen, fibronectin, von Willebrand factor and vitronectin on the procoagulant state of adherent platelets.* Biomaterials, 2000. **21**(22): p. 2243-2252.
31. Loike, J.D., et al., *CD11c/CD18 on neutrophils recognizes a domain at the N terminus of the A alpha chain of fibrinogen.* Proceedings of the National Academy of Sciences, 1991. **88**(3): p. 1044-1048.
32. Morley, D. and I. Feuerstein, *Adhesion of polymorphonuclear leukocytes to protein-coated and platelet adherent surfaces.* Thrombosis and haemostasis, 1989. **62**(07): p. 1023-1028.
33. Kazatchkine, M. and M. Carreno, *Activation of the complement system at the interface between blood and artificial surfaces.* Biomaterials, 1988. **9**(1): p. 30-35.
34. Bowers, V., et al., *A micromechanical technique for monitoring cell—substrate adhesiveness: measurements of the strength of red blood cell adhesion to glass and polymer test surfaces.* Journal of biomedical materials research, 1989. **23**(12): p. 1453-1473.
35. Puri, R.N., R.W. Colman, and M.A. Liberman, *ADP-Induced Platelet Activation.* Critical reviews in biochemistry and molecular biology, 1997. **32**(6): p. 437-502.
36. Ogata, H., et al., *KEGG: Kyoto encyclopedia of genes and genomes.* Nucleic acids research, 1999. **27**(1): p. 29-34.
37. Sarma, J.V. and P.A. Ward, *The complement system.* Cell and tissue research, 2011. **343**(1): p. 227-235.

38. Tegla, C.A., et al., *Membrane attack by complement: the assembly and biology of terminal complement complexes.* Immunologic research, 2011. **51**(1): p. 45-60.
39. Jaffer, I., et al., *Medical device-induced thrombosis: what causes it and how can we prevent it?* Journal of Thrombosis and Haemostasis, 2015. **13**: p. S72-S81.
40. Krisinger, M.J., et al., *Thrombin generates previously unidentified C5 products that support the terminal complement activation pathway.* Blood, The Journal of the American Society of Hematology, 2012. **120**(8): p. 1717-1725.
41. Carroll, M.C., *The complement system in regulation of adaptive immunity.* Nature immunology, 2004. **5**(10): p. 981-986.
42. Conrad, S.A. and P.T. Rycus, *Extracorporeal membrane oxygenation in critical care: past, present, and future.* Journal of Cardiac Critical Care TSS, 2017. **1**(02): p. 60-64.
43. Bartlett, R. and L. Gattinoni, *Current status of extracorporeal life support (ECMO) for cardiopulmonary failure.* Minerva Anestesiol, 2010. **76**(7): p. 534-540.
44. Barbaro, R.P., et al., *Extracorporeal membrane oxygenation support in COVID-19: an international cohort study of the Extracorporeal Life Support Organization registry.* The Lancet, 2020. **396**(10257): p. 1071-1078.
45. Mulder, M., I. Fawzy, and M. Lancé, *ECMO and anticoagulation: a comprehensive review.* Neth J Crit Care, 2018. **26**(1): p. 6-13.
46. Doyle, A.J. and B.J. Hunt, *Current understanding of how extracorporeal membrane oxygenators activate haemostasis and other blood components.* Frontiers in medicine, 2018. **5**: p. 352.
47. Firstenberg, M.S., *Extracorporeal membrane oxygenation: advances in therapy*. 2016: BoD–Books on Demand.
48. Hirsh, J., et al., *Mechanism of action and pharmacology of unfractionated heparin*. 2001, Am Heart Assoc.
49. Grecu, L., *Anticoagulation for extracorporeal membrane oxygenation: between the rock and the hard place.* Critical care medicine, 2020. **48**(2): p. 264-266.
50. Zhang, M., et al., *Anti-thrombogenic Surface Coatings for Extracorporeal Membrane Oxygenation: A Narrative Review.* ACS Biomaterials Science & Engineering, 2021. **7**(9): p. 4402-4419.
51. Siedlecki, C., *Hemocompatibility of Biomaterials for Clinical Applications*. 2018, Elsevier.
52. Maitz, M.F., et al., *The blood compatibility challenge. Part 4: Surface modification for hemocompatible materials: Passive and active approaches to guide blood-material interactions.* Acta biomaterialia, 2019. **94**: p. 33-43.
53. Werner, C., M.F. Maitz, and C. Sperling, *Current strategies towards hemocompatible coatings.* Journal of materials chemistry, 2007. **17**(32): p. 3376-3384.
54. Gott, V.L., J.D. Whiffen, and R.C. Dutton, *Heparin bonding on colloidal graphite surfaces.* Science, 1963. **142**(3597): p. 1297-1298.
55. Larm, O., R. Larsson, and P. Olsson, *A new non-thrombogenic surface prepared by selective covalent binding of heparin via a modified reducing terminal residue.* Biomaterials, medical devices, and artificial organs, 1983. **11**(2-3): p. 161-173.
56. Videm, V., et al., *Reduced complement activation with heparin-coated oxygenator and tubings in coronary bypass operations.* The Journal of thoracic and cardiovascular surgery, 1992. **103**(4): p. 806-813.

57. Wendel, H.P. and G. Ziemer, *Coating-techniques to improve the hemocompatibility of artificial devices used for extracorporeal circulation.* European journal of cardio-thoracic surgery, 1999. **16**(3): p. 342-350.
58. Teligui, L., et al., *An ex vivo evaluation of blood coagulation and thromboresistance of two extracorporeal circuit coatings with reduced and full heparin dose.* Interact Cardiovasc Thorac Surg, 2014. **18**(6): p. 763-9.
59. Reser, D., et al., *Retrospective analysis of outcome data with regards to the use of Phisio(R)-, Bioline(R)- or Softline(R)-coated cardiopulmonary bypass circuits in cardiac surgery.* Perfusion, 2012. **27**(6): p. 530-4.
60. Schulze, C.J., et al., *Phosphorylcholine-coated circuits improve preservation of platelet count and reduce expression of proinflammatory cytokines in CABG: a prospective randomized trial.* J Card Surg, 2009. **24**(4): p. 363-8.
61. Nunes, A.D.C., et al., *Albumin Coating Prevents Cardiac Effect of the Magnetic Nanoparticles.* IEEE Trans Nanobioscience, 2019. **18**(4): p. 640-650.
62. Shimamoto, A., et al., *Biocompatibility of silicone-coated oxygenator in cardiopulmonary bypass.* Ann Thorac Surg, 2000. **69**(1): p. 115-20.
63. Weber, N., H.P. Wendel, and G. Ziemer, *Hemocompatibility of heparin-coated surfaces and the role of selective plasma protein adsorption.* Biomaterials, 2002. **23**(2): p. 429-439.
64. Johnson, G., et al., *In vitro assessment of blood compatibility: Residual and dynamic markers of cellular activation.* Journal of Biomaterials Applications, 2013. **27**(8): p. 925-936.
65. Kottke-Marchant, K., et al., *Effect of albumin coating on the in vitro blood compatibility of Dacron® arterial prostheses.* Biomaterials, 1989. **10**(3): p. 147-155.
66. Sivaraman, B. and R.A. Latour, *The adherence of platelets to adsorbed albumin by receptor-mediated recognition of binding sites exposed by adsorption-induced unfolding.* Biomaterials, 2010. **31**(6): p. 1036-1044.
67. Hanson, S.R., E.I. Tucker, and R.A. Latour, *Blood coagulation and blood–material interactions*, in *Biomaterials science*. 2020, Elsevier. p. 801-812.
68. Silverberg, M., et al., *Autoactivation of human Hageman factor. Demonstration utilizing a synthetic substrate.* Journal of Biological Chemistry, 1980. **255**(15): p. 7281-7286.
69. Schmaier, A., *The contact activation and kallikrein/kinin systems: pathophysiologic and physiologic activities.* Journal of Thrombosis and Haemostasis, 2016. **14**(1): p. 28-39.
70. Ratnoff, O.D. and J.M. Rosenblum, *Role of Hageman factor in the initiation of clotting by glass: evidence that glass frees Hageman factor from inhibition.* The American Journal of Medicine, 1958. **25**(2): p. 160-168.
71. Zhao, M., et al., *Characterization of a heparin binding site on the heavy chain of factor XI.* Journal of Biological Chemistry, 1998. **273**(47): p. 31153-31159.
72. Ziats, N., et al., *Adsorption of Hageman factor (factor XII) and other human plasma proteins to biomedical polymers.* The Journal of laboratory and clinical medicine, 1990. **116**(5): p. 687-696.
73. Mulzer, S. and J. Brash, *Identification of plasma proteins adsorbed to hemodialyzers during clinical use.* Journal of biomedical materials research, 1989. **23**(12): p. 1483-1504.
74. Cornelius, R.M. and J.L. Brash, *Identification of proteins adsorbed to hemodialyser membranes from heparinized plasma.* Journal of Biomaterials Science, Polymer Edition, 1993. **4**(3): p. 291-304.

75. Matata, B., et al., *Determination of contact phase activation by the measurement of the activity of supernatant and membrane surface‐adsorbed factor XII (FXII): Its relevance as a useful parameter for the in vitro assessment of haemodialysis membranes.* Journal of Biomedical Materials Research: An Official Journal of The Society for Biomaterials and The Japanese Society for Biomaterials, 1996. **31**(1): p. 63-70.
76. Elam, J.-H. and H. Nygren, *Adsorption of coagulation proteins from whole blood on to polymer materials: relation to platelet activation.* Biomaterials, 1992. **13**(1): p. 3-8.
77. Van der Kamp, K. and W. Van Oeveren, *Factor XII fragment and kallikrein generation in plasma during incubation with biomaterials.* Journal of biomedical materials research, 1994. **28**(3): p. 349-352.
78. Van der Kamp, K., et al., *Contact activation during incubation of five different polyurethanes or glass in plasma.* Journal of biomedical materials research, 1995. **29**(10): p. 1303-1306.
79. Hong, J., et al., *A new in vitro model to study interaction between whole blood and biomaterials. Studies of platelet and coagulation activation and the effect of aspirin.* Biomaterials, 1999. **20**(7): p. 603-611.
80. Burman, J.F., et al., *Role of factor XII in thrombin generation and fibrinolysis during cardiopulmonary bypass.* The Lancet, 1994. **344**(8931): p. 1192-1193.
81. Faxälv, L., P. Tengvall, and T.L. Lindahl, *Imaging of blood plasma coagulation and its propagation at surfaces.* Journal of Biomedical Materials Research Part A: An Official Journal of The Society for Biomaterials, The Japanese Society for Biomaterials, and The Australian Society for Biomaterials and the Korean Society for Biomaterials, 2008. **85**(4): p. 1129-1134.
82. Monroe, D.M., M. Hoffman, and H.R. Roberts, *Platelets and thrombin generation.* Arteriosclerosis, thrombosis, and vascular biology, 2002. **22**(9): p. 1381-1389.
83. Kador, K., et al., *Sequential co-immobilization of thrombomodulin and endothelial protein C receptor on polyurethane: activation of protein C.* Acta Biomaterialia, 2011. **7**(6): p. 2508-2517.
84. Andersson, J., et al., *Binding of C3 fragments on top of adsorbed plasma proteins during complement activation on a model biomaterial surface.* Biomaterials, 2005. **26**(13): p. 1477-1485.
85. Nilsson, U., et al., *Modification of the complement binding properties of polystyrene: Effects of end‐point heparin attachment.* Scandinavian journal of immunology, 1993. **37**(3): p. 349-354.
86. Garred, P., et al., *A journey through the lectin pathway of complement—MBL and beyond.* Immunological reviews, 2016. **274**(1): p. 74-97.
87. Hein, E., et al., *Heparin-coated cardiopulmonary bypass circuits selectively deplete the pattern recognition molecule ficolin-2 of the lectin complement pathway in vivo.* Clinical & Experimental Immunology, 2015. **179**(2): p. 294-299.
88. Lachmann, P. and N. Hughes-Jones. *Initiation of complement activation*. in *Springer seminars in immunopathology*. 1984. Springer.
89. Sahu, A. and J.D. Lambris, *Complement inhibitors: a resurgent concept in anti-inflammatory therapeutics.* Immunopharmacology, 2000. **49**(1-2): p. 133-148.
90. Riedel, T., et al., *Complement Activation Dramatically Accelerates Blood Plasma Fouling On Antifouling Poly (2‐Hydroxyethyl Methacrylate) Brush Surfaces.* Macromolecular Bioscience, 2021: p. 2100460.

91. Lhotta, K., et al., *Rapid activation of the complement system by cuprophane depends on complement component C4.* Kidney international, 1998. **53**(4): p. 1044-1051.
92. Tengvall, P., A. Askendal, and I. Lundström, *Studies on protein adsorption and activation of complement on hydrated aluminium surfaces in vitro.* Biomaterials, 1998. **19**(10): p. 935-940.
93. Engberg, A.E., et al., *Inhibition of complement activation on a model biomaterial surface by streptococcal M protein-derived peptides.* Biomaterials, 2009. **30**(13): p. 2653-2659.
94. Engberg, A.E., et al., *Prediction of inflammatory responses induced by biomaterials in contact with human blood using protein fingerprint from plasma.* Biomaterials, 2015. **36**: p. 55-65.
95. Meri, S. and H. Jarva, *Complement regulation.* Vox sanguinis, 1998. **74**(S2): p. 291-302.
96. Pangburn, M.K., M. Atkinson, and S. Meri, *Localization of the heparin-binding site on complement factor H.* Journal of Biological Chemistry, 1991. **266**(25): p. 16847-16853.
97. Ormsby, R.J., et al., *Localization of the third heparin-binding site in the human complement regulator factor H1.* Molecular immunology, 2006. **43**(10): p. 1624-1632.
98. Sakariassen, K.S., et al., *Collagen type III induced ex vivo thrombogenesis in humans. Role of platelets and leukocytes in deposition of fibrin.* Arteriosclerosis, 1990. **10**(2): p. 276-84.
99. Meyer, A.D., et al., *Effect of blood flow on platelets, leukocytes, and extracellular vesicles in thrombosis of simulated neonatal extracorporeal circulation.* J Thromb Haemost, 2020. **18**(2): p. 399-410.
100. Biran, R. and D. Pond, *Heparin coatings for improving blood compatibility of medical devices.* Adv Drug Deliv Rev, 2017. **112**: p. 12-23.
101. Bayly-Jones, C., D. Bubeck, and M.A. Dunstone, *The mystery behind membrane insertion: a review of the complement membrane attack complex.* Philosophical Transactions of the Royal Society B: Biological Sciences, 2017. **372**(1726): p. 20160221.
102. Li, H.H., *Self-administered C1 esterase inhibitor concentrates for the management of hereditary angioedema: usability and patient acceptance.* Patient Prefer Adherence, 2016. **10**: p. 1727-37.
103. Krishnaswamy, S., *The transition of prothrombin to thrombin.* J Thromb Haemost, 2013. **11 Suppl 1**: p. 265-76.
104. Quaranta, M., et al., *The physiologic and therapeutic role of heparin in implantation and placentation.* PeerJ, 2015. **3**: p. e691.
105. Visser, M., et al., *Role of Factor XIa and Plasma Kallikrein in Arterial and Venous Thrombosis.* Thromb Haemost, 2020. **120**(6): p. 883-993.
106. Gailani, D. and G.J. Broze, Jr., *Factor XII-independent activation of factor XI in plasma: effects of sulfatides on tissue factor-induced coagulation.* Blood, 1993. **82**(3): p. 813-9.
107. Panagiotou, A., M. Trendelenburg, and M. Osthoff, *The Lectin Pathway of Complement in Myocardial Ischemia/Reperfusion Injury-Review of Its Significance and the Potential Impact of Therapeutic Interference by C1 Esterase Inhibitor.* Front Immunol, 2018. **9**: p. 1151.
108. Naudin, C., et al., *Factor XII Contact Activation.* Semin Thromb Hemost, 2017. **43**(8): p. 814-826.

109. Liu, W., et al., *Rare heparin induced thrombocytopenia type I reaction in a hemodialysis patient: Case report.* Medicine (Baltimore), 2018. **97**(50): p. e13609.
110. Riedel, R., et al., *[Heparin-induced thrombocytopenia type II (HIT II) : A medical-economic view].* Med Klin Intensivmed Notfmed, 2017. **112**(4): p. 334-346.
111. Chang, J.J.Y. and C.R. Parikh, *When heparin causes thrombosis: Significance, recognition, and management of heparin-induced thrombocytopenia in dialysis patients.* Seminars in Dialysis, 2006. **19**(4): p. 297-304.
112. Grouzi, E., *Update on argatroban for the prophylaxis and treatment of heparin-induced thrombocytopenia type II.* J Blood Med, 2014. **5**: p. 131-41.
113. Johnson, R.J., *Complement activation by biomaterials.* Prog Clin Biol Res, 1990. **337**: p. 507-12.
114. Lander, H., M. Zammert, and D. FitzGerald, *Anticoagulation management during cross-clamping and bypass.* Best Pract Res Clin Anaesthesiol, 2016. **30**(3): p. 359-70.
115. Reddy, K.R., et al., *Temperature regime and carbon dioxide enrichment alter cotton roll development and fiber properties.* Agronomy Journal, 1999. **91**(5): p. 851-858.
116. Krajewski, S., et al., *Hypercoagulant Abdominal Swabs in Cardiac Surgery: Potential Problems and Background.* Thorac Cardiovasc Surg, 2016. **64**(7): p. 589-595.
117. Shimamoto, T., *Polyurethane sheet: a potential substitute of surgical cotton gauze.* J Cardiothorac Surg, 2011. **6**: p. 26.
118. Sutton, S.W., et al., *Clinical benefits of continuous leukocyte filtration during cardiopulmonary bypass in patients undergoing valvular repair or replacement.* Perfusion, 2005. **20**(1): p. 21-9.
119. Blair, P. and R. Flaumenhaft, *Platelet alpha-granules: basic biology and clinical correlates.* Blood Rev, 2009. **23**(4): p. 177-89.
120. Mansour, A., et al., *Platelet Functions During Extracorporeal Membrane Oxygenation. Platelet-Leukocyte Aggregates Analyzed by Flow Cytometry as a Promising Tool to Monitor Platelet Activation.* J Clin Med, 2020. **9**(8).
121. Lacy, P., *Mechanisms of degranulation in neutrophils.* Allergy Asthma Clin Immunol, 2006. **2**(3): p. 98-108.
122. Zhang, J.N., et al., *Platelet aggregation and activation under complex patterns of shear stress.* Thromb Haemost, 2002. **88**(5): p. 817-21.
123. Osterud, B. and E. Bjorklid, *Sources of tissue factor.* Semin Thromb Hemost, 2006. **32**(1): p. 11-23.
124. Kambas, K., et al., *Autophagy mediates the delivery of thrombogenic tissue factor to neutrophil extracellular traps in human sepsis.* PLoS One, 2012. **7**(9): p. e45427.
125. Zelaya, H., A.S. Rothmeier, and W. Ruf, *Tissue factor at the crossroad of coagulation and cell signaling.* Journal of Thrombosis and Haemostasis, 2018. **16**(10): p. 1941-1952.
126. Zhuo, R., C.A. Siedlecki, and E.A. Vogler, *Autoactivation of blood factor XII at hydrophilic and hydrophobic surfaces.* Biomaterials, 2006. **27**(24): p. 4325-4332.
127. Mandle, R., Jr. and A.P. Kaplan, *Hageman factor substrates. Human plasma prekallikrein: mechanism of activation by Hageman factor and participation in hageman factor-dependent fibrinolysis.* J Biol Chem, 1977. **252**(17): p. 6097-104.

128. Wiggins, R.C., et al., *Role of high-molecular-weight kininogen in surface-binding and activation of coagulation Factor XI and prekallikrein.* Proc Natl Acad Sci U S A, 1977. **74**(10): p. 4636-40.
129. Dray, A. and M. Perkins, *Bradykinin and inflammatory pain.* Trends Neurosci, 1993. **16**(3): p. 99-104.
130. Trunk, S., et al., *Inflammatory potential of cotton-based surgically invasive devices: Implications for cardiac surgery.* J Biomed Mater Res B Appl Biomater, 2019. **107**(6): p. 1877-1888.
131. Dinarello, C.A., *Blocking IL-1 in systemic inflammation.* J Exp Med, 2005. **201**(9): p. 1355-9.
132. Norris, C.A., et al., *Synthesis of IL-6 by Hepatocytes Is a Normal Response to Common Hepatic Stimuli.* Plos One, 2014. **9**(4).
133. Janowski, M., *Functional diversity of SDF-1 splicing variants.* Cell Adh Migr, 2009. **3**(3): p. 243-9.
134. McCandless, E.E., et al., *IL-1R Signaling within the Central Nervous System Regulates CXCL12 Expression at the Blood-Brain Barrier and Disease Severity during Experimental Autoimmune Encephalomyelitis.* Journal of Immunology, 2009. **183**(1): p. 613-620.
135. Chatterjee, M., et al., *SDF-1alpha induces differential trafficking of CXCR4-CXCR7 involving cyclophilin A, CXCR7 ubiquitination and promotes platelet survival.* FASEB J, 2014. **28**(7): p. 2864-78.
136. Sun, X.Q., et al., *CXCL12/CXCR4/CXCR7 chemokine axis and cancer progression.* Cancer and Metastasis Reviews, 2010. **29**(4): p. 709-722.
137. Massberg, S., et al., *Platelets secrete stromal cell-derived factor 1alpha and recruit bone marrow-derived progenitor cells to arterial thrombi in vivo.* J Exp Med, 2006. **203**(5): p. 1221-33.
138. Chatterjee, M., et al., *Platelet-derived CXCL12 regulates monocyte function, survival, differentiation into macrophages and foam cells through differential involvement of CXCR4-CXCR7.* Cell Death & Disease, 2015. **6**.
139. Clancy, D.M., et al., *Extracellular Neutrophil Proteases Are Efficient Regulators of IL-1, IL-33, and IL-36 Cytokine Activity but Poor Effectors of Microbial Killing.* Cell Rep, 2018. **22**(11): p. 2937-2950.
140. Hernandez, M.R., et al., *Biocompatibility of cellulosic and synthetic membranes assessed by leukocyte activation.* Am J Nephrol, 2004. **24**(2): p. 235-41.
141. Castelli, W.A., et al., *Cheek mucosa response to silk, cotton, and nylon suture materials.* Oral Surg Oral Med Oral Pathol, 1978. **45**(2): p. 186-9.
142. Jang, J. and W.S. Go, *Continuous photografting of HEMA onto polypropylene fabrics with benzophenone photoinitiator.* Fibers and Polymers, 2008. **9**(4): p. 375-379.

7 Anhang:

7.1 Liste aller wissenschaftlichen Veröffentlichungen

Katharina Gerling, Sabrina Ölschläger, Meltem Avci-Adali, Bernd Neumann, Ernst Schweizer, Christian Schlensak, Hans Peter Wendel, Sandra Stoppelkamp

"A Novel C1-esterase inhibitor oxygenator coating prevents FXII activation in human blood." Biomolecules 10.7 (2020): 1042

Katharina Gerling*, Lisa Maria Herrmann*, Christoph Salewski, Melanie Wolf, Pia-Müllerbader, Dorothea Siegel-Axel, Hans-Peter Wendel, Christian Schlensak, Meltem Avci-Adali und Sandra Stoppelkamp

* gleichermaßen beigetragen

"Synthetic Material Abdominal Swabs Reduce Activation of Platelets and Leukocytes Compared to Cotton Materials." Biomolecules 11.7 (2021): 1023

Heidrun Steinle, Josefin Weber, Sandra Stoppelkamp, **Katharina Große-Berkenbusch**, Sonia Golombek, Marbod Weber, Tuba Canak-Ipek, Sarah-Maria Trenz, Christian Schlensak, Meltem Avci-Adali

"Delivery of synthetic mRNAs for tissue regeneration." Advanced drug delivery reviews 179 (2021): 114007.

Katharina Große-Berkenbusch, Meltem Avci-Adali, Madeleine Arnold, Linda Cahalan, Patrick Cahalan, Ana Velic, Boris Maček, Christian Schlensak, Hans Peter Wendel, Sandra Stoppelkamp

"Profiling of time-dependent human plasma protein adsorption on non-coated and heparin-coated oxygenator membranes." Biomaterials Advances 139 (2022): 213014.

Lena Witzdam, Berlind Vosberg, **Katharina Große-Berkenbusch**, Sandra Stoppelkamp, Hans Peter Wendel, Cesar Rodriguez-Emmenegger

"Tackling the Root Cause of Surface-Induced Coagulation: Inhibition of FXII Activation to Mitigate Coagulation Propagation and Prevent Clotting." Macromolecular Bioscience 24.2 (2024): 2300321.

Katharina Große-Berkenbusch, Meltem Avci-Adali, Patrick Cahalan, Linda Cahalan, Ana Velic, Boris Maček, Christian Schlensak, Hans Peter Wendel, Sandra Stoppelkamp

“Comparative study of flow rate- and material-dependent human plasma protein adsorption on oxygenator membranes and heat exchanger materials”. Frontiers in Cardiovascular Medicine, 12, 1578538

7.2 Anteil an gemeinschaftlichen Veröffentlichungen

Erklärung nach § 5 Abs. 2 Nr. 8 der Promotionsordnung der Math.-Nat. Fakultät
-Anteil an gemeinschaftlichen Veröffentlichungen-
Nur bei kumulativer Dissertation erforderlich!

List of Publications

1. A Novel C1-esterase inhibitor oxygenator coating prevents FXII activation in human blood." Biomolecules 10.7 (2020): 1042

List of authors: Katharina Gerling, Sabrina Ölschläger, Meltem Avci-Adali, Bernd Neumann, Ernst Schweizer, Christian Schlensak, Hans Peter Wendel, Sandra Stoppelkamp

2. Synthetic Material Abdominal Swabs Reduce Activation of Platelets and Leukocytes Compared to Cotton Materials." Biomolecules 11.7 (2021): 1023

List of authors: Katharina Gerling*, Lisa Maria Herrmann*, Christoph Salewski, Melanie Wolf, Pia Müllerbader, Dorothea Siegel-Axel, Hans-Peter Wendel, Christian Schlensak, Meltem Avci-Adali und Sandra Stoppelkamp (* contributed equally)

3. Profiling of time-dependent human plasma protein adsorption on non-coated and heparin-coated oxygenator membranes." Biomaterials Advances 139 (2022): 213014.

List of authors: Katharina Große-Berkenbusch, Meltem Avci-Adali, Madeleine Arnold, Linda Cahalan, Patrick Cahalan, Ana Velic, Boris Maček, Christian Schlensak, Hans Peter Wendel, Sandra Stoppelkamp

4. Comparative study of flow rate-and material-dependent human plasma protein adsorption on oxygenator membranes and heat exchanger materials." Frontiers in Cardiovascular Medicine 12 (2025): 1578538.

List of authors: Katharina Große-Berkenbusch, Meltem Avci-Adali, Patrick Cahalan, Linda Cahalan, Ana Velic, Boris Maček, Christian Schlensak, Hans Peter Wendel, Sandra Stoppelkamp

Nr.	**Accepted publication yes/no**	**List of authors**	Position of candidate in list of authors	Scientific ideas by the candidate (%)	Data generation by the candidate (%)	Analysis and Interpretation by the candidate (%)	Paper writing done by the candidate (%)
1	yes	see 1	1.	60	90	90	75
2	yes	see 2	1. (shared)	40	50	80	70
3	yes	see 3	1.	40	80	85	70
4	yes	see 4	1.	20	80	50	35

8 Wissenschaftliche Veröffentlichungen im Original

8.1 Publikation I:

Profiling of time-dependent human plasma protein adsorption on non-coated and heparin-coated oxygenator membranes

139 (2022) 213014

Contents lists available at ScienceDirect

Biomaterials Advances

journal homepage: www.journals.elsevier.com/materials-science-and-engineering-c

Profiling of time-dependent human plasma protein adsorption on non-coated and heparin-coated oxygenator membranes

Katharina Große-Berkenbusch [a], Meltem Avci-Adali [a], Madeleine Arnold [a], Linda Cahalan [b], Patrick Cahalan [b], Ana Velic [c], Boris Maček [c], Christian Schlensak [a], Hans Peter Wendel [a], Sandra Stoppelkamp [a,*]

[a] Clinical Research Laboratory, Department of Thoracic and Cardiovascular Surgery, University Hospital Tübingen, University of Tübingen, Calwerstr. 7/1, 72076 Tübingen, Germany
[b] Ension Inc, 508 Pittsburg Road, Butler, PA 16002, United States of America
[c] Proteome Center Tübingen, Interfaculty Institute for Cell Biology, University of Tübingen, Auf der Morgenstelle 15, 72076 Tübingen, Germany

ARTICLE INFO

Keywords:
ECMO
Hollow fiber membrane
Heparin-coating
Plasma protein adsorption
Complement
Coagulation

ABSTRACT

Patients with severe lung diseases are highly dependent on lung support systems. Despite many improvements, long-term use is not possible, mainly because of the strong body defence reactions (e.g. coagulation, complement system, inflammation and cell activation). The systematic characterization of adsorbed proteins on the gas exchange membrane of the lung system over time can provide insights into the course of various defence reactions and identify possible targets for surface modifications. Using comprehensive mass spectrometry analyses of desorbed proteins, we were able to identify for the first time binding profiles of over 500 proteins over a period of six hours on non-coated and heparin-coated PMP hollow fiber membranes. We observed a higher degree of remodeling of the protein layer on the non-coated membrane than on the coated membrane. In general, there was a higher protein binding on the coated membrane with exception of proteins with a heparin-binding site. Focusing on the most important pathways showed that almost all coagulation factors bound in higher amounts to the non-coated membranes. Furthermore, we could show that the initiator proteins of the complement system bound stronger to the heparinized membranes, but the subsequently activated proteins bound stronger to the non-coated membranes, thus complement activation on heparinized surfaces is mainly due to the alternative complement pathway. Our results provide a comprehensive insight into plasma protein adsorption on oxygenator membranes over time and point to new ways to better understand the processes on the membranes and to develop new specific surface modifications.

1. Introduction

Critically ill patients with lung disease are highly dependent on lung support or replacement systems. The need for such systems has also increased due to the COVID-19 pandemic. Currently, extracorporeal membrane oxygenation (ECMO) is the only treatment option for replacing lung function [1]. The central element of ECMO is the gas exchange membrane. The deoxygenated blood is diverted from the body and flows along the hollow fiber membranes (HFMs). Oxygen passes through the inner lumen of the membrane fibers and diffuses into the blood, while carbon dioxide is removed [2]. Mostly, HFM made of polypropylene (PP) or polymethylpentene (PMP) are used [3], where untreated PP is prone to plasma leakage [4], but can be treated to prolong its tightness [5]. Usually, a PMP membrane is used for long-term ECMO to avoid complications due to plasma leakage [6]. In addition, PMP is an efficient and low resistance artificial gas exchange membrane. Other blood-contacting components of ECMO are the blood reservoir, mechanical blood pump, heat exchanger, and circulatory tubing system

Abbreviations: ECMO, extracorporeal membrane oxygenation; HFM, hollow fiber membranes; PP, polypropylene; PMP, polymethylpentene; EBS, Ension Bioactive Surface; PEI, polyethyleneimine; NAD, nitrous acid-degraded; PVC, polyvinylchloride; TAT, thrombin-antithrombin III complex; PMN, polymorphonuclear; PRM, pattern recognition molecule.

* Corresponding author at: Clinical Research Laboratory, Department of Thoracic and Cardiovascular Surgery, University Hospital Tübingen, University of Tübingen, Calwerstr. 7/1, 72076 Tübingen, Germany.
E-mail address: Sandra.Stoppelkamp@klinikum.uni-tuebingen.de (S. Stoppelkamp).

https://doi.org/10.1016/j.bioadv.2022.213014
Received 11 March 2022; Received in revised form 2 June 2022; Accepted 30 June 2022
Available online 5 July 2022

[2,7]. Despite the benefits of assisting the patient's oxygenation, its use is also associated with various risks to the patient. Common complications include the occurrence of thromboembolic complications or bleeding at the cannula site due to the need for systemic anticoagulation [8].

A large membrane surface area is necessary for adequate oxygenation, but it can lead to various reactions such as coagulation, complement activation, and inflammation [9]. It is known that protein adsorption plays a crucial role in the course of biological reactions and cellular interactions with a large foreign surface [10,11]. The proteins adsorb within a few seconds to the artificial surface when material comes into contact with a living system, and a protein monolayer is formed within a few minutes [12,13]. A better understanding of the relationship between protein adsorption and the progression of biological pathways on surfaces is critical for the development of new biomaterials [14–16]. The study of competing proteins during adsorption is also important, as biomaterials are exposed to protein mixtures with different affinities for the surface [17–19]. Using proteomics, it is possible to determine the identity and concentration of hundreds of proteins in a complex sample simultaneously [20]. In the past, adsorption of a few proteins such as albumin, immunoglobulin-γ (IgG), and fibrinogen have been studied [21,22]. However, also other proteins are known to be present in the adsorbed layer. Often the interactions between the proteins on the surface are non-covalent [23] but examples of covalent binding have also been described [12]. Protein adsorption on biomaterials can be specific or nonspecific due to differences in surface chemistry and properties, and competitive adsorption [24].

The main goal of this study was to determine the time-dependent differences in protein adsorption to non-coated and heparin-coated oxygenator membranes. The binding profile of proteins from plasma to heparin-coated and non-coated membranes was analyzed in loop circuits over 6 h.

2. Materials and methods

2.1. Miniature devices with hollow-fiber oxygenator membranes

For the miniature devices, PMP HFMs (OXYPLUS®, 3 M Membrana, Wuppertal, Germany) with an outer fiber diameter of 380 ± 30 μm and a wall thickness of 90 ± 10 μm, resulting in an inner diameter of 200 ± 50 μm, were used. One HFM piece (14 × 10 cm, approx. 210 cm^2 surface area) (coated and non-coated, respectively) was coiled and placed in a 3/8-in. polyvinylchloride tubing (Raumedic, Helmbrechts, Germany). A 3/8 in. to 1/4-in. polycarbonate straight connector was attached to both ends. The volume of the whole device was approx. 10 ml. No oxygen supply was connected. A schematic of the miniature devices is shown in Supplementary Fig. 1a.

2.2. Heparin-coating of the miniature devices

The HFMs and all other blood contacting surfaces of miniature devices were covalently coated with heparin using the Ension Bioactive Surface (EBS) coating technology. The fundamental concepts of EBS coating have been described by Johnson et al. [19]. Briefly, aqueous free radical activation and oxygenation of the material surface were performed followed by coupling of a polyethyleneimine (PEI, BASF, Ludwigshafen, Germany) spacer to which nitrous acid-degraded (NAD) heparin (Celsus, Cincinnati, OH) was coupled. The successful coating with PEI is demonstrated by ponceau S staining and heparin coating is detected by toluidine blue staining Supplementary Fig. 1b-c. The coating technology yields approx. 3.5 μg heparin per cm^2 as tested by the coating specialists from Ension. According to the analyses of the coating technology, bioactivity correlates with the amount of heparin on the surface.

2.3. Experimental setup

To characterize the adsorption of plasma proteins, heparin-coated and non-coated PMP membranes were inserted into miniature devices and a loop circuit was created using a 1/4-in. polyvinylchloride (PVC) tubing (Raumedic, Helmbrechts, Germany) (Fig. 1). The volume of the whole circuit was approx. 50 ml. Before starting, the test system was filled with isotonic saline (0.9 % NaCl, Fresenius Kabi, Bad Homburg, Germany), which was circulated (flow rate 1 l/min) for approximately 10 to 15 min to rinse and wet all surfaces. The NaCl solution was drained and replaced by blood or plasma.

2.4. Blood and plasma sampling

Whole blood and plasma for the studies were obtained from the donor pool of the transfusion service of the University Hospital Tuebingen. Frozen citrated plasma was used for the plasma experiments. After thawing, 3 IU/ml sodium heparin (25.000 I.E/5 ml; LEO Pharma GmbH, Neu-Isenburg, Germany) was added and recalcified with calcium chloride (Baxter, Glenview, USA) depending on the citrate concentration (calculated by the transfusion service). For the whole blood experiments, 500 ml of fresh, heparinisized (3 IU/ml) whole blood from the transfusion service was used. The whole blood was diluted with 100 ml ringer lactate solution (Fresenius, Bad Homburg, Germany) consisting of 1.3 % glucose solution (Delta-Pharma GmbH, Pfullingen, Germany) and 53 mM $NaHCO_3$ (Braun Melsungen AG, Melsungen, Germany).

2.5. Incubation with plasma

Since the simultaneous performance of loop circuits with miniature devices containing non-coated or heparin-coated PMP membranes required a large plasma volume, it was not possible to perform this with blood from a single donor. Therefore, the comparative analyses over time were performed using pooled human plasma instead. Each pool consisted of plasma from three donors. For time-dependent protein adsorption on heparin-coated and non-coated PMP membranes, a separate circulation system was operated for each different time point. For this purpose, the separate circulation systems were filled with 50 ml plasma, the plasma was pumped through the system for either 1, 5, 10, 30, 60, 180, or 360 min at a flow rate of 1 l/min. After the appropriate incubation time, the system was rinsed with 1 l NaCl solution and the washed membrane was removed. To desorb the proteins, the membrane was dynamically incubated for 30 min in 10 ml lysis buffer containing 1 % LDS (Carl Roth, Karlsruhe, Germany) in phosphate-buffered saline (PBS; Thermo Scientific, Waltham, USA), phosphatase inhibitors (1 mM sodium orthovanadate, 5 mM glycerol-2-phosphate, 5 mM sodium

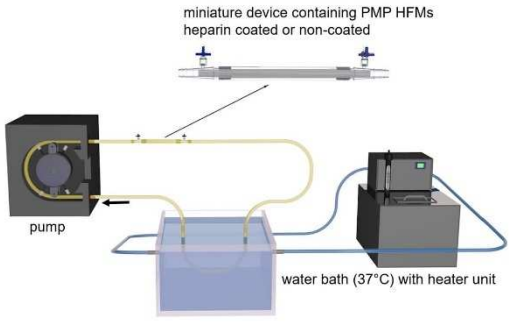

Fig. 1. Schematic representation of the experimental setup for the analysis of plasma protein adsorption over time on oxygenator membranes in a miniature device.

fluoride (all from Sigma-Aldrich, St. Louis, USA), and protease inhibitor cocktail (Roche complete, Mannheim, Germany). The protein solution was concentrated using Amicon Ultra-15 PLBC Ultracel-PL Membrane 3 kDa (Merck, Darmstadt, Germany) at 4000 x g for 45 min. The protein concentration of each sample was determined using Pierce™ BCA Protein Assay Kit (Thermo Fisher Scientific, Waltham, USA) as described by the manufacturer.

2.6. Incubation with whole blood

For the experiments with heparinized whole blood (3 IU/ml), a blood reservoir was connected to the loop circuit. Before starting the incubation, a baseline sample was taken to determine the initial values of the individual parameters in the blood of the respective donor. A miniature device containing heparin-coated PMP membrane was connected to the loop circuit and filled with whole blood. Blood flow was 1 l/min and the temperature was 37 °C. Blood samples were taken from the loop circuit at different time points during the 360-min circulation period (1, 5, 10, 30, 60, 90, 180, and 360 min after the start of circulation).

The blood samples obtained were investigated using ELISA for changes in activation of the coagulation (thrombin-antithrombin III complex (TAT)), complement system (SC5b-9), platelets (β-thromboglobulin (β-TG), and inflammation (polymorphonuclear (PMN) elastase). Depending on the manufacturer's instructions, various anticoagulants were added and plasma was obtained by centrifugation. Plasma samples were shock-frozen and stored at −20 °C or −80 °C. All ELISAs were performed according to the manufacturer's instructions. SC5b-9 (MicroVue™ Complement, Quidel, Osteomedical GmbH, Sissach, Switzerland) was determined in EDTA plasma, TAT (Enzygnost® TAT micro, Siemens Healthcare, Erlangen, Germany), and PMN elastase (PMN Elastase ELISA, Demeditec Diagnostics, Kiel, Germany) in citrated plasma and β-TG (Asserachrome® β-TG, Diagnostica Stago, Parsippany, NJ, USA) in CTAD-anticoagulated plasma. The blood cell counts were measured directly with an automatic cell counter (ABX Micros 60, Horiba Medical, Kyoto, Japan). To evaluate if both plasma or blood incubation of PMP HFM lead to similar time-dependent protein adsorption, the desorbed proteins after plasma and blood incubations were compared after 360 min. Protein adsorption was performed in the same way as described in Section 2.5.

2.7. Mass spectroscopy(MS) analysis of adsorbed proteins

SDS-PAGE short gel purification and in-gel digestion with Trypsin were performed as described previously [25]. The extracted peptides were desalted using C18 StageTips [26] and subjected to LC-MS/MS analysis. LC-MS/MS analyses were performed on an Easy-nLC 1200 UHPLC (ultra-high-performance liquid chromatography) (Thermo Fisher Scientific) coupled to an QExactive HF Orbitrap mass spectrometer (Thermo Fisher Scientific) as described elsewhere [27]. Peptides were eluted with a 60 min segmented gradient at a flow rate of 200 nl/min, with the 20 most intensive peaks selected for fragmentation with higher-energy collisional dissociation (HCD). The MS data were processed with MaxQuant software suite v. 1.5.2.8 and v.1.6.7.0 [28]. The label-free-quantification (LFQ) was enabled. Database search was performed using the Andromeda search engine against human (96,817 entries) UniProt database [29].

2.8. Statistics

Experiments were performed with the blood from three independent donors and three different plasma pools. Significant differences of individual proteins adhered to the heparin-coated or non-coated membranes were analyzed using unpaired two-tailed Student's *t*-tests assuming equal variance. All data sets for ELISAs showing normal distribution were analyzed with a one-way analysis of variance (ANOVA) and Bonferroni's post hoc test for multiple comparisons to detect differences between the time points. For non-normally-distributed data sets, Kruskal–Wallis test with Dunn's multiple comparison test was used. Statistical significance was defined as $p < 0.05$. Statistical analysis was performed using Microsoft Excel 365 (Microsoft, Albuquerque, USA) and GraphPad Prism version 6.01 (GraphPad Software Inc., La Jolla, CA, USA).

3. Results

3.1. Comparison of adsorbed proteins after blood or plasma incubation

The main scope of our research was to ascertain the time-dependent plasma protein adsorption on the oxygenator membranes. An initial comparison between the protein adsorption from blood or plasma was performed at 360 min to ascertain differential outcomes. In total (blood and plasma, after 360 min), 1371 desorbed proteins were detected by MS. A considerably high number of those (1280 proteins) were seen after incubation with blood. These were mainly intracellular proteins from cells, which were still adherent to the membrane after washing. A relatively small number, 256 proteins, was detected after incubation with plasma and 163 proteins were found after both types of incubation (blood and plasma). The biggest part of these proteins (101 proteins) was mostly not significantly different in their abundance. A detailed comparison is given in the supplementary data (Supplementary Fig. 2), along with a full list of desorbed proteins measured by MS (Supplementary Table 1). Overall, the data showed a high level of congruency between blood and plasma, especially for complement-related proteins (Supplementary Fig. 3). Since we wanted to focus on differences in time-dependent plasma protein adsorption, the protein adsorption differences between 1 min and 6 h were investigated with plasma.

3.2. Differentially detected proteins on heparin-coated and non-coated membranes

MS analyses over time revealed a lower number of different adsorbed proteins (353) on heparinized PMP-HFMs than on non-coated HFMs (525) (Table 1). A total of 106 proteins were detected only on the heparin-coated membranes, while 278 proteins were detected only on the non-coated membranes. In general, these proteins detected only on one type of membrane tended to be proteins bound in lower quantities. The number of proteins detected on both types of membranes, non-coated and heparinized, was 247 (corresponding to 39.1 %) (Fig. 2a). Looking at those proteins present at each of the time points (Fig. 2b), the overlap was even higher with over 55 % present on both membrane types. All proteins detected over time are listed in Supplementary Table 1.

Apart from describing the pure presence of adsorbed proteins, their relative abundances (measured as LFQ) are important to evaluate the remodeling of the protein layer. Therefore, we first compared the changes in abundances of the adsorbed proteins over time (1 min compared to 360 min) on non-coated (Fig. 3a) and heparin-coated (Fig. 3b) HFM. The proportion of proteins that decreased significantly over time (50 proteins; 23 %) was higher on non-coated HFMs than on heparinized HFMs (2 proteins; CFH and APOC2; 1 %). On the other hand, the proportion of proteins that significantly increased over time was higher on heparinized HFMs (31 %) than on non-coated HFMs (12 %), although the total numbers of changed proteins were very similar (27 vs. 26, respectively). The comparison of the effect of coating at each time point showed that heparinization of the membrane significantly lowered the relative amount of bound proteins between 36 % to 73 % (Supplementary Fig. 4), whereas only 3 %–22 % of proteins significantly increased on the coating. The latter were mostly proteins with affinity for heparin, such as ATIII, ficolin, and C1. The greatest effect of increase or decrease in proteins was observed at 10 min.

Table 1
Number of desorbed proteins measured at different time points on non-coated and heparin-coated PMP membranes via MS, $n = 3$.

		Incubation time (min)							
	PMP membrane	1	5	10	30	60	90	180	360
Numbers of desorbed proteins	Non-coated	340	335	365	341	365	358	372	356
	Heparin-coated	276	251	269	303	269	272	246	256

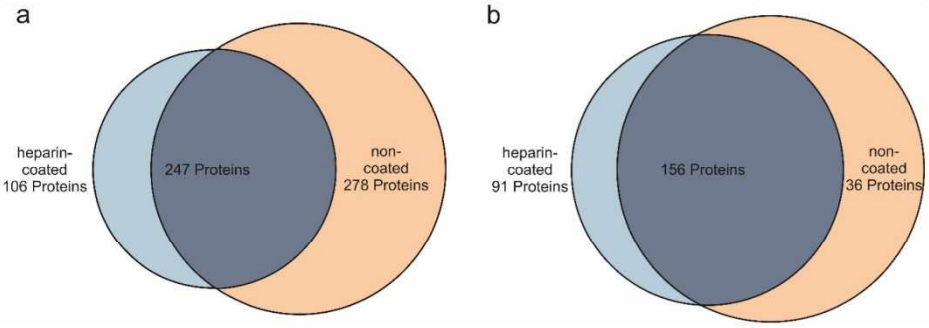

Fig. 2. Venn-Diagrams showing the number of proteins detected on heparin- and/or non-coated HFMs with human plasma. (a) total numbers of proteins on the membrane types present at least at one of the time points; (b) total numbers of proteins on the membrane types present at each time point.

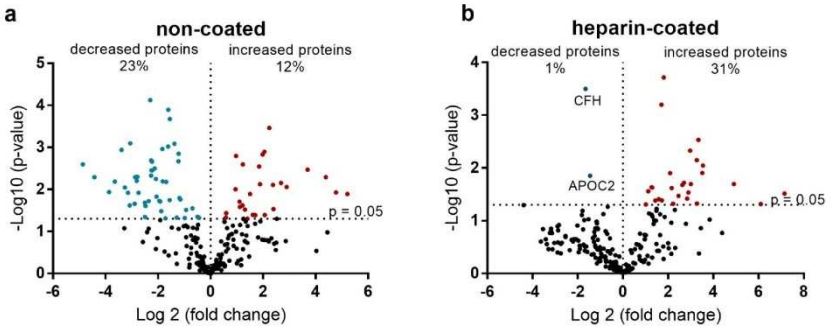

Fig. 3. Volcano plot showing the change in protein abundance from 1 min compared to 360 min. (a) On the non-coated membrane, the abundance of 50 proteins (23 %) decreased and 26 proteins (12 %) increased after 360 min. (b) While the heparin coating resulted in a decrease of only 2 proteins (1 %; CFH and APOC2) and an increase of 27 proteins (31 %) after 360 min.

3.3. Identifying the most abundant proteins on heparin-coated and non-coated membranes

The 10 most abundant proteins detected on non-coated (Table 2) and coated PMP membranes (Table 3) were identified to gain a better understanding of the main protein layer composition. The order of abundance of all proteins is provided in Supplementary Table 1. Proteins shaded in Tables 2 and 3 in gray indicate significantly increased protein amounts compared to the coated or non-coated membrane type. Notably, large differences between membrane types were observed already after 1 min (gray-shaded proteins, Table 2) and in general, more significantly higher abundances were observed on the non-coated membrane, supporting the observations in the volcano plots (Supplementary Fig. 4). The adhesion of fibrinogen (FGA, FGB, FGG) was significantly lower on the heparin-coated surface already after 1 min, which was further reduced after 10, 30, 90, and 180 min. However, even with the coated membrane, fibrinogen was among the 10 most abundant proteins at all time points. Significantly higher abundance within these 10 proteins was also observed for apolipoprotein A1 (APOA1), inter-alpha-trypsin inhibitor heavy chain family member 4 (ITIH4), and clusterin (CLU) after 1 min. On the coated membrane, only ficolin-2 (FCN2) (1 min, 10 min) and antithrombin III (SERPINC1) (5, 10, 30, 60 min) showed significantly higher abundance than on the non-coated membrane. The reason therefore could be the specific binding of both ficolin-2 [30] and antithrombin III [31] to heparin. A closer look at the order of abundance revealed that different apolipoproteins bind very frequently on both the coated and the non-coated membranes (Supplementary Table 1). Significantly lower binding of vitronectin was observed on the coated membrane after 1 min (Table 2), but also after 5, 10, 30, and 360 min (Supplementary Table 1). Vitronectin was replaced by other proteins in the first minutes and was no longer among the ten most abundant proteins on the non-coated membrane after 1 min, indicating lower cell-activating properties than the non-coated membrane in this respect. In addition, the binding of the von Willebrand

factor occurred significantly more frequently on the non-coated membrane after 10 min (Supplementary Table 1). In contrast to the other proteins involved in platelet adhesion, there were no significant differences in the binding of fibronectin between the coated and non-coated membranes (Table 2 and Supplementary Table 1). Serum amyloid P is known to promote leukocyte and possibly platelet aggregation by binding [32] and it was detected in higher amounts on the non-coated membrane after 5 to 360 min (Supplementary Table 1). Despite these observed differences, after 360 min, the eight most abundant proteins on both membrane types were FGA, FGB, FGG, ITIH4, C3, ALB, FN1, and APOB, with a slight change in order. Only FGA showed significantly higher abundance on the non-coated membrane than on the heparin-coated membrane. This indicates that the positive effects such as reduction of coagulation and complement of heparinization may last only a few hours.

3.4. Analysis of coagulation pathway-related proteins

The precise detection of proteins by MS allowed a detailed analysis of the presence of coagulation pathway-related proteins over time. The presence of coagulation pathway-related proteins was compared between the first (1 min) and last (360 min) time points, and a color-coded schematic illustrates the changes in protein binding on coated (right side of the protein name) and non-coated (left side of the protein name) PMP membranes over time (Fig. 4). The binding profiles of the coagulation system proteins on the heparin-coated and non-coated membranes showed that most of the proteins did not change over time (colored yellow). These proteins either bound immediately after blood contact and then remained stably attached to the membrane, or an equilibrium state occurred in which the proteins detached and rebounded. On the non-coated membranes (Fig. 4, left sides of protein names), a decrease (colored blue) in binding was observed over time for FIX, FXII, kallikrein, and kininogen. The binding abundance of these proteins remained constant on the coated membranes over time (yellow, right side of protein names), except for FIX, whose binding even significantly increased on the coated membranes (red). Over time, the coating increased the binding of the coagulation cascade proteins FVII, FIX, FX, thrombin, and HCII, but also of vWF, α2AP, and plasmin (Fig. 4, right side of the box, red).

The quantities of the major coagulation-related proteins at each time point are shown in Fig. 5. Notably, a decrease in initial contact phase activation proteins (FXII, FXI, kallikrein, and kininogen) was observed on the non-coated membranes over time. Compared with coated membranes, significantly higher FXII(a), kallikrein, and KNG binding were detected on non-coated membranes during the first time points. After approximately 60 min, no significant differences were observed between coated and non-coated membranes. FXI(a) was mainly present on the coated membranes. Interestingly, FIX, which is activated by FXI, showed higher adsorption to non-coated membranes, but the amount decreased over time to the levels on the heparinized membranes. Although FX showed significantly increased binding to the non-coated membranes only after 1 min and no differences were detected between non-coated and coated membranes. FV, which usually forms the prothrombinase complex together with FX [34], was present in a significantly higher amount on non-coated surfaces at almost all time points. Significantly higher amounts of fibrinogen were detected on non-coated membranes at all time points. Similar to FXI(a), significantly higher amounts of ATIII were observed on coated membranes than on non-coated membranes at all time points, likely due to the affinity for heparin [35]. Increased plasmin binding was observed only after 1 min on the non-coated membrane compared with the heparin-coated membrane. No significant differences were detected in thrombin binding.

In addition to protein adsorption on the membranes over time, the effect of heparin-coated PMP membranes on coagulation was measured in human blood over time (Supplementary Fig. 5). As coagulation occurs in close interaction between plasma proteins and cells, the observation of platelet activation and coagulation activation in blood over time provides an additional indication of the sequence of events. Over time, an increase in coagulation activation, measured by TAT, and platelet activation, measured by β-TG, was detected in the blood. While platelet activation was seen already after the first minute with constantly rising values, TAT remained relatively low up to 90 min and then increased considerably. This increase in TAT measured in blood was not paralleled by an increased thrombin adsorption on the membranes after 90 min.

3.5. Analysis of complement system activation-related proteins

In addition to the analysis of proteins involved in the coagulation pathway, the binding profiles of proteins related to the complement system were analyzed. The presence of complement system-related

Table 2

non-coated	1 min	5 min	10 min	30 min	60 min	90 min	180 min	360 min
1	FGA	FGA	FGG	FGB	FGB	FGA	FGA	FGA
2	FGG	FGG	FGA	FGA	FGA	FGG	FGG	FGB
3	FGB	FGB	FGB	FGG	FGG	FGB	FGB	FGG
4	ALB	ALB	ALB	ALB	ALB	ALB	ITIH4	ITIH4
5	APOA1	APOA1	APOA1	ITIH4	C3	ITIH4	ALB	C3
6	FN1	ITIH4	FN1	C3	ITIH4	C3	C3	ALB
7	ITIH4	FN1	C3	APOB	IGHG1	FN1	APOB	FN1
8	VTN	APOE	ITIH4	FN1	APOB	APOB	FN1	APOB
9	APOE	APOB	APOB	APOA1	FN1	APOA1	CLU	CLU
10	CLU	C3	IGHG1	IGHG1	APOA1	IGHG1	APOA1	IGHG1

The ten most abundant proteins on non-coated PMP membranes. Gray-shaded proteins are significantly more abundant than on the coated membrane. Gene names: ALB: serum albumin, CP: ceruloplasmin, GSN: gelsolin, RBP4: retinol-binding protein 4, C3: complement C3, HPX: hemopexin, APOA1: apolipoprotein A1, A2M: alpha-2-macroglobulin, APOD: apolipoprotein D, SERPINC1: antithrombin III, FGA: fibrinogen alpha chain, FGG: fibrinogen gamma chain, FGB: fibrinogen beta chain, FN1: fibronectin 1, ITIH4: inter-alpha-trypsin inhibitor heavy chain family member 4, VTN: vitronectin, APOE: apolipoprotein E, CLU: clusterin, APOB: apolipoprotein B, IGHG1: g gamma-1 chain C region; LBP: lipopolysaccharide-binding protein, FCN2: ficolin 2, TF: transferrin.

Table 3

coated	1 min	5 min	10 min	30 min	60 min	90 min	180 min	360 min
1	APOB	ALB	APOB	ALB	FGA	APOB	ALB	FGA
2	ALB	FGG	FGG	APOB	APOB	FGA	FGG	FGB
3	SERPINC1	FGA	ALB	FGG	FGB	FGB	APOB	APOB
4	FGG	FGB	FGA	FGA	FGG	FGG	FGA	FGG
5	FGA	APOB	SERPINC1	FGB	ALB	ALB	FGB	ALB
6	APOE	FN1	FGB	SERPINC1	SERPINC1	SERPINC1	ITIH4	ITIH4
7	FGB	SERPINC1	APOE	APOE	FN1	APOE	C3	FN1
8	LBP	C3	FN1	C3	APOE	C3	FN1	C3
9	FCN2	APOE	FCN2	TF	C3	FN1	SERPINC1	SERPINC1
10	FN1	TF	LBP	FN1	ITIH4	ITIH4	APOE	APOE

The ten most abundant proteins on heparin-coated PMP membranes. Gray shaded proteins are significantly more abundant than on the non-coated membrane. Gene names: ALB: serum albumin, CP: ceruloplasmin, GSN: gelsolin, RBP4: retinol-binding protein 4, C3: complement C3, HPX: hemopexin, APOA1: apolipoprotein A1, A2M: alpha-2-macroglobulin, APOD: apolipoprotein D, SERPINC1: antithrombin III, FGA: fibrinogen alpha chain, FGG: fibrinogen gamma chain, FGB: fibrinogen beta chain, FN1: fibronectin 1, ITIH4: inter-alpha-trypsin inhibitor heavy chain family member 4, VTN: vitronectin, APOE: apolipoprotein E, CLU: clusterin, APOB: apolipoprotein B, IGHG1: g gamma-1 chain C region; LBP: lipopolysaccharide-binding protein, FCN2: ficolin 2, TF: transferrin.

proteins was compared between the first (1 min) and last (360 min) time points of incubation and a color-coded schematic illustrates the changes in protein binding on coated (right side of the protein name) and non-coated (left side of the protein name) PMP membranes over time (Fig. 6). The presence of a few complement system proteins remained stable over time. Especially, the initiator proteins of the classical pathway and the complement factor H-related proteins (CFHR) were detected stably over time on both membrane types (colored yellow). Complement factor H was significantly reduced over time (blue) on both membrane types and C5, C7, and C9 were significantly increased over time (red). The other proteins did not show the same adsorption pattern on the coated membrane as on the non-coated membrane. Especially ficolins, as initiators of the lectin pathway showed significantly decreased binding on the non-coated membrane over time ($p = 0.0502$) while those were not significantly different on the heparinized membrane. Central components of the MAC complex (C6, C8) were bound significantly stronger on the heparinized membranes. Two of the C3 convertase-related proteins, C3 and FB, were increased on non-coated membranes but the amount was stable over time on heparinized membranes, while the amount of C4 was increased on coated membranes and stable on non-coated membranes.

The quantities of the major proteins of the complement at each time point are shown in Fig. 7. Interestingly, the initiator proteins of the classical pathway (C1-complex) and the lectin pathway (ficolin-1, ficolin-2, MASP-1, MASP-2) were detected in significantly higher amounts on the coated membranes. In contrast, complement factors C4 and C2, which form the C3 convertase after activation by initiator proteins, were detected in higher amounts on non-coated membranes. Complement factor B (FB), the central complement factor C3, FH, and FI were detected in increased amounts on the non-coated membrane. Such an increase was also observed for the components of the MAC complex and the inhibitors of the complement system (Supplementary Table 1). An exception was C1-INH, which was found significantly increased on coated membranes (Supplementary Table 1). Although complement FH serves as a cofactor for FI, FH and FI do not show the same binding profile as other binding partners (see C1q and C1r/C1s or ficoline and MASP, Figs. 6 and 7). FH still binds relatively frequently to the heparin-coated surface, FI binds only sporadically or not at all to the coated membrane.

To investigate the effect of heparin-coated membrane contact with blood on activation of the complement system and the initiation of inflammatory processes the concentration of sC5b-9 and PMN elastase were measured by ELISA in the blood (Supplementary Fig. 6). An increased sC5b-9 level as well as a higher PMN elastase release from the neutrophils was observed after 180 min. The formation of the sC5b-9 complex in blood showed a similar increase over time as the adsorption of the sC5b-9 proteins on the membrane. This means that a high adsorption of the proteins C5,C6,C7,C8 and C9 is accompanied by strong activation of the complement system.

4. Discussion

In this study, the binding of plasma proteins to non-coated and heparin-coated PMP oxygenator membranes was characterized over time. Adsorption of plasma proteins occurred already within the first minute of blood or plasma contact. In addition, the changes in the protein composition over time were investigated and over 500 time-dependent protein binding profiles on PMP membranes were detected.

The observed difference in total protein amounts between blood and plasma was mainly due to intracellular proteins. However, there was a small proportion of proteins only detected after plasma incubation with the HFM. This can be ascribed to proteins that preferentially bind to cells and are therefore not found adhering to HFM after incubation with blood. The overall high congruency of protein amounts after both types of incubation indicates that protein adsorption analyses with plasma can be used to deduce plasma protein adsorption occurring during blood incubations.

Over time, fewer plasma proteins (less different and also lower amounts) were adsorbed to the heparinized HFM than to the non-coated HFM, indicating different adsorption behavior of proteins to these

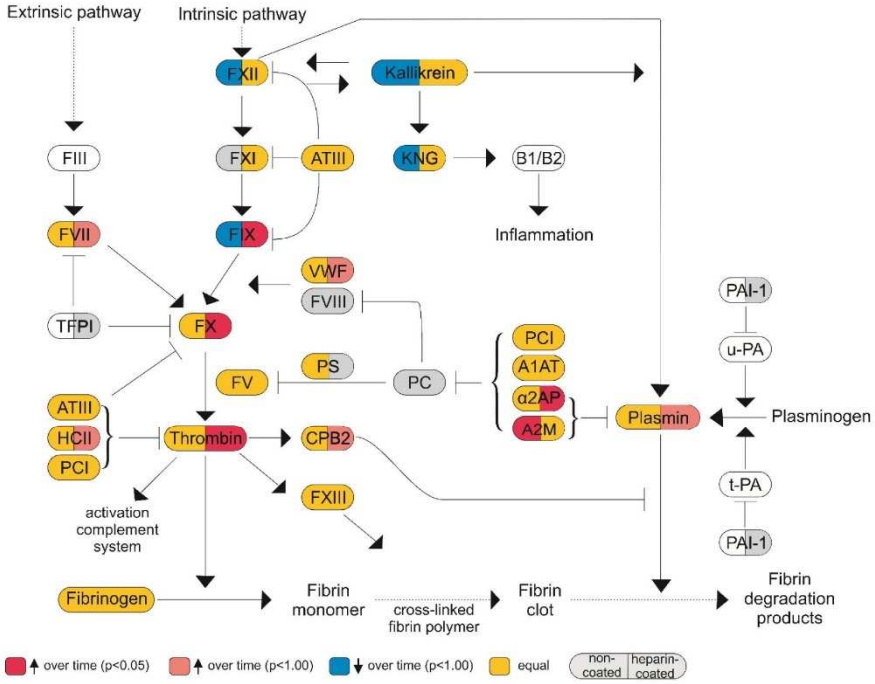

Fig. 4. Protein changes over time associated with coagulation. Color-coded schematic of time-dependent changes in protein adsorption associated with the coagulation pathway on non-coated (left side of the protein name) and heparin-coated (right side of the protein name) PMP membranes. Proteins that show a constant binding profile are colored yellow, those that increase significantly over 360 min are colored red ($p < 0.05$) or light red ($p < 0.1$), and proteins that are found less frequently over time are colored blue ($p < 0.05$). Proteins with white background could not be detected, gray ones only sporadically. Statistical analyses are based on LFQ intensities and were performed using a paired two-tailed *t*-test to determine differences after 1 and 360 min. $n = 3$; *$p < 0.05$, **$p < 0.01$. (For interpretation of the references to color in this figure legend, the reader is referred to the web version of this article.)

surfaces. A considerable proportion of the proteins on the non-coated membrane decreased over time, which was not prominent with the heparin-coated membrane. These changes in protein abundance on membranes indicate the remodeling of the protein layer over time. Furthermore, this suggests that the protein layer on heparinized membranes changed less than that on non-coated membranes. In another study, different protein binding behavior between heparin-coated and non-coated PVC tubings was also discovered [36], but no decrease in protein amount could be detected using SDS-PAGE over 120 min. Transient adsorption of plasma proteins on the surface begins immediately in the first seconds, especially fibrinogen, and dynamic displacement of proteins, is known as the Vroman effect [37]. The findings in this study indicate that more dynamic protein displacement occurs on non-coated membranes than on heparinized membranes and that a change in the protein layer does not only occur in the start phase but throughout the entire 6 h period. Brash et al. also pointed out that protein-surface interactions in blood contact are dynamic and it seems unlikely that the layer maintains its composition over long periods [38].

FGA was the most abundant protein on the non-coated membrane at all time points and the most abundant protein on the coated membrane after 60 and 360 min of contact. For both membranes and all time points, fibrin or fibrinogen, albumin, or apolipoproteins were detected most abundantly. These proteins are also reported in the literature to bind most frequently regardless of surface property [39]. Various proteins, such as fibrinogen, fibronectin, vitronectin, and von Willebrand factor are involved in platelet aggregation induced by adenosine diphosphate (ADP) [40–42]. Although no cell activations could be investigated by incubation with plasma, the adsorption of proteins involved in platelet aggregation indicate subsequent cell activation on those surfaces.

The investigation of coagulation and complement system-related proteins on non-coated and heparin-coated PMP membranes revealed increased binding of contact phase proteins except for FXI on the non-coated membranes. Since FXI has a heparin-binding site [33], this increased adsorption on the heparin-coated membrane can be explained. After 360 min of blood incubation, the contact phase proteins and FIX could not be detected.

The increased binding of most coagulation factors to the non-coated membrane shows increased interaction with this membrane type. Moreover, increased anti-thrombin III binding was detected on the heparin-coated membrane due to its high affinity for heparin. The binding of proteins that inhibit clotting, such as antithrombin, is generally considered positive [43]. It is assumed that the initially formed protein film consists of a monolayer and that complement activation takes place on this layer [44,45]. Coagulation and the complement system are closely crosslinked [46].

The lectin pathway of the complement system is activated by soluble pattern recognition molecules (PRMs), which include the three ficolins, ficolin-1, -2, and -3, and the mannose-binding lectin (MBL). Ficolin 1 and MBL could not be detected on either coated or non-coated membranes. However, ficolin 2 and 3 were detected in significantly more amounts on heparin-coated membrane than on the non-coated

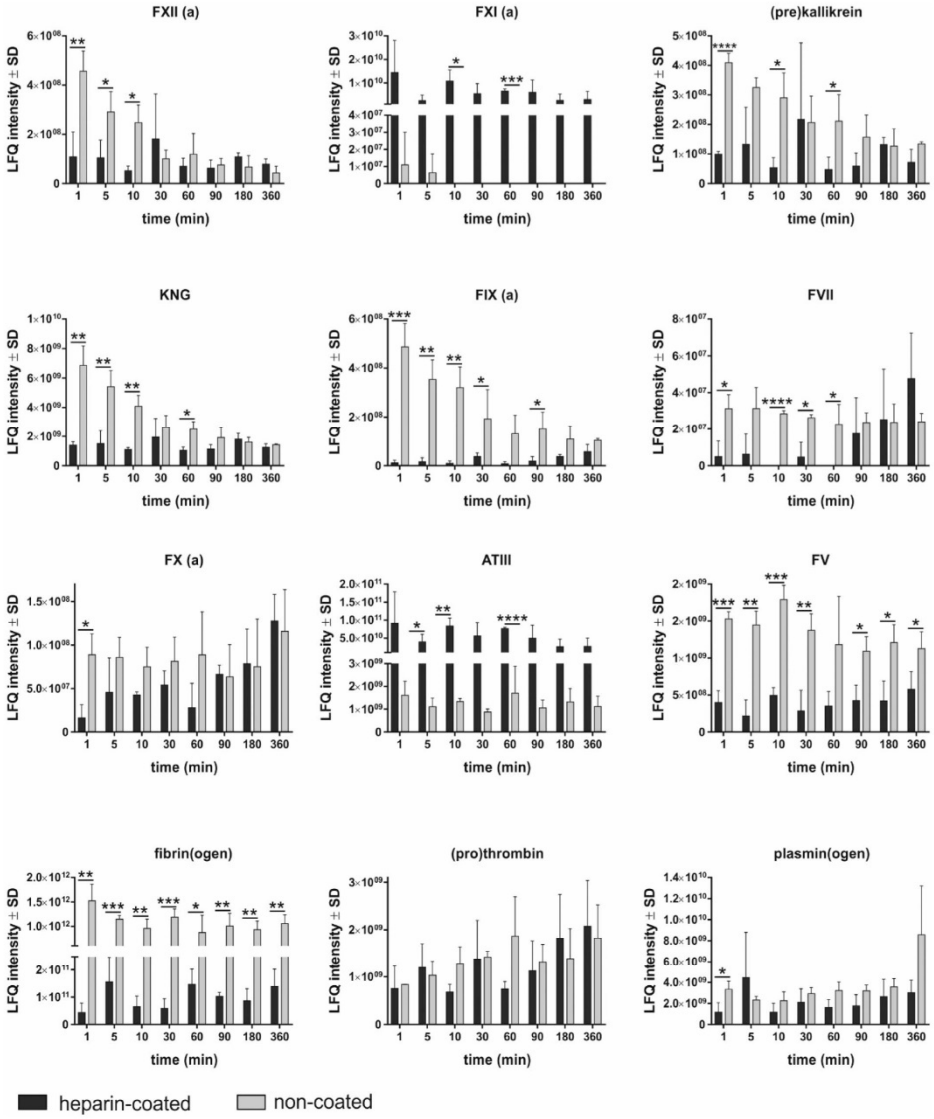

Fig. 5. Binding differences of major coagulation components on coated and non-coated membranes. The contact phase proteins (FXII, FXI, kallikrein), kininogen (KNG), and FIX) were bound more frequently on the non-coated membrane at the beginning (up to 60 min), except for FXI, which has a heparin-binding site. FIX showed high protein adsorption on non-coated membranes, which decreased over time to the levels on heparinized membranes. Except for after 1 min, there were no discernible differences in the binding of FX. FV and fibrinogen were bound more strongly to the non-coated membrane over the entire time. Whereas for ATIII a reverse effect is evident due to specific heparin binding. Increased plasmin binding was detected only after 1 min on non-coated membrane compared to heparin-coated membrane. No significant differences were detected in thrombin binding. The data are shown as mean LFQ Intensity ± SD. Statistical analysis was performed using unpaired two-tailed *t*-test to determine the differences between heparin-coated and non-coated PMP-membranes at every time point, $n = 3$; ***$p < 0.001$, **$p < 0.01$, *$p < 0.05$.

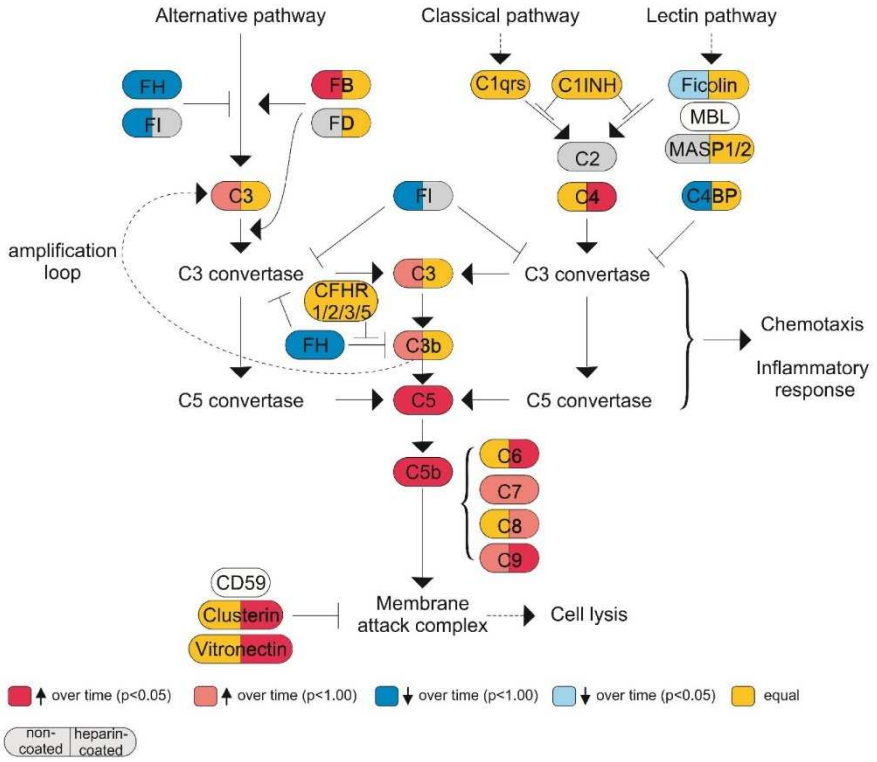

Fig. 6. Protein changes over time associated with the complement system. Color-coded schematic of time-dependent changes in the protein adsorption associated with the complement system pathway on non-coated (left side of the protein name) and heparin-coated (right side of the protein name) PMP membranes. Proteins showing a constant binding profile are colored in yellow, those significantly increasing over 360 min are colored in red ($p < 0.05$) or light red ($p < 0.1$), and proteins found less frequently over time are colored in blue ($p < 0.05$) or light blue ($p < 0.01$). Proteins with a white background could not be detected, gray ones only sporadically. Statistical analyses are based on LFQ intensities and were performed using paired two-tailed *t*-test to determine the differences between 1 min and 360 min. $n = 3$. (For interpretation of the references to color in this figure legend, the reader is referred to the web version of this article.)

membrane at different time points. Hein et al. observed a similar effect for ficolin-2 by comparing PRM levels after cardiopulmonary bypass treatment of patients with two differently coated cardiopulmonary bypass circuits, Phisio® (phosphorylcholine polymer coating) and Bioline® (albumin-heparin coating) [47]. In their study, significantly lower ficolin-2 levels were detected in plasma samples of Bioline® group than the Phisio® group. Hein et al. concluded that this reduction was related to the specific binding of ficolin-2 to heparin [47]. The reduced ficolin-2 concentration in blood by increased binding to heparin-coated surfaces could lead to an increased postoperative susceptibility to infections after extracorporeal circulation procedures. Once PRMs are bound to the target structure, the cascade is initiated by the activation of MBL/ficolin-associated serine proteases (MASPs). Both MASP1 and MASP2 were also detected significantly more frequently on the heparin-coated membrane. This suggests that the properties of ficolin are retained after binding to heparin.

The initiation of the classical pathway is similar to the lectin pathway and requires the C1 complex, which consists of a large subunit C1q and two serine proteases (C1r and C1s). In our study, C1q binds significantly more often to the heparin-coated membrane. This is probably due to the high binding affinity of C1q to heparin [48]. Nilsson et al. investigated the effect of heparin-coated polystyrene surfaces of microtitre plates on the complement system [45] and observed also an increased affinity of C1q to the heparin-coated polystyrene. They assumed an increased activation of the classical pathway by the increased binding of C1q. In our study, increased binding of C1r and C1s, as well as C1 esterase inhibitor (C1-INH) was also observed on the heparin-coated membrane. Thus, we conclude that the binding sites for C1r, C1s, and C1-INH are still present after binding of C1q to heparin on the coated membrane, which could result in the activation of the classical pathway. However, this does not seem very likely because C2, which is required for the formation of the active C3 convertase, C4b2a, was only sporadically detected on both membranes (on heparin coating only after 5 and 30 min) and in very low amounts. However, a significantly higher C2 binding was detected on the non-coated membrane after 10 min. Moreover, C4 was found more pronounced on the non-coated membranes than on the heparin-coated membranes. The increased binding of C4 to the non-coated membrane suggests a stronger activation of the classical and lectin pathways by the non-coated membrane, despite the initial findings of increased ficolin and C1 adsorption to heparin-coated membranes. However, from 90 min onwards, C4 adsorption increased slightly on the heparinized membranes, so that the differences between membranes were not significant any longer.

Our results, therefore, suggest that the main trigger for the activation

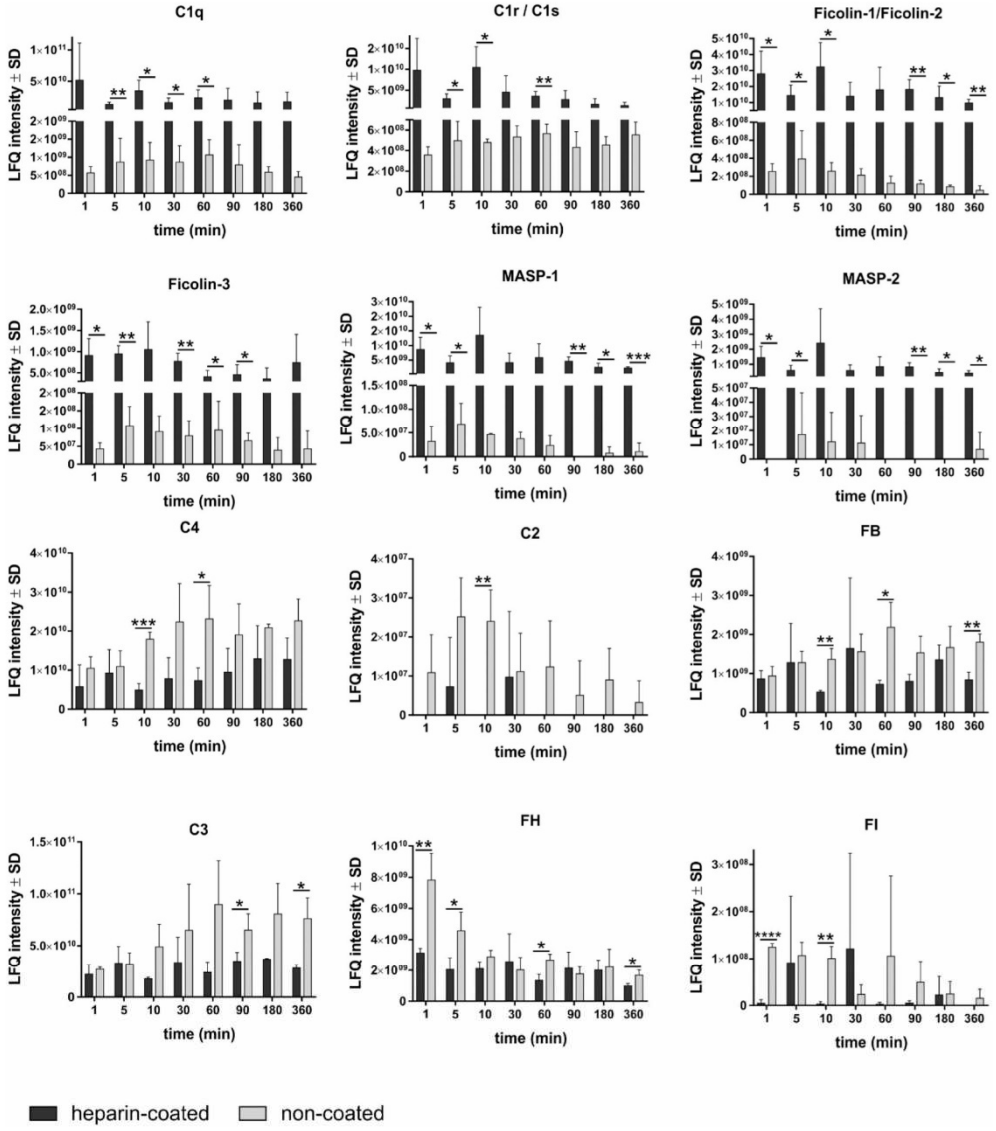

Fig. 7. Binding differences of major complement components of the classical pathway, lectin pathway, alternative pathway, and inhibitors to the non-coated and heparin-coated membrane. While the initiator molecules of the classical pathway and lectin pathway bound more abundantly on the coated membrane this effect was reversed for the later components C2 and C4. FB bound more strongly to the non-coated membrane C3 was detected more abundantly on the non-coated membrane. The inhibitor FH bound more strongly to the non-coated membrane, but it is noteworthy that FI for which FH acts as a cofactor did not bind to the coated membrane at all or bound with very low abundance. LFQ Intensity ± SD. Statistical analysis was performed using unpaired two-tailed *t*-test to determine the differences between heparin-coated and non-coated PMP-membranes at every time point, $n = 3$; * * * $p < 0.001$, * * $p < 0.01$, * $p < 0.05$.

of the complement system was the alternative pathway. In this pathway, C3 is spontaneously hydrolyzed to yield C3(H_2O) (the "tick-over" mechanism), which is enhanced by FB, FD, and properdin. The C3 convertase produced by the alternative pathway has a special significance because it can reproduce itself by producing C3b. This means that the alternative pathway can act as an amplifier loop and rapidly increase C3b production once some C3b molecules have been formed [49]. This is triggered by foreign surfaces that do not provide sufficient down-regulation of convertase [50]. Recently, Riedel et al. also found evidence that the alternative pathway of the complement system through

the "tick-over" mechanism of spontaneous C3 activation plays an important role in fouling on surfaces coated with poly(2-hydroxyethyl methacrylate) polymer brushes [51]. Antifouling polymer brushes usually successfully suppress fouling, but some coatings show extremely high variability of fouling by different donors, likely due to activation of the complement system [51]. These observations are in contrast to the results of Nilsson et al., who suggested that the classical complement pathway is activated stronger on heparinzed surfaces, but this activation was compensated by lower activation of the alternative pathway [45].

All three pathways of the complement system culminate in the formation of the membrane attack complex. Consistent with the increased binding of the components of the membrane attack complex to the coated and non-coated PMP membrane, we observed a time-dependent increase of sC5b-9 in blood. This suggests the activation of the complement system occurring on the membrane with subsequent binding of the late complement proteins on the HFM rather than adsorption of single individual proteins. Despite extensive research, there is still no clear consensus in the literature as to which protein(s) initially trigger complement activation on biomaterial surfaces. Bound IgG, C1q, and C4 have been proposed as initiators [50,52,53]. Our results suggest that C1q is not the main trigger of the complement cascade on heparinized biomaterials. C1q binds significantly more frequently to the heparin-coated membrane, but heparin coating has been shown to reduce the activation of the complement system [54].

Complement activation is under tight control by several regulators. In general, the regulators FH, C4BP, and FI were bound more frequently to non-coated membranes, but showed a significant decrease over time. C4BP remained constant, albeit at slightly lower levels, on the heparin-coated membrane. The C4BP binding might explain the lack of C2 binding, as C2 is displaced by C4BP [55]. C4BP consists of seven identical α-chains, each of which can bind a C4b moiety and facilitate its down-regulation by factor I to iC4b. Even after binding, most of the α-chains should retain their function, which is why C4BP retains a substantial part of its co-factor function after binding to a biomaterial [56]. In our study, we observed on the non-coated membranes a decrease in the amount of C4BP over time, which could have an amplifying effect on complement activation.

Factor H has a single-chain structure with multiple binding sites for C3b, all of which must bind C3b to allow efficient degradation of C3b to iC3b. Thus, it has been shown that the cofactor activity of FH is lost when FH is bound in a denatured conformation [57,58]. In addition, FH has multiple heparin-binding sites with a high affinity for heparin [59,60]. The measured FH bonds on the coated membrane are therefore more likely to be due to binding to heparin than to C3b. This assumption is supported by the barely present FI on the coated membrane, which cannot bind to FH bound to heparin. Due to FH binding more likely to heparin instead of C3b, no FI is bound to FH.

C1-INH is also one of the regulators of the complement system as it inhibits the activation of C1 by covalent binding. In a previous study, we could show that bound C1-INH can improve the hemocompatibility of oxygenator membranes [61]. With increased C1 binding on the coated membrane, we also observed increased C1-INH binding over the non-coated membrane at all time points. This increase was approx. 1.5-fold increased over the non-coated membrane, and especially at 30 min (4.5-fold) and at 180 min (2.5-fold) a stronger increased binding was observed on heparinized than on non-coated membrane. If C1-INH is still active after binding to C1, it can inhibit the serine proteases C1r and C1s, which has the beneficial effect of reducing complement activation, which may be contributing to the lack of C2 activation on the heparinized membranes.

To confirm these findings with final certainty, conformational analyses of individual proteins would be useful.

Our analyses of plasma protein adsorption showed that specific interactions between the coating and plasma proteins were still present after six hours. The results indicate that the development of strategies involved in complement activation, such as the use of complement inhibitors could be useful. We have already chosen this approach for our novel C1-INH coating [61]. However, in this study, we detected that the alternative pathway seems to play an important role in the activation of the complement system by HFMs. Therefore, the use of inhibitors of the alternative pathway could be advantageous. To prevent coagulation activation, antithrombin-heparin complexes could be considered, such as those already used by Klement et al. [62]. Our results further showed that fibrinogen can be displaced by albumin as the most abundant protein at the heparin-coated membrane. However, this lasts only for 180 min. This displacement effect could potentially be prolonged by a combination coating of albumin and heparin-ATIII complexes. Albumin coating has been used previously to improve the biocompatibility of vascular grafts, resulting in less cell deposition [63]. The commercially used Bioline® coating consists of a recombinant human albumin layer with covalently bound heparin [64]. Improved haemocompatibility was shown by Andersson and colleagues when using heparinized surfaces with an ATIII binding capacity of 6–12 pmol/cm^2, corresponding to the bioactivity of about 1.5 μg heparin/cm^2 [65]. The heparin coating used in our study corresponded to approximately 3.5 μg bioactive heparin/cm^2, thus ranging in the described ATII binding capacity of Andersson et al. So far, comparable protein adsorption studies of other coating approaches have not been published. Based on our findings with the end-point attached heparin, it can be assumed that proteins with affinities for the molecules used for biofunctionalisation can be also attracted to the membrane, e.g. C1 protein on the surface of the C1-INH coating. This in turn can affect the protein adsorption on those biofunctionalised membranes. The data presented in the current study suggest that a combination of a biopassive layer of albumin with a bioactive heparin-ATIII complex and/or complement inhibitors could be suitable candidates for a novel coating to improve long-term haemocompatibility.

5. Conclusion

In summary, this study is the first to demonstrate and compare time-dependent plasma protein adsorption on non-coated and heparin-coated PMP membranes over 6 h. During this period, a dynamic plasma protein layer was detected. The binding mechanisms of proteins were altered by surface modification with heparin and resulted in less protein binding on heparin-coated membranes. Particularly, significantly higher amounts of proteins with heparin-binding side were detected on heparin-coated membranes. Furthermore, a higher degree of remodeling of the protein layer on the non-coated membrane than on the heparin-coated membrane was detected. Fibrinogen (FGA/FGB/FGG) was most abundant at all time points with higher protein concentrations on non-coated than on heparinized membranes. The strongest changes in proteins were detected 10 min after contact with the plasma. Precise pathway analyses allowed to further elucidate the mechanisms of coagulation and component activation triggered by PMP membranes. Almost all coagulation factors were bound in higher amounts on non-coated membranes. Interestingly, complement system initiator proteins showed increased binding to heparinized membranes but downstream complement factors were found in increased amounts on non-coated membranes. Thus, we suggest that novel coating strategies preventing the activation of the complement system could significantly improve the hemocompatibility of artificial surfaces.

Supplementary data to this article can be found online at https://doi.org/10.1016/j.bioadv.2022.213014.

CRediT authorship contribution statement

The authors of the manuscript contributed in several ways to the study: conceptualization, KGB, HPW, CS, MAA, and SS; methodology, KGB, MA, LC, PC, AV, and BM; validation, KGB, MAA, BM, AV and SS.; formal analysis, KGB, MA, BM, AV, and SS; investigation, KGB, MA, AV, PC, and LC; resources, HPW, CS, MAA, and SS; writing—original draft preparation, KGB, MA, LC, PC, HPW, MAA, and SS; writing—Review &

Editing, KGB, MAA, and SS; visualization, KGB, MA, MAA and SS; supervision, HPW, CS, and MAA, project administration, SS; funding acquisition, SS. All authors have read and agreed to the published version of the manuscript.

Funding

This research was funded by the Deutsche Forschungsgemeinschaft (DFG) (STO 1176/1-1) within the priority programme SPP2014 "Towards an implantable lung".

Declaration of competing interest

The authors declare no conflict of interest. The DFG had no role in the design of the study; in the collection, analyses, or interpretation of data; in the writing of the manuscript, or in the decision to publish the results. Patrick and Linda Cahalan are employees of Ension, Inc.

Acknowledgments

The authors would like to thank Melanie Wolf, Pia Müllerbader, and Bernd Neumann for their support with the experimental setup and performing the ELISAs. Furthermore, we acknowledge the support by the DFG.

References

[1] J.M. Blum, W.R. Lynch, C.M. Coopersmith, Clinical and billing review of extracorporeal membrane oxygenation, Chest 147 (2015) 1697–1703.
[2] S.F. Marasco, G. Lukas, M. McDonald, J. McMillan, B. Ihle, Review of ecmo (extra corporeal membrane oxygenation) support in critically ill adult patients, Heart Lung Circ. 17 (2008) S41–S47.
[3] G. Lafçı, A.B. Budak, A.Ü. Yener, O.F. Cicek, Use of extracorporeal membrane oxygenation in adults, Heart Lung Circ. 23 (2014) 10–23.
[4] H. Iwahashi, K. Yuri, Y. Nosé, Development of the oxygenator: past, present, and future, J. Artif. Organs 7 (2004) 111–120.
[5] C.J.D.Kwantai Cho, Robert English Johnston. Microporous Hollow Fiber Blood Oxygenator. A61M/114; A61M/136; A61M/134; A61M/3700, Celgard Inc, 1998.
[6] J.M. Toomasian, R.J. Schreiner, D.E. Meyer, M.E. Schmidt, S.E. Hagan, G. W. Griffith, R.H. Bartlett, K.E. Cook, A polymethylpentene fiber gas exchanger for long-term extracorporeal life support, ASAIO J. 51 (2005) 390–397.
[7] L. Lequier, S.B. Horton, D.M. McMullan, R.H. Bartlett, Extracorporeal membrane oxygenation circuitry, Pediatr. Crit. Care Med. 14 (2013) S7.
[8] E. Øvrum, T.E. Mollnes, E. Fosse, E.Å. Holen, G. Tangen, M.-A.L. Ringdal, V. Videm, High and low heparin dose with heparin-coated cardiopulmonary bypass: activation of complement and granulocytes, Ann. Thorac. Surg. 60 (1995) 1755–1761.
[9] T. Miyashita, A.K. Ahmed, S. Nakanuma, K. Okamoto, S. Sakai, J. Kinoshita, I. Makino, K. Nakamura, H. Hayashi, K. Oyama, A three-phase approach for the early identification of acute lung injury induced by severe sepsis, In Vivo 30 (2016) 341–349.
[10] M.B. Gorbet, M.V. Sefton, Biomaterial-associated thrombosis: roles of coagulation factors, complement, platelets and leukocytes, Biomaterials 25 (2004) 5681–5703.
[11] X. Liu, L. Yuan, D. Li, Z. Tang, Y. Wang, G. Chen, H. Chen, J.L. Brash, Blood compatible materials: state of the art, J. Mater. Chem. B 2 (2014) 5718–5738.
[12] T. Göppert, R. Müller, Adsorption kinetics of plasma proteins on solid lipid nanoparticles for drug targeting, Int. J. Pharm. 302 (2005) 172–186.
[13] S. Schöttler, G. Becker, S. Winzen, T. Steinbach, K. Mohr, K. Landfester, V. Mailänder, F.R. Wurm, Protein adsorption is required for stealth effect of poly (ethylene glycol)-and poly (phosphoester)-coated nanocarriers, Nat. Nanotechnol. 11 (2016) 372–377.
[14] J.L. Brash, T.A. Horbett, Proteins at Interfaces: Physicochemical and Biochemical Studies, ACS Publications, 1987.
[15] T.A. Horbett, J.L. Brash, Proteins at Interfaces ii, ACS Publications, 1995.
[16] S. Mulzer, J. Brash, Identification of plasma proteins adsorbed to hemodialyzers during clinical use, J. Biomed. Mater. Res. 23 (1989) 1483–1504.
[17] H.M. Verheul, K. Hoekman, S.L.-D. Bakker, C.A. Eekman, C.C. Folman, H. J. Broxterman, H.M. Pinedo, Platelet: transporter of vascular endothelial growth, Clin. Cancer Res. 3 (1997) 2187–2190.
[18] J. Tan, W.G. McClung, J.L. Brash, Non-fouling biomaterials based on blends of polyethylene oxide copolymers and polyurethane: simultaneous measurement of platelet adhesion and fibrinogen adsorption from flowing whole blood, J. Biomater. Sci. Polym. Ed. 24 (2013) 497–506, https://doi.org/10.1080/09205063.2012.690286.
[19] G. Johnson, B. Curry, L. Cahalan, R. Prater, M. Beeler, M. Gartner, J. Biggerstaff, P. Cahalan, In vitro assessment of blood compatibility: Residual and dynamic markers of cellular activation, J. Biomater. Appl. 27 (2013) 925–936, https://doi.org/10.1177/0885328211428525.
[20] L. Vroman, A. Adams, G. Fischer, P. Munoz, Interaction of High Molecular Weight Kininogen, Factor xii, and Fibrinogen in Plasma at Interfaces, 1980.
[21] C.D. Walkey, J.B. Olsen, F. Song, R. Liu, H. Guo, D.W.H. Olsen, Y. Cohen, A. Emili, W.C. Chan, Protein corona fingerprinting predicts the cellular interaction of gold and silver nanoparticles, ACS Nano 8 (2014) 2439–2455.
[22] P. Wojciechowski, P. Ten Hove, J. Brash, Phenomenology and mechanism of the transient adsorption of fibrinogen from plasma (vroman effect), J. Colloid Interface Sci. 111 (1986) 455–465.
[23] R.M. Cornelius, J.G. Archambault, L. Berry, A.K. Chan, J.L. Brash, Adsorption of proteins from infant and adult plasma to biomaterial surfaces, J. Biomed. Mater. Res. 60 (2002) 622–632.
[24] T.S. Tsapikouni, Y.F. Missirlis, Protein–material interactions: from micro-to-nano scale, Mater. Sci. Eng. B 152 (2008) 2–7.
[25] N. Borchert, C. Dieterich, K. Krug, W. Schütz, S. Jung, A. Nordheim, R.J. Sommer, B. Macek, Proteogenomics of pristionchus pacificus reveals distinct proteome structure of nematode models, Genome Res. 20 (2010) 837–846.
[26] J. Rappsilber, M. Mann, Y. Ishihama, Protocol for micro-purification, enrichment, pre-fractionation and storage of peptides for proteomics using stagetips, Nat. Protoc. 2 (2007) 1896–1906.
[27] M. Schmitt, T. Sinnberg, N.C. Nalpas, A. Maass, B. Schittek, B. Macek, Quantitative proteomics links the intermediate filament nestin to resistance to targeted braf inhibition in melanoma cells, Mol. Cell. Proteomics 18 (2019) 1096–1109.
[28] J. Cox, M. Mann, Maxquant enables high peptide identification rates, individualized ppb-range mass accuracies and proteome-wide protein quantification, Nat. Biotechnol. 26 (2008) 1367–1372.
[29] J. Cox, N. Neuhauser, A. Michalski, R.A. Scheltema, J.V. Olsen, M. Mann, Andromeda: a peptide search engine integrated into the maxquant environment, J. Proteome Res. 10 (2011) 1794–1805.
[30] E. Gout, V. Garlatti, D.F. Smith, M. Lacroix, C. Dumestre-Pérard, T. Lunardi, L. Martin, J.-Y. Cesbron, G.J. Arlaud, C. Gaboriaud, Carbohydrate recognition properties of human ficolins: glycan array screening reveals the sialic acid binding specificity of m-ficolin, J. Biol. Chem. 285 (2010) 6612–6622.
[31] U. Lindahl, G. Bäckström, M. Höök, L. Thunberg, L.-A. Fransson, A. Linker, Structure of the antithrombin-binding site in heparin, Proc. Natl. Acad. Sci. 76 (1979) 3198–3202.
[32] W. Feng, X. Gao, G. McClung, S. Zhu, K. Ishihara, J.L. Brash, Methacrylate polymer layers bearing poly (ethylene oxide) and phosphorylcholine side chains as non-fouling surfaces: in vitro interactions with plasma proteins and platelets, Acta Biomater. 7 (2011) 3692–3699.
[33] M. Zhao, T. Abdel-Razek, M.-F. Sun, D. Gailani, Characterization of a heparin binding site on the heavy chain of factor xi, J. Biol. Chem. 273 (1998) 31153–31159.
[34] S.A. Smith, The cell-based model of coagulation, J. Vet. Emerg. Crit. Care 19 (2009) 3–10.
[35] E. Ersdal-Badju, A. Lu, Y. Zuo, V. Picard, S.C. Bock, Identification of the antithrombin iii heparin binding site, J. Biol. Chem. 272 (1997) 19393–19400.
[36] N. Weber, H.P. Wendel, G. Ziemer, Hemocompatibility of heparin-coated surfaces and the role of selective plasma protein adsorption, Biomaterials 23 (2002) 429–439.
[37] L. Vroman, A.L. Adams, Identification of rapid changes at plasma–solid interfaces, J. Biomed. Mater. Res. 3 (1969) 43–67.
[38] J.L. Brash, T.A. Horbett, R.A. Latour, P. Tengvall, The blood compatibility challenge. Part 2: protein adsorption phenomena governing blood reactivity, Acta Biomater. 94 (2019) 11–24.
[39] J.L. Brash, Protein surface interactions and biocompatibility: a forty year perspective, in: T. Horbett, J.L. Brash, W. Norde (Eds.), Proteins at Interfaces iii State of the Art, ASC Symposium Series eBooks, 2012, pp. 277–300.
[40] J. Grunkemeier, W. Tsai, C. McFarland, T. Horbett, The effect of adsorbed fibrinogen, fibronectin, von willebrand factor and vitronectin on the procoagulant state of adherent platelets, Biomaterials 21 (2000) 2243–2252.
[41] C. Blaszykowski, S. Sheikh, M. Thompson, A survey of state-of-the-art surface chemistries to minimize fouling from human and animal biofluids, Biomater. Sci. 3 (2015) 1335–1370.
[42] W.B. Tsai, J.M. Grunkemeier, C.D. McFarland, T.A. Horbett, Platelet adhesion to polystyrene-based surfaces preadsorbed with plasmas selectively depleted in fibrinogen, fibronectin, vitronectin, or von willebrand's factor, J. Biomed. Mater. Res. 60 (2002) 348–359.
[43] K. Kador, T. Mamedov, M. Schneider, A. Subramanian, Sequential co-immobilization of thrombomodulin and endothelial protein c receptor on polyurethane: activation of protein c, Acta Biomater. 7 (2011) 2508–2517.
[44] J. Andersson, K.N. Ekdahl, J.D. Lambris, B. Nilsson, Binding of c3 fragments on top of adsorbed plasma proteins during complement activation on a model biomaterial surface, Biomaterials 26 (2005) 1477–1485.
[45] U. Nilsson, O. Larm, B. Nilsson, K.E. Storm, H. Elwing, K.N. Ekdahl, Modification of the complement binding properties of polystyrene: effects of end-point heparin attachment, Scand. J. Immunol. 37 (1993) 349–354.
[46] A.T. Long, E. Kenne, R. Jung, T.A. Fuchs, T. Renné, Contact system revisited: an interface between inflammation, coagulation, and innate immunity, J. Thromb. Haemost. 14 (2016) 427–437.
[47] E. Hein, L. Munthe-Fog, A. Thiara, A. Fiane, T. Mollnes, P. Garred, Heparin-coated cardiopulmonary bypass circuits selectively deplete the pattern recognition molecule ficolin-2 of the lectin complement pathway in vivo, Clin. Exp. Immunol. 179 (2015) 294–299.
[48] S. Almeda, R.D. Rosenberg, D.H. Bing, The binding properties of human complement component c1q. Interaction with mucopolysaccharides, J. Biol. Chem. 258 (1983) 785–791.

[49] P. Lachmann, N. Hughes-Jones, Initiation of complement activation, in: Springer Seminars in Immunopathology, Springer, 1984, pp. 143–162.
[50] A. Sahu, J.D. Lambris, Complement inhibitors: a resurgent concept in anti-inflammatory therapeutics, Immunopharmacology 49 (2000) 133–148.
[51] T. Riedel, A.D.L.S. Pereira, J. Táborská, Z. Riedelová, O. Pop-Georgievski, P. Májek, K. Pečánková, C. Rodriguez-Emmenegger, Complement activation dramatically accelerates blood plasma fouling on antifouling poly (2-hydroxyethyl methacrylate) brush surfaces, Macromol. Biosci. 2100460 (2021).
[52] K. Lhotta, R. Würzner, F. Kronenberg, M. Oppermann, P. König, Rapid activation of the complement system by cuprophane depends on complement component c4, Kidney Int. 53 (1998) 1044–1051.
[53] P. Tengvall, A. Askendal, I. Lundström, Studies on protein adsorption and activation of complement on hydrated aluminium surfaces in vitro, Biomaterials 19 (1998) 935–940.
[54] V. Videm, J.L. Svennevig, E. Fosse, G. Semb, T.E. Mollnes, H. Nielsen, Reduced complement activation with heparin-coated oxygenator and tubings in coronary bypass operations, J. Thorac. Cardiovasc. Surg. 103 (1992) 806–813.
[55] S. Meri, H. Jarva, Complement regulation, Vox Sang. 74 (1998) 291–302.
[56] A.E. Engberg, P.H. Nilsson, S. Huang, K. Fromell, O.A. Hamad, T.E. Mollnes, J. P. Rosengren-Holmberg, K. Sandholm, Y. Teramura, I.A. Nicholls, Prediction of inflammatory responses induced by biomaterials in contact with human blood using protein fingerprint from plasma, Biomaterials 36 (2015) 55–65.
[57] J. Andersson, R. Larsson, R. Richter, K.N. Ekdahl, B. Nilsson, Binding of a model regulator of complement activation (rca) to a biomaterial surface: surface-bound factor h inhibits complement activation, Biomaterials 22 (2001) 2435–2443.
[58] J. Andersson, F. Bexborn, J. Klinth, B. Nilsson, K.N. Ekdahl, Surface-attached peo in the form of activated pluronic with immobilized factor h reduces both coagulation and complement activation in a whole-blood model, J. Biomed. Mater. Res. A 76 (2006) 25–34.
[59] M.K. Pangburn, M. Atkinson, S. Meri, Localization of the heparin-binding site on complement factor h, J. Biol. Chem. 266 (1991) 16847–16853.
[60] R.J. Ormsby, T.S. Jokiranta, T.G. Duthy, K.M. Griggs, T.A. Sadlon, E. Giannakis, D. L. Gordon, Localization of the third heparin-binding site in the human complement regulator factor h1, Mol. Immunol. 43 (2006) 1624–1632.
[61] K. Gerling, S. Ölschläger, M. Avci-Adali, B. Neumann, E. Schweizer, C. Schlensak, H.-P. Wendel, S. Stoppelkamp, A novel c1-esterase inhibitor oxygenator coating prevents fxii activation in human blood, Biomolecules 10 (2020) 1042.
[62] P. Klement, Y.J. Du, L. Berry, M. Andrew, A.K.C. Chan, Blood-compatible biomaterials by surface coating with a novel antithrombin-heparin covalent complex, Biomaterials 23 (2002) 527–535.
[63] K. Kottke-Marchant, J.M. Anderson, Y. Umemura, R.E. Marchant, Effect of albumin coating on the in vitro blood compatibility of dacron arterial prostheses, Biomaterials 10 (1989) 147–155.
[64] R. Biran, D. Pond, Heparin coatings for improving blood compatibility of medical devices, Adv. Drug Deliv. Rev. 112 (2017) 12–23, https://doi.org/10.1016/j.addr.2016.12.002.
[65] J. Andersson, J. Sanchez, K.N. Ekdahl, G. Elgue, B. Nilsson, R. Larsson, Optimal heparin surface concentration and antithrombin binding capacity as evaluated with human non-anticoagulated blood in vitro, J. Biomed. Mater. Res. A 67 (2003) 458–466, https://doi.org/10.1002/jbm.a.10104.

8.2 Publikation II:

Comparative study of flow rate- and material-dependent human plasma protein adsorption on oxygenator membranes and heat exchanger materials

frontiers | Frontiers in Cardiovascular Medicine

TYPE Original Research
PUBLISHED 17 June 2025
DOI 10.3389/fcvm.2025.1578538

OPEN ACCESS

EDITED BY
Zhaoliang Cui,
Nanjing Tech University, China

REVIEWED BY
Stephen R. Baker,
Wake Forest University, United States
Iva Pruner,
Nationwide Children's Hospital, United States

*CORRESPONDENCE
Sandra Stoppelkamp
sandra.stoppelkamp@klinikum.uni-tuebingen.de

RECEIVED 18 February 2025
ACCEPTED 28 May 2025
PUBLISHED 17 June 2025

CITATION
Große-Berkenbusch K, Avci-Adali M, Cahalan P, Cahalan L, Velic A, Maček B, Schlensak C, Wendel HP and Stoppelkamp S (2025) Comparative study of flow rate- and material-dependent human plasma protein adsorption on oxygenator membranes and heat exchanger materials.
Front. Cardiovasc. Med. 12:1578538.
doi: 10.3389/fcvm.2025.1578538

Comparative study of flow rate- and material-dependent human plasma protein adsorption on oxygenator membranes and heat exchanger materials

Katharina Große-Berkenbusch[1], Meltem Avci-Adali[1], Patrick Cahalan[2], Linda Cahalan[2], Ana Velic[3], Boris Maček[3], Christian Schlensak[1], Hans Peter Wendel[1] and Sandra Stoppelkamp[1]*

[1]Clinical Research Laboratory, Department of Thoracic and Cardiovascular Surgery, University Hospital Tübingen, Tübingen University, Tübingen, Germany, [2]Ension Inc., Butler, PA, United States, [3]Proteome Center Tübingen, Interfaculty Institute for Cell Biology, University of Tübingen, Tübingen, Germany

Artificial lungs support patients with acute or chronic lung diseases. However, complications such as the activation of blood components leading to thrombosis and inflammation limit their long-term applicability. The systematic characterization of protein adhesion events on different material parts of the oxygenators at different flow rates can shed light on the initial reaction of blood to foreign materials. Miniaturized extracorporeal circuit devices with heparin-coated gas (PMP) or heat-exchange (PET) hollow-fiber membranes were exposed to high and low flow rates. Hemocompatibility and adsorption of plasma proteins were measured after one minute to six hours using mass spectroscopy analyses. Approximately 150–200 different proteins were present on the membranes, with almost no variation in the 10 most abundant proteins. Protein adsorption to the membrane types did not vary to a large extent, but a decreased flow rate significantly reduced the differences in protein adsorption between both membrane types and led to the adhesion of significantly higher amounts of inhibitory proteins C1INH and α1-AT. At the higher flow rate, coagulation-associated proteins adsorbed significantly more to PET membranes, whereas complement-activating-related proteins adsorbed more on PMP membranes. Our results highlight the importance of analyzing all circuit components to understand the activation of blood components during ECMO. The primary contributor to increased protein adsorption and activation of blood components was an increased flow rate. Therefore, flow rate adjustments should ideally aim to achieve optimal oxygenation levels of around 80% while minimizing protein adsorption and blood activation during ECMO. Notably, at a low flow rate, PMP HFM exhibited a significant increase in binding of complement and inflammation inhibitors, suggesting a potential benefit of lowering the flow rate apart from the general reduction in protein adsorption.

KEYWORDS

ECMO, hollow fiber membrane, PMP, PET, heparin-coating, plasma protein adsorption, hemocompatibility

1 Introduction

Extracorporeal membrane oxygenation (ECMO) is a potentially life-saving procedure used to support the lungs of critically ill patients. With its tubes and cannulas, pump, heat exchanger, and hollow fiber membrane (HFM) oxygenator, ECMO creates a large artificial surface that comes into contact with blood. Of all components, the oxygenator accounts for the largest part (>90%) of the blood-contacting area with 0.8–2.5 m^2. In addition, the tubes form a surface area of 0.05–0.15 m^2 (1). Due to this large foreign surface area and the necessary systemic anticoagulation, hemostatic changes often occur during ECMO, including both bleeding and thrombotic events (2).

To prevent complications during ECMO and to increase hemocompatibility, the ECMO systems are coated. Heparin-albumin coatings are mainly used in long-term applications for up to 30 days (3). For this purpose, tip-to-tip coating is usually used, which means that all blood-contacting surfaces of the ECMO are modified (4). When developing new coatings and testing hemocompatibility, great attention is usually paid to HFMs for gas exchange. In contrast, the membranes for heat exchange receive little attention, but they are also a significant part of the blood-contacting surface. In addition to the different materials that come into contact with blood during ECMO treatment, the selected flow rate has also an influence on hemocompatibility (5). In adults, the flow rate during ECMO is 4–6 L/min (60–80 ml/kg/min) (6). This flow rate is necessary to maintain adequate gas exchange. During weaning, the flow rate is gradually reduced to less than 30%. These recommended flow rates are well documented (7); however, it is not well understood how different flow rates affect coagulation and hemolysis.

The flow rate can determine the speed of cell and protein adsorption on the surface. Furthermore, by varying the flow rate, the degree of receptor expression on platelets and leukocytes can change (8). Since platelets play a crucial role in thrombus formation, numerous studies have focussed on the impact of flow rate on platelet behavior (9–14). High flow rates and the associated increase in shear forces led to increased deposition of platelets (15, 16). Low flow rates had the opposite effect (17). On the other hand, it has been described that fibrin deposition decreased with increasing wall shear rate (18).

The importance of flow is widely known, but the current understanding of the influence of flow is mainly limited to platelets. Less is known about the effects of flow rate on the activation of the coagulation system. However, it is known that the formation of factor Xa increases with increasing shear rate (19) and that thrombin formation is influenced by flow velocity (20). In addition, cannulas and centrifugal pumps required for ECMO support can alter fluid dynamics by creating turbulent flows and high shear stresses, thus altering hemodynamic effects (21, 22). This results in damage to circulating blood cells and hemostatic proteins. In addition, it has been shown that extracorporeal life support can lead to acquired von Willebrand syndrome, which is characterized by the loss of high molecular weight (HMW) multimers of von Willebrand factor (vWF) due to high shear stress and leads to impaired binding of vWF to collagen and platelets (23). This leads to impaired primary hemostasis and patients develop a bleeding tendency.

This study aims to assess the material- and flow rate-dependent plasma protein binding over time, and to investigate the effects of plasma protein binding on thrombosis and inflammation by detecting various hemocompatibility markers. For this purpose, a mock-loop system was developed in which polymethyl pentene (PMP) gas exchange HFM membranes and polyethylene terephthalate (PET) heat exchange membranes were incubated with human whole blood or human plasma at two different flow rates (0.2 L/min and 1 L/min) for six hours.

Abbreviations

ECMO, extracorporeal membrane oxygenation; HFM, hollow fiber membranes; PP, polypropylene; PMP, polymethyl pentene; EBS, Ension Bioactive Surface; PEI, polyethyleneimine; NAD, nitrous acid-degraded; PVC, polyvinylchloride; TAT, thrombin-antithrombin III complex; PMN, polymorphonuclear; PRM, pattern recognition molecule.

2 Materials and methods

2.1 Miniature devices with heparin-coated hollow-fiber oxygenator membranes

Miniature devices were used with gas exchange or heat exchange membranes. The gas exchange membrane was a PMP hollow-fiber membrane (OXYPLUS^{TM}, 3M Membrana, Wuppertal, Germany) and the heat exchange membrane was a PET hollow-fiber membrane (HEXPET^{TM}, Capillary, Type 60/670, 3M Membrana, Wuppertal, Germany). The miniature device components were individually coated as previously described (24) and then assembled under sterile conditions. Heparin-coated PMP or PET membrane pieces (14 × 10 cm, approx. 210 cm^2 surface area) were placed in a 3/8-in (0.95 cm) polyvinylchloride (PVC) tube (Raumedic, Helmbrechts, Germany) with a 3/8-in–1/4-in (0.95–0.65 cm) polycarbonate straight connector at both ends. The miniature devices were covalently coated with the EBS (Ension Bioactive Surface) coating technology as described before (24). The fundamental concepts of the EBS coating are described by Johnson et al. (25).

2.2 Blood and plasma sampling

The citrated plasma and heparinized whole blood were obtained from the donor pool of the Transfusion Service of the University Hospital Tübingen. The frozen citrated plasma was mixed with 3 IU/ml sodium heparin (25,000 IU/5 ml; LEO Pharma GmbH, Neu-Isenburg, Germany) after thawing and recalcified with calcium chloride (Baxter, Glenview, USA) depending on the citrate concentration.

For the hemocompatibility studies, 500 ml fresh heparinized (3 IU/ml) whole blood obtained directly from the transfusion service was used. The whole blood was diluted with 100 ml diluent solution containing 1.3% glucose solution (Delta-Pharma GmbH, Pfullingen, Germany) and 53 mM $NaHCO_3$ (Braun Melsungen AG, Melsungen, Germany) in ringer lactate solution (Fresenius, Bad Homburg, Germany).

2.3 Experimental setup

To characterize the adsorption of plasma proteins and the hemocompatibility parameters on heparin-coated PMP and PET membranes at different blood flows, a 1/4-in PVC tubing system (Raumedic, Helmbrechts, Germany) was set up with the miniature devices as described previously (24). For time-dependent protein adsorption analyses on heparin-coated PMP and PET membranes, separate circulation systems were run with two different flows (0.2 L/min and 1 L/min). The flow rates were adjusted to the miniature model with a smaller tube diameter to simulate the flow rates of the patient oxygenators. The higher flow corresponds approximately to the normal cardiac output of an adult and thus the normal ECMO pumping rate of approximately 4–6 L/min. The reduced flow of 0.2 L/min corresponds approximately to the ECMO flow during weaning (approximately 1.5 L/min). For this purpose, the system with the miniature device was filled with plasma and stopped after different time points. After the appropriate incubation time, the system was rinsed with 1 L of 0.9% NaCl solution and the washed membrane was removed. The adsorbed proteins were desorbed as previously described (24).

2.4 Hemocompatibility tests

For the experiments with whole blood, a blood reservoir was added to the circulation system described earlier (24). To determine the baseline values, a baseline sample was taken before the start of incubation. The diluted whole blood described in Section 2.2 was divided to allow simultaneous determination of the two different membrane types (PMP and PET) with the same donor blood. The experiments were carried out with a blood flow of 1 L/min and 0.2 L/min and a temperature of 37°C. Blood was collected from the system at different time points (1, 5, 10, 30, 60, 90, 180, and 360 min after the start of circulation). Blood cell counts were determined directly using an automated cell counter (ABX Micros 60, Horiba Medical, Kyoto, Japan). Furthermore, collected serum or plasma samples were cryopreserved and later the activation of coagulation, complement system, platelets, and inflammation were determined by ELISAs. All ELISAs were performed according to the manufacturer's instructions and the following ELISAs were used: SC5b-9 (MicroVue™ Complement, Quidel, Osteomedical GmbH, Sissach, Switzerland), thrombin-antithrombin III complex (TAT) (Enzygnost® TAT micro, Siemens Healthcare, Erlangen, Germany), polymorphonuclear (PMN) elastase (PMN elastase ELISA, Demeditec Diagnostics, Kiel, Germany), and β-thromboglobulin (β-TG) (Asserachrome® β-TG, Diagnostica Stago, Parsippany, NJ, USA). In addition, protein adsorption to the membranes was determined at the end of whole blood incubation as described in Section 2.3.

2.5 Mass spectrometry (MS) analysis

SDS PAGE short gel purification was run and in-gel digestion with trypsin was conducted as described previously (26). Extracted peptides were desalted using C18 StageTips (27) and subjected to LC-MS/MS analysis. LC-MS/MS analyses were performed on an Easy-nLC 1200 UHPLC (ultra-high performance liquid chromatography) (Thermo Fisher Scientific) coupled to an QExactive HF Orbitrap mass spectrometer (Thermo Fisher Scientific) as described elsewhere (28). Peptides were eluted with a 60 min segmented gradient at a flow rate of 200 nl/min, selecting the 20 most intensive peaks for fragmentation with HCD (higher-energy collisional dissociation). The MS data was processed with MaxQuant software suite v. 1.5.2.8 and v.1.6.7.0 (29) The LFQ (label-free-quantification) was used for analyses. Database search was provided against human (96,817 entries) UniProt database using the Andromeda search engine (30).

2.6 Statistics

Experiments were performed with the blood from four independent donors ($n = 4$) and three different plasma ($n = 3$ independent experiments, each plasma consisted of a pool from 3 donors). Significant differences were analyzed using unpaired two-tailed Student's t-tests assuming equal variance. Statistical significance was defined as $p < 0.05$ and statistical analysis was performed using Microsoft Excel 365 (Microsoft, Albuquerque, USA) and GraphPad Prism version 6.01 (GraphPad Software Inc., La Jolla, CA, USA).

3 Results

In this research work, the influence of two different membranes, PMP gas exchange or PET heat exchange membranes, and different flow rates (1.0 L/min and 0.2 L/min) on the surface plasma protein binding over time was investigated. Only heparin-coated miniature devices were used. Part of the data, namely heparinized PMP devices with 1.0 L/min, were discussed previously (24), but all experiments shown here were performed at the same time. To be able to draw conclusions about the effects of various endogenous defense reactions, various markers of blood coagulation, the complement system, inflammation, and platelet activation were determined using ELISAs in addition to the detection of adsorbed proteins using MS.

3.1 Comparison of total numbers of desorbed proteins

In total, 532 different desorbed proteins were detected by MS in the four conditions. A full list of desorbed proteins measured by MS can be found in Supplementary Tables S1–S4. The total number of different proteins found at both membrane types and

10.3389/fcvm.2025.1578538

TABLE 1 Number of desorbed proteins after contact with plasma that were present at all time points on heparin-coated PMP and PET membranes at different flow rates (1 L/min and 0.2 L/min) presented as percentage of the total protein number found in general and present at the respective condition.

Type of membrane	Flow rate	# of different proteins	% of proteins present at all time points	
			Per condition	From total
PMP	1 L/min	373	40.8	29.0
	0.2 L/min	311	47.9	28.4
PET	1 L/min	403	35.2	27.0
	0.2 L/min	306	48.7	28.4

at the low and high flow rates are listed in Table 1. The highest total number of different proteins was detected for PET (heat exchange) membranes at 1 L/min while both membranes (PMP and PET) at lower flow rates (0.2 L/min) showed similar protein numbers. However, the number of proteins present at all individual time points showed a different result. Here, the lower flow rates showed higher proportions of proteins that were present at each time point at both membrane types that at the higher flow rates.

The numbers of proteins at each time point are shown in Figure 1. Here, the PMP membranes at the high flow rate had mostly the highest number of proteins desorbed. Already here it becomes apparent that the influence of different membrane materials is not high, if both are heparin-coated, especially at a low flow rate. While at a faster flow rate of 1 L/min, there was occasionally a higher difference in the number of bound proteins (1 L/min, black lines), the number of bound proteins at a flow rate of 0.2 L/min was almost identical (0.2 L/min, grey lines). Comparing the different flow rates, it is evident that a faster flow rate also leads to a higher number of bound proteins on the PMP membrane; this trend was evident throughout the entire time. A similar behavior was observed with the PET membrane. However, after 5 min the opposite behaviour was observed once, with a lower number of proteins desorbed from the high-flow device. In the period between 10 and 90 min, the protein number was almost identical before it increased at 180 min with a higher flow rate and then settled again at a similar level after 360 min. Overall, 133 proteins were found at each individual time point in all conditions. The number of proteins differing between conditions can be seen in the Venn-Diagrams (Figures 2a–d). It is apparent that only few (5–15) differed at most in their binding profile. For each parameter comparison, i.e., flow rates on PMP (Figure 2a) or PMP (Figure 2b), and materials at 1 L/min (Figure 2c) or 0.2 L/min (Figure 2d), that are consistently present at all time points in one condition but absent at some time points in the other are named.

3.2 Identifying the most abundant proteins on different membrane types and flow rates

To determine the composition of the protein layer on the membranes, the relative amount of each protein in relation to the other proteins was determined. This can provide information about the statistically most likely present proteins and binding partners, and thus define the influence of the material and the flow rate more accurately. Tables 2–5 show the ten most abundant proteins on the PMP and PET membranes at flow rates of 1 L/min and 0.2 L/min, respectively. The order of abundance of all proteins is shown in Supplementary Tables S1–S4.

The proteins that bind with the highest abundance were very similar for both membrane types and flow rates. Eight (APOB, ALB, SERPINC1, FGG, FGA, FGB, APOE, FN1) out of ten were among the ten most abundant proteins in all conditions (i.e., on both membrane types, flow rates, and at all time points), albeit in a slightly different order. While the order of the most abundant proteins on the PMP membranes (Table 3) and the

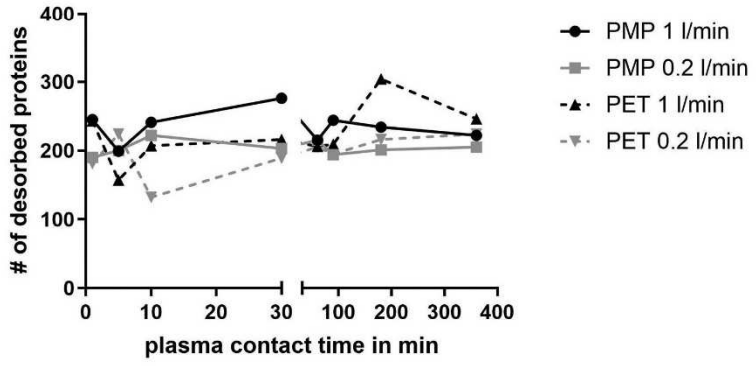

FIGURE 1
Number of different desorbed proteins after plasma contact over time on different surfaces (PMP and PET) and under different conditions (flow rates 1 L/min and 0.2 L/min).

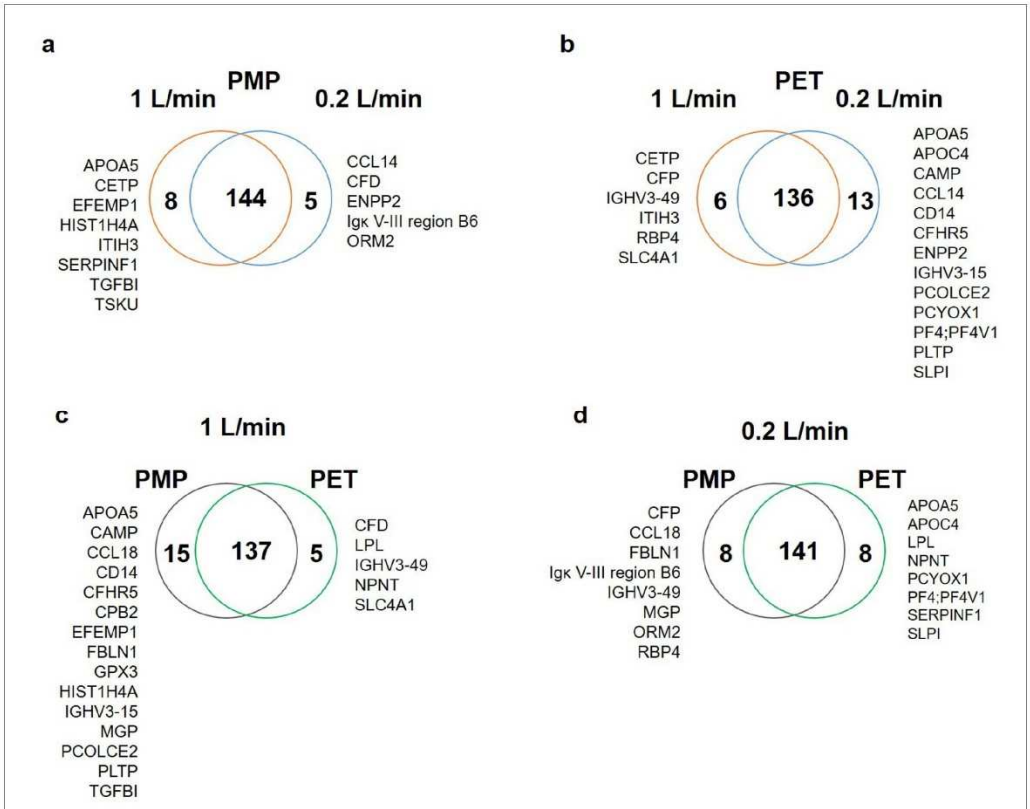

FIGURE 2
Venn-Diagrams presenting the number of proteins present at all time points in the individual conditions in comparison. **(a)** On the PMP membrane 144 proteins were present at both flow rates, whereas 8 proteins were only seen at all time points at high flow, and 5 at low flow. **(b)** On the PET membranes 136 proteins were present at all time points, but 6 only at the higher flow and 13 only at the lower flow rate at all time points. **(c)** At the high flow rate 137 proteins were found at each time point on both membrane types, but 15 were present only on PMP at each time point, and 5 on PET at each time point. **(d)** At the lower flow rate 141 proteins were found at each time point on both membrane types, but 8 were not present at all time points on PMP or PET, respectively.

TABLE 2 The ten most abundant proteins on heparin-coated PMP membranes incubated with a flow rate of 1 L/min.

PMP 1 L/min	1 min	5 min	10 min	30 min	60 min	90 min	180 min	360 min
1	APOB	ALB	APOB	ALB	FGA	APOB	ALB	FGA
2	ALB	FGG	FGG	APOB	APOB	FGA	FGG	FGB
3	SERPINC1	FGA	ALB	FGG	FGB	FGB	APOB	APOB
4	FGG	FGB	FGA	FGA	FGG	FGG	FGA	FGG
5	FGA	APOB	SERPINC1	FGB	ALB	ALB	FGB	ALB
6	APOE	FN1	FGB	SERPINC1	SERPINC1	SERPINC1	ITIH4	ITIH4
7	FGB	SERPINC1	APOE	APOE	FN1	APOE	C3	FN1
8	LBP	C3	FN1	C3	APOE	C3	FN1	C3
9	FCN2	APOE	FCN2	TF	C3	FN1	SERPINC1	SERPINC1
10	FN1	TF	LBP	FN1	ITIH4	ITIH4	APOE	APOE

Reproduced with permission from "The ten most abundant proteins on heparin-coated PMP membranes" by Katharina Große-Berkenbusch, Meltem Avci-Adali, Madeleine Arnold, Linda Cahalan, Patrick Cahalan, Ana Velic, Boris Maček, Christian Schlensak, Hans Peter Wendel and Sandra Stoppelkamp.

TABLE 3 The ten most abundant proteins on heparin-coated PMP membranes incubated with a flow rate of 0.2 L/min.

PMP 0.2 L/min	1 min	5 min	10 min	30 min	60 min	90 min	180 min	360 min
1	ALB	ALB	ALB	FGA	FGA	ALB	ALB	APOB
2	FGA	FGB	APOB	FGB	FGB	FGA	APOB	FGA
3	FGB	FGA	FGA	APOB	FGG	FGB	FGA	FGB
4	APOB	FGG	FGB	FGG	APOB	FGG	FGB	FGG
5	FGG	FN1	FGG	ALB	ALB	APOB	FGG	ALB
6	SERPINC1	APOB	SERPINC1	SERPINC1	SERPINC1	C3	SERPINC1	APOE
7	FN1	SERPINC1	FN1	APOE	FN1	FN1	APOE	FN1
8	APOE	APOE	APOE	FN1	APOE	SERPINC1	C3	SERPINC1
9	LBP	C3	FCN2	FCN2	FCN2	APOE	FCN2	C3
10	C3	IGHG1	ANG	C3	C3	FCN2	FN1	LPA

TABLE 4 The ten most abundant proteins on heparin-coated PET membranes incubated with a flow rate of 1 L/min.

PET 1 L/min	1 min	5 min	10 min	30 min	60 min	90 min	180 min	360 min
1	FGA	FGA	FGA	FGA	FGA	FGA	FGA	FGA
2	FGB	FGB	ALB	FGB	FGB	FGB	FGB	APOB
3	FGG	FGG	FGB	ALB	ALB	ALB	ALB	FGB
4	ALB	ALB	FGG	FGG	FGG	FGG	FGG	FGG
5	APOB	FN1	APOB	APOB	APOB	APOB	APOB	ALB
6	SERPINC1	APOB	SERPINC1	FN1	SERPINC1	C3	C3	ITIH4
7	FN1	SERPINC1	FN1	APOE	FN1	FN1	FN1	FN1
8	APOE	APOE	APOE	SERPINC1	C3	ITIH4	ITIH4	C3
9	LBP	C3	C3	C3	ITIH4	SERPINC1	SERPINC1	SERPINC1
10	C3	ANG	LBP	ITIH4	APOE	APOE	APOE	APOE

TABLE 5 The ten most abundant proteins on heparin-coated PET membranes incubated with a flow rate of 0.2 L/min.

PET 0.2 L/min	1 min	5 min	10 min	30 min	60 min	90 min	180 min	360 min
1	FGA	ALB	FGB	FGA	ALB	FGA	APOB	ALB
2	FGB	FGA	FGA	FGB	FGA	FGB	ALB	APOB
3	FGG	FGB	FGG	FGG	FGB	FGG	FGA	FGA
4	ALB	FGG	ALB	ALB	FGG	APOB	FGB	FGB
5	FN1	APOB	FN1	APOB	APOB	ALB	FGG	FGG
6	APOB	SERPINC1	APOB	SERPINC1	SERPINC1	SERPINC1	SERPINC1	C3
7	SERPINC1	FN1	SERPINC1	APOE	C3	APOE	C3	APOE
8	APOE	APOE	APOE	C3	APOE	FN1	APOE	SERPINC1
9	C3	C3	ANG	LBP	FN1	C3	FN1	FN1
10	TF	TF	C3	FN1	TF	LBP	LBP	TF

PET membranes (Table 5) changed frequently over time with the lower flow rate, it was remarkably stable on the PET membrane at a flow rate of 1 L/min (Table 4). FGA was the most frequently bound, followed by FGB, which was the second most bound protein except for 10 min and 360 min. Only minor differences were observed in the order of the subsequent proteins of Table 4.

When comparing the abundance of proteins related to the complement pathways, especially the complement activating proteins C3, C1, ficolins, and MASP1/2, but also the regulatory proteins CFH, vitronectin, and clusterin were found among the ~50 most common proteins in all samples. Thrombosis-activating proteins that were present in larger abundance in all conditions included fibrinogen, prothrombin (F2), tissue factor (F2), F11, kininogen, and vWF, as well as the inhibitory proteins ATIII, protein C inhibitor (PCI), and α-2-macroglobulin (A2M) and the fibrinolysis-related proteins fibronectin and inter-alpha-trypsin inhibitor proteins (ITIH2/3/4).

3.3 Differences in protein binding over time

Although the most frequently bound proteins were relatively stable over time for both membrane types and at both flow rates (Tables 2–5), clear differences were observed when comparing the relative abundance (LFQ) of proteins present at all time points over time. The significant changes occurring between 1 and 360 min indicate the remodeling of the protein layer (Figure 3). A stronger remodeling of the protein layer occurred

10.3389/fcvm.2025.1578538

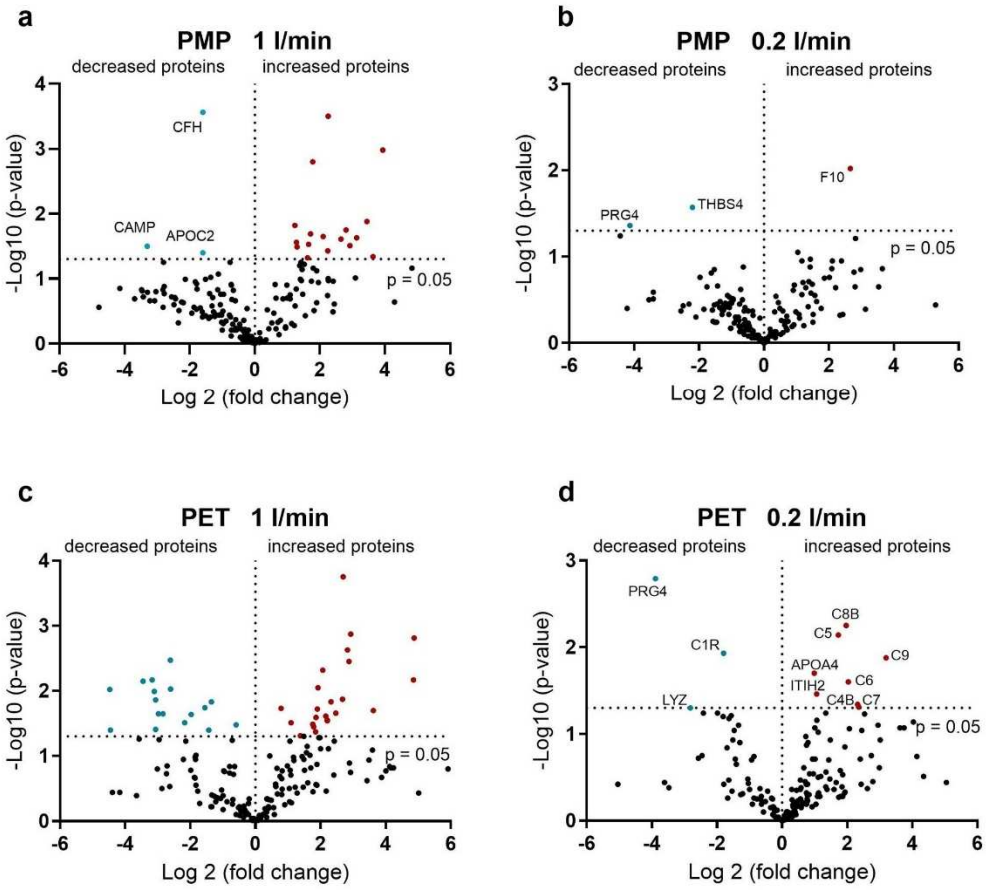

FIGURE 3
Volcano plot showing the change in protein abundance after 360 min compared to one minute. (a) On the PMP membranes at a high flow rate, some of the proteins showed an increasing abundance over time. (b) On the PMP membranes at a low flow rate, almost all proteins showed a constant binding profile over time. (c) On the PET membranes at a high flow rate, both an increase and a decrease in protein binding over time were observed. (e) On the PET membrane at a low flow rate, a lower number of proteins were detected with an increase and a decrease over time. Significant differences were analyzed using unpaired two-tailed Student's *t*-tests assuming equal variance (significance level $p < 0.05$), $n = 3$.

with higher flow rates on both membrane types (Figures 3a vs. b,c vs. d). An interesting observation here was the higher level of significant changes in protein binding over time on the PET membranes compared to the PMP membranes at the same flow rates (Figures 3a vs. c,b vs. d). While only three proteins (CFH, CAMP, and APOC2) with a significantly decreased (3-fold lower) binding abundance over time were detected on the PMP membrane at a high flow rate (Figure 3a), significantly decreased binding abundance over time occurred more frequently and with larger (up to 20-fold) changes on the PET membrane (Figure 3c). Increased protein abundance on the PMP membrane was mostly observed for lipid transport related proteins (CETP, PLTP), inhibitors of trypsin (ITIH3 and 4) and chymotrypsin (SERPIND1), fibrinogen, von Willebrand factor, and complement inhibitors clusterin and vitronectin as well as complement factor 9 (C9).

By reducing the flow rate, significant changes in binding frequency over time can be almost eliminated for both membrane types. However, at low blood flow, the few proteins that increase significantly over time are of crucial importance. On the PMP membrane, binding of the central factor of the coagulation cascade, FX, increased 6-fold over time. In contrast, on the PET membrane with lower flow rate, proteins of the complement system mainly increased significantly over time, with C9 increasing the most (9-fold).

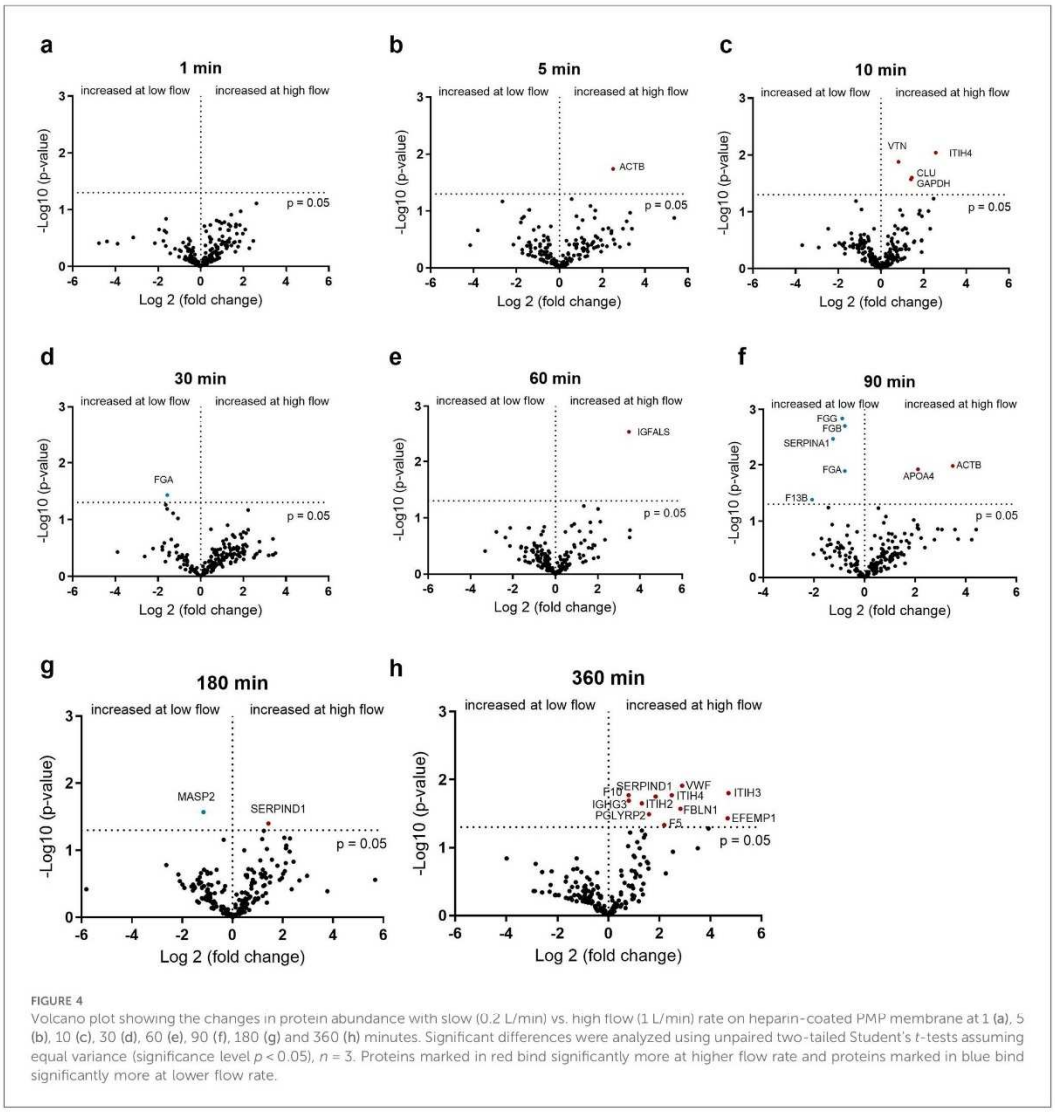

FIGURE 4
Volcano plot showing the changes in protein abundance with slow (0.2 L/min) vs. high flow (1 L/min) rate on heparin-coated PMP membrane at 1 (**a**), 5 (**b**), 10 (**c**), 30 (**d**), 60 (**e**), 90 (**f**), 180 (**g**) and 360 (**h**) minutes. Significant differences were analyzed using unpaired two-tailed Student's *t*-tests assuming equal variance (significance level $p < 0.05$), $n = 3$. Proteins marked in red bind significantly more at higher flow rate and proteins marked in blue bind significantly more at lower flow rate.

3.4 Identifying the effect of flow rate on plasma protein binding

Since different degrees of protein remodeling were observed during the 6 h under the four conditions, the individual time points were investigated in more detail. First, the adsorbed proteins were compared between a slow (0.2 L/min) and fast (1 L/min) flow rate with PMP and PET membranes. The effects of flow rate on protein adsorption on the PMP membrane are shown in Figure 4. At most time points, no significant increase in protein adsorption was observed at low flow rates. Significantly increased protein binding was detected for some proteins [α-1-antitrypsin (SERPINA1), FXIII (F13B), and fibrinogen] after 90 min at a low flow rate on PMP membranes (Figure 4f). At a low flow rate, increased fibrinogen binding was also observed after 30 min (Figure 4d), as well as increased MASP1 binding after 180 min (Figure 4g). In particular, after 360 min at a faster flow rate (Figure 4h), increased numbers of significantly elevated proteins, including proteins of the coagulation cascade (VWF, F10, SERPIND1, F5) were detected.

The influence of the flow rate on the PET membrane is shown in Figure 5. In contrast to the PMP membrane, differences in protein adsorption can already be seen after 5 min. Here, fibrinogen binds significantly more at a higher flow rate (Figure 5b). This is in contrast to the PMP membrane, where fibrinogen was bound significantly more at a lower flow rate. Within the first 60 min, the 5 min time point showed the most alterations in protein abundance

10.3389/fcvm.2025.1578538

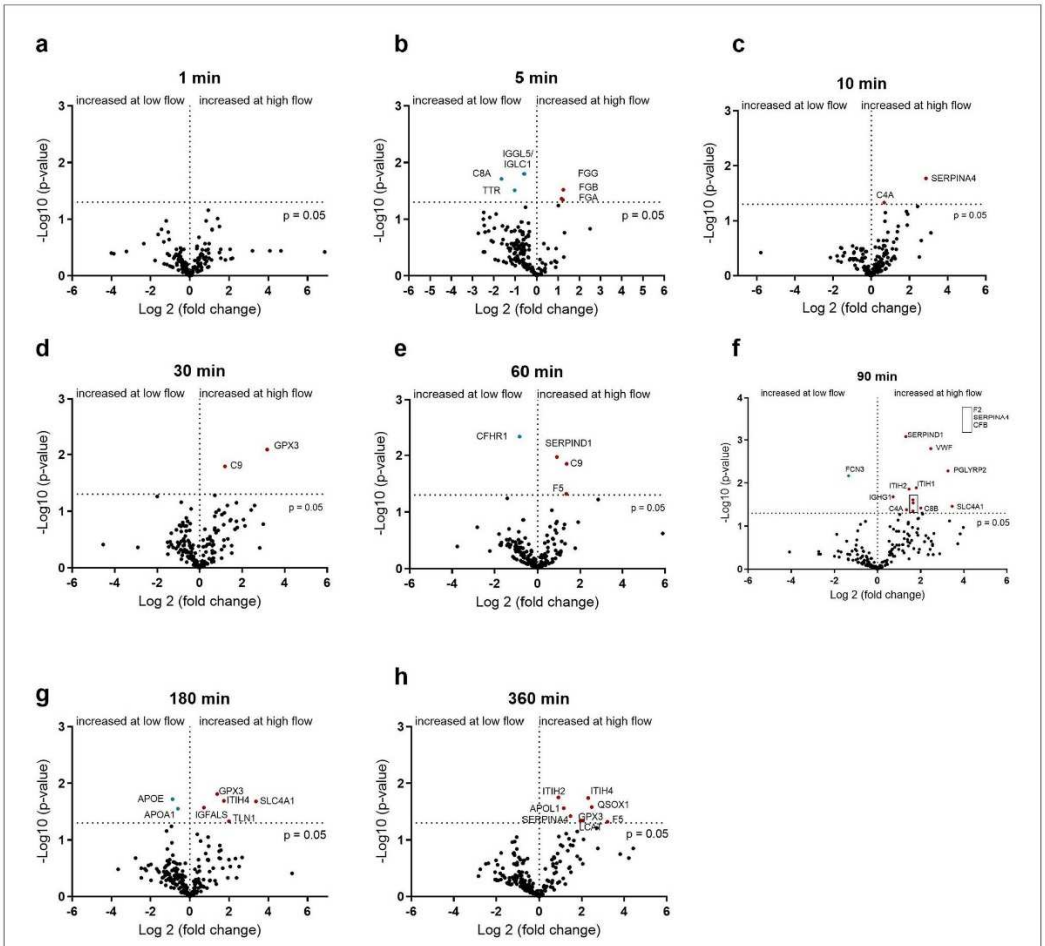

FIGURE 5
Volcano plot showing the changes in protein abundance with slow (0.2 L/min) vs. high flow (1 L/min) rate on heparin-coated PET membrane at 1 (**a**), 5 (**b**), 10 (**c**), 30 (**d**), 60 (**e**), 90 (**f**), 180 (**g**) and 360 (**h**) minutes. Significant differences were analyzed using unpaired two-tailed Student's *t*-tests assuming equal variance (significance level $p < 0.05$), $n = 3$. Proteins marked in red bind significantly more at higher flow rate and proteins marked in blue bind significantly more at lower flow rate.

due to flow intensity and an increased C9 binding after 30 and 60 min at a higher flow rate could be detected. From 90 min onwards, several proteins again showed increased binding due to a faster flow rate. These included proteins of the coagulation cascade (VWF, F2) and complement factor B (CFB).

3.5 Identifying the effect of the surface on plasma protein binding

In addition to the influence of the flow rate, the dependence of protein binding on the membrane type was also investigated. The differences in protein binding between PMP and PET membranes at a fast flow rate are shown in Figure 6. In the initial phase, after 5 min, FCN3, MASP1, and APOM were significantly higher on PMP membranes, and significantly higher fibrinogen binding was detected on PET membranes. In general, the greatest differences in binding frequency were observed after 10 min, indicating the strongest influence of the material at this time. Thereafter, only a few differences (mainly on the PMP membrane) were observed. This shows that more significant protein changes over the entire time were seen on PMP membranes at the high flow rate, but a stronger remodeling occurred on PET membranes at 10 min.

If the flow was reduced to 0.2 L/min, the membrane type played almost no role, in contrast to a higher flow rate of

10.3389/fcvm.2025.1578538

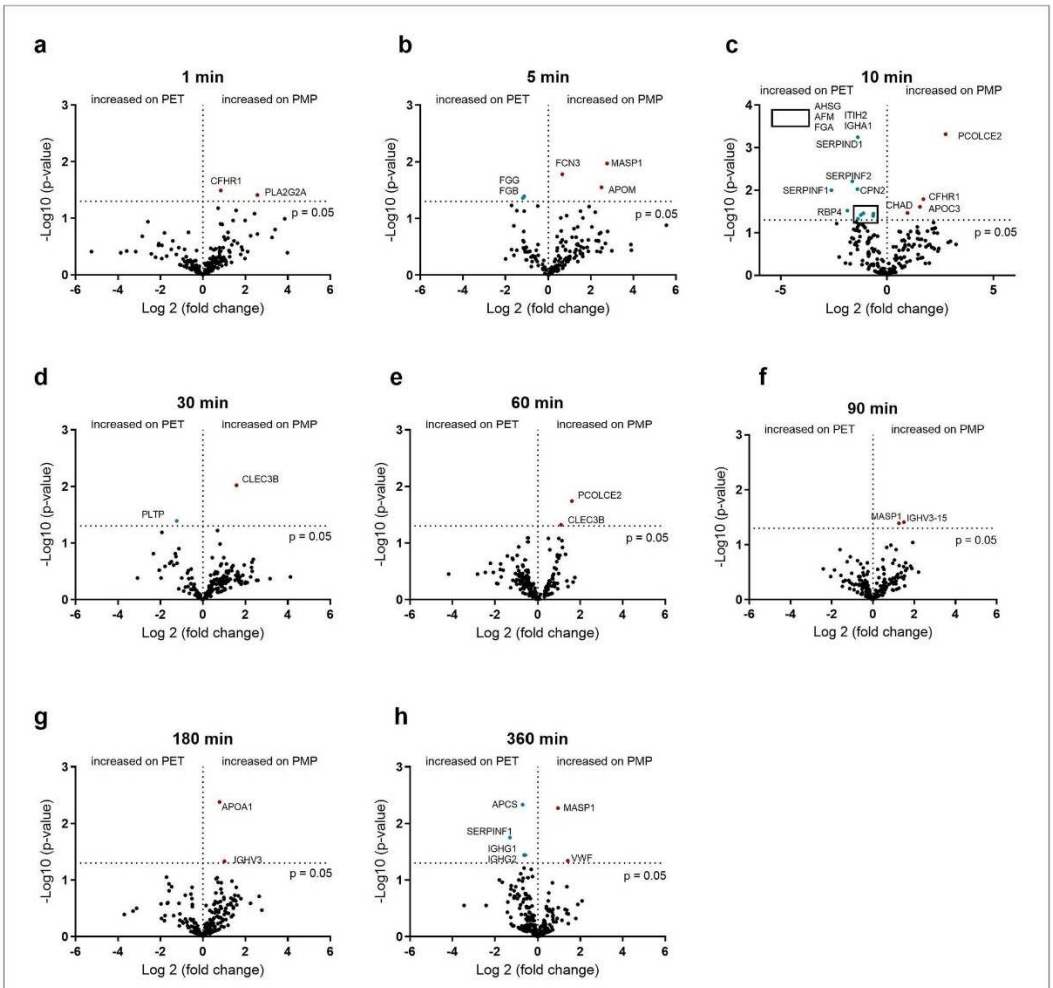

FIGURE 6
Volcano plot showing the changes in protein abundance on heparin-coated PMP membrane vs. heparin-coated PET membrane with a high flow from 1 L/min at 1 (**a**), 5 (**b**), 10 (**c**), 30 (**d**), 60 (**e**), 90 (**f**), 180 (**g**) and 360 (**h**) minutes. Significant differences were analyzed using unpaired two-tailed Student's *t*-tests assuming equal variance (significance level $p < 0.05$), $n = 3$. Proteins marked in red bind significantly more on PMP membrane, proteins marked in blue bind significantly more on PET membrane. The 5 proteins in the box in (**c**) are named in the upper left quadrant of the diagram due to space issues.

1 L/min. The small differences in the binding abundance are shown in Figure 7. Although only very few proteins differed significantly in their binding abundance, these could be of significance. The increased binding of C9 and heparin co-factor 2 (SERPIND1) on the PET membrane after 30 min, the increased binding of ficolin-3 (FCN3) after 60 min as well as the increased binding of C1-esterase inhibitor (SERPING1) and α-1-antitrypsin (SERPINA1) on the PMP membrane after 90 min should be emphasized here.

The individual binding profiles of all coagulation and complement components that showed significant differences in Figures 3–6 are shown in Supplementary Figures S1 (complement) and S2 (coagulation).

3.6 Comparison of the hemocompatibility

To determine the effects of protein binding on the course of the body's various defense reactions, the blood cell counts and plasma levels of various hemocompatibility markers were determined over time (Figure 8). Blood cell counts and hematological parameters were assessed at all time points. The numbers of white blood

10.3389/fcvm.2025.1578538

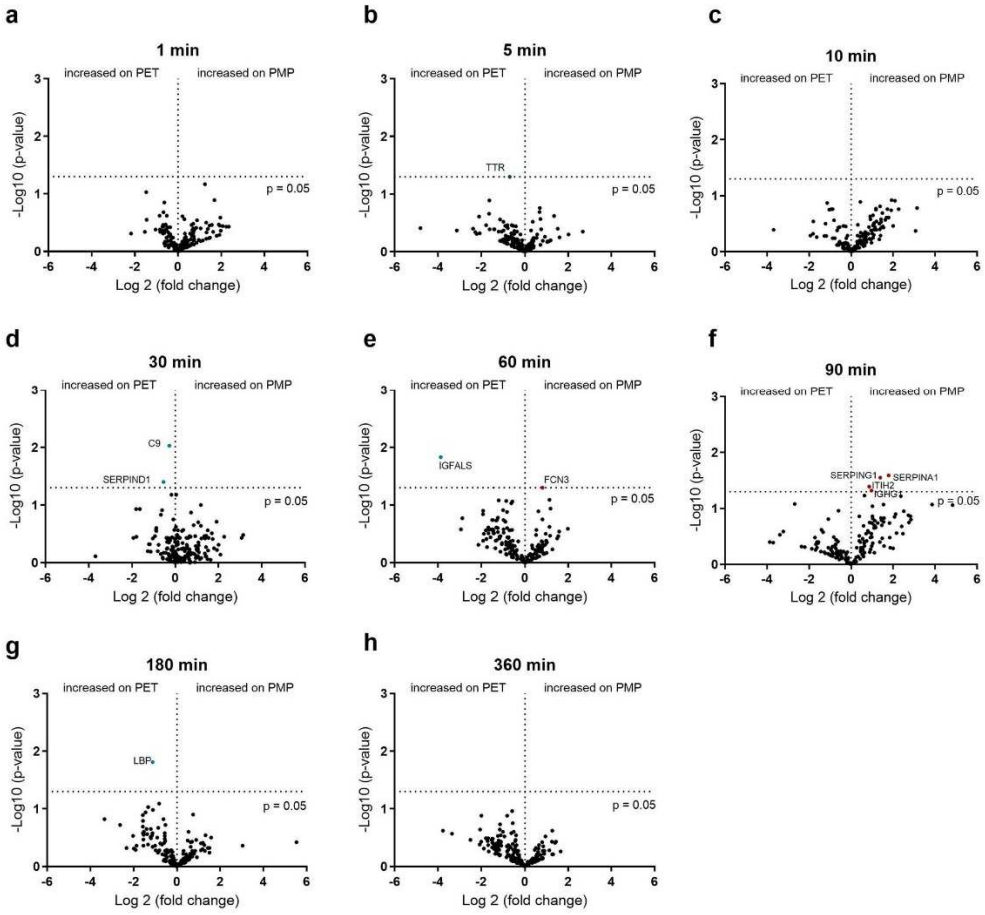

FIGURE 7
Volcano plot showing the changes in protein abundance on heparin-coated PMP membrane vs. a heparin-coated PET membrane with a low flow from 0.2 L/min at 1 (a), 5 (b), 10 (c), 30 (d), 60 (e), 90 (f), 180 (g) and 360 (h) minutes. Significant differences were analyzed using unpaired two-tailed Student's *t*-tests assuming equal variance (significance level $p < 0.05$), $n = 3$. Proteins marked in red bind significantly more on PMP membrane, proteins marked in blue bind significantly more on PET membrane.

cells, red blood cells, platelets, as well as hemoglobin and hematocrit levels remained constant throughout the experiment, with no significant differences over time or between high and low flow rate time points and the different membrane types (data not shown). Inflammation (PMN elastase), complement (SC5b-9), coagulation (TAT complex), and platelet (β-TG) activation markers increased over time with both membrane types and flow rates, but only after 6 h a significantly increased activation of inflammation, complement system, and platelets were detected ($p < 0.05$ labeled with $). Although not statistically significant, the highest TAT levels were also observed after 6 h of incubation.

A lower flow rate with PMP and PET membranes resulted in lower PMN elastase, SC5b-9, and β-TG levels across the different time points than at higher flow rate. At 360 min, TAT values were also lower in samples obtained from low flow rate conditions for both membrane types. The incubation of PET membranes with the lower flow rate led to significantly lower platelet activation (β-TG) at 1 min ($^*p < 0.05$) and inflammatory activation (PMN elastase) at 90 min ($^*p < 0.05$) (Figure 8d). Furthermore, at 5 min, significantly lower β-TG levels were observed in samples incubated with PMP membranes at a low flow rate compared to a high flow rate ($^{**}p < 0.01$) (Figure 8b). This is remarkable as no significant differences in protein binding due to flow rates were observed at this early stage (Figure 4). Complement activation was significantly reduced in blood samples incubated with the PET membrane after 360 min

10.3389/fcvm.2025.1578538

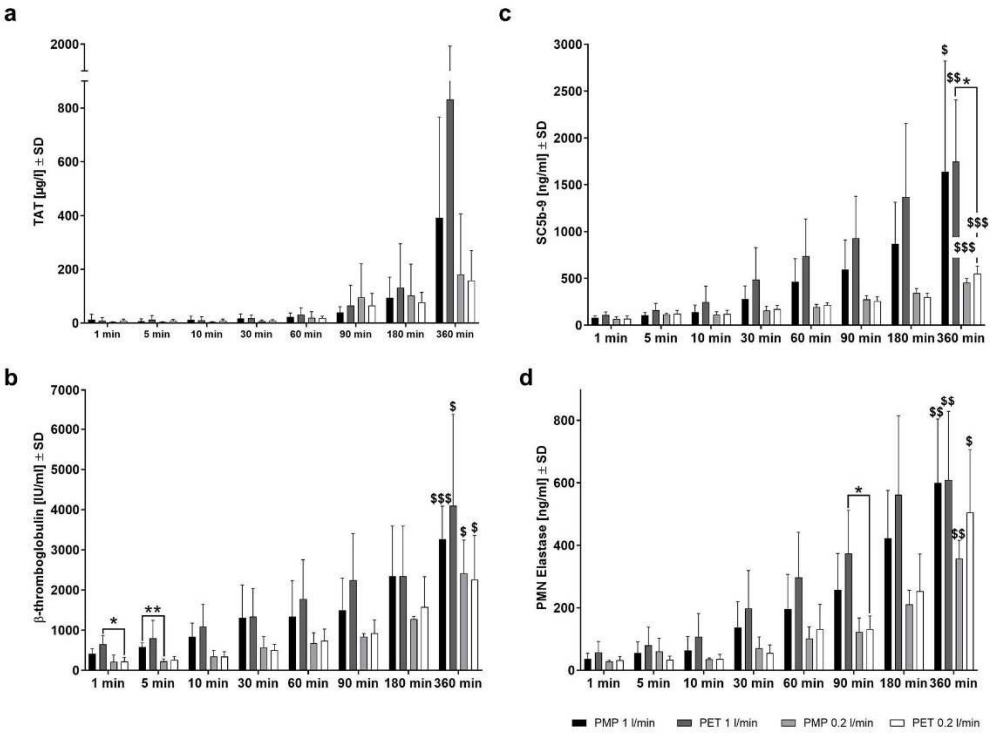

FIGURE 8
Hemocompatibility parameters measured after whole blood incubation at different time points. Plasma levels of (a) coagulation activation (TAT), (b) inflammation activation (PMN-elastase), (c) complement activation (SC5b-9), and (d) platelet activation (β-TG) were measured in a mock loop system with either a heparin-coated PMP membrane or a heparin-coated PET membrane and at a high (1.0 L/min) or low (0.2 L/min) flow rate. Differences were detected by unpaired two-tailed Student's *t*-test $*p < 0.05$, $**p < 0.01$ show significant differences between materials or settings within the same time point; "$" denotes significant differences compared to 1 min of the same material or setting, $ $p < 0.05$, $$ $p < 0.01$, $$$ $p < 0.001$, $n = 4$.

at a lower flow rate ($*p < 0.05$) (Figure 8c). This was also indicated by significantly increased C9 binding to the PET membrane after 30 (Figure 5d) and 60 min (Figure 5e) of plasma contact at higher flow rates and increased C8B binding after 90 min (Figure 5f).

4 Discussion

In this study, the influence of different HFM membrane materials and flow rates on the binding of plasma proteins over time was investigated for the first time. Therefore, heparin-coated miniature devices with HFM membranes were used, and the desorbed plasma proteins on HFMs were compared over time using MS. In addition, various markers of blood activation, i.e., coagulation, complement system, inflammation, and platelets were measured using ELISAs. In the miniature devices, heparin was covalently coupled to the surface by a reductive amination reaction between the terminal aldehydes of the heparin chains and the primary amines in the primer matrix. This form of binding is referred to as end-point attachment (EPA) and reflects the simple covalent binding of the heparin molecules to the substrate. EPA results in the specific binding of proteins with a heparin-binding side, as discussed in detail in our previous study (24).

Considering the overall quantity (LFQ) of proteins, a comparable amount of proteins adsorbed to both membrane types at both flow conditions, but the number of different proteins was mostly highest over time on PMP membranes at the high flow rate. When comparing the heparin-coated PMP and PET membranes, it could be detected that higher flow rates led to increased adsorption of various proteins on both membrane types. Among the 10 most abundant proteins under all conditions were the proteins APOB, ALB, ATIII, FGG, FGA, FGB, APOE, and FN1. This is in part consistent with previous reports of protein layers detected on diverse biomaterials in which fibrinogen, albumin, vitronectin, and ApoA1 were found (31). The order of abundance is certainly modulated by the

heparinization of the HFM. Many of these 10 most abundant proteins have a heparin-binding site (such as APOB, APOE, FN1, FCN2, and SERPINC1 ref. UniProt). Therefore, their presence on heparinized surfaces is to be expected. Considering their general relative abundance in blood, the order of the 10 most abundant proteins detected here could be expected as follows: ALB > TF > C3 > APOB > FN1 > Fibrinogen > IGHG1 > SERPINC1 > ITIH4 > APOE > FCN2 > LBp > ANG (32). Interestingly, in our study, the two proteins with the highest concentration in blood (albumin with 40 g/L and transferrin with 20 g/L), neither of which has a heparin-binding site, were adsorbed quite differently to the HFM membranes. Albumin was found on all membranes, whereas transferrin was only sporadically found among the first 10 proteins. Other proteins harbouring a heparin-binding site and are present in relatively high amounts in blood are e.g., SERPING1 and SERPIND1 (32), but these proteins were found on the membranes around the first 50–100 detected proteins. Of the two proteins with similar abundance in blood, APOB and C3 (32), APOB was found in higher amounts (often the most abundant protein) than C3, probably because APOB has a heparin-binding site. The binding of C3 to membranes, despite lacking a heparin binding site, is most likely due to its thioester bond exposed after activation (33, 34).

Although it has been reported that HMWK and HDL can displace fibrinogen (31), we could not detect such an effect in our study over 6 h. KNG1 was found among the first 42–62 detected proteins (once as the 19th most abundant protein on PMP membranes at 0.2 L/min) and proteins associated with HDL (such as the apolipoproteins A, C, D, E, F, M) were not found increased on the membranes over time. Only APOE was among the 10 most abundant proteins. Although we did not observe the described displacement, the order of abundance varied over time as described by Vroman (35, 36), and FGA consistently bound most abundantly on the PMP and PET membranes at a flow rate of 1 L/min.

Gore et al. (37) describe that the amount and reduction of plasma protein binding alone are not sufficient to improve hemocompatibility and hypothesize that specific antithrombin binding is mainly responsible for the improved hemocompatibility of the heparin coating. In our study, we also detected high ATIII (SERPINC1) binding under all measured conditions (rank 3–12). Importantly, a general observation was that lower flow rates resulted in less significant protein changes on the membranes than higher flow rates. More interestingly, PMP membranes showed less significant changes in proteins over 6 h than PET membranes.

The findings by Blezer et al. (38) underscore the dual nature of heparinized surfaces in their interaction with the coagulation system. While these surfaces are inherently thrombogenic, the immobilization of heparin combined with the plasma serine protease inhibitor antithrombin shifts their behavior towards strong antithrombotic activity by effectively slowing the propagation of blood clotting. This mechanism depends on the ability of the immobilized heparin-antithrombin complex to inhibit serine proteases such as thrombin. Thus, the effectiveness of heparinized surfaces in inhibiting the activation of serine proteases may also be influenced by diffusion processes. Specifically, the bioactivity of the heparinized surface could depend on how effectively its target molecules, such as serine protease inhibitors, diffuse to interact with heparin.

4.1 Influence of flow rate on protein binding

The process of thrombus formation and complement activation is initiated when blood comes into contact with artificial surfaces or damaged endothelium (39). The first step in this process is the adsorption of blood proteins, followed by the adhesion and activation of platelets. These processes are influenced by the fluid mechanics of the blood flow, in particular by the wall shear stress, which is the force per area of the wall caused by the flow. The constant wall shear stress in normal blood circulation indicates its important function (5). When blood comes into contact with a biomaterial, fluid mechanics, especially shear stress, can damage erythrocytes and platelets (40). Although experiments performed with blood plasma cannot accurately consider the effects of cell interaction with the surfaces, differential binding of plasma proteins was observed at different flow rates.

It was striking that an increased binding of the proteins of the coagulation cascade (PMP: VWF, F10, SERPIND1, F5; PET: VWF, F2) occurred especially at the late time point (360 min) at a high flow rate, while complement inhibitor proteins (VTN, CLU) were bound significantly more at the beginning (10 min, 1 L/min). Despite the commonly observed tendency of increased protein binding with increased flow rate, fibrinogen, F13B, and α-1-antitrypsin (SERPINA1) were found significantly more on PMP membranes at low flow rate. Increased fibrinogen deposition at a lower flow rate was observed previously (41). The simultaneous presence of both SERPINA1 and F13B is not surprising as α-1-antitrypsin is one of the most abundant proteins in fibrin clots (42) and the F13b subunit accelerates the crosslinking of fibrin by binding to FXIII-A, fibrinogen, and thrombin (43). Shear stress caused by blood flow can trigger the activation of von Willebrand factor (vWF) and its binding to the platelet glycoprotein Ib receptor (GPIb), followed by activation of GPIIb/IIIa receptor, which binds vWF or fibrinogen and mediates platelet aggregation (44). Thus, high shear stress and the resulting conformational changes in vWF could increase its binding to the HFM surfaces, as observed *in vitro* with isolated platelets subjected to increased shear stress. When platelets were suspended in HEPES-buffer alone, elevated shear stress created in stainless steel viscosimeter with rotating cone and stationary plate led to increased platelet binding. However, the addition of fibrinogen, vWF multimeric forms, or both, significantly increased shear-induced platelet adhesion (45). On the PET membrane, in addition to the increased binding of coagulation proteins at a higher flow rate, there was also increased binding of complement proteins (C4A; C9; CFB; C8B; Supplementary Figure S1) at some time points. The significantly increased sC5b-9 levels after the incubation of blood with the PET membrane for 360 min at a high flow rate compared to the low flow rate also indicate a possible correlation with the increased binding of complement proteins to the membranes. Our studies with whole blood also showed that high flow rates led to increased activation of

platelets, neutrophils, and the complement system, resulting in a deterioration of hemocompatibility. Medium flow rates for long-time ECMO are therefore desirable for reducing the protein adsorption to the HFM as well as reducing shear stress to cell components (46). This however, is only possible for some patients as the arterial oxygen saturation of 80% or higher is the main goal of ECMO (47) and the flow rates have to be adjusted accordingly.

4.2 Influence of membrane type on protein binding

The influence of the membrane types was only significant for very few proteins, especially at the low flow rate. This indicates that the flow rate has a greater influence on the adsorption of plasma proteins. Nevertheless, the influence of the material should not be underestimated. PMP and PET are both thermoplastic materials commonly used in medical devices and other applications (48, 49). However, they have some differences in their properties and characteristics. PMP is an amorphous polymer composed of repeating units of methylpentene monomers (50), while PET is a semi-crystalline polymer composed of repeating units of ethylene glycol and terephthalic acid (51). The comparison of the adsorbed plasma proteins on both materials showed that the fibrinogen (FGG, FGB, and FGA) and some other proteins associated with the inhibition of coagulation (SERPIND1) and fibrinolysis (SERPINF2) bind significantly more frequently to the PET membrane than to the PMP membrane at a high flow rate. Proteins of the complement system (MASP1, FCN3), but also of the coagulation cascade (VWF) were more frequently bound to the PMP membrane at high flow. This indicates that at high flow rates, PET HFM seems to have more influence on coagulation activation, whereas complement activation seems to be more prominent for PMP HFM. Under low flow conditions, two inhibitory proteins, C1-esterase inhibitor (SERPING1) and alpha-1-antitrypsin (SERPINA1), showed increased binding to the PMP membrane at 90 min, indicating that their presence could help to mitigate complement activation and inflammation. In a previous study, heparin-coating of PMP HFM not only reduced the overall number of adsorbed proteins compared to non-coated PMP HFM but also significantly decreased adsorption of coagulation-related proteins (FXII, FIX, FV, FX, fibrinogen, kalikrein, kininogen) and complement activation- related proteins (C3, C4, FH) (24). On the other hand, some proteins with heparin-binding sites [FXI, ATIII (=SERPINC1), C1INH (=SERPING1)] were more abundant on heparin-coated PMP HFM. We could therefore conclude that the heparin-coating generally led to reduced protein adsorption, particularly for proteins involved in coagulation and complement activation, while enhancing the binding of proteins that inhibit these processes. Compared to the present study, where both membrane types were heparin-coated, some similarities were observed: (1) for both heparin-coated membrane types, the number of adsorbed proteins present at all time points were reasonably similar; (2) activation-related proteins previously shown to bind more to non-coated PMP HFM did not show significant differences in binding between heparin-coated PMP and PET membranes; (3) levels of C1INH (SERPING1), ATIII (SERPINC1), and FXI were also not significantly different between heparin-coated PMP and PET HFM. Thus, heparinization of both membrane types has likely reduced overall protein adsorption and decreased binding of coagulation and complement activation-related proteins. When assessing hemocompatibility and developing new coating approaches, the literature often only considers the gas exchange membrane and neglects the heat exchange membrane (52–54). Our findings indicate that this approach is acceptable if the heat exchange membrane is also heparinized, as plasma protein adsorption on both membrane types was relatively similar and the flow rate played the most decisive role. Especially, considering increased presence of C1INH (SERPING1) and alpha-1-antitrypsin (SERPINA1) on PMP HFM at the lower flow rate.

5 Conclusion

In this study, the binding of plasma proteins to the surfaces of heparin-coated PMP or PET membranes was investigated at low and high flow rates over 6 h using miniature devices, and the adsorbed proteins on the membranes were measured by MS. The adsorption of plasma proteins on both membrane types was relatively similar, which could be related to the heparin-coating of both membrane materials. In contrast, the flow rate played the most decisive role. The main differences in protein binding occurred at early time points and higher flow rate and were no longer present after 6 h at a low flow rate. The studies with whole blood also showed an increased activation of thrombocytes, inflammation, and complement system at high flow rate for both material types compared to low flow rate. The main differences between materials observed were the increased binding of coagulation-associated proteins on PET HFM and complement activation-associated proteins on PMP HFM at the higher flow rate. Notably, at a low flow rate, PMP HFM exhibited a significant increase in binding of complement and inflammation inhibitors, suggesting a potential benefit of lowering the flow rate apart from the general reduction in protein adsorption.

Data availability statement

The original contributions presented in the study are included in the article/Supplementary Material, further inquiries can be directed to the corresponding author.

Ethics statement

The studies involving humans were approved by Ethics commitee of the University of Tübingen. The studies were conducted in accordance with the local legislation and institutional requirements. The human samples used in this study were acquired from a by- product of routine care or industry. Written informed consent for participation was not

required from the participants or the participants' legal guardians/ next of kin in accordance with the national legislation and institutional requirements.

Author contributions

KG-B: Conceptualization, Formal analysis, Investigation, Methodology, Validation, Visualization, Writing – original draft, Writing – review & editing. MA-A: Conceptualization, Resources, Supervision, Validation, Visualization, Writing – original draft, Writing – review & editing. PC: Investigation, Methodology, Writing – original draft, Writing – review & editing. LC: Investigation, Methodology, Writing – original draft, Writing – review & editing. AV: Formal analysis, Investigation, Methodology, Validation, Writing – original draft, Writing – review & editing. BM: Formal analysis, Investigation, Methodology, Validation, Writing – original draft, Writing – review & editing. CS: Conceptualization, Resources, Supervision, Writing – original draft, Writing – review & editing. HW: Conceptualization, Resources, Supervision, Writing – original draft, Writing – review & editing. SS: Conceptualization, Formal analysis, Funding acquisition, Project administration, Resources, Validation, Visualization, Writing – original draft, Writing – review & editing.

Funding

The author(s) declare that financial support was received for the research and/or publication of this article. This research was funded by the Deutsche Forschungsgemeinschaft (DFG) (STO 1176/1-1) within the priority programme SPP2014 "Towards an implantable lung". Part of the publication costs were covered by the Open Access Publishing Fund of University of Tübingen.

Acknowledgments

The authors would like to thank Bernd Neumann for his support with the experimental setup. Furthermore, we acknowledge the support by DFG. Furthermore, we acknowledge the support by DFG and Open Access Publishing Fund of University of Tübingen.

Conflict of interest

The DFG had no role in the design of the study; in the collection, analyses, or interpretation of data; in the writing of the manuscript, or in the decision to publish the results. PC and LC are employees of Ension, Inc.

The remaining authors declare that the research was conducted in the absence of any commercial or financial relationships that could be construed as a potential conflict of interest.

Generative AI statement

The authors declare that no Generative AI was used in the creation of this manuscript.

Publisher's note

All claims expressed in this article are solely those of the authors and do not necessarily represent those of their affiliated organizations, or those of the publisher, the editors and the reviewers. Any product that may be evaluated in this article, or claim that may be made by its manufacturer, is not guaranteed or endorsed by the publisher.

Supplementary material

The Supplementary Material for this article can be found online at: https://www.frontiersin.org/articles/10.3389/fcvm.2025.1578538/full#supplementary-material

SUPPLEMENTARY FIGURE 1
Binding profiles of complement components with differences between the materials and flow rates. Statistical analysis was performed using unpaired two-tailed *t*-test to determine the differences between heparin-coated PMP membrane and heparin-coated PET membrane, and the differences between 1 L/min and 0.2 L/min flow rate. Shown are mean values ± SD, $n = 3$; * $p < 0.05$; ** $p < 0.01$.

SUPPLEMENTARY FIGURE 2
Binding profiles of coagulation components with differences between the materials and flow rates. Statistical analysis was performed using unpaired two-tailed *t*-test to determine the differences between heparin-coated PMP membrane and heparin-coated PET membrane, and the differences between 1 L/min and 0.2 L/min flow rate. Shown are mean values ± SD, $n = 3$; * $p < 0.05$; ** $p < 0.01$.

References

1. Firstenberg MS. *Extracorporeal Membrane Oxygenation: Advances in Therapy*. Rijeka: BoD–Books on Demand (2016).

2. Thiagarajan RR, Barbaro RP, Rycus PT, Mcmullan DM, Conrad SA, Fortenberry JD, et al. Extracorporeal life support organization registry international report 2016. *ASAIO J.* (2017) 63(1):60–7. doi: 10.1097/MAT.0000000000000475

3. Zhang M, Pauls JP, Bartnikowski N, Haymet AB, Chan CH, Suen JY, et al. Anti-thrombogenic surface coatings for extracorporeal membrane oxygenation: a narrative review. *ACS Biomater Sci Eng.* (2021) 7(9):4402–19. doi: 10.1021/acsbiomaterials.1c00758

4. Marcum JA, Rosenberg RD. The biochemistry and physiology of anticoagulantly active heparin-like molecules. In: Simionescu N, Simionescu M, editors. *Endothelial Cell Biology in Health and Disease*. Boston, MA: Springer (1988). doi: 10.1007/978-1-4613-0937-6_10

5. Spijker H, Graaff R, Boonstra P, Busscher H, van Oeveren W. On the influence of flow conditions and wettability on blood material interactions. *Biomaterials.* (2003) 24(26):4717–27. doi: 10.1016/S0142-9612(03)00380-6

6. Peek GJ, Mugford M, Tiruvoipati R, Wilson A, Allen E, Thalanany MM, et al. Efficacy and economic assessment of conventional ventilatory support versus extracorporeal membrane oxygenation for severe adult respiratory failure (cesar): a multicentre randomised controlled trial. *Lancet.* (2009) 374(9698):1351–63. doi: 10.1016/S0140-6736(09)61069-2

7. Di Nardo M, Vercaemst L, Swol J, Barret N, Taccone FS, Malfertheiner MV, et al. A narrative review of the technical standards for extracorporeal life support devices (pumps and oxygenators) in Europe. *Perfusion*. (2018) 33(7):553–61. doi: 10.1177/0267659118772452

8. Gorbet MB, Sefton MV. Biomaterial-associated thrombosis: roles of coagulation factors, complement, platelets and leukocytes. *Biomaterials*. (2004) 25(26):5681–703. doi: 10.1016/j.biomaterials.2004.01.023

9. Zhang T, Liu L, Huang X, Gao X, Huan X, He C, et al. The rapid change of shear rate gradient is beneficial to platelet activation. *Platelets*. (2024) 35(1):1–10. doi: 10.1080/09537104.2023.2288679

10. Zhang T, Huang X, Gao X, Liu L, Chen D, Huan X, et al. Effect of pathological high shear exposure time on platelet activation and aggregation. *Clin Hemorheol Microcirc*. (2023) 84(2):125–39. doi: 10.3233/CH-221567

11. Scavone M, Bozzi S, Mencarini T, Podda G, Cattaneo M, Redaelli A. Platelet adhesion and thrombus formation in microchannels: the effect of assay-dependent variables. *Int J Mol Sci*. (2020) 21(750):1–11. doi: 10.3390/ijms21030750

12. Zhussupbekov M, Rojano RM, Wu W-T, Antaki JF. Von Willebrand factor unfolding mediates platelet deposition in a model of high-shear thrombosis. *Biophys J*. (2022) 121(1):4033–47. doi: 10.1016/j.bpj.2022.09.040

13. Goel MS, Diamond SL. Neutrophil enhancement of fibrin deposition under flow through platelet-dependent and -independent mechanisms. *Arterioscler Thromb Vasc Biol*. (2001) 21(12):2093–108. doi: 10.1161/hq1201.100255

14. Matsunari Y, Sugimoto M, Doi M, Matsui H, Kawaguchi M. Functional characterization of tissue factor in von Willebrand factor-dependent thrombus formation under whole blood flow conditions. *Int J Hematol*. (2016) 104(6):661–8. doi: 10.1007/s12185-016-2086-z

15. Shenkman B, Savion N, Dardik R, Tamarin I, Varon D. Testing of platelet deposition on polystyrene surface under flow conditions by the cone and plate(let) analyzer: role of platelet activation, fibrinogen and von willebrand factor. *Thromb Res*. (2000) 99(4):353–61. doi: 10.1016/S0049-3848(00)00255-3

16. Baumgartner HR. The role of blood flow in platelet adhesion, fibrin deposition, and formation of mural thrombi. *Microvasc Res*. (1973) 5(2):167–79. doi: 10.1016/0026-2862(73)90069-1

17. Turitto VT, Weiss HJ, Baumgartner HR. The effect of shear rate on platelet interaction with subendothelium exposed to citrated human blood. *Microvasc Res*. (1980) 19(3):352–65. doi: 10.1016/0026-2862(80)90054-0

18. Gersh KC, Edmondson KE, Weisel JW. Flow rate and fibrin fiber alignment. *J Thromb Haemost*. (2010) 8(12):2826–8. doi: 10.1111/j.1538-7836.2010.04118.x

19. Gemmell CH, Nemerson Y, Turitto V. The effects of shear rate on the enzymatic activity of the tissue factor-factor viia complex. *Microvasc Res*. (1990) 40(3):327–40. doi: 10.1016/0026-2862(90)90031-L

20. von Appen K, Goolsby C, Mehl P, Goewert R, Ivanovich P. Leukocyte adhesion molecules as biocompatibility markers for hemodialysis membranes. *ASAIO J*. (1994) 40(3):M609–15. doi: 10.1097/00002480-199407000-00071

21. De Bartolo C, Nigro A, Fragomeni G, Colacino FM, Wang D, Jones CC, et al. Numerical and experimental flow analysis of the Wang-Zwische double-lumen cannula. *Asaio Journal*. (2011) 57(4):318–27. doi: 10.1097/MAT.0b013e31821c08bc

22. Tauber H, Ott H, Streif W, Weigel G, Loacker L, Fritz J, et al. Extracorporeal membrane oxygenation induces short-term loss of high-molecular-weight von Willebrand factor multimers. *Anesth Analg*. (2015) 120(4):730–6. doi: 10.1213/ANE.0000000000000554

23. Heilmann C, Geisen U, Beyersdorf F, Nakamura L, Benk C, Trummer G, et al. Acquired von Willebrand syndrome in patients with extracorporeal life support (ECLS). *Intensive Care Med*. (2012) 38(1):62–8. doi: 10.1007/s00134-011-2370-6

24. Große-Berkenbusch K, Avci-Adali M, Arnold M, Cahalan L, Cahalan P, Velic A, et al. Profiling of time-dependent human plasma protein adsorption on non-coated and heparin-coated oxygenator membranes. *Biomater Adv*. (2022) 139:213014. doi: 10.1016/j.bioadv.2022.213014

25. Johnson G, Curry B, Cahalan L, Prater R, Beeler M, Gartner M, et al. *In vitro* assessment of blood compatibility: residual and dynamic markers of cellular activation. *J Biomater Appl*. (2013) 27(8):925–36. doi: 10.1177/0885328211428525

26. Borchert N, Dieterich C, Krug K, Schütz W, Jung S, Nordheim A, et al. Proteogenomics of pristionchus pacificus reveals distinct proteome structure of nematode models. *Genome Res*. (2010) 20(6):837–46. doi: 10.1101/gr.103119.109

27. Rappsilber J, Mann M, Ishihama Y. Protocol for micro-purification, enrichment, pre-fractionation and storage of peptides for proteomics using stagetips. *Nat Protoc*. (2007) 2(8):1896–906. doi: 10.1038/nprot.2007.261

28. Schmitt M, Sinnberg T, Nalpas NC, Maass A, Schittek B, Macek B. Quantitative proteomics links the intermediate filament nestin to resistance to targeted braf inhibition in melanoma cells. *Mol Cell Proteomics*. (2019) 18(6):1096–109. doi: 10.1074/mcp.RA119.001302

29. Cox J, Mann M. Maxquant enables high peptide identification rates, individualized ppb-range mass accuracies and proteome-wide protein quantification. *Nat Biotechnol*. (2008) 26(12):1367–72. doi: 10.1038/nbt.1511

30. Cox J, Neuhauser N, Michalski A, Scheltema RA, Olsen JV, Mann M. Andromeda: a peptide search engine integrated into the maxquant environment. *J Proteome Res*. (2011) 10(4):1794–805. doi: 10.1021/pr101065j

31. Brash JL, Horbett TA, Latour RA, Tengvall P. The blood compatibility challenge. Part 2: protein adsorption phenomena governing blood reactivity. *Acta Biomater*. (2019) 94:11–24. doi: 10.1016/j.actbio.2019.06.022

32. Atlas THP. The blood protein section. (2024).

33. Alcorlo M, López-Perrote A, Delgado S, Yébenes H, Subías M, Rodríguez-Gallego C, et al. Structural insights on complement activation. *FEBS J* (2015) 282(20):3883–91. doi: 10.1111/febs.13399

34. Law SKA, Dodds AW. The internal thioester and the covalent binding properties of the complement proteins c3 and c4. *Protein Sci*. (1997) 6(2):263–74. doi: 10.1002/pro.5560060201

35. Hirsh SL, McKenzie DR, Nosworthy NJ, Denman JA, Sezerman OU, Bilek MMM. The vroman effect: competitive protein exchange with dynamic multilayer protein aggregates. *Colloids Surf B Biointerfaces*. (2013) 103:395–404. doi: 10.1016/j.colsurfb.2012.10.039

36. Vroman L, Adams AL, Fischer GC, Munoz PC. Interaction of high molecular weight kininogen, factor xii, and fibrinogen in plasma at interfaces. *Blood*. (1980) 55(1):156–9. doi: 10.1182/blood.V55.1.156.156

37. Gore S, Andersson J, Biran R, Underwood C, Riesenfeld J. Heparin surfaces: impact of immobilization chemistry on hemocompatibility and protein adsorption. *J Biomed Mater Res B Appl Biomater*. (2014) 102(8):1817–24. doi: 10.1002/jbm.b.33154

38. Blezer R, Fouache B, Willems GM, Lindhout T. Activation of blood coagulation at heparin-coated surfaces. *J Biomed Mater Res A*. (1997) 37(1):108–13. doi: 10.1002/(SICI)1097-4636(199710)37:1<108::AID-JBM13>3.0.CO;2-C

39. Courtney J, Lamba N, Sundaram S, Forbes C. Biomaterials for blood-contacting applications. *Biomaterials*. (1994) 15(10):737–44. doi: 10.1016/0142-9612(94)90026-4

40. Dasi LP, Simon HA, Sucosky P, Yoganathan AP. Fluid mechanics of artificial heart valves. *Clin Exp Pharmacol Physiol*. (2009) 36(2):225–37. doi: 10.1111/j.1440-1681.2008.05099.x

41. Sakariassen KS, Joss R, Muggli R, Kuhn H, Tschopp TB, Sage H, et al. Collagen type iii induced ex vivo thrombogenesis in humans. Role of platelets and leukocytes in deposition of fibrin. *Arteriosclerosis*. (1990) 10(2):276–84. doi: 10.1161/01.ATV.10.2.276

42. Talens S, Malfliet JJMC, van Hal PTW, Leebeek FWG, Rijken DC. Identification and characterization of α1 -antitrypsin in fibrin clots. *J Thromb Haemost*. (2013) 11(7):1319–28. doi: 10.1111/jth.12288

43. Souri M, Osaki T, Ichinose A. The non-catalytic b subunit of coagulation factor XIII accelerates fibrin cross-linking. *J Biol Chem*. (2015) 290(19):12027–39. doi: 10.1074/jbc.M114.608570

44. Andrews RK, Gardiner EE, Shen Y, Whisstock JC, Berndt MC. Glycoprotein Ib-IX-V. *Int J Biochem Cell Biol*. (2003) 35(8):1170–4. doi: 10.1016/S1357-2725(02)00280-7

45. Moake JL, Turner NA, Stathopoulos NA, Nolasco L, Hellums JD. Shear-induced platelet aggregation can be mediated by vwf released from platelets, as well as by exogenous large or unusually large vwf multimers, requires adenosine diphosphate, and is resistant to aspirin. *Blood*. (1988) 71(5):1366–74. doi: 10.1182/blood.V71.5.1366.1366

46. Meyer AD, Rishmawi A, Kamucheka R, Lafleur C, Batchinsky AI, Mackman N, et al. Effect of blood flow on platelets, leukocytes, and extracellular vesicles in thrombosis of simulated neonatal extracorporeal circulation. *J Thromb Haemost*. (2020) 18(2):399–410. doi: 10.1111/jth.14661

47. Rabah H, Rabah A. Extracorporeal membrane oxygenation (ecmo): what we need to know. *Cureus*. (2022) 14(7):e26735. doi: 10.7759/cureus.26735

48. Bohnen NI, Kaufer DI, Ivanco LS, Lopresti B, Koeppe RA, Davis JG, et al. Cortical cholinergic function is more severely affected in parkinsonian dementia than in Alzheimer disease: an *in vivo* positron emission tomographic study. *Arch Neurol*. (2003) 60(12):1745–8. doi: 10.1001/archneur.60.12.1745

49. Friedman M, Walsh G. High performance films: review of new materials and trends. *Polym Eng Sci*. (2002) 42(8):1756–88. doi: 10.1002/pen.11069

50. Lopez LC, Wilkes GL, Stricklen PM, White SA. Synthesis, structure, and properties of poly (4-methyl-1-pentene). *J Macromol Sci C*. (1992) 32(3–4):301–406. doi: 10.1080/15321799208021429

51. Lepoittevin B, Roger P. Poly (ethylene terephthalate). In: Sabu Thomas VPM, editor. *Handbook of Engineering and Speciality Thermoplastics*. Salem, MA: Scrivener Publishing LLC (2011) 3. p. 97–126. doi: 10.1002/9781118104729.ch4

52. Gerling K, Ölschläger S, Avci-Adali M, Neumann B, Schweizer E, Schlensak C, et al. A novel c1-esterase inhibitor oxygenator coating prevents fxii activation in human blood. *Biomolecules*. (2020) 10(7):1042. doi: 10.3390/biom10071042

53. Obstals F, Vorobii M, Riedel T, de los Santos Pereira A, Bruns M, Singh S, et al. Improving hemocompatibility of membranes for extracorporeal membrane oxygenators by grafting nonthrombogenic polymer brushes. *Macromol Biosci*. (2018) 18(3):1700359. doi: 10.1002/mabi.201700359

54. Canjuga D, Hansen C, Halbrügge F, Hann L, Weiß S, Schlensak C, et al. Improving hemocompatibility of artificial lungs by click conjugation of glycoengineered endothelial cells onto blood-contacting surfaces. *Biomater Adv*. (2022) 137:212824. doi: 10.1016/j.bioadv.2022.212824

8.3 Publikation III:

A Novel C1-Esterase Inhibitor Oxygenator Coating Prevents FXII Activation in Human Blood

biomolecules

MDPI

Article

A Novel C1-Esterase Inhibitor Oxygenator Coating Prevents FXII Activation in Human Blood

Katharina Gerling [1], Sabrina Ölschläger [1], Meltem Avci-Adali [1], Bernd Neumann [1], Ernst Schweizer [2], Christian Schlensak [1], Hans-Peter Wendel [1] and Sandra Stoppelkamp [1,*]

[1] University Hospital Tuebingen, Clinic for Thoracic and Cardiovascular Surgery, Calwerstr, 7/1, 72076 Tuebingen, Germany; Katharina.Gerling@uni-tuebingen.de (K.G.); Sabrina.Oelschlaeger@med.uni-tuebingen.de (S.Ö.); meltem.avci-adali@uni-tuebingen.de (M.A.-A.); Bernd.Neumann@klinikum.uni-tuebingen.de (B.N.); Christian.Schlensak@med.uni-tuebingen.de (C.S.); Hans-Peter.Wendel@med.uni-tuebingen.de (H.-P.W.)

[2] University Hospital Tuebingen, Section Medical Materials and Technology, Osianderstr, 2-8, 72076 Tuebingen, Germany; Ernst.Schweizer@med.uni-tuebingen.de

* Correspondence: sandra.stoppelkamp@klinikum.uni-tuebingen.de; Tel.: +49-7071-29-83340

Received: 7 June 2020; Accepted: 9 July 2020; Published: 13 July 2020

Abstract: The limited hemocompatibility of currently used oxygenator membranes prevents long-term use of artificial lungs in patients with lung failure. To improve hemocompatibility, we developed a novel covalent C1-esterase inhibitor (C1-INH) coating. Besides complement inhibition, C1-INH also prevents FXII activation, a very early event of contact phase activation at the crossroads of coagulation and inflammation. Covalently coated heparin, as the current anticoagulation gold standard, served as control. Additionally, a combination of both coatings (C1-INH/heparin) was established. The coatings were tested for their hemocompatibility by dynamic incubation with freshly drawn human whole blood. The analysis of various blood and plasma parameters revealed that C1-INH-containing coatings were able to markedly reduce FXIIa activity compared to heparin coating. Combined C1-INH/heparin coatings yielded similarly low levels of thrombin-antithrombin III complex formation as heparin coating. In particular, adhesion of monocytes and platelets as well as the diminished formation of fibrin networks were observed for combined coatings. We could show for the first time that a covalent coating with complement inhibitor C1-INH was able to ameliorate hemocompatibility. Thus, the early inhibition of the coagulation cascade is likely to have far-reaching consequences for the other cross-reacting plasma protein pathways.

Keywords: ECMO; hollow-fiber membranes; C1-esterase inhibitor; anti-thrombogenic; novel coating; inflammation; hemocompatibility

1. Introduction

Critically ill patients with chronic lung disease are dependent on long-term lung replacement methods. As the demand for donor lungs exceeds the availability [1], an alternative long-term oxygenation system is needed urgently. Currently, extra-corporeal membrane oxygenation (ECMO) is the only treatment option that can be used for a maximum of a few weeks at best [2].

The ECMO circuit consists of a series of components whose key element is the gas exchange membrane. It ensures the exchange of O_2 and CO_2. Oxygen-deficient blood is drained from the body to flow along the gas exchange membranes. There, oxygen streams through the inner lumen of the membrane fibers and diffuses through the membrane into the blood, while carbon dioxide is removed [3]. Various membranes can be used for gas exchange [4]. While polypropylene (PP) has good gas permeability properties, plasma-leakage remains a major limitation for long-term use [5,6].

To circumvent the plasma-leakage complications, polymethylpentene (PMP) with its good plasma tightness is most often used for ECMO. In addition to the plasma tightness, PMP is an efficient and low-resistance artificial gas exchange membrane. Further components of the ECMO are the blood reservoir, mechanical blood pump, heat exchanger, and circulatory tube system [3,7].

Despite the benefits of supporting patient oxygenation, using an ECMO/extra-corporeal life support (ECLS) system is also associated with several risks for patients. The most common complications are the occurrence of thromboembolic complications due to the extra-corporeal circuit or bleeding at the cannulation site caused by the required systemic anticoagulation. The large membrane surface is essential for an adequate oxygen supply but can lead to various complications such as acute respiratory distress syndrome (ARDS), systemic inflammatory response syndrome (SIRS), or multi-organ dysfunction syndrome (MODS) [8]. The reason for this is the complex interaction of several blood activation pathways upon contact with foreign surfaces. These include interactions between mechanical and chemical cell activation, dysfunction of the immune regulation and activation of the coagulation cascade. The reaction of the diverse blood components depends on the chemical and physical properties of the materials used (i.e., their hemocompatibility), interactions of the foreign surface with plasma proteins and surface coatings [9–13].

The main goal of optimizing ECMO membranes is to develop a non-activating surface [14]. Therefore, activation of coagulation and inflammation can be effectively prevented. The key reaction of coagulation is the thrombin formation that eventually leads to insoluble fibrin clots [15] (see Figure 1). Thrombin generation from prothrombin is mediated by activated factor X (FXa). This key step is inhibited by endogenous serine-protease inhibitor antithrombin III (AT) that targets factor (F) X. Heparin greatly increases the inhibitory function of AT [16]. Thus, heparin-coated oxygenators and tubings as well as systemic heparin are used to prevent activation of coagulation and clot formation. Inflammation on the other hand can be mediated either by anaphylatoxins C3a and C5a generated by the complement pathway or by activation of the kallikrein-kinin pathway [17,18]. None of these are targeted by heparin. On top of this, the crosstalk of the diverse pathways of plasma proteins complicate interventions even further. The contact phase system is activated by autoactivation of FXII on neutral or charged foreign surfaces [19] or by polyphosphates released from activated platelets [20,21]. The following activation of kallikrein leads to the amplification of FXII activation. This in turn activates FXI and forms the link to the coagulation pathway by subsequently activating factors IX and X. Kallikrein on the other hand can digest the high molecular-weight kininogen to liberate the small pro-inflammatory molecule bradykinin [22]. Moreover, FXII and subsequent kallikrein activation have also been reported to occur by misfolded proteins [22,23] suggesting a role of FXII in the induction of inflammation in misfolded protein diseases.

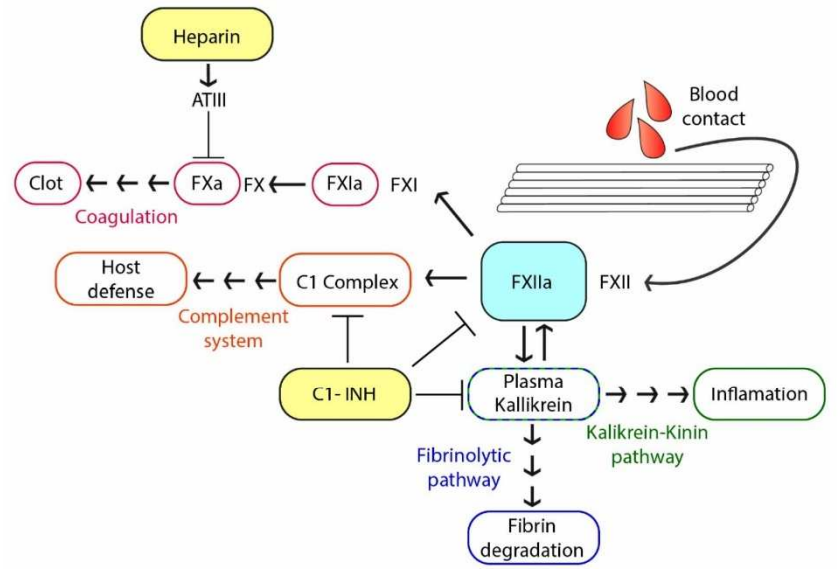

Figure 1. Schematic representation of the contact activation system. The contact of the blood with the artificial surface (polymethylpentene membrane) leads to the activation of factor (F) XII to FXIIa. FXIIa can then activate four different downstream pathways: (i) the coagulation pathway by cleaving the zymogen FXI to FXIa, eventually leading to thrombin activation and fibrin formation, (ii) the complement system by activation of the C1qrs-complex subunits C1r and C1s, (iii) the fibrinolytic pathway by plasma kallikrein activating plasmin to eventually degrade fibrin, (iv) the inflammatory kallikrein-kinin signaling pathway by plasma kallikrein cleaving high-molecular-weight kininogen liberating the pro-inflammatory molecule bradykinin [15]. Heparin and C1-INH are both able to inhibit one or more of these pathways. While heparin only inhibits coagulation, C1-INH positively affects coagulation, the complement system, fibrin degradation, and inflammation [16,24].

Preventing early reactions, such as the activation of the plasma contact system [25,26], therefore plays an important part here. These pathways are well-known in vitro, but especially the role of FXII in vivo is not fully elucidated yet [19,23]. Diverse coatings in combination with systemic anticoagulation are used to reduce these reactions. The currently used coatings can be divided into non-heparin-based biopassive coatings and heparin-based coatings [14]. For the long-term ECMO mostly heparin-based coatings are used, e.g., Carmeda® BioActive Surface, Bioline coating. A combination of covalent heparin coating and systemic anticoagulation is of clinical benefit as lower doses of systemically applied heparin reduce blood transfusion [27,28].

The anticoagulant effect of heparin can be achieved via a systemic administration or by functionalization of artificial surfaces [27,29]. Covalent coating of tubings and membranes with heparin is especially suited for longer-term use [30]. The mode of action of heparin on the surface is considered either as amplifying the action of AT [31] or as modifying the surface properties towards a more hemocompatible layer [29]. According to Weber and colleagues [29], the effect of heparin coatings on hemocompatibility is probably at least partly due to the adsorption of proteins on the coating, which gives an overall anticoagulant feature. The C1-esterase inhibitor (C1-INH) was one of the proteins adsorbed quite early after blood contact. Since covalent surface modification is a very convenient strategy to achieve a longer-lasting effect, we have established a novel C1-INH covalent coating. C1-INH is an acute-phase protein belonging to the serpin superfamily of serine-protease inhibitors. The primary function of serpins includes the inhibition of proteases. They are also involved

in biological interactions with microorganisms and endothelial cells [24,32]. Under physiological conditions, C1-INH can have a positive effect on the complement system, the contact phase system, the kallikrein-kinin system, the fibrinolysis, and the coagulation pathways [33]. In particular, inhibitory effects exerted on FXII and kallikrein make C1-INH a promising candidate for improving ECMO membrane hemocompatibility.

Thus, by coating ECMO membranes with C1-INH, the blood activation and inflammation processes might be reduced. To the best of our knowledge, we are the first group to show the development of a novel covalent C1-INH coating for blood-contacting surfaces. Although the coating is primarily developed for oxygenators to increase hemocompatibility, its design also allows the coating of other surfaces. Another special feature of the coating is that other proteins with a positive impact on hemocompatibility can be covalently bound using the same principle. Thus, to combine the advantages of the current gold standard heparin and the novel C1-INH coating, an additional coating containing both components was also developed. Here, we compared the effect of the covalently coated C1-INH in addition to covalently attached heparin on the hemocompatibility of oxygenator membranes.

2. Materials and Methods

2.1. Hollow-Fiber Oxygenator Membranes

Polymethylpentene (PMP, OXYPLUS®,) hollow-fiber gas exchange membranes with an outer fiber diameter of 380 ± 30 µm and a wall thickness of 90 ± 10 µm, resulting in an inner diameter of 200 ± 50 µm were bought from 3M Membrana (Wuppertal, Germany). PMP membranes with an area of 1 cm^2 were coated and tested for their hemocompatibility.

2.2. Coating of the Membranes

Three different covalent coatings were applied: C1-INH, heparin, and a combination of C1-INH and heparin. A reactive layer of amino groups was generated for all coatings using layer-by-layer technology, originally reported by Decher and Hong on polyelectrolyte multilayers in 1991 [34]. Briefly, the surface was pretreated using 5% ammonium persulfate (55 °C) (Sigma–Aldrich, Darmstadt, Germany). This was followed by alternating layers of the cationic polymer polyethyleneimine (PEI) (0.01% or 0.1%, room temperature (RT)) (Sigma–Aldrich, Darmstadt, Germany) and the anionic polysaccharide dextran sulfate (0.01%, 55 °C) (Sigma–Aldrich, Darmstadt, Germany) in borate buffer (50 mmol/L, pH 8.5) (Thermo Scientific, Waltham, MA, USA). The first layer of PEI was stabilized with 4 mmol/L crotonaldehyde (Sigma–Aldrich, Darmstadt, Germany). After each reaction step, the membranes were washed thoroughly to prevent neutralization of charged molecules. The reaction time for each step was 25 min. The covalent bonding of C1-INH is based on the formation of amidine bonds (see schematic representation in Figure 2a). These were generated by dimethyl suberimidate (DMS) (Thermo Scientific, Waltham, MA, USA) a crosslinker containing two amine-reactive imidoester groups. PMP membranes were placed in a mixture of 3 IU/mL C1-INH (Berinert®, CSL Behring, PA, USA) and 3.33 mg/mL DMS dissolved in 0.2 mol/L triethanolamine (Sigma–Aldrich, Darmstadt, Germany) buffer (pH 8.0). After 1 h at RT, the reaction was stopped by incubation with 50 mmol/L Tris buffer (Sigma–Aldrich, Darmstadt, Germany) (pH 8.0) for 30 min. Heparin (Fragmin 2500 IE, Pfizer, New York, NY, USA) (1.6 IU/mL) was covalently bound (Figure 2b) by reductive amination. Here, 0.05% sodium cyanoborohydride (Sigma–Aldrich, Darmstadt, Germany) served as the reducing agent. The reduction reaction was performed at 55 °C in a sterile 9% NaCl solution (VWR Chemicals, Darmstadt, Germany) for 2 h. For the combined coating of C1-INH and heparin (Figure 2c), C1-INH was first covalently bound as described above, followed by the heparin-binding step. After coating, all membranes were washed with isotonic saline solution (0.9%, Fresenius Kabi, Bad Homburg, Germany) and sterile water for injection (Ampuwa; Fresenius Kabi, Bad Homburg, Germany) before drying in a desiccator.

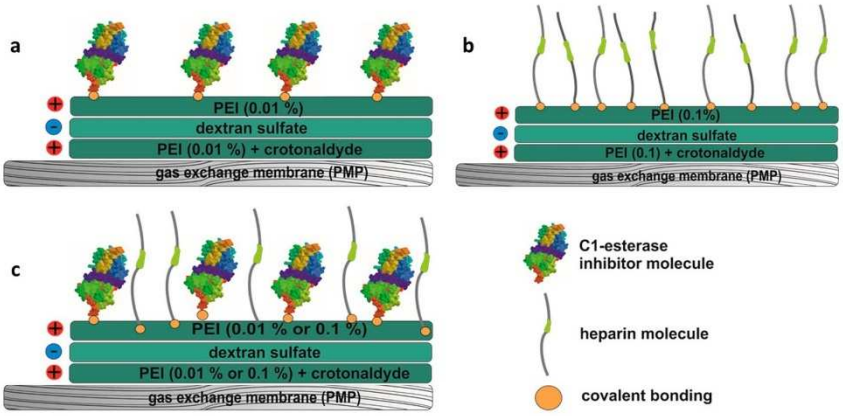

Figure 2. Schematic representation of the generated coatings. (**a**) C1-INH coating, (**b**) heparin coating, (**c**) the combined coating of C1-INH and heparin.

2.3. Detection of Bound C1-INH and Heparin

For the detection of surface-bound C1-INH on the hollow-fiber membranes, the TECHNOCHROM®C1-INH kit (Haemochrom Diagnostica, Germany) was used. The membranes (1 cm^2) with immobilized C1-INH were placed in a 24-well plate and filled with sample buffer from the kit to equalize the volume to that of the standard dilutions of C1-INH. The subsequent steps were performed according to the manufacturer's instructions. Biologically active heparin concentrations were determined by the Chromogenix Coamatic Heparin kit (Haemochrom Diagnostica, Germany) according to the manufacturer's instructions.

2.4. Blood Sampling

Blood was obtained from five voluntary healthy adults by venipuncture (Safety-Multifly® 20 Gx3/4 TW needle; Sarstedt, Nümbrecht, Germany) after giving their informed consent. To enable conclusive in vitro blood experiments, relatively low anticoagulation with 1 IU/mL sodium heparin 25,000 (Ratiopharm, Ulm, Germany) was used. To guarantee the quality of the blood, strict exclusion criteria were applied to blood donors: e.g., smoking and medication were prohibited. In particular, the intake of drugs inhibiting coagulation and inflammation in the last two weeks before blood donation was not allowed. The blood collection procedures described and the use of blood in the experimental settings were approved by the Research and Ethics Department of the University of Tuebingen (project approval number 287/2020BO2).

2.5. Blood Incubation

To demonstrate the anti-inflammatory and anti-thrombogenic effects of the coatings, the differently coated membranes and an untreated membrane (each 1 cm^2) were dynamically incubated with 9 mL freshly drawn heparinized human whole blood in polypropylene tubes (Becton Dickinson (BD) Biosciences, Heidelberg, Germany) at 37 °C for 90 min. Heparinized blood incubated without sample material served as control. Basal activity of each measured marker was obtained from blood that was transferred into the corresponding anti-coagulated monovettes immediately after collection. Changes to the basal levels were determined in dynamically incubated blood samples after 90 min. Blood cell counts (platelets, erythrocytes, and lymphocytes) were measured directly with an automated cell counter (ABX Micros 60, Horiba Medical, Kyoto, Japan). All other activation markers were evaluated from plasma that was shock-frozen and stored at −20 °C or −80 °C, depending on the

manufacturer's instructions. For the FXIIa activity test, the heparin was neutralized with protamine (ME 1000 I.E/mL, MEDA, Solna, Sweden). Anti-coagulating reagents were: Ethylenediaminetetraacetic acid (EDTA; Sarstedt, Nümbrecht, Germany) for blood cell count measurement and complement enzyme-linked immunosorbent assay (ELISA), CTAD (a mixture of citrate, theophylline, adenosine, and dipyridamole; BD Biosciences, Heidelberg, Germany) for platelet activation ELISA, and citrate (Sarstedt, Nümbrecht, Germany) for FXIIa activation test, thrombin-antithrombin III complex ELISA, and leukocyte activation ELISA.

2.6. Soluble Activation Markers

Changes in the activation of the complement system, contact phase system, blood coagulation, platelets, and monocyte activation were detected by ELISA for the corresponding activation markers. All ELISAs were performed according to the manufacturer's instructions. C3a fragment (C3a MicroVue™, Quidel, Osteomedical GmbH, Sissach, Switzerland) was determined from EDTA plasma, while thrombin-antithrombin III complex (TAT) (Enzygnost® TAT micro, Siemens Healthcare, Erlangen, Germany) and polymorphonuclear (PMN) elastase (PMN Elastase ELISA, Demeditec Diagnostics, Kiel, Germany) were measured in citrated plasma. Activation of platelets was quantified by β-thromboglobulin (β-TG) release (Asserachrom® β-TG, Diagnostica Stago, Parsippany, NJ, USA) in CTAD-anticoagulated plasma. Blood coagulation was measured with an assay for Factor XIIa-like activity (Unitest Factor XIIa-like activity, Haemochrom Diagnostica, Germany).

2.7. Scanning Electron Microscopy

After blood incubation, the membranes were rinsed thoroughly with 0.9% saline solution (Fresenius Kabi, Bad Homburg, Germany) until all excess and non-adsorbed blood components were removed. The rinsed PMP membranes were fixed for one day in 2.5% glutaraldehyde (Sigma–Aldrich, Darmstadt, Germany) in phosphate-buffered saline (PBS; Thermo Scientific, Waltham, USA). Dehydration was performed by an ascending ethanol series before mounting and critically point drying. Dried samples were finally sputtered with gold-palladium particles (Baltec SCD 050, Bal-Tec AG, Balzers, Liechtenstein) and imaged by a scanning electron microscope (LEO 1430, Zeiss, Oberkochen, Germany). In each case, 100-fold, 500-fold, and 1000-fold magnifications were taken.

2.8. Fluorescence Microscopy

Surface cell adhesion was determined by 4′,6-Diamidine-2′-phenylindole (DAPI) cell staining. The surface was washed thoroughly with 0.9% saline solution and the adsorbed cells fixed in formaldehyde (4%; Fischar, Saarbrücken, Germany) for at least one hour. To stain the cells, the samples were incubated in 0.2 µg/mL DAPI (Sigma–Aldrich, Darmstadt, Germany) in PBS for 5 min. The adherent cells were visualized by fluorescence microscopy (Optiphot-2 Nikon) equipped with a remote control digital single-lens reflex camera (Nikon 550 D, Nikon, Japan). Quantification was performed via the program "ImageJ" from 20 independent images per parameter at 10x objective magnification. For quantification, the background was subtracted by setting the rolling ball radius to 50 pixels, setting a threshold, and counting the colored particles with a size (pixels^2) of 250 to infinity.

2.9. Statistical Analyses

Experiments were repeated from five independent samples (donors). Obtained results were first tested for normal distribution by the Shapiro–Wilk normality test. All data sets showing normal distribution were analyzed with a one-way analysis of variance (ANOVA) with Bonferroni's multiple comparison post hoc test to ascertain differences between the groups (hemocompatibility parameters). The Kruskal–Wallis test with Dunn's multiple comparison test was used for non-normal distributed datasets. Statistical significance was defined as $p < 0.05$. All analyses were performed using the statistical software package GraphPad Prism version 6.01 (GraphPad Software Inc., La Jolla, CA, USA). Non-marked bars are considered not significant to each other.

3. Results

3.1. Quantification of Immobilized C1-INH and Heparin on PMP Membranes

Covalent attachment of the three different surface modifications was quantified by modified C1-INH and FXa assays. Similar amounts of covalently coated bioactive C1-INH could be detected when PMP membranes were coated with C1-INH alone (0.087 ± 0.021 IU/cm^2) or in combination with heparin (Figure 3a). Combined C1-INH/heparin coatings were tested with two different PEI concentrations (0.1% and 0.01% PEI). The incorporation of PEI did not significantly influence the conjugated C1-INH amount on PMP membrane surface, but the lower PEI concentration led to more homogenous amounts of coated C1-INH. In contrast, in combined coatings, heparin concentration was significantly lower than the coatings with only heparin (Figure 3b). Heparin amounts dropped from 1.143 ± 0.688 IU/cm^2 for only heparin coatings to 0.226 ± 0.046 IU/cm^2 (PEI = 0.1%) and 0.261 ± 0.047 IU/cm^2 (PEI = 0.01%) for combined coatings. This effect was likely due to the sequential coating of C1-INH before heparin in combined coatings. Overall, we could successfully immobilize bioactive C1-INH and bioactive heparin on PMP membrane surfaces.

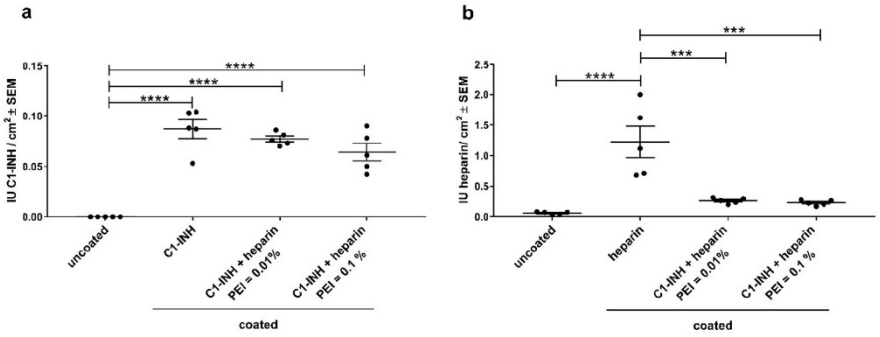

Figure 3. Detection of bioactive (**a**) C1-INH or (**b**) heparin amounts on PMP membranes. Significantly increased amounts of C1-INH were detected compared to the uncoated samples. However, only heparin-coating resulted in significantly increased immobilization of heparin compared to untreated samples. The results are shown as mean ± scanning electron microscopy (SEM). Statistical analysis was performed using one-way ANOVA with Bonferroni's multiple comparison post hoc test. $n = 5$; **** $p < 0.0001$, *** $p < 0.001$.

3.2. Analysis of Hemocompatibility

An ideal coating should confer near-natural properties to oxygenator membranes, minimizing coagulation and inflammatory activation of blood. To evaluate the impact of the coated membranes on the diverse blood components, e.g., coagulation and complement system, and activation of blood cells, differently coated PMP membranes were incubated dynamically with heparinized, fresh human whole blood. After incubation, the blood cell counts, and various hematological markers were determined and compared between coatings and to an uncoated membrane. Variations in blood cell count indicate cell loss due to adhesion or activation of platelets, adhesion of leukocytes, or hemolysis of erythrocytes.

The number of erythrocytes was not significantly different before (baseline) and after dynamic incubation (Figure 4a), indicating no destruction of erythrocytes by hemolysis due to material contacts or the incubation procedure. There was no reduction of white blood cell numbers compared to the controls without a membrane (baseline = before incubation; control = after incubation) (Figure 4b). Similarly, no reduction of platelet counts was observed for all coated membranes and the uncoated membrane (Figure 4c). This shows that all membranes, coated and uncoated, do not lead to marked cell loss or hemolysis.

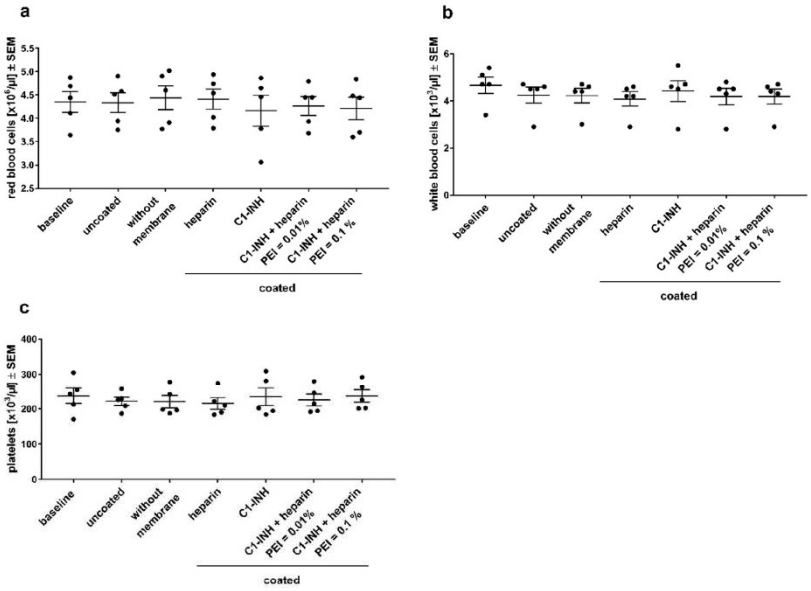

Figure 4. Comparative analyses of the blood cell number before (baseline) and after dynamic incubation revealed no significant loss of leukocytes and platelets after incubation with either coated or uncoated membranes. Shown are mean numbers of red blood cells (RBCs) (**a**), white blood cells (WBCs) (**b**), and platelets (**c**) per microliter heparinized whole blood ± SEM. Statistical analysis was performed using one-way ANOVA with Bonferroni's multiple comparison post hoc test (**a**,**c**), or Kruskal–Wallis test with Dunn's multiple comparison post hoc test (**b**). $n = 5$.

Activation of the different cross-reacting blood pathways (contact phase system—FXIIa-like activity; coagulation—TAT; complement system—C3a; platelet activation β–TG; leukocyte activation PMN-elastase) was determined from freshly frozen plasma samples (Figure 5). Comparing blood without a membrane (control) and blood incubated with uncoated membranes indicates the effect of the material PMP itself. A clear effect was observed for contact phase activation (Figure 5a) and coagulation (Figure 5b). The C1-INH coating significantly reduced FXII activation compared to heparin coating and uncoated membranes. The combined coatings of heparin and C1-INH showed a larger variation between donors, thus no significant differences were seen compared to heparin coating or C1-INH coating, but mean FXIIa activity was on the same level as blood without membrane. Significantly reduced TAT complex generation was detected after the incubation of blood with only heparin or C1-INH/heparin (PEI 0.01%) coated membranes compared to uncoated membranes (Figure 5b). Heparin-coated membranes were able to significantly reduce TAT formation back to control levels. The significant reduction of TAT complex back to the same low TAT levels as heparin by the combined coating (PEI 0.01%) shows the effective prevention of thrombin formation by C1-INH/heparin coating. There were no significant differences measured between the coatings regarding neutrophil granulocytes (Figure 5c), complement system (Figure 5d), and platelet activation (Figure 5e).

3.3. Membrane Surface Analyses

Activation of cells usually precedes cellular adhesion and aggregation. This later event of cell adhesion was investigated using fluorescence microscopy of DAPI-stained membranes and using scanning electron microscopy (SEM). DAPI-staining was supposed to indicate the number of nucleated cells (mainly neutrophils) attached to the membranes after blood contact. Figure 6a shows

the mean number of adhered cells of representative fluorescence microscope images. All coatings significantly reduced the cell adhesion compared to the untreated membrane, but cell adhesion did not differ between coatings. The proportional amount of reduction is visualized in the scatter plot in Figure 6b. Interestingly, while heparin reduced cell adhesion significantly ($p < 0.01$), the reduction by C1-INH-containing coatings was highly significant ($p < 0.001$) indicating an additional effect of C1-INH to reduce adhesion of nucleated cells.

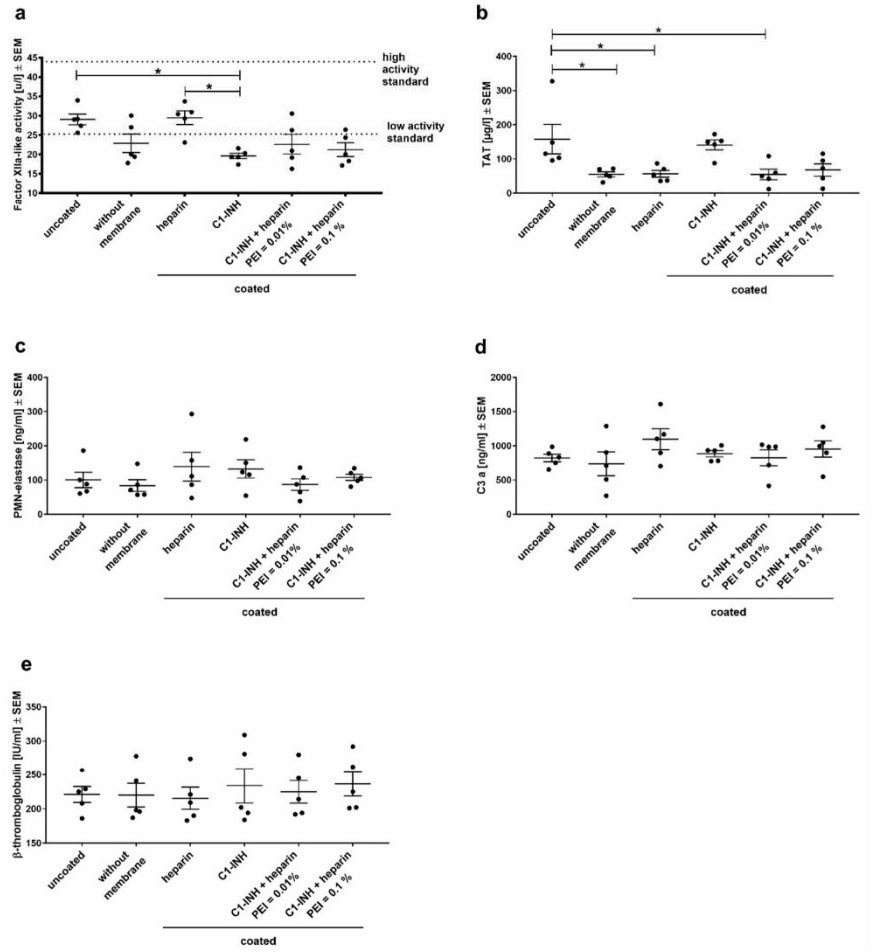

Figure 5. C1-INH coating prevented FXII activation, while heparin coating prevented TAT formation. Hemocompatibility analysis of differently coated PMP membranes: blood markers for the contact phase system (FXIIA-like activity) (**a**), coagulation (TAT) (**b**), activation of neutrophils (PMN-elastase) (**c**), complement system (C3a) (**d**), and platelet activation (β-thromboglobulin) (**e**). Statistical analysis was performed using one-way ANOVA with Bonferroni's multiple comparison post hoc test. The mean value of each column was compared with the mean value of each other column. $n = 5$; * $p < 0.05$.

In addition to the adhesion of neutrophils, there is typically a rapid adhesion and aggregation of activated platelets on artificial surfaces, which is associated with fibrin adhesion and clot formation.

These events were investigated using SEM. All coatings significantly reduced adhesion and aggregation of activated platelets as well as fibrin adhesion and clot formation. Particularly few deposits can be seen in the combined coatings (Figure 7). The combination of C1-INH and heparin was able to prevent platelet aggregation and fibrin formation almost completely. However, in the untreated membrane, several adhered platelets and large fibrin networks were visible.

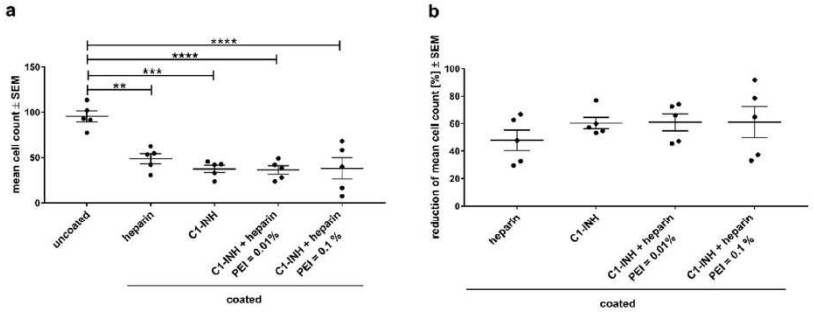

Figure 6. Fluorescence microscopy revealed reduced cell adhesion on single C1-INH and heparin as well as combined coatings. Mean cell counts ± SEM of DAPI-stained membranes show the significant reduction of nucleated cells on the surface of coated membranes (**a**), proportional reduction of mean adhered nucleated cells visualize the effect in direct comparison of the different coatings (**b**). Statistical analysis was performed using one-way ANOVA with Bonferroni's multiple comparison post hoc test. The mean value of each column was compared with the mean value of each other column. $n = 5$; **** $p < 0.0001$, *** $p < 0.001$, ** $p < 0.01$.

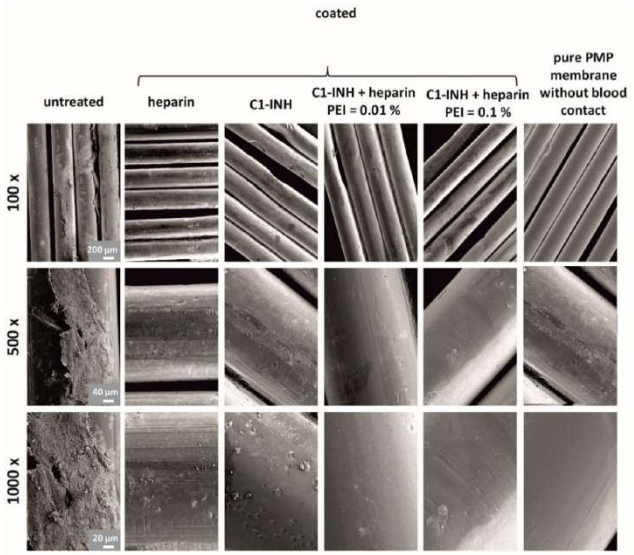

Figure 7. SEM images show an obvious decrease in platelet aggregation and fibrin formation. This effect is particularly noticeable with the combined coatings of heparin and C1-INH. For each type of coating, images were taken with a 100×, 500×, and 1000× magnification. For a visual comparison of the effects, images of an uncoated PMP membrane without blood contact are also shown (last column).

4. Discussion

This study aimed to improve the hemocompatibility of ECMO membranes by using a novel coating that inhibits early events in the activation of plasma proteins. Our approach was to use the serine-protease inhibitor C1-INH, a plasma protein acting as a complement inhibitor as well as an inhibitor of other signaling pathways such as the contact system, fibrinolysis, and coagulation [33]. The usual protein interactions are reported to change in their bound state [35]. Although this mechanism is not fully described yet, it is assumed that this is dependent on the adsorption-related conformational changes of proteins [29]. Hylton at al. showed that the binding of fibrinogen and serum albumin increases the tendency to thrombus formation [35]. However, the change in the mode of action of bound proteins does not necessarily have to be accompanied by negative effects. Weber et al. showed that at least part of the improved blood compatibility of heparin-coated biomaterials is due to the selective uptake and cleavage of plasma proteins [29]. It was also shown that increased adsorption of C1-INH took place on surfaces coated with heparin. This indicates a positive influence of bound C1-INH on blood compatibility [29].

In the present study, such a positive effect of C1-INH coating was also detected. We could show that coating with C1-INH improves hemocompatibility. This is particularly evident in the pronounced inhibition of Factor XIIa by C1-INH coating. Here, the heparin coating did not show a marked reduction in FXIIa activity. In contrast, the very early event in activation of several blood plasma pathways by FXII was significantly blocked by C1-INH. Particularly coagulation and inflammation are dreaded adverse events in ECMO. An increase in the formation of thrombin-antithrombin III (TAT) complex in plasma is proportional to the activation of FX, since FXa (as catalytic part of the prothrombinase complex) cleaves prothrombin to thrombin that is captured by AT to form the TAT complex [36,37]. As expected, heparin, which is known to enhance the effect of AT, significantly reduced TAT plasma levels. C1-INH coating on the other hand did not show a similar effect, indicating that the possible FX activation for increasing TAT plasma levels was not solely caused by FXII and its downstream actions. Although the initiation of coagulation by medical devices is often reported to start with FXII activation leading to downstream activation of FXI, FIX and FX [38,39], this exact sequence of events seems unlikely here, since FXII was significantly inhibited by C1-INH coating, while TAT levels were not reduced. It is possible that the activation of the coagulation was started independently of FXII by FXI autoactivation. FXI itself was reported to be autoactivated by negatively charged surfaces and the activation was accelerated by thrombin [40]. Thus, a small amount of thrombin formed can autoactivate FXI leading to further downstream events. FXI is also a target of C1-INH [24], therefore either the amount of C1-INH was not sufficient to block both FXII and FXI or there have been other activating events. Looking at the combined coatings of C1-INH and heparin, both showed similar TAT levels as heparin coating alone although the amount of heparin was approx. 3-times lower (compare Figure 2). Thus, the incorporation of C1-INH into heparin coating indicates an improvement of heparins action on the surface.

Although there was no obvious difference in activation of neutrophils (PMN-elastase), complement activation (C3a), and platelet activation (β-TG) between coatings, there was a significant reduction of leukocyte attachment to the coated membranes (Figure 6). The combined coatings of C1-INH and heparin even showed a highly significant decrease in leukocyte binding. This suggests that the adhesion of cells could be further decreased by the incorporation of C1-INH into heparin coatings. The investigation of fibrin formation and platelet adhesion by SEM reinforces this assumption. Almost no platelet adhesion or fibrin networks were seen on membranes coated with C1-INH and even less in combined coatings (Figure 7). Heparin-coated membranes showed decreased adhesion of platelets and generation of fibrin networks than uncoated membranes, but there were more accumulations seen than on the other coated membranes. This result demonstrates that there must be another underlying effect of C1-INH coating than preventing activation of coagulation. The adhesion of plasma proteins may be one of the underlying events. As reported previously [29], the adsorption of C1-INH was detected on heparinized surfaces. The authors suggested a role of adsorbed C1-INH and other proteins

for improved hemocompatibility of heparinized surfaces. By directly coating C1-INH to the surface of PMP membrane, the adsorption of plasma proteins may have been steered towards a hemocompatible non-activating surface. Moreover, FXII can be activated by misfolded proteins [41]. Inhibition of FXII activation by C1-INH could therefore also reduce the negative effect of proteins that adsorb to the surface and undergo a change in conformation. This activation of FXII would usually promote unwanted inflammation, whereas preventing protein adsorption and misfolding on the surface can reduce the binding of fibrinogen and platelets to the surface [42]. The mechanism of bound C1-INH preventing platelet and leukocyte adhesion is not clear but should be investigated further. In particular, the role of protein adsorption to the surface and direct interaction of diverse coagulation factors with C1-INH are of particular interest to understand the observed reduction in cell adhesion. Irrespective of the mechanism, the direct advantage of C1-INH coating for a group of patients reacting to heparin is directly obvious. In some cases, patients can develop heparin-induced thrombocytopenia (HIT) when exposed to heparin. Although type 1 of this disease is non-immune mediated and the drop in platelet counts stabilizes during continuous heparin treatment [43], type 2 HIT is an immune reaction with life-threatening thromboembolic complications [44]. IgG antibodies are produced within 5 days and form a complex with heparin and platelet factor 4 leading to platelet aggregation and thrombosis [45]. The occurrence of such IgG is common, whereas HIT type 2 is relatively rare [46]. Nevertheless, substituting heparin coating with C1-INH could prevent HIT and make ECMO safer for such patients. In the case of HIT, the formed antibodies can lead to the activation of the classical complement pathway leading to inflammation [47]. Thus, the presence of C1-INH in combined C1-INH/heparin coating could prevent antibody- and C1-induced complement activation if HIT would occur.

5. Conclusions

Our novel covalent C1-INH coating demonstrated improved hemocompatibility by inhibition of FXII activation. The reduced adhesion of leukocytes and platelets was obvious for all types of coatings; however, C1-INH/heparin coatings showed the lowest adhesion of cells. As the membrane sizes in this in vitro study is relatively small compared to the full-sized oxygenator, we expect an even more distinct effect in large-scale models. The combined C1-INH/heparin coatings showed the most promising results in preventing platelet adhesion and fibrin networks. Therefore, these combinations will be extended in different ratios in the next study to reveal the optimal ratio of coated heparin to C1-INH before larger-scale models are investigated. Furthermore, the mechanism behind C1-INH coating leading to the observed events will be analyzed in more detail by biochemical methods.

Author Contributions: The authors of the manuscript contributed all in several ways to the study: conceptualization, K.G., S.S., S.Ö., B.N., C.S., M.A.-A., E.S. and H.-P.W.; methodology, K.G., B.N., S.Ö., E.S., H.-P.W., M.A.-A. and S.S.; validation, K.G., S.S., S.Ö., C.S., M.A.-A., B.N., E.S. and H.-P.W.; formal analysis, K.G., S.Ö., S.S., B.N., E.S. and M.A.-A.; investigation, K.G., S.S., S.Ö., B.N., E.S. and M.A.-A.; resources, C.S., H.-P.W. and S.S.; writing—original draft preparation, K.G., S.S., S.Ö., M.A.-A., H.-P.W., B.N., E.S. and C.S.; writing-revision, S.S., K.G. and M.A.-A.; visualization, K.G., E.S. and S.S.; supervision, S.S., H.-P.W. and M.A.-A.; project administration, S.S.; funding acquisition, S.S., H.-P.W., S.Ö. and C.S. All authors have read and agreed to the published version of the manuscript.

Funding: This research was partly funded by the Deutsche Forschungsgemeinschaft (DFG), grant number AOBJ: 640574, and internal resources.

Acknowledgments: The authors would like to thank Lutz Scheideler for the opportunity of using the Optiphot-2 Nikon microscope and to Melanie Wolf, Pia Müllerbader, Hanna Haag, and Julia Krieg for their support with the ELISAs. Furthermore, we acknowledge the support by Deutsche Forschungsgemeinschaft and Open Access Publishing Fund of University of Tübingen.

Conflicts of Interest: The authors declare no conflict of interest. The funders had no role in the design of the study; in the collection, analyses, or interpretation of data; in the writing of the manuscript, or in the decision to publish the results.

References

1. Gulack, B.C.; Hirji, S.A.; Hartwig, M.G. Bridge to lung transplantation and rescue post-transplant: The expanding role of extracorporeal membrane oxygenation. *J. Thorac. Dis.* **2014**, *6*, 1070–1079. [CrossRef] [PubMed]
2. Blum, J.M.; Lynch, W.R.; Coopersmith, C.M. Clinical and billing review of extracorporeal membrane oxygenation. *Chest* **2015**, *147*, 1697–1703. [CrossRef] [PubMed]
3. Marasco, S.F.; Lukas, G.; McDonald, M.; McMillan, J.; Ihle, B. Review of ECMO (Extra Corporeal Membrane Oxygenation) Support in Critically Ill Adult Patients. *Hear. Lung Circ.* **2008**, *17*, S41–S47. [CrossRef] [PubMed]
4. Betit, P. Technical Advances in the Field of ECMO. *Respir. Care* **2018**, *63*, 1162–1173. [CrossRef]
5. MONTOYA, J.P.; SHANLEY, C.J.; MERZ, S.I.; BARTLETT, R.H. Plasma Leakage through Microporous Membranes. *ASAIO J.* **1992**, *38*, M399–M405. [CrossRef]
6. Mottaghy, K.; Oedekoven, B.; Starmans, H.; Müller, B.; Kashefi, A.; Hoffmann, B.; Böhm, S. Technical aspects of plasma leakage prevention in microporous capillary membrane oxygenators. *ASAIO Trans.* **1989**, *35*, 640–643. [CrossRef]
7. Lequier, L.; Horton, S.B.; McMullan, D.M.; Bartlett, R.H. Extracorporeal membrane oxygenation circuitry. *Pediatr. Crit. Care Med.* **2013**, *14*, S7–S12. [CrossRef]
8. Miyashita, T.; Ahmed, A.; Nakanuma, S.; Okamoto, K.; Sakai, S.; Kinoshita, J.; Makino, I.; Nakamura, K.; Hayashi, H.; Oyama, K.; et al. A Three-phase Approach for the Early Identification of Acute Lung Injury Induced by Severe Sepsis. *In Vivo (Brooklyn)* **2016**, *30*, 341–350.
9. Tisoncik, J.R.; Korth, M.J.; Simmons, C.P.; Farrar, J.; Martin, T.R.; Katze, M.G. Into the Eye of the Cytokine Storm. *Microbiol. Mol. Biol. Rev.* **2012**, *76*, 16–32. [CrossRef]
10. Sniecinski, R.M.; Chandler, W.L. Activation of the hemostatic system during cardiopulmonary bypass. *Anesth. Analg.* **2011**, *113*, 1319–1333. [CrossRef]
11. Zakkar, M.; Guida, G.; Suleiman, M.-S.; Angelini, G.D. Cardiopulmonary Bypass and Oxidative Stress. *Oxid. Med. Cell. Longev.* **2015**, *2015*, 1–8. [CrossRef] [PubMed]
12. Hein, E.; Munthe-Fog, L.; Thiara, A.S.; Fiane, A.E.; Mollnes, T.E.; Garred, P. Heparin-coated cardiopulmonary bypass circuits selectively deplete the pattern recognition molecule ficolin-2 of the lectin complement pathway in vivo. *Clin. Exp. Immunol.* **2015**, *179*, 294–299. [CrossRef]
13. Kraft, F.; Schmidt, C.; Van Aken, H.; Zarbock, A. Inflammatory response and extracorporeal circulation. *Best Pract. Res. Clin. Anaesthesiol.* **2015**, *29*, 113–123. [CrossRef] [PubMed]
14. Palanzo, D.; Qiu, F.; Baer, L.; Clark, J.B.; Myers, J.L.; Ündar, A. *Artificial Organs*; John Wiley & Sons, Ltd (10.1111): Hoboken, NJ, USA, 1 November 2010; pp. 869–873.
15. Weber, M.; Steinle, H.; Golombek, S.; Hann, L.; Schlensak, C.; Wendel, H.P.; Avci-Adali, M. Blood-Contacting Biomaterials: In Vitro Evaluation of the Hemocompatibility. *Front. Bioeng. Biotechnol.* **2018**, *6*. [CrossRef] [PubMed]
16. Gray, E.; Hogwood, J.; Mulloy, B. The anticoagulant and antithrombotic mechanisms of heparin. *Handb. Exp. Pharmacol.* **2012**, *207*, 43–61. [CrossRef]
17. Dunkelberger, J.R.; Song, W.C. Complement and its role in innate and adaptive immune responses. *Cell Res.* **2010**, *20*, 34–50. [CrossRef]
18. Schmaier, A.H. The contact activation and kallikrein/kinin systems: Pathophysiologic and physiologic activities. *J. Thromb. Haemost.* **2016**, *14*, 28–39. [CrossRef]
19. Renné, T.; Schmaier, A.H.; Nickel, K.F.; Blombäck, M.; Maas, C. In vivo roles of factor XII. *Blood* **2012**, *120*, 4296–4303.
20. Müller, F.; Mutch, N.J.; Schenk, W.A.; Smith, S.A.; Esterl, L.; Spronk, H.M.; Schmidbauer, S.; Gahl, W.A.; Morrissey, J.H.; Renné, T. Platelet Polyphosphates Are Proinflammatory and Procoagulant Mediators In Vivo. *Cell* **2009**, *139*, 1143–1156. [CrossRef]
21. Morrissey, J.H. Polyphosphate: A link between platelets, coagulation and inflammation. *Int. J. Hematol.* **2012**, *95*, 346–352. [CrossRef]
22. Weidmann, H.; Heikaus, L.; Long, A.T.; Naudin, C.; Schlüter, H.; Renné, T. The plasma contact system, a protease cascade at the nexus of inflammation, coagulation and immunity. *Biochim. Biophys. Acta - Mol. Cell Res.* **2017**, *1864*, 2118–2127. [CrossRef] [PubMed]

23. Renné, T.; Schmaier, A.H.; Nickel, K.F.; Blombäck, M.; Maas, C.; Dc, W.; Schmaier, A.H.; Nickel, K.F.; Blomba, M. In vivo roles of factor XII Review article In vivo roles of factor XII. *Blood* **2014**, *120*, 4296–4303. [CrossRef]
24. Panagiotou, A.; Trendelenburg, M.; Osthoff, M. The Lectin pathway of complement in myocardial ischemia/reperfusion injury-review of its significance and the potential impact of therapeutic interference by C1 esterase inhibitor. *Front. Immunol.* **2018**, *9*, 1151. [CrossRef] [PubMed]
25. Björkqvist, J.; Nickel, K.F.; Stavrou, E.; Renné, T. In vivo activation and functions of the protease factor XII. *Thromb. Haemost.* **2014**, *112*, 868–875. [CrossRef]
26. Gailani, D.; Bane, C.E.; Gruber, A. Factor XI and contact activation as targets for antithrombotic therapy. *J. Thromb. Haemost.* **2015**, *13*, 1383–1395. [CrossRef]
27. Øvrum, E.; Tangen, G.; Tølløfsrud, S.; Skeie, B.; Ringdal, M.A.L.; Istad, R.; Øystese, R. Heparinized cardiopulmonary bypass circuits and low systemic anticoagulation: An analysis of nearly 6000 patients undergoing coronary artery bypass grafting. *J. Thorac. Cardiovasc. Surg.* **2011**, *141*, 1145–1149. [CrossRef]
28. Ranucci, M.; Balduini, A.; Ditta, A.; Boncilli, A.; Brozzi, S. A Systematic Review of Biocompatible Cardiopulmonary Bypass Circuits and Clinical Outcome. *Ann. Thorac. Surg.* **2009**, *87*, 1311–1319. [CrossRef]
29. Weber, N.; Wendel, H.P.; Ziemer, G. Hemocompatibility of heparin-coated surfaces and the role of selective plasma protein adsorption. *Biomaterials* **2002**, *23*, 429–439. [CrossRef]
30. Begovac, P.C.; Thomson, R.C.; Fisher, J.L.; Hughson, A.; Gällhagen, A. Improvements in GORE-TEX® vascular graft performance by Carmeda®bioactive surface heparin immobilization. *Eur. J. Vasc. Endovasc. Surg.* **2003**, *25*, 432–437. [CrossRef]
31. Biran, R.; Pond, D. Heparin coatings for improving blood compatibility of medical devices. *Adv. Drug Deliv. Rev.* **2017**, *112*, 12–23. [CrossRef]
32. Cai, S.; Dole, V.S.; Bergmeier, W.; Scafidi, J.; Feng, H.; Wagner, D.D.; Davis, A.E. A Direct Role for C1 Inhibitor in Regulation of Leukocyte Adhesion. *J. Immunol.* **2005**, *174*, 6462–6466. [CrossRef] [PubMed]
33. Li, H.(Henry). Self-administered C1 esterase inhibitor concentrates for the management of hereditary angioedema: usability and patient acceptance. *Patient Prefer. Adherence* **2016**, *10*, 1727–1737. [CrossRef]
34. Decher, G.; Hong, J.-D. Buildup of ultrathin multilayer films by a self-assembly process, 1 consecutive adsorption of anionic and cationic bipolar amphiphiles on charged surfaces. *Makromol. Chemie. Macromol. Symp.* **1991**, *46*, 321–327. [CrossRef]
35. Hylton, D.M.; Shalaby, S.W.; Latour, R.A. Direct correlation between adsorption-induced changes in protein structure and platelet adhesion. *J. Biomed. Mater. Res. Part A* **2005**, *73A*, 349–358. [CrossRef] [PubMed]
36. Krishnaswamy, S. The transition of prothrombin to thrombin. *J. Thromb. Haemost.* **2013**, *11*, 265–276. [CrossRef] [PubMed]
37. Quaranta, M.; Erez, O.; Mastrolia, S.A.; Koifman, A.; Leron, E.; Eshkoli, T.; Mazor, M.; Holcberg, G. The physiologic and therapeutic role of heparin in implantation and placentation. *PeerJ* **2015**, *3*, e691. [CrossRef]
38. Jaffer, I.H.; Fredenburgh, J.C.; Hirsh, J.; Weitz, J.I. Medical device-induced thrombosis: What causes it and how can we prevent it? *J. Thromb. Haemost.* **2015**, *13*, S72–S81. [CrossRef]
39. Visser, M.; Heitmeier, S.; Ten Cate, H.; Spronk, H.M.H. Role of Factor XIa and Plasma Kallikrein in Arterial and Venous Thrombosis. *Thromb. Haemost.* **2020**, *120*, 883–993. [CrossRef]
40. Gailani, D.; Broze, G.J. Factor XII-independent activation of factor XI in plasma: effects of sulfatides on tissue factor-induced coagulation. *Blood* **1993**, *82*, 813–819. [CrossRef]
41. Naudin, C.; Burillo, E.; Blankenberg, S.; Butler, L.; Renné, T. Factor XII Contact Activation. *Semin. Thromb. Hemost.* **2017**, *43*, 814–826. [CrossRef]
42. Zhang, L.; Casey, B.; Galanakis, D.K.; Marmorat, C.; Skoog, S.; Vorvolakos, K.; Simon, M.; Rafailovich, M.H. The influence of surface chemistry on adsorbed fibrinogen conformation, orientation, fiber formation and platelet adhesion. *Acta Biomater.* **2017**, *54*, 164–174. [CrossRef] [PubMed]
43. Liu, W.; Zhang, C.; Bai, Q.; Zhang, Z. Rare heparin induced thrombocytopenia type I reaction in a hemodialysis patient Case report. *Med. (United States)* **2018**, *97*. [CrossRef]
44. Riedel, R.; Schmieder, A.; Koster, A.; Kim, S.; Baumgarten, G.; Schewe, J.C. Heparin-induced thrombocytopenia type II (HIT II): A medical-economic view. *Medizinische Klin. Intensivmed. und Notfallmedizin* **2017**, *112*, 334–346. [CrossRef] [PubMed]

45. Chang, J.J.Y.; Parikh, C.R. HEMATOLOGY: ISSUES IN THE DIALYSIS PATIENT: When Heparin Causes Thrombosis: Significance, Recognition, and Management of Heparin-Induced Thrombocytopenia in Dialysis Patients. *Semin. Dial.* **2006**, *19*, 297–304. [CrossRef]
46. Grouzi, E. Update on argatroban for the prophylaxis and treatment of heparin-induced thrombocytopenia type II. *J. Blood Med.* **2014**, *5*, 131. [CrossRef]
47. Chaplin, D.D. Overview of the immune response. *J. Allergy Clin. Immunol.* **2010**, *125*, S3. [CrossRef]

8.4 Publikation IV:

Synthetic Material Abdominal Swabs Reduce Activation of Platelets and Leukocytes Compared to Cotton Materials

biomolecules

MDPI

Article

Synthetic Material Abdominal Swabs Reduce Activation of Platelets and Leukocytes Compared to Cotton Materials

Katharina Gerling [1,†], Lisa Maria Herrmann [1,†], Christoph Salewski [1], Melanie Wolf [1], Pia Müllerbader [1], Dorothea Siegel-Axel [2,3], Hans Peter Wendel [1], Christian Schlensak [1], Meltem Avci-Adali [1] and Sandra Stoppelkamp [1,*]

1 Clinical Research Laboratory, Department of Thoracic and Cardiovascular Surgery, University Hospital Tübingen, Eberhard Karls University of Tübingen, 72076 Tübingen, Germany; Katharina.Gerling@uni-tuebingen.de (K.G.); lisa-maria.herrmann@student.uni-tuebingen.de (L.M.H.); Christoph.salewski@med.uni-tuebingen.de (C.S.); melanie.wolf@klinikum.uni-tuebingen.de (M.W.); Pia.Muellerbader@klinikum.uni-tuebingen.de (P.M.); Hans-Peter.Wendel@med.uni-tuebingen.de (H.P.W.); Christian.schlensak@med.uni-tuebingen.de (C.S.); meltem.avci-adali@uni-tuebingen.de (M.A.-A.)
2 German Center for Diabetes Research (DZD e.V.) and Institute for Diabetes Research and Metabolic Diseases of the Helmholtz Center Munich at the Eberhard Karls University of Tübingen, 85764 Neuherberg, Germany; dorothea.axel@med.uni-tuebingen.de
3 Department of Internal Medicine IV, Division of Endocrinology, Diabetology and Nephrology, University Hospital Tübingen, 72076 Tübingen, Germany
* Correspondence: Sandra.Stoppelkamp@klinikum.uni-tuebingen.de; Tel.: +49-(0)7071-29-83340
† These authors have contributed equally to the work.

check for updates

Citation: Gerling, K.; Herrmann, L.M.; Salewski, C.; Wolf, M.; Müllerbader, P.; Siegel-Axel, D.; Wendel, H.P.; Schlensak, C.; Avci-Adali, M.; Stoppelkamp, S. Synthetic Material Abdominal Swabs Reduce Activation of Platelets and Leukocytes Compared to Cotton Materials. *Biomolecules* **2021**, *11*, 1023. https://doi.org/10.3390/biom11071023

Academic Editor: Vladimir N. Uversky

Received: 9 June 2021
Accepted: 10 July 2021
Published: 13 July 2021

Publisher's Note: MDPI stays neutral with regard to jurisdictional claims in published maps and institutional affiliations.

Abstract: During surgical procedures, cotton abdominal swabs with their high absorptive capacity and malleability are used to retain organs and absorb blood or other body fluids. Such properties of the natural material cotton are advantageous for most operations, but in cardiopulmonary bypass (CPB) surgery, a high blood volume can accumulate in the thoracic cavity that is quickly retransfused via the heart–lung machine (HLM). This common practice is supposed to be safe due to the high anticoagulation. However, in vitro analyses showed that blood cells and plasma proteins were activated despite a high anticoagulation, which can propagate especially an inflammatory response in the patient. Thus, we investigated patients' blood during CPB surgery for inflammatory and coagulation-associated activation after contact to the HLM and either cotton or synthetic abdominal swabs. Contact with cotton significantly increased thrombocyte and neutrophil activation measured as β-thromboglobulin and PMN-elastase secretion, respectively, compared to synthetic abdominal swabs. Both inflammatory cytokines, interleukin (IL) 1β and IL6, were also significantly increased in the cotton over the synthetic patient group, while SDF-1α was significantly lower in the synthetic group. Our data show for the first time that cotton materials can activate platelets and leukocytes despite a high anticoagulation and that this activation is lower with synthetic materials. This additional activation due to the material on top of the activation exerted by the tissue contact that blood is exposed to during CPB surgery can propagate further reactions in patients after surgery, which poses a risk for this already vulnerable patient group.

Keywords: cardiopulmonary bypass surgery; systemic inflammation; heart–lung machine; cotton; abdominal swabs

1. Introduction

Abdominal swabs are often used in surgical procedures to absorb blood or body fluids from the surgical field or to retain organs [1]. Mostly cotton abdominal swabs are used due to the high absorbency; however, cotton as a natural product is subject to various influences during the growing process, which can affect the quality of the raw material [2]. In addition, the manufacturing process can influence blood compatibility [3]. Although contact time is usually only a few hours, blood components (cells and proteins) can get activated.

In most surgeries, where heavy bleeding is expected, such as hip replacement, open-heart, or aorta surgeries, blood is aspirated using a vacuum blood sucker and retransfusion of the aspirated blood is routinely performed to avoid allogeneic blood transfusions [4]. The coagulation, fibrinolysis, and inflammation in the sucked blood are strongly activated [5,6]. Furthermore, cells are exposed to shear stress, which can lead to their destruction [7]. Thus, the sucked blood is processed in a cell saver to remove cell fragments, human plasma, clotting factors, free hemoglobin, and tissue debris. Solely erythrocytes are retransfused to the patient [8], which prevents the transfer of activated mediators into the systemic circulation and thereby reduces complications [9,10].

Abdominal swabs are also routinely used in the field of cardiovascular surgery [11]. During cardiopulmonary bypass operations, the blood is pumped through the HLM and it comes into contact with foreign surfaces, resulting in the activation of cells and the secretion of pro-inflammatory and -coagulant mediators [12]. Thus, to prevent the activation of blood coagulation, the patient's blood is anticoagulated with approximately 3 IU high-molecular-weight (HMW) heparin/mL blood, which leads to an activated clotting time (ACT) of >300–480 s. Since the blood is highly anticoagulated, in many heart centers, it is common that the blood from the surgical site is wrung out of the used abdominal swabs and sucked into the cardiotomy reservoir of the HLM. Then, the aspirated blood is retransfused without the purification via a cell saver, since a possible activation of the coagulation system for thromboembolic events is considered negligible [13].

In previous studies, a possible procoagulant potential of cotton abdominal swabs was detected using a simple clotting test [14]. Hypercoagulant swabs reduced the ACT and the concentration of free heparin [3]. Further studies showed that even sterilized abdominal swabs were able to activate inflammatory processes in human blood [15], which indicates that the material itself has a certain inflammation activation potential. The retransfusion of sucked blood, which came in contact with the cotton abdominal swabs, without purification might lead to a higher risk of postoperative complications, such as thromboembolic or inflammatory events.

For some years, there have been comparable abdominal swabs available made out of synthetic fibers e.g., viscose or polyester [16]. Most steps during the manufacturing process of synthetic fibers can be controlled, and therefore, it is possible to influence the quality and characteristics of the synthetic product. The previous observation that cotton swabs could induce an inflammatory response despite a high anticoagulation led us to the question of whether there might be a benefit of using a synthetic material with lower activating potential, as activated cells and cytokines retransfused could have an effect on the development of a systemic inflammatory response syndrome (SIRS). Therefore, we set out to investigate this in a small clinical study with 20 cardiac patients undergoing elective surgery involving the HLM, which is divided in two groups of 10 patients each. In one of the groups, cotton abdominal swabs were used in the thoracic cavity and in the other group, synthetic non-woven fiber swabs were employed. To analyze the effect of the two materials in cardiac surgery, blood counts, activation of coagulation, or inflammation with cytokine and chemokine secretion between groups were directly compared.

2. Materials and Methods

2.1. Abdominal Swab Materials

Cotton (white) abdominal swabs from different manufacturers were used, depending on the current status of the central stock at the University Hospital Tübingen (e.g., from Lohmann & Rauscher GmbH & Co. KG, Neuwied, Germany; Paul Hartmann AG, Heidenheim, Germany). The synthetic non-woven (white) abdominal swabs were obtained from Mölnlycke Health Care GmbH, Düsseldorf, Germany.

2.2. Preparation of Sample Swabs for in Vitro Tests

Commercially available processed abdominal swabs (Table 1) were prepared in a laminar flow clean bench with pyrogen-free materials. First, the abdominal swabs were

cut into 2.5 × 1 cm pieces. For the following monocyte activation test (MAT), untreated cotton or synthetic abdominal swabs and pyrogen-impregnated abdominal swabs were prepared. The pyrogen solution (Lipopolysaccharide, LPS; 2000 endotoxin units (EU)/mL; World Health Organization, Geneva, Switzerland) of different concentrations (1 EU/mL, 10 EU/mL) was dried overnight on the material under pyrogen-free conditions, yielding a concentration of 0.1 and 1 EU/mL LPS in the test tubes, respectively, when incubated with blood.

Table 1. Overview of the abdominal swabs used to compare the pyrogenicity between cotton and synthetic abdominal swabs using the MAT.

Abdominal Swabs	Material	Lot	Company	Size
Telasorb white	cotton	299900005	Paul Hartmann AG	20 × 30 cm
BARRIER special non-woven abdominal swabs white	synthetic	17395462	Mölnlycke Health Care GmbH	40 × 40 cm

2.3. Blood Sampling for in Vitro Tests

Whole blood was collected by venipuncture (Safety-Multifly® 20 Gx3/4 TW needle; Sarstedt, Nümbrecht, Germany) in heparin- (19 I.U./mL, Sarstedt, Germany) or EDTA- containing monovettes (EDTA-K 1.6 mg/mL, Sarstedt, Germany) after donors were informed and gave their written informed consent. The blood of four healthy donors was pooled for each procedure. The blood pooling was carried out according to specific instructions in the European Pharmacopoiea (EP) [17]. The strict exclusion criteria for blood donors of the EP also applied: no non-steroidal anti-inflammatory drugs (e.g., ibuprofen) at least 48 h before blood sampling and no steroidal anti-inflammatory drugs 7 days prior to blood sampling. The blood collection procedures were approved by the research and ethics unit of the University of Tübingen (project approval number 287/2020BO2).

2.4. Monocyte Activation Test (MAT)

The MAT was performed with human whole blood as described before [15]. Briefly, the cotton or synthetic swabs (untreated or pyrogen-impregnated) were placed in sterile 2 mL DNA LoBind Eppendorf reaction tubes, and 1.5 mL of 1:10 diluted pooled human whole blood was added and incubated for 18 h at 37 °C. Increasing 2-fold concentrations from 0.0125 to 0.5 EU/mL LPS (concentrations correspond to the volume in the incubation to enable a comparison to a solid swab material) were added to the diluted blood to detect the immune activation potential of the pooled blood to pyrogens (standard dilution row). A concentration of LPS in the middle of the used standard curve (0.1 EU/mL) served as liquid LPS spike and as the lower concentration for LPS impregnation of the swabs. Half of the sterile, non-impregnated swabs were spiked with liquid LPS directly at the time of incubation (yielding 0.1 EU/mL in the incubation) to detect potential interferences with the swabs. The LPS-impregnated samples (0.1 EU/mL and 1.0 EU/mL) were incubated with blood under the same conditions as the sterile swabs.

After the incubation, the samples were centrifuged at 300 g for 5 min, and the supernatant was analyzed for cytokine secretion by enzyme-linked immunosorbent assay (ELISA). Cytokine production triggered by the abdominal swabs was measured by ELISA (human IL1β Duo-Set; R&D Systems/BioTechne, Wiesbaden, Germany) according to the manufacturer's instructions. The quantification of secreted IL1β was performed using Gen5 software (Biotek, Bad Friedrichshall, Germany).

2.5. Patients for the Clinical Study

The study performed was reviewed and approved by the local institutional ethics committee of the Eberhard Karls University of Tübingen (project approval number: 301/2018BO2). The design of the study aims to examine the influence of the abdominal swab material on

biomarkers of inflammation and coagulation activation. Therefore, 20 patients requiring cardiac surgery with the heart–lung machine (HLM) were enrolled and gave their written, informed consent. The patients were divided randomly into two groups. In group one, cotton abdominal swabs were used as is currently the standard procedure. In group two, a synthetic abdominal swab was used instead of cotton in the thoracic cavity during the whole cardiopulmonary bypass. Patient blood was collected at three time points: (1) from HLM directly after connection, (2) from HLM shortly before hemostasis, (3) wrung out from the abdominal swab after antagonizing heparin with protamine. The latter samples were obtained at the time of hemostasis from blood that would not be retransfused to safe patient blood during surgery. Although those samples were not exactly the same samples that were retransfused to the patients, they give an indication of the activating potential of the swab types. Only patients undergoing planned surgery with HLM support were recruited, and special attention was paid to only include patients that did not take immunosuppressant drugs. The two groups consisted of patients of similar age, weight, BMI, comorbidities, and hospitalization periods. The operations were performed under the same conditions. The duration of the operation, the bypass, and the aortic clamping were identical in both groups (Table 2). Additionally, inflammatory markers (C-reactive protein (CRP), procalcitonin (PCT), SIRS, and sepsis-related organ failure assessment (SOFA score) were evaluated from patient files. Criteria for SIRS were two or more of the following: temperature >38 °C or <36 °C, heart rate >90 beats/min, respiratory rate >20 breaths/min or paCO2 <32 mmHg, white blood cell count of >12.000 cells/mm^3 or <4000 cells/mm^3 [18]. The SOFA score was assessed as the sum of the severity scale (0–4) of six organ parameters: oxygenation index (pO_2/FiO_2) for lung, Glasgow Coma Scale for nervous system, mean arterial blood pressure for cardiovascular system, bilirubin for liver, thrombocytes for coagulation, and creatinine for kidney [19].

Table 2. Data of patients where cotton (n = 10) or synthetic (n = 10) swabs were used during the surgery. Data are presented as mean ± SD or percentage of patients per group. Differences between groups were assessed by Student's t-test.

Patients	Cotton	Synthetic	p Values
Number	10	10 (1 death day 5)	
Age (years)	66.7 ± 7.0	68.9 ± 7.5	0.885
Gender (male/female)	7/3	6/4	0.639
Height (cm)	170.2 ± 10.1	169.3 ± 8.7	0.544
Weight (kg)	82.1 ±14.2	75.5 ± 20.1	0.244
BMI (kg/m^2)	28.7 ± 4.7	25.9 ± 5.1	0.761
Body surface area (m^2)	1.9 ± 0.2	1.9 0.3	0.272
Hospitalization (days)	13.4 ± 5.7	11.0 ± 3.5	0.118
Duration of surgery (min)	245.7 ± 47.0	229.0 ± 50.5	0.675
Duration of bypass (min)	133.7 ±45.7	103.6 ± 37.7	0.357
Duration of aortic clamping (min)	101.4 ± 36.1	76.3 ± 31.9	0.704
Intensive postoperative treatment (days)	2.0 ± 2.1	1.4 ± 1.2	0.305
Comorbidities			
BMI (kg/m^2) <25	20%	30%	
BMI (kg/m^2) ≥ 25-<30	50%	50%	
BMI (kg/m^2) ≥30-<35	20%	20%	
BMI (kg/m^2) ≥35-<40	10%		
Diabetes mellitus	20%	50%	
(Arterial) hypertension	60%	70%	

Table 2. *Cont.*

Patients	Cotton	Synthetic	*p* Values
Inflammatory markers (post-surgery)			
Maximal CRP (mg/dl)	14.57 ± 5.88	12.16 ± 3.32	0.275
CRP at discharge (mg/dl)	4.26 ± 2.23	4.49 ± 2.67	0.855
Patients with PCT >2 (ng/mL)	2	1	
SIRS symptoms (1 day post-surgery)	5/10	2/10	
SOFA score (1 day post-surgery)	5.6 ± 3.5	4.2 ± 2.3	0.302

BMI: body mass index; CRP: C-reactive protein; PCT: procalcitonin; SIRS: systemic inflammatory response syndrome; SOFA score: sepsis-related organ failure assessment score.

2.6. Plasma and Blood Sampling from Patients

During surgery, 3 different blood samples were taken: (1) After the establishment of the HLM connection, blood was taken directly from the HLM. (2) Towards the end of the surgery, during the phase of hemostasis, blood was again taken directly from the HLM. (3) Blood was collected from the blood-soaked abdominal swab by wringing out. Blood cell counts were additionally measured at patient admission, post-surgery, and at discharge. The blood was collected into ethylenediaminetetraacetic acid (EDTA; Sarstedt, Nümbrecht, Germany) containing monovettes for the measurement of the blood cell counts, complement activation ELISA, and multiplex immunoassay. CTAD (a mixture of citrate, theophylline, adenosine, and dipyridamol; BD Biosciences, Heidelberg, Germany) vacutainer were used for platelet activation ELISA, and citrate monovettes (Sarstedt, Nümbrecht, Germany) was used for coagulation activation (thrombin–antithrombin III complex; TAT) and leukocyte activation ELISAs (PMN-elastase). After the collection, the blood was analyzed or processed as soon as possible but after one hour at the latest. The blood cell counts (thrombocytes, erythrocytes, and lymphocytes) were measured directly with an automatic cell counter (ABX Micros 60, Horiba Medical, Kyoto, Japan). For all other activation markers, plasma was obtained by centrifugation (1800× *g*, 18 min at room temperature for citrated blood and 2500× *g*, 20 min at 4 °C for EDTA and CTAD blood). The plasma was shock frozen and stored at −20 °C (citrate and CTAD plasma) or −80 °C (EDTA plasma).

2.7. Soluble Activation Markers

The influence of the two different abdominal swab materials on the activation of the complement system, blood clotting, activation of platelets, and activation of neutrophils was evaluated by the detection of different activation markers using ELISAs, which were performed according to the manufacturer's instructions. For this purpose, the shock frozen plasmas were used. The following activation markers were measured: terminal complement complex (sC5b-9) (MicroVue™ Complement, Quidel, Osteomedical GmbH, Sissach, Switzerland) in EDTA plasma, thrombin–antithrombin III complex (TAT) (Enzygnost® TAT micro, Siemens Healthcare, Erlangen, Germany) and the polymorphonuclear (PMN)-elastase (PMN-elastase ELISA, demeditec, Kiel, Germany) in citrated plasma, β-thromboglobulin (β-TG) (Asserachrom® β-TG, Diagnostica Stago, Düsseldorf, Germany) in CTAD plasma.

2.8. Cytokine and Chemokine Assessment

Cytokine concentrations of IL1β, IL6, SDF-1α, MCP-1, and TNFα were determined using a multiplex immunoassay (Human High Sensitivity Cytokine Luminex Performance Assay; R&D Systems/Bio-Techne, Wiesbaden, Germany) according to the manufacturer's instructions. For the measurement, frozen EDTA plasma samples were diluted 1:4 with calibration diluent RD6-40 and measured with polystyrene microparticle beads in a Bioplex 200 (BioRad, Feldkirchen, Germany).

2.9. Statistics

The statistical analyses were performed using the software package GraphPad Prism version 6.01 (GraphPad Software Inc., La Jolla, CA, USA). After analyzing the samples for normal distribution by Shapiro–Wilk normality test, either Student's unpaired *t*-tests or Mann–Whitney U tests were performed. Statistical significance was defined as $p < 0.05$.

3. Results

3.1. Preliminary In Vitro Test Shows Marked Differences between Materials

In a preliminary in vitro test, the inflammatory activation of blood by synthetic and cotton abdominal swabs was investigated using the monocyte activation test (MAT). As observed previously [15], cotton abdominal swabs themselves induced relatively strong secretion of the inflammatory cytokine IL1β, whereas blood incubated with the synthetic material showed no measurable IL1β secretion, actually the same response as blood without LPS or materials (Figure 1). The significantly different responses between swab types ($p < 0.0001$) indicate that the synthetic material does not activate the blood monocytes and thus shows different material properties than cotton, which induced a similar IL1β secretion in blood as the middle of the LPS standard curve (0.1 EU/mL) (Figure 1). On the other hand, the addition of liquid LPS to the incubating swabs did only marginally increase the cytokine secretion with a recovery rate of roughly 42% and 22%, respectively (Table 3). Two concentrations of LPS dried on the surface were almost not detectable any longer. According to the EP, LPS recovery rates below 50% show interference of LPS with the test substance [17]. Therefore, both materials, synthetic and cotton, inhibited the recovery of LPS, giving them similar properties in this respect. This behavior is generally advantageous for the abdominal swab materials, since this indicates that potential contaminants, e.g., when used for wounds, would be rather trapped than stimulate an immune response. Due to the interesting marked differences in the inflammatory response of whole blood to the materials alone, an in vivo study with two patient groups was planned and conducted.

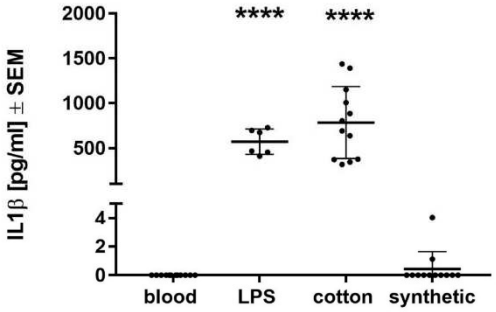

Figure 1. The MAT with human whole blood revealed inflammatory activation by cotton to a similar extend as 0.1 EU/mL liquid LPS added to blood, but there was no activation by synthetic swabs. Secretion of IL1β by blood monocytes is presented as scatter plot with means ± SEM. **** $p < 0.0001$, significantly different from blood without additives. One-way ANOVA with Tukey multiple comparison post hoc test.

Table 3. Proportional LPS recovery rates when added as liquid spike or when impregnated to the surface of the materials.

	Cotton	Synthetic
+0.1 EU/mL liquid LPS	42.3%	21.8%
+0.1 EU/mL impregnated LPS	0%	2.2%
+1.0 EU/mL impregnated LPS	0%	17.7%

3.2. Leukocyte Counts Increased at the End of HLM Only in the Cotton Group

As a first indicator of differences between operations performed with the two materials, blood cell counts were ascertained (Figure 2). In addition to the blood samples obtained during the operation, the blood cell counts from the patient's records were used to get a more complete picture of the clinical outcome. No significant changes in platelet counts (Figure 2a) or red blood cell counts (RBC) (Figure 2b) were observed between cotton and synthetic abdominal swab groups, but significant decreases compared to admission values were seen within both groups. While RBC counts were similarly decreased compared to admission in both groups, platelet counts showed significant decreases in the cotton group for HLM start, HLM end, and post-surgery, but only for HLM start in the synthetic group. However, this was likely due to the generally larger variability of platelet counts in the patient group with synthetic swabs. The lower RBC counts during HLM is explained by the blood loss and dilution of blood with the priming fluid. The platelet and RBC counts in the blood samples obtained from the cotton and synthetic abdominal swabs are reduced and clearly in the pathological range, indicating a possible adhesion and activation of thrombocytes to the material and also trapping of RBCs in the swabs or hemolysis of RBCs.

Interestingly, there was only a significant increase in white blood cells (WBC) between HLM start and post-surgery in the synthetic group, whereas in the cotton group, the time points HLM end and post-surgery were significantly increased compared to admission and HLM start (Figure 2c). Moreover, the WBC count at the end of HLM was significantly elevated compared to discharge. Between groups, at the start of the HLM, WBC counts were significantly lower in the synthetic group than in the cotton group, but for both groups, the values were in the physiological range. Shortly before stopping the HLM, the WBC counts of patients from the synthetic group were still in the physiological range, but those from the cotton group were not. Additionally, leukocyte counts were significantly elevated in the cotton group at the end of HLM compared to the synthetic group. WBC counts in the blood obtained by wringing of the swabs were not significantly different between the two groups.

3.3. Hemocompatibility Parameters Differed for Leukocyte and Thrombocyte Activation

The activation of the complement system (sC5b-9), inflammation (PMN-elastase), coagulation (TAT), and platelets (β-TG) was analyzed in the blood samples from the beginning and end of HLM as well as in the blood samples obtained by wringing out of abdominal swabs (Figure 3). At the end of HLM, all measured hemocompatibility markers were significantly increased in both cotton and synthetic groups (Figure 3a–d), indicating that the activation of blood through the HLM treatment predominated over possible differences between the materials. While complement activation was similar between materials (Figure 3a), blood obtained from cotton swabs showed significantly higher activation of inflammation (PMN-elastase, Figure 3b), the coagulation cascade (TAT, Figure 3c), and platelets (β-TG, Figure 3d). The most marked difference was observed for PMN-elastase levels, where the activation of the blood by the synthetic material was only slightly higher than the activation seen at the end of HLM (Figure 3b). In contrast, cotton increased PMN-elastase levels to a much larger extend.

3.4. IL6 and IL1β Secretion was Lower with Synthetic Swabs

Similar to the in vitro experiments, inflammatory cytokine secretion was also investigated in vivo. Compared to the start of HLM, IL6 and TNFα levels were significantly increased in both groups at the end of HLM showing an inflammatory activation during HLM, while IL1β secretion was not significantly different (Figure 4). Between the groups, both IL1β and IL6 secretion was significantly lower at the end of HLM in the synthetic compared to the cotton group (Figure 4a,b), while TNFα secretion did not differ (Figure 4c). This difference between groups points toward an influence of the materials. Especially for IL6, this was also seen in blood obtained directly from the swabs (Figure 4b).

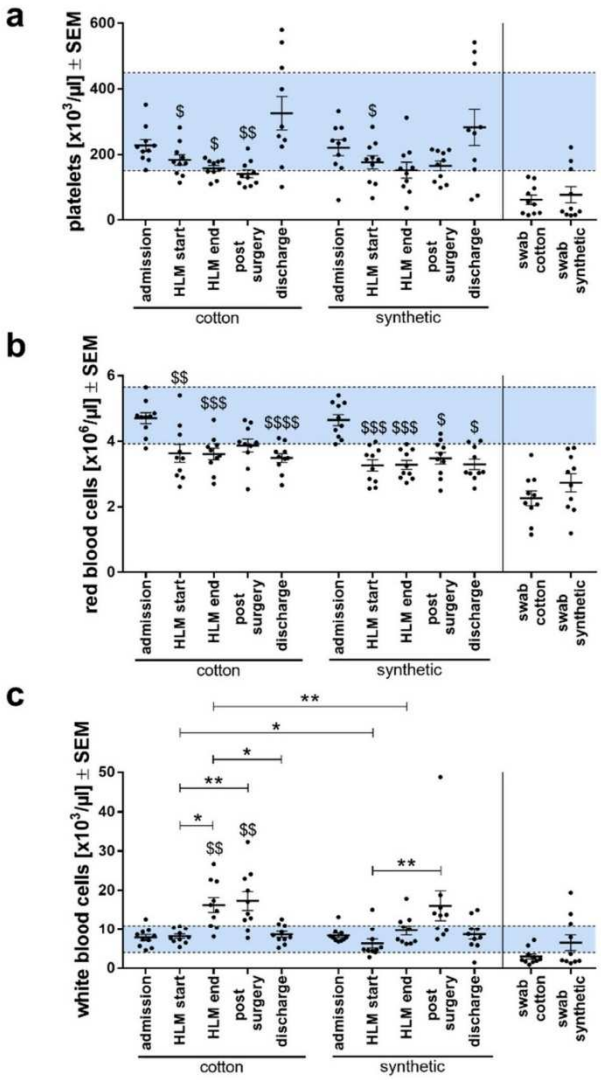

Figure 2. Analyses of blood cell counts of both patient groups (cotton swabs and synthetic swabs) measured at time of admission, during (HLM start, HLM end, and swab), and post-surgery as well as before discharge. (**a**) Platelets, (**b**) red blood cells, (**c**) white blood cells. Cell counts are presented as means ± SEM per study group. The horizontal line indicates the threshold values to pathological levels, the blue areas between the lines indicate the physiological ranges. Differences between groups were analyzed using Student's *t*-test, differences within groups were analyzed using a one-way analysis of variance (ANOVA) with Bonferroni's multiple comparison post-hoc test. The symbol "$" denotes significant differences compared to admission. * or $ $p < 0.05$; ** or $$ $p < 0.01$; $$$ $p < 0.001$; $$$$ $p < 0.0001$.

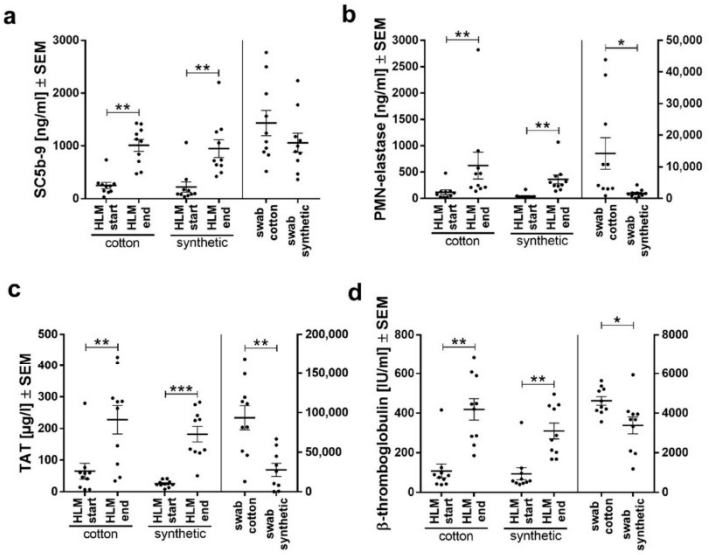

Figure 3. Hemocompatibility parameters measured from plasma of both patient groups indicate lower activation of neutrophils and platelets when synthetic swabs are used. Plasma levels of (**a**) complement, SC5b-9; (**b**) inflammation, PMN-elastase; (**c**) coagulation, TAT; and (**d**) platelet, β-TG activation from patients of both groups (cotton swabs and synthetic swabs) are presented as means ± SEM per study group. Differences were detected by Student's *t*-test * $p < 0.05$, ** $p < 0.01$, *** $p < 0.001$.

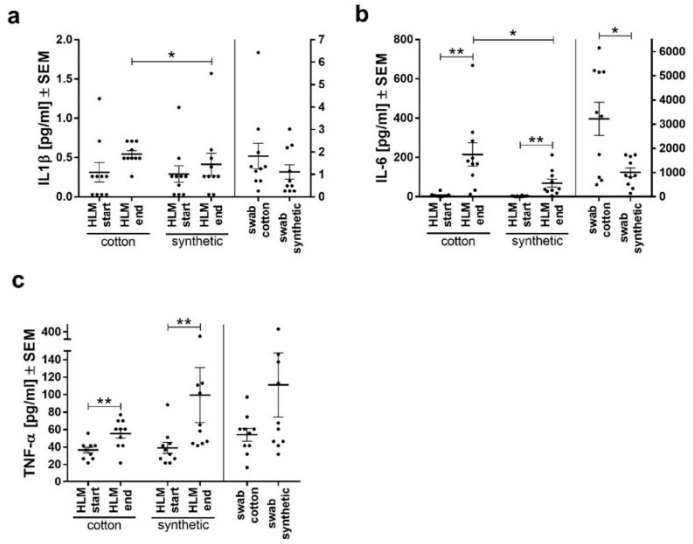

Figure 4. Interleukin levels of (**a**) IL1β and (**b**) IL6 from patients of both groups (cotton swabs and synthetic swabs) were lower with synthetic abdominal swabs than with cotton swabs, while no differences were seen with (**c**) TNFα secretion. Cytokine levels are presented as means ± SEM per study group. * $p < 0.05$, ** $p < 0.01$, student's *t*-test.

3.5. Levels of Chemokines MCP-1 and SDF1-α Reflect Inflammatory Processes

In addition to inflammatory cytokines, the chemokines monocyte chemoattractant protein-1 (MCP-1/CCL2) and stromal cell-derived factor 1 (SDF-1α) were measured. In our experiments, we could see an increase in MCP-1 levels during HLM (start HLM vs. end HLM) (Figure 5a), but not between groups or materials. SDF-1α was significantly increased at the end of HLM in both groups (Figure 5b). Interestingly, in blood wrung from the swabs, the synthetic material induced a significantly stronger activation of this marker than cotton.

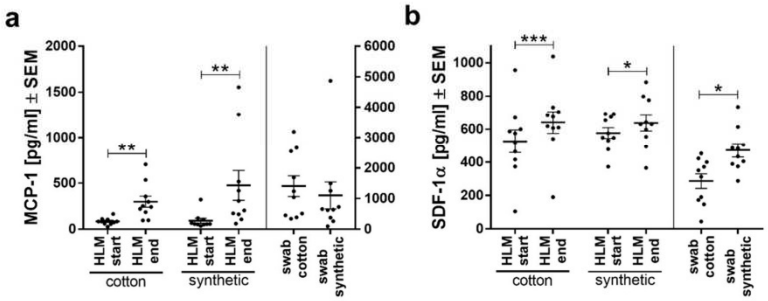

Figure 5. Plasma levels of chemokines are increased during HLM. Shown are plasma levels of (**a**) MCP-1 and (**b**) SDF-1α as means ± SEM per study group. Differences are measured with Student's *t*-test. * $p < 0.05$, ** $p < 0.01$, *** $p < 0.001$.

4. Discussion

The aim of the current study was to ascertain whether or not abdominal swab material may influence blood parameters in addition to cardiopulmonary bypass surgery and thus reveal a possible source for unwanted additional activation of blood that could be avoided. The obtained data have to be discussed in two different aspects: (1) changes occurring during HLM/surgery reflect combined effects of the surgery, the HLM circuit, and the abdominal swab material, (2) parameters measured from blood that was wrung out of the abdominal swabs are mainly due to effects of the material and applied shear stress. As the surgery parameters and HLM contact times were not significantly different between groups, the differences observed at the HLM end between groups likely reflect the additional influence of the used swab material.

The significantly lower RBC and platelet counts at the beginning of HLM are explained by dilution of the blood with priming fluid [20]. The activation of blood parameters during cardiopulmonary bypass using the HLM has been described for the complement system, coagulation, leukocyte activation, and inflammatory cytokines [21–23]. The effects observed in our study reflect these observations to a large extend. Moreover, the similarities in blood cell counts between the blood samples wrung from the abdominal swabs indicates that the adhesion of platelets and leukocytes or the destruction of erythrocytes due to the shear stress from wringing [24,25] was reasonably similar between the materials.

However, the different activation parameters during HLM between patient groups point toward an additional effect of the material. Here, the samples taken from the swabs can be used to support the material-induced activation. The pathologically increased leukocytes at the end of HLM and post-surgery that were only observed in the cotton group cannot only be explained by the procedure but are likely due to stronger activation and cell proliferation [26] caused by the material. There are two possibilities of how the material-induced activation may have occurred: (1) directly on the leukocytes or (2) through triggering of other blood cells or proteins that affected the leukocytes. The natural material cotton consists of subunits belonging to the β-glucans, which are known to trigger an immune response in mammals [27] and plants [28]. Although it is not known

whether this interaction of glucan molecules with cell surface receptors also applies to the material woven from cotton fibers [16], NF-kb activation over Toll-like receptor (TLR) 2-stimulation was observed in a monocyte cell line [29]. The strong IL1β secretion after contact of blood with cotton seen in our in vitro experiment strengthens the assumption that cotton stimulates monocytes to secrete IL1β. This cytokine, released by monocytes upon stimulation and inflammasome processing [30], is a very potent trigger of fever [31,32] but also stimulates endothelial cells to secrete NO and express adhesion molecules and chemokines, thus facilitating neutrophil extravasation [31,33,34]. However, thrombocytes have been reported to also liberate IL1β upon stimulation [35]. There is a strong mutual interaction and activation between platelets and leukocytes (especially neutrophils and macrophages) [36]. Therefore, the increase in leukocyte numbers only in the cotton group during HLM is likely related to the stimulation of proliferation and differentiation of neutrophil precursors by IL1β [30], which is released by either monocytes or platelets and can induce the mobilization of granulocyte progenitor cells and maturation of neutrophils in the bone marrow [37].

PMN-elastase, released from activated neutrophils, was significantly higher at the end of HLM in both groups, and in blood from the cotton swabs compared to the synthetic swabs. This suggests that in addition to the HLM procedure, the material itself induced increased neutrophil degranulation. Since the groups were not significantly different at the end of HLM, the activating effect induced by the extracorporeal procedure likely concealed the effect of the material. Therefore, the increase in neutrophil counts at the end of HLM observed only for the cotton group was not synonymous with neutrophil activation and degranulation alone, as PMN-elastase was similarly increased at the end of HLM in both groups. Neutrophil degranulation can be induced by several stimuli such as contact phase FXIIa, kallikrein [38], LPS [39], or IL8 [40]. The latter is produced by activated monocytes [41]. Activated platelets secrete thrombocyte activating (e.g., platelet-activating factor, ADP, von Willebrand Factor, [42]) but also neutrophil-activating (neutrophil-activating peptide 2) and other inflammation-triggering mediators such as reactive oxygen species [36]. Therefore, the significantly higher activation of platelets, measured by β-TG release, in blood wrung from cotton could be responsible for the increased neutrophil activation. Platelets themselves are readily activated at negatively charged surfaces [39] or by shear stress [43] from the HLM or wringing of the swabs. Tissue-factor expressing cells, such as activated monocytes [44], or neutrophil extracellular traps (NET) from activated neutrophils [45], can trigger the coagulation cascade [46], but also contact phase activation (by hydrolysis of FXII [47]) through the artificial surfaces of the HLM or swabs can occur and promote coagulation and inflammation [48–51]. A significant coagulation activation (measured by TAT complex formation) was observed in blood taken from the HLM despite the high anticoagulation regime used to prevent this [52,53]. In comparison to the levels during HLM, the very high TAT formation in blood taken from both swabs reflects in part the beginning protamine treatment antagonizing heparin and the adsorption of the anticoagulant heparin to the material [3], thus preventing thrombin formation less efficiently than during HLM. However, there was a significantly stronger activation in cotton than in synthetic swabs, pointing to a stronger activation of the coagulation cascade by stronger contact phase activation or platelet activation.

The significantly higher IL6 secretion in blood wrung from cotton swabs likely reflects a material-induced inflammatory activation of monocytes [15], whereas the significant increase at the end of HLM in the cotton compared to the synthetic group for both inflammatory cytokines (IL1β and IL6) can be induced by activated monocytes, platelets, or endothelial cells [54,55]. The SDF-1α expression can be upregulated by inflammatory mediators such as IL1β or TNFα [56,57]. In our study, this chemokine was significantly increased during HLM in both groups, but in blood wrung from swabs, the synthetic swabs induced a significantly higher expression than cotton swabs. This observation seems contradicting to the other observations as it has aggravating effects on platelet aggregation upon binding to the platelet surface receptors CXRC4 or CXCR7 [58]. In line with

cotton's stronger activation of platelets and leukocytes, we would therefore expect to see the opposite effect. Although it has long been assumed that SDF-1α originates mainly from bone marrow and endothelium [59], there is also a pool of SDF-1α released from platelets [60]. Especially this SDF-1α has been shown to promote platelet survival [58] and regulate monocyte differentiation and survival [61]. Thus, SDF-1α measured from swabs and during HLM may come from different sources. While SDF-1α levels in blood taken from HLM are not different between patient groups, the levels measured from swabs are, indicating a possible role of platelet-derived SDF-1α after direct contact with the materials and thus having a protective rather than a destructive role for platelets and monocytes in this case.

Our data strongly suggest that an inflammatory activation of monocytes, degranulation of neutrophils, and activation of platelets has occurred due to the material, not least due to the strong IL1β secretion in vitro in contact with cotton but the almost complete abrogation in contact with the synthetic material. Although most measured parameters were similarly elevated at the end of HLM in both patient groups, there was a significant increase in the inflammatory parameters at the end of HLM in the cotton group. This stronger activation of blood components by cotton than the synthetic material poses an additional risk for patients to develop a sterile inflammatory response (SIRS) when the activated blood components enter the systemic circulation. PMN-elastase has been reported to further cytokine release [62], and the other pro-inflammatory mediators and substances released from activated thrombocytes contribute as well. Looking at the CRP levels and SOFA score in both groups, we could not see a significant difference between groups. However, in the cotton group, half of the patients (five) showed symptoms of SIRS, whereas in the synthetic group, only two patients had SIRS symptoms. Therefore, the synthetic material seems to be the safer choice for patients in CPB surgery where blood is retransfused without using the cell saver to remove inflammatory mediators.

Similar observations concerning synthetic materials have been observed in other studies. Hernández et al., were able to show in patients with hemodialysis that the leukocyte activation was higher when cellulosic membranes were used than synthetic membranes [63]. In monkeys, oral sutures made from nylon showed nearly no inflammatory tissue reaction and therefore were superior to sutures made from cotton [64]. The same tendency of a lower inflammatory reaction to synthetic polymers than to cotton was visible in our study.

However, all operating surgeons in our study described the synthetic materials as inferior regarding absorbency and moldability. This subjective view may base on the surgeons being familiar with the cotton swabs. At least for the adsorptive capacity of the synthetic material polyurethane, there was no disadvantage over cotton materials seen even after the repeated use of one swab [16]. When comparing the spread of blood drops on this material, it was visible that the spread on the synthetic material was less. In clinical use, this could be an advantage in locating the exact origin of bleedings [16]. However, the described stiffness of the synthetic material is a disadvantage that needs to be considered. Modifications of synthetic materials to improve wettability or haptic properties may be applied such as the photografting of 2-hydroxyethyl methacrylate (HEMA), a possible material for a biocompatible hydrogel [65], onto polypropylene, which resulted in significantly increased absorbency and decreased water wetting time of the polymer [66]. Overall, patient safety in terms of adverse reactions such as SIRS and optimal properties during surgery need to be evaluated.

5. Conclusions

For the first time, the current clinical study provided evidence for an additional activation of blood components due to cotton abdominal swabs. Especially in cardiopulmonary bypass surgery, if no cell saver is used, the retransfusion of the activated blood components may pose a further risk for the already critically ill patients. Whether or not this necessarily contributes to serious complications cannot be predicted by this small study with limited patient numbers but requires a larger cohort comparing post-surgery complications in

patients where the materials have been used. Our data unequivocally show that despite its advantageous properties, the natural material cotton activates blood components. Ideally, the cotton material would be modified to show less activation or the malleability of the synthetic material improved. Nevertheless, the common practice of retransfusion should be reconsidered when using cotton materials, as the increased cytokine secretion may contribute to or aggravate systemic inflammatory reactions following surgery. A cost–benefit analysis for the use of materials, cell saver, and allogenic blood products is advisable.

Author Contributions: Conceptualization: C.S. (Christoph Salewski), S.S., C.S. (Christian Schlensak), M.A.-A. and H.P.W.; methodology: C.S. (Christoph Salewski), S.S. and H.P.W.; validation: S.S., C.S. (Christoph Salewski), K.G., L.M.H., D.S.-A. and M.A.-A.; formal analysis: K.G., L.M.H., S.S. and C.S. (Christoph Salewski); investigation: K.G., L.M.H., M.W., P.M, D.S.-A. and C.S. (Christoph Salewski); resources: C.S. (Christian Schlensak), M.A.-A. and H.P.W.; data curation: C.S. (Christoph Salewski), C.S. (Christian Schlensak), L.M.H. and K.G.; writing—original draft preparation: S.S., K.G., L.M.H., C.S. (Christoph Salewski), M.A.-A., P.M., M.W., H.P.W. and D.S.-A.; writing—resubmission: S.S., K.G. and C.S. (Christoph Salewski); visualization: K.G., L.M.H. and S.S.; supervision: S.S., K.G., L.M.H. and C.S. (Christoph Salewski); project administration: C.S. (Christian Schlensak), C.S. (Christoph Salewski), S.S., H.P.W. and M.A.-A.; funding acquisition: C.S. (Christian Schlensak) and H.P.W. All authors have read and agreed to the published version of the manuscript.

Funding: This research did not receive any specific grant from funding agencies in the public, commercial, or not-for-profit sectors.

Institutional Review Board Statement: The study was conducted according to the guidelines of the Declaration of Helsinki, and approved by the Institutional Ethics Committee of the Eberhard Karls University of Tübingen, medical faculty (301/2018BO2; 08.08.2018).

Informed Consent Statement: Informed consent was obtained from all subjects involved in the study.

Acknowledgments: The authors are very grateful to Mölnlycke Healthcare AB for providing access to synthetic non-woven abdominal swab sets in Germany. We would also like to thank the whole team of surgeons for their support in this study and Birgit Schreiner for her assistance in the Bioplex assay. Furthermore, we acknowledge the support by Open Access Publishing Fund of University of Tübingen.

Conflicts of Interest: The authors declare no conflict of interest.

References

1. Criscitelli, T. *Fast Facts for the Operating Room Nurse, Second Edition: An Orientation and Care Guide in a Nutshell*; Springer Publishing Company: New York, NY, USA, 2018; p. 81.
2. Reddy, K.R.; Davidonis, G.H.; Johnson, A.S.; Vinyard, B.T. Temperature regime and carbon dioxide enrichment alter cotton boll development and fiber properties. *Agron. J.* **1999**, *91*, 851–858. [CrossRef]
3. Krajewski, S.; Hierlemann, T.; Neumann, B.; Nathan, T.; Abel, M.; Koggel, A.; Schlensak, C.; Wendel, H.P. Hypercoagulant abdominal swabs in cardiac surgery: Potential problems and background. *Thorac Cardiovasc Surg* **2016**, *64*, 589–595.
4. Zhao, H.; Ma, H.; Meng, L.; Zhao, Z.; Quan, X.; Cheng, Z. Application of autologous blood cell salvage in off-pump coronary artery bypass graft operation. *Heart Surg. Forum* **2017**, *20*, E107–E110. [CrossRef]
5. Tu, L.N.; Hsieh, L.; Kajimoto, M.; Charette, K.; Kibiryeva, N.; Forero, A.; Hampson, S.; Marshall, J.A.; O'brien, J.; Scatena, M. Shear stress associated with cardiopulmonary bypass induces expression of inflammatory cytokines and necroptosis in monocytes. *JCI Insight* **2021**, *6*, e141341. [CrossRef]
6. Edmunds, L.H.; Colman, R.; Niewiarowski, S. Blood-Surface Interactions during Cardiopulmonary Bypass. In *Blood Use in Cardiac Surgery*; Springer: Heidelberg, Germany, 1991; pp. 27–36.
7. Gregoretti, S. Suction-induced hemolysis at various vacuum pressures: Implications for intraoperative blood salvage. *Transfusion* **1996**, *36*, 57–60. [CrossRef]
8. Konig, G.; Waters, J.H. Washing and filtering of cell-salvaged blood–does it make autotransfusion safer? *Transfus. Altern. Transfus. Med.* **2012**, *12*, 78–87. [CrossRef] [PubMed]
9. Gunaydin, S.; Robertson, C.; Budak, A.B.; Gourlay, T. Comparative evaluation of blood salvage techniques in patients undergoing cardiac surgery with cardiopulmonary bypass. *Perfusion* **2018**, *33*, 105–109. [CrossRef] [PubMed]
10. Damgaard, S.; Nielsen, C.H.; Andersen, L.W.; Bendtzen, K.; Tvede, M.; Steinbrüchel, D.A. Cell saver for on-pump coronary operations reduces systemic inflammatory markers: A randomized trial. *Ann. Thorac. Surg.* **2010**, *89*, 1511–1517. [CrossRef] [PubMed]
11. Taggart, D. *Core Concepts in Cardiac Surgery*; OUP OxfordL: Oxford, UK, 2018; p. 40.

12. Hakim, R.M. Complement activation by biomaterials. *Cardiovasc. Pathol.* **1993**, *2*, 187–197. [CrossRef]
13. Lander, H.; Zammert, M.; Fitzgerald, D. Anticoagulation management during cross-clamping and bypass. *Best Pr. Res. Clin. Anaesthesiol* **2016**, *30*, 359–370. [CrossRef] [PubMed]
14. Krajewski, S.; Nathan, T.; Neumann, B.; Hoffmann, S.; Abel, M.; Koggel, A.; Schlensak, C.; Wendel, H.P. Simple clotting test to detect procoagulant abdominal swabs. *J. Mater. Sci Mater. Med.* **2015**, *26*, 106. [CrossRef] [PubMed]
15. Trunk, S.; Mullerbader, P.; Hennig, U.; Abel, M.; Koggel, A.; Stang, K.; Altreuter, Y.; Steger, V.; Schlensak, C.; Wendel, H.P.; et al. Inflammatory potential of cotton-based surgically invasive devices: Implications for cardiac surgery. *J. Biomed. Mater. Res. B Appl. Biomater.* **2019**, *107*, 1877–1888. [CrossRef] [PubMed]
16. Shimamoto, T. Polyurethane sheet: A potential substitute of surgical cotton gauze. *J. Cardiothorac Surg* **2011**, *6*, 26. [CrossRef] [PubMed]
17. European Council. European-Pharmacopoeia. Monocyte Activation Test. Edition 9.2; 2017; Chapter 2.6.30.
18. Stoppelkamp, S.; Veseli, K.; Stang, K.; Schlensak, C.; Wendel, H.P.; Walker, T. Identification of predictive early biomarkers for sterile-sirs after cardiovascular surgery. *PLoS ONE* **2015**, *10*, e0135527. [CrossRef] [PubMed]
19. Robert-Koch-Institut. Epidemiologisches Bulletin. Available online: https://www.rki.de/DE/Content/Infekt/EpidBull/Archiv/2017/Ausgaben/37_17.pdf?__blob=publicationFile (accessed on 30 June 2021).
20. Brauer, S.D.; Applegate Ii, R.L.; Jameson, J.J.; Hay, K.L.; Lauer, R.E.; Herrmann, P.C.; Bull, B.S. Association of plasma dilution with cardiopulmonary bypass-associated bleeding and morbidity. *J. Cardiothorac. Vasc. Anesth.* **2013**, *27*, 845–852. [CrossRef]
21. Sniecinski, R.M.; Chandler, W.L. Activation of the hemostatic system during cardiopulmonary bypass. *Anesth. Analg.* **2011**, *113*, 1319–1333. [CrossRef]
22. Wehlin, L.; Vedin, J.; Vaage, J.; Lundahl, J. Activation of complement and leukocyte receptors during on-and off pump coronary artery bypass surgery. *Eur. J. Cardio-Thorac. Surg.* **2004**, *25*, 35–42. [CrossRef]
23. Plötz, F.B.; Van Oeveren, W.; Bartlett, R.H.; Wildevuur, C.R. Blood activation during neonatal extracorporeal life support. *J. Thorac. Cardiovasc. Surg.* **1993**, *105*, 823–832. [CrossRef]
24. Leverett, L.; Hellums, J.; Alfrey, C.; Lynch, E. Red blood cell damage by shear stress. *Biophys. J.* **1972**, *12*, 257–273. [CrossRef]
25. Watts, T.; Barigou, M.; Nash, G.B. Comparative rheology of the adhesion of platelets and leukocytes from flowing blood: Why are platelets so small? *Am. J. Physiol. Heart Circ. Physiol.* **2013**, *304*, H1483–H1494. [CrossRef]
26. Sutton, S.; Patel, A.; Chase, V.; Schmidt, L.; Hunley, E.; Yancey, L.; Hebeler, R.; Cheung, E.; Henry Iii, A.; Meyers, T. Clinical benefits of continuous leukocyte filtration during cardiopulmonary bypass in patients undergoing valvular repair or replacement. *Perfusion* **2005**, *20*, 21–29. [CrossRef]
27. Akramienė, D.; Kondrotas, A.; Didžiapetrienė, J.; Kėvelaitis, E. Effects of ß-glucans on the immune system. *Medicina* **2007**, *43*, 597. [CrossRef] [PubMed]
28. Kim, H.S.; Hong, J.T.; Kim, Y.; Han, S.-B. Stimulatory effect of β-glucans on immune cells. *Immune Netw.* **2011**, *11*, 191–195. [CrossRef]
29. Vogt, L.M.; Boekschoten, M.V.; De Groot, P.J.; Faas, M.M.; De Vos, P. Cellulose alters the expression of nuclear factor kappa b-related genes and toll-like receptor-related genes in human peripheral blood mononuclear cells. *J. Funct. Foods* **2015**, *18*, 520–531. [CrossRef]
30. Köffel, R.; Meshcheryakova, A.; Warszawska, J.; Hennig, A.; Wagner, K.; Jörgl, A.; Gubi, D.; Moser, D.; Hladik, A.; Hoffmann, U. Monocytic cell differentiation from band-stage neutrophils under inflammatory conditions via mkk6 activation. *Blood* **2014**, *124*, 2713–2724. [CrossRef] [PubMed]
31. Dinarello, C.A. Infection, fever, and exogenous and endogenous pyrogens: Some concepts have changed. *J. Endotoxin Res.* **2004**, *10*, 201–222.
32. Fennrich, S.; Hennig, U.; Toliashvili, L.; Schlensak, C.; Wendel, H.P.; Stoppelkamp, S. More than 70 years of pyrogen detection: Current state and future perspectives. *Altern. Lab. Anim.* **2016**, *44*, 239–253. [CrossRef] [PubMed]
33. Sahni, A.; Sahni, S.K.; Francis, C.W. Endothelial cell activation by il-1β in the presence of fibrinogen requires αvβ3. *Arterioscler. Thromb. Vasc. Biol.* **2005**, *25*, 2222–2227. [CrossRef] [PubMed]
34. Gross, S.S.; Jaffe, E.A.; Levi, R.; Kilbourn, R.G. Cytokine-activated endothelial cells express an isotype of nitric oxide synthase which is tetrahydrobiopterin-dependent, calmodulin-independent and inhibited by arginine analogs with a rank-order of potency characteristic of activated macrophages. *Biochem. Biophys. Res. Commun.* **1991**, *178*, 823–829. [CrossRef]
35. Hottz, E.D.; Monteiro, A.P.T.; Bozza, F.A.; Bozza, P.T. Inflammasome in platelets: Allying coagulation and inflammation in infectious and sterile diseases? *Mediat. Inflamm.* **2015**. [CrossRef]
36. Mansour, A.; Roussel, M.; Gaussem, P.; Nédelec-Gac, F.; Pontis, A.; Flécher, E.; Bachelot-Loza, C.; Gouin-Thibault, I. Platelet functions during extracorporeal membrane oxygenation. Platelet–leukocyte aggregates analyzed by flow cytometry as a promising tool to monitor platelet activation. *J. Clin. Med.* **2020**, *9*, 2361. [CrossRef] [PubMed]
37. Brugger, W.; Mocklin, W.; Heimfeld, S.; Berenson, R.J.; Mertelsmann, R.; Kanz, L. Ex vivo expansion of enriched peripheral blood cd34+ progenitor cells by stem cell factor, interleukin-1 beta (il-1 beta), il-6, il-3, interferon-gamma, and erythropoietin. *Blood* **1993**, *81*, 579–584. [CrossRef]
38. Wachtfogel, Y.T.; Kucich, U.; James, H.L.; Scott, C.F.; Schapira, M.; Zimmerman, M.; Cohen, A.B.; Colman, R. Human plasma kallikrein releases neutrophil elastase during blood coagulation. *J. Clin. Investig.* **1983**, *72*, 1672–1677. [CrossRef]
39. Lacy, P. Mechanisms of degranulation in neutrophils. *Allergy Asthma Clin. Immunol.* **2006**, *2*, 98. [CrossRef]

40. Taub, D.D.; Anver, M.; Oppenheim, J.J.; Longo, D.L.; Murphy, W.J. T lymphocyte recruitment by interleukin-8 (il-8). Il-8-induced degranulation of neutrophils releases potent chemoattractants for human t lymphocytes both in vitro and in vivo. *J. Clin. Investig.* **1996**, *97*, 1931–1941. [CrossRef]
41. Lopez-Castejon, G.; Brough, D. Understanding the mechanism of il-1β secretion. *Cytokine Growth Factor Rev.* **2011**, *22*, 189–195. [CrossRef] [PubMed]
42. Blair, P.; Flaumenhaft, R. Platelet α-granules: Basic biology and clinical correlates. *Blood Rev.* **2009**, *23*, 177–189. [CrossRef] [PubMed]
43. Zhang, J.-N.; Bergeron, A.L.; Yu, Q.; Sun, C.; Mcintire, L.V.; López, J.A.; Dong, J.-F. Platelet aggregation and activation under complex patterns of shear stress. *Thromb. Haemost.* **2002**, *88*, 817–821. [CrossRef]
44. Østerud, B.; Bjørklid, E. Sources of tissue factor. *Semin. Thromb. Hemost.* **2006**, *32*, 11–23. [CrossRef]
45. Kambas, K.; Mitroulis, I.; Apostolidou, E.; Girod, A.; Chrysanthopoulou, A.; Pneumatikos, I.; Skendros, P.; Kourtzelis, I.; Koffa, M.; Kotsianidis, I. Autophagy mediates the delivery of thrombogenic tissue factor to neutrophil extracellular traps in human sepsis. *PLoS ONE* **2012**. [CrossRef]
46. Zelaya, H.; Rothmeier, A.; Ruf, W. Tissue factor at the crossroad of coagulation and cell signaling. *J. Thromb. Haemost.* **2018**, *16*, 1941–1952. [CrossRef] [PubMed]
47. Zhuo, R.; Siedlecki, C.A.; Vogler, E.A. Autoactivation of blood factor xii at hydrophilic and hydrophobic surfaces. *Biomaterials* **2006**, *27*, 4325–4332. [CrossRef]
48. Green, D. Coagulation cascade. *Hemodial. Int.* **2006**, *10*, S2–S4. [CrossRef] [PubMed]
49. Mandle, R.; Kaplan, A. Hageman factor substrates. Human plasma prekallikrein: Mechanism of activation by hageman factor and participation in hageman factor-dependent fibrinolysis. *J. Biol. Chem.* **1977**, *252*, 6097–6104. [CrossRef]
50. Wiggins, R.C.; Bouma, B.N.; Cochrane, C.G.; Griffin, J.H. Role of high-molecular-weight kininogen in surface-binding and activation of coagulation factor xi and prekallikrein. *Proc. Natl. Acad. Sci. USA* **1977**, *74*, 4636–4640. [CrossRef]
51. Dray, A.; Perkins, M. Bradykinin and inflammatory pain. *Trends Neurosci.* **1993**, *16*, 99–104. [CrossRef]
52. Gouault-Heilmann, M.; Huet, Y.; Contant, G.; Payen, D.; Bloch, G.; Rapin, M. Cardiopulmonary bypass with a low-molecular-weight heparin fraction. *Lancet* **1983**, *322*, 1374. [CrossRef]
53. Massonnet-Castel, S.; Pelissier, E.; Dreyfus, G.; Deloche, A.; Abry, B.; Guibourt, P.; Terrier, E.; Passelecq, J.; Jaulmes, B.; Carpentier, A. Low-molecular-weight heparin in extracorporeal circulation. *Lancet* **1984**, *323*, 1182–1183. [CrossRef]
54. Dinarello, C.A. Blocking il-1 in systemic inflammation. *J. Exp. Med.* **2005**, *201*, 1355–1359. [CrossRef]
55. Norris, C.A.; He, M.; Kang, L.-I.; Ding, M.Q.; Radder, J.E.; Haynes, M.M.; Yang, Y.; Paranjpe, S.; Bowen, W.C.; Orr, A. Synthesis of il-6 by hepatocytes is a normal response to common hepatic stimuli. *PLoS ONE* **2014**, *9*, e96053. [CrossRef] [PubMed]
56. Janowski, M. Functional diversity of sdf-1 splicing variants. *Cell Adhes. Migr.* **2009**, *3*, 243–249. [CrossRef] [PubMed]
57. Mccandless, E.E.; Budde, M.; Lees, J.R.; Dorsey, D.; Lyng, E.; Klein, R.S. Il-1r signaling within the central nervous system regulates cxcl12 expression at the blood-brain barrier and disease severity during experimental autoimmune encephalomyelitis. *J. Immunol.* **2009**, *183*, 613–620. [CrossRef] [PubMed]
58. Chatterjee, M.; Seizer, P.; Borst, O.; Schönberger, T.; Mack, A.; Geisler, T.; Langer, H.F.; May, A.E.; Vogel, S.; Lang, F. Sdf-1α induces differential trafficking of cxcr4-cxcr7 involving cyclophilin a, cxcr7 ubiquitination and promotes platelet survival. *FASEB J.* **2014**, *28*, 2864–2878. [CrossRef] [PubMed]
59. Sun, X.; Cheng, G.; Hao, M.; Zheng, J.; Zhou, X.; Zhang, J.; Taichman, R.S.; Pienta, K.J.; Wang, J. Cxcl12/cxcr4/cxcr7 chemokine axis and cancer progression. *Cancer Metastasis Rev.* **2010**, *29*, 709–722. [CrossRef] [PubMed]
60. Massberg, S.; Konrad, I.; SchüRzinger, K.; Lorenz, M.; Schneider, S.; Zohlnhoefer, D.; Hoppe, K.; Schiemann, M.; Kennerknecht, E.; Sauer, S. Platelets secrete stromal cell–derived factor 1α and recruit bone marrow–derived progenitor cells to arterial thrombi in vivo. *J. Exp. Med.* **2006**, *203*, 1221–1233. [CrossRef]
61. Chatterjee, M.; Von Ungern-Sternberg, S.N.; Seizer, P.; Schlegel, F.; Büttcher, M.; Sindhu, N.; Müller, S.; Mack, A.; Gawaz, M. Platelet-derived cxcl12 regulates monocyte function, survival, differentiation into macrophages and foam cells through differential involvement of cxcr4–cxcr7. *Cell Death Dis.* **2015**, *6*, e1989. [CrossRef]
62. Clancy, D.M.; Sullivan, G.P.; Moran, H.B.; Henry, C.M.; Reeves, E.P.; Mcelvaney, N.G.; Lavelle, E.C.; Martin, S.J. Extracellular neutrophil proteases are efficient regulators of il-1, il-33, and il-36 cytokine activity but poor effectors of microbial killing. *Cell Rep.* **2018**, *22*, 2937–2950. [CrossRef]
63. Hernández, M.R.; Galán, A.M.; Cases, A.; Lopez-Pedret, J.; Pereira, A.; Tonda, R.; Bozzo, J.; Escolar, G.; Ordinas, A. Biocompatibility of cellulosic and synthetic membranes assessed by leukocyte activation. *Am. J. Nephrol.* **2004**, *24*, 235–241. [CrossRef]
64. Castelli, W.A.; Nasjleti, C.F.; Diaz-Perez, R.; Caffesse, R.G. Cheek mucosa response to silk, cotton, and nylon suture materials. *Oral Surg. Oral Med. Oral Pathol.* **1978**, *45*, 186–189. [CrossRef]
65. Wichterle, O.; Lim, D. Hydrophilic gels for biological use. *Nature* **1960**, *185*, 117–118. [CrossRef]
66. Jang, J.; Go, W.-S. Continuous photografting of hema onto polypropylene fabrics with benzophenone photoinitiator. *Fibers Polym.* **2008**, *9*, 375–379. [CrossRef]